UNCLASSIFIED
SECURITY CLASSIFICATION OF THIS PAGE (When Data Entered)

REPORT DOCUMENTATION PAGE

READ INSTRUCTIONS BEFORE COMPLETING FORM

1. REPORT NUMBER: DTNSRDC-81/026
2. GOVT ACCESSION NO.
3. RECIPIENT'S CATALOG NUMBER

4. TITLE (and Subtitle): STATUS OF HYDRODYNAMIC TECHNOLOGY AS RELATED TO MODEL TESTS OF HIGH-SPEED MARINE VEHICLES
5. TYPE OF REPORT & PERIOD COVERED: Final
6. PERFORMING ORG. REPORT NUMBER

7. AUTHOR(s): Robert A. Wilson, D. Savitsky, M.J. Stevens, R.J. Balquet, B. Müller-Graf, T. Murakami, S.D. Prokhorov, P. van Oossanen
8. CONTRACT OR GRANT NUMBER(s)

9. PERFORMING ORGANIZATION NAME AND ADDRESS: David W. Taylor Naval Ship Research and Development Center, Bethesda, MD 20084
10. PROGRAM ELEMENT, PROJECT, TASK AREA & WORK UNIT NUMBERS: Task Area - SF43400391; Program Element - 62543N; Work Unit 1507-101

11. CONTROLLING OFFICE NAME AND ADDRESS: Naval Sea Systems Command (03R11), Washington, D.C. 20362
12. REPORT DATE: July 1981
13. NUMBER OF PAGES: 185

14. MONITORING AGENCY NAME & ADDRESS (if different from Controlling Office)
15. SECURITY CLASS. (of this report): UNCLASSIFIED
15a. DECLASSIFICATION/DOWNGRADING SCHEDULE

16. DISTRIBUTION STATEMENT (of this Report)

APPROVED FOR PUBLIC RELEASE; DISTRIBUTION UNLIMITED

17. DISTRIBUTION STATEMENT (of the abstract entered in Block 20, if different from Report)

18. SUPPLEMENTARY NOTES

19. KEY WORDS (Continue on reverse side if necessary and identify by block number)

High Speed Marine Vehicles
Model Tests
ITTC
SWATH
Semidisplacement Round Bilge Vessels
Planning Hulls
Submerged Hydrofoil Craft
Surface Effect Ships
Air Cushion Vehicles

20. ABSTRACT (Continue on reverse side if necessary and identify by block number)

The High Speed Marine Vehicle Panel of the 16th International Towing Tank Conference prepared hydrodynamic technology status reports related to model tank tests of SWATH, semidisplacement round bilge hulls, planing hulls, semisubmerged hydrofoils, surface effect ships, and air cushion vehicles. Each status report, plus the results of an initial survey of worldwide towing tanks conducting model experiments of high speed vessels, are contained herein. Hydrodynamic problems related to model testing and the full-scale extrapolation of the data for these vehicle types are also presented.

DD FORM 1 JAN 73 1473 EDITION OF 1 NOV 65 IS OBSOLETE.
S/N 0102-014-6601

UNCLASSIFIED
SECURITY CLASSIFICATION OF THIS PAGE (When Data Entered)

TABLE OF CONTENTS

LIST OF FIGURES

LIST OF TABLES

ABSTRACT

The High Speed Marine Vehicle Panel of the 16th International Towing Tank Conference prepared hydrodynamic technology status reports related to model tank tests of SWATH, semidisplacement round bilge hulls, planing hulls, semisubmerged hydrofoils, surface effect ships, and air cushion vehicles. Each status report, plus the results of an initial survey of worldwide towing tanks conducting mode experiments of high speed vessels, are contained herein. Hydrodynamic problems related to model testing and the full-scale extrapolation of the data for these vehicle types are also presented.

ADMINISTRATIVE INFORMATION

The 16th International Towing Tank Conference requested the assistance of the David W. Taylor Naval Ship Research and Development Center, Bethesda, Md, in coordinating the preparation and publication of the complete findings of the High Speed Marine Vehicle Panel. This report contains the in-depth contributions of the High Speed Marine Vehicle Panel members who were: Daniel Savitsky (Chairman), Davidson Laboratory, Stevens Institute of Technology, USA; Martin J. Stevens (Secretary), Experimental and Electronic Laboratories, British Hovercraft Corporation, England; Robert J. Balquet, Basin d'Essais des Carenes, France; Burkhard Müller-Graf, Versuchsanstalt fur Wasserbau und Schiffbau, West Germany; Toshikazu Murakami, Japan Defense Agency, Japan; Sergei D. Prokhorov, Krylov Ship Research Institute, USSR; Peter van Ossanen, Maritime Research Institute Netherlands, Netherlands Ship Model Basin, The Netherlands; Robert A. Wilson, David W. Taylor Naval Ship Research and Development Center, USA. This report can be obtained by contacting the National Technical Information Service, 5285 Port Royal Road, Springfield, Virginia 22161. The editing and publication of this report was sponsored by the Naval Sea Systems Command under Task Area SF 43400391, Program Element 62543N, and DTNSRDC Work Unit 1507-101.

1.0 INTRODUCTION

Worldwide interest in high speed marine vehicles such as SWATH, semidisplacement round bilge hulls, planing hulls, hydrofoils, surface effect ships, and air cushion vehicles (shown in Figure 1.1) is continuing to grow, but the classical model test

technologies are inadequate to define the performance of these advanced vehicles. As a means of providing a better understanding of the types of model experiments conducted on these vehicles, the Executive Committee of the 15th ITTC created a High-Speed Marine Vehicle Panel at The Hague, Netherlands, in 1978. The panel members, each of whom had considerable experience in conducting towing tank experiments of high speed marine vehicles, prepared a series of in-depth status reports on the vehicle types. These contributions are contained in this report together with the complete results of an initial survey of the extent of involvement of worldwide towing tanks conducting model experiments of high speed vessels.

Each individual contribution is directed toward identifying the status of hydrodynamic technology and identifying those model test procedures unique to each high speed marine vehicle studied. Hydrodynamic problems related to these model tests and their full-scale extrapolation procedures are also identified. The procedures discussed are those presently being used in the contributors facility and in other facilities where information was available; these procedures, however, are not necessarily those recommended for all investigations of the specific type of vehicle.

Because the hydrodynamic technologies of these craft are in a constant state of evolution, the information contained in this report should be considered as a base for future work and should be updated as new information or new vehicle types become available.

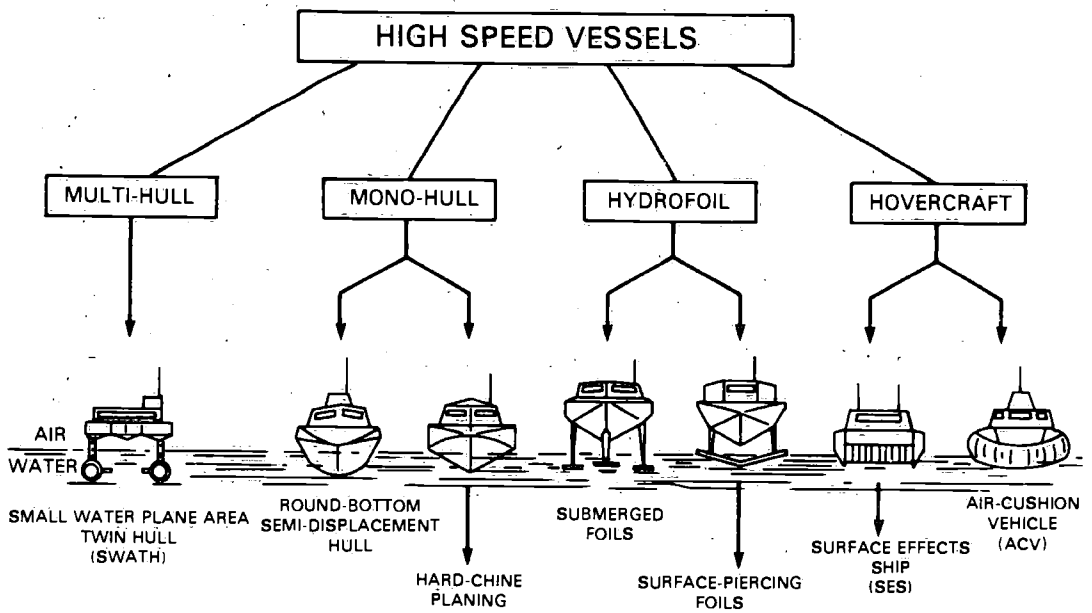

Figure 1.1 High Speed Marine Vehicles

2.0 RESULTS OF THE HIGH SPEED VESSEL PANEL QUESTIONNAIRE

2.1 INTRODUCTION

The main objects of the questionnaire were to obtain an indication of the extent to which ITTC members are involved in high speed craft activities, and to obtain their opinions concerning the major problem areas associated with model tests on high speed craft.

Seventy questionnaires were dispatched and forty-four replies were received. Of these, thirty-seven indicated that they were to some extent involved in testing high speed vessels. These thirty-seven establishments are listed in Table 2.1, and it seems reasonable to assume that they represent the majority of ITTC members who have any significant involvement in high speed vessel activities.

2.2 SUMMARY OF RESULTS

2.2.1 GENERAL

Members were asked to give their replies relative to six defined vehicle types (denoted A to F, respectively) and ten defined types of tests (denoted 1 to 10, respectively). They were asked to define any additional type of vehicle or test appropriate to their particular activities.

The defined types of craft and tests are listed in Table 2.2, together with examples of the additional craft types and tests specified in the replies to the questionnaire. In the following analysis of the results these additional types of craft and tests have each been grouped together under the general heading of "other."

2.2.2 TYPES OF HIGH SPEED CRAFT TESTED AND TYPES OF TESTS PERFORMED

Figure 2.1 shows the number of establishments that have tested specified types of craft (a) within the last five years and (b) more than five years ago. Figure 2.2 is a similar illustration with respect to types of tests. Figure 2.3 shows the number of establishments that have carried out specified tests on the specified vehicle types within the last five years.

It appears that high speed vessel activity has increased in the last five years in all areas except tests on hydrofoils, where the number of establishments testing them has decreased.

More establishments are involved in hard-chine and round-bilge craft than other types, and the greatest increases in activity have occurred in these areas.

The types of tests most often conducted are towed resistance tests, followed by towed tests in regular waves.

2.2.3 EXTENT OF INVOLVEMENT IN HIGH SPEED RESEARCH AND THE NATURE OF THIS RESEARCH

For the majority of establishments, high speed craft represent 20 percent or less of their total model test activity (see Figure 2.4). For over half the establishments, 20 percent or less of their total high speed vessel activity is devoted to basic research (see Figure 2.5), and for a significant proportion of establishments over 80 percent of their high speed work is development or commercial research on particular prototypes.

Some establishments carryout high speed work which does not fall within these two classifications (e.g., educational work), but this was generally a comparatively small percentage and is not shown on Figure 2.5.

2.2.4 FULL-SCALE AND MODEL-SCALE CORRELATION

Members were asked to indicate the areas in which they had direct full-scale and model-scale correlation data, and Figure 2.6 indicates the results that could be made available to the ITTC. Additional data have been obtained by many establishments but because these are not available, for proprietary or other reasons, they have not been included in Figure 2.5.

2.2.5 TYPE OF FACILITIES AND TYPICAL MODEL SIZES

For simplicity, the types of facilities have been analyzed only in respect to the maximum speed attainable (see Figure 2.7). The great majority of facilities fall within the speed range 0 to 15 m/s.

As might be expected, establishments with more than one high speed facility often employ differently sized models in each. Figure 2.8, therefore, shows the percentage distribution of model lengths for all the model sizes quoted in the questionnaire replies.

The most popular length for models is in the range 2 to 3 meters.

2.2.6 RESEARCH INVESTIGATIONS WHICH ARE INTENDED TO BE CONDUCTED IN THE FUTURE

Research investigations which are intended to be conducted have been broadly classified into the following groups. The most popular craft for proposed investigations are SWATH vessels and ACVs.

Investigation	Number of Establishments
SWATH Tests (Various)	9
ACV Tests (Various)	6
Hydrofoil Tests (Various)	5
Hard-Chine Vessel Tests (Various)	5
Round-Bilge Vessel Tests (Various)	4
Interaction Effects (Various)	3
Wave-Induced Motions and Hull Loads	3
SES Tests (Various)	3
Appendage Resistance Investigations	2
Scale Effect Investigations	2
Effect of Speed on Transverse Stability	2
Resistance Reduction of High Speed Hulls	2
Cavitation Investigations	2
Correlation of Propulsion Tests, Systematic Series, and Wetted Surface Determination	1 each

2.2.7 RESEARCH INVESTIGATIONS WHICH SHOULD BE CARRIED OUT

The areas in which members consider that research should be carried out have been grouped together in the following table. The areas in which most establishments consider research ought to be conducted are seakeeping and scale effect.

Investigation	Number of Establishments
Seakeeping Investigations - including nonlinearities, directional stability, habitability, motions in oblique waves, testing techniques, and instrumentation.	18
Scale effect investigations - including flexible skirts, running trim, appendages, methods of turbulence stimulation, and correct modelling techniques.	10
Drag component separation and interaction effects of propulsors.	8

Investigation	Number of Establishments
Effects of blockage and shallow water, tank boundary effects above critical speed.	4
Propulsive performance and added resistance in rough water.	4
Estimates of propulsive performance from model tests and determination of propulsive coefficients.	3
Model and full-scale correlation.	3
Effects of running trim and possibilities of automatic trim control.	2
Performance of propulsors in inclined flow, roll-yaw interaction of planing craft, ACV lift systems, effects of shallow water on SES, spray formation on round-bilge hulls, SES full-scale and model scale correlation.	1 each

2.2.8 GENERAL COMMENTS

The additional comments provided by members suggested that there was a requirement for a statement on experimental methodology for defined high speed vessels, including a list of references. Guidance was also required on such matters as the definition of wetted areas and turbulence stimulation, effects of trim and trim corrections, propeller-hull interaction effects, and measurement of resistance components.

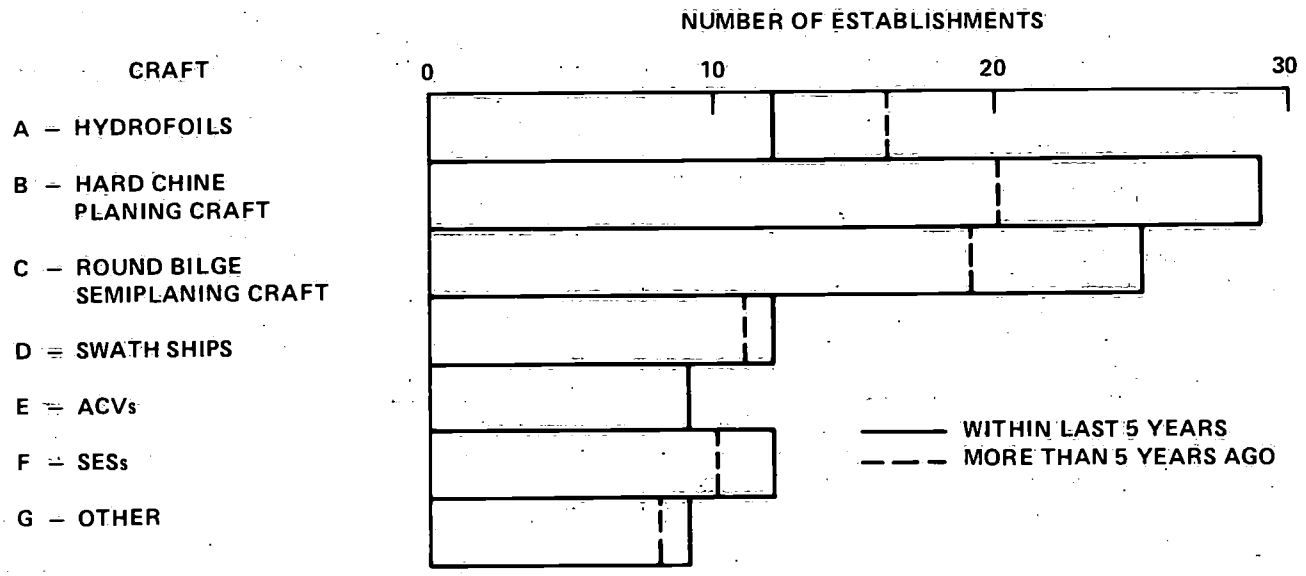

Figure 2.1 - Number of Establishments that have Tested Specified Types of High Speed Craft

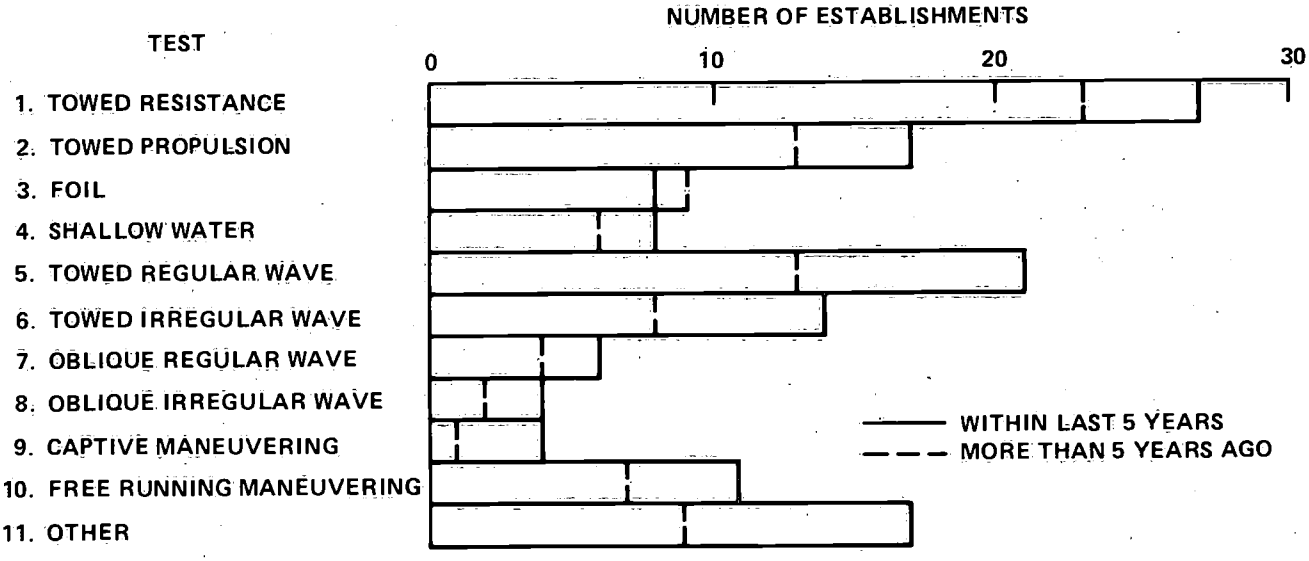

Figure 2.2 - Number of Establishments that have Conducted Specified Types of Test on High Speed Craft

Craft / Test		A	B	C	D	E	F
		Hydrofoils	Hard Chine	Round Bilge	SWATH Ships	ACV's	SES's
1	Towed Resistance	6	24	22	10	8	8
2	Towed Propulsion	0	10	9	5	2	3
3	Foil	8	0	0	0	0	0
4	Shallow Water	1	5	5	1	1	0
5	Regular Wave	6	13	14	9	5	4
6	Irregular Wave	1	11	10	6	4	2
7	Oblique Regular Wave	1	3	1	4	1	2
8	Oblique Irregular Wave	0	1	1	4	1	1
9	Captive Maneuvering	1	1	2	1	2	2
10	Free Run Maneuvering	0	0	5	3	3	1

Figure 2.3 - Number of Establishments that have Conducted Specific Tests on Defined Vehicle Types

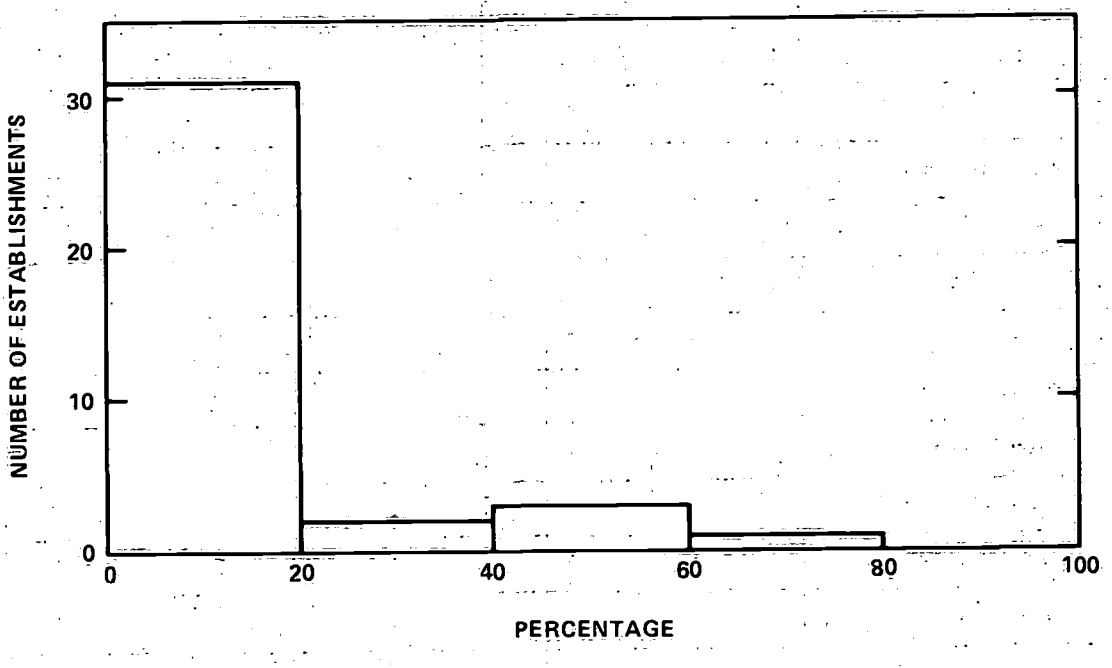

Figure 2.4 - Percentage of Total Activity that is High Speed Work at each Establishment

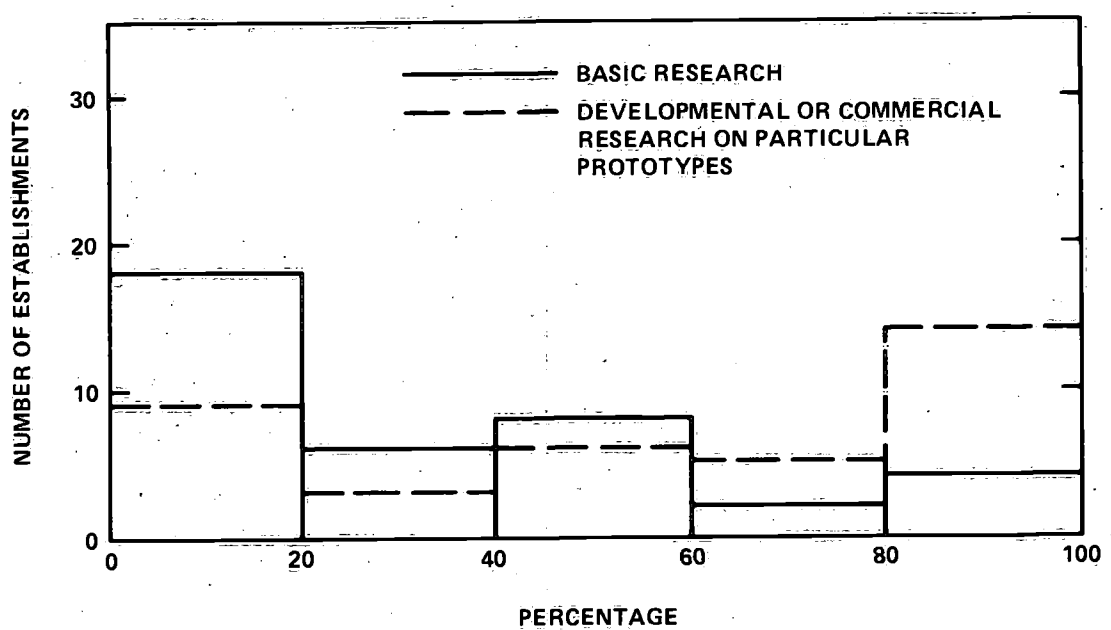

Figure 2.5 - Nature of High Speed Work

Craft / Test		A	B	C	D	E	F
		Hydrofoils	Hard Chine	Round Bilge	SWATH Ships	ACV's	SES's
1	Towed Resistance	2	2	2	0	1	3
2	Towed Propulsion	1	3	1	0	0	1
3	Foil	0	1	0	0	0	0
4	Shallow Water	0	1	0	0	0	0
5	Regular Wave	0	0	1	0	0	0
6	Irregular Wave	0	0	1	0	0	0
7	Oblique Regular Wave	0	1	1	0	0	0
8	Oblique Irregular Wave	0	0	1	0	0	0
9	Captive Maneuvering	0	0	1	0	0	0
10	Free Run Maneuvering	0	0	1	0	0	0

Figure 2.6 - Number of Establishments Having Correlation Data which could be made Available to the ITTC

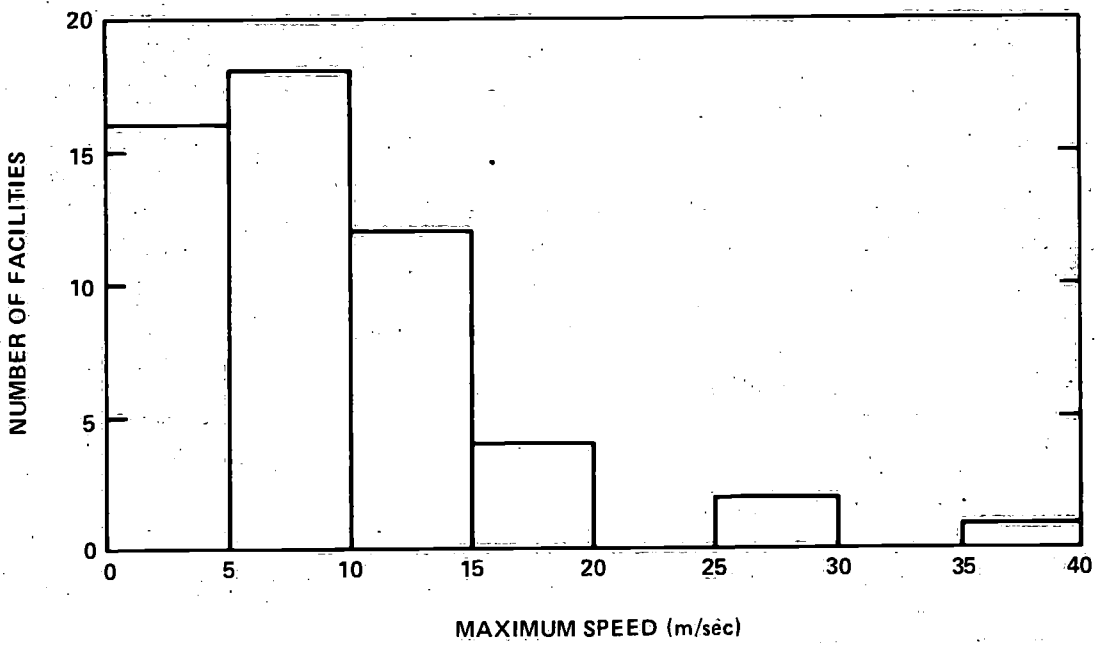

Figure 2.7 - Maximum Speed of High Speed Facilities

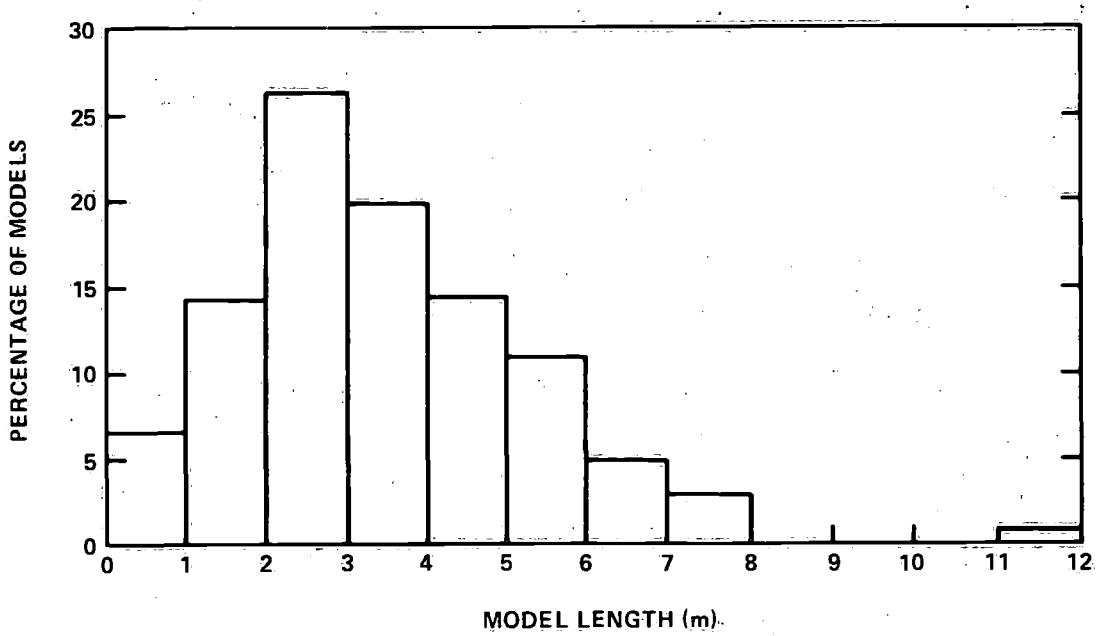

Figure 2.8 - Model Lengths Employed

TABLE 2.1 - ESTABLISHMENTS FROM WHICH REPLIES WERE RECEIVED

Admiralty Marine Technological Establishment (Haslar), U.K.

*Applied Research Laboratory, Pennsylvania State University, State College, Pennsylvania, U.S.A.

*Bulgarian Ship Hydrodynamics Centre, Varna, Bulgaria

Canal de Experiencias Hidrodinamicas, Madrid, Spain

China Ship Scientific Research Centre, Wusih, China

*College of Engineering, Seoul National University, S. Korea

Davidson Laboratory, Stevens Institute of Technology, Hoboken, New Jersey, U.S.A.

Delft University of Technology, The Netherlands

David W. Taylor Naval Ship Research and Development Center, Bethesda, Maryland, U.S.A.

Experimental and Electronic Laboratories, British Hovercraft Corporation, E. Cowes, U.K.

Hamburgische Schiffbau Versuchsanstalt, W. Germany

Hydromechanics Laboratory, U.S. Naval Academy, Annapolis, Maryland, U.S.A.

Hydronautics Ship Model Basin, Laurel, Maryland, U.S.A.

*Indian Institute of Technology, Kharagpur, India

Institut fur Schiffstechnik, Berlin, W. Germany

Institute Nazionale per Studi ed Esperienze di Architettura Navale, Rome, Italy

Institute Policattedra di Ingegneria Navale, Genoa, Italy

Institute de Pesquisas Technologicas do Estado de Sao Paulo, Brazil

Kamewa Marine Laboratory, Sweden

Krylov Shipbuilding Research Institute, Leningrad, U.S.S.R.

Nagaski Experimental Tank, Japan

National Maritime Institute, Feltham, U.K.

Norwegian Hydrodynamic Laboratories, Trondheim, Norway

Netherlands Ship Model Basin, Wageningen, The Netherlands

Offshore Technology Corporation, Escondido, California, U.S.A.

Research Institute Ishikawajima - Harima Heavy Industries Company Limited, Japan

Schiffbautechnische Versuchsanstalt, Vienna, Austria

Shanghai Ship Design and Research Institute, China

Ship Design and Research Centre, Gdansk, Poland

Ship Dynamics Division, Ship Research Institute, Tokyo, Japan

Ship Hydrodynamics Division, Poona, India

Ship Hydrodynamics Laboratories, Helsinki, Finland

Ship Hydrodynamics Laboratories, Shanghai, Chiao-Tung University, China

Ship Hydrodynamics Laboratory, University of Michigan, Ann Arbor, Michigan, U.S.A.

Swedish Maritime Research Centre, S.S.P.A., Gothenburg, Sweden

*University of Iowa, Iowa City, U.S.A.

University of Newcastle, U.K.

University of Osaka, Japan

*University of Rostock, German Democratic Republic

U.S. Army Cold Region Experimental Laboratory, Hanover, New Hampshire, U.S.A.

Versuchsanstalt fur Wasserbau und Schiffbau, Berlin, W. Germany

Vosper Thornycroft (U.K.) Limited, U.K.

*Wartsila, Helsinki, Finland

Yokohama National University, Japan

*These establishments reported they are presently doing no significant high speed work.

TABLE 2.2 - DEFINITIONS OF CRAFT AND TESTS

Types of Craft

A Hydrofoils
B Hard-Chine Planing Craft
C Round-Bilge Semi-Planing Craft
D SWATH Ships
E Air Cushion Vehicles (Amphibious)
F Surface Effect Ships (Not Amphibious)
G Others:
Hard Chine Semi-Planing Craft
HYSWAS
SWASH
Catamarans
Hybrids, etc.

Types of Test

1. Towed Resistance Tests
2. Towed Propulsion Tests
3. Foil Tests
4. Shallow Water Tests
5. Regular Wave Tests (Towed)
6. Irregular Wave Tests (Towed)
7. Regular Oblique Wave Tests (Towed)
8. Irregular Oblique Wave Tests (Towed)
9. Captive Maneuvering Tests
10. Free-Running Maneuvering Tests
11. Others:
Cavitation Tests (Various)

3.0 STATUS OF VEHICLE TYPE INVESTIGATIONS

3.1 SMALL-WATERPLANE-AREA, TWIN-HULL (SWATH) SHIPS

by

Dr. Peter Van Oossanen

Maritime Research Institute Netherlands

Netherlands Ship Model Basin

3.1.1 CONCEPT DEFINITION

The SWATH concept, which stands for small-waterplane-area, twin-hull ship, features two fully submerged hulls connected to an above-water, box-like deck structure, by one or more relatively thin struts attached to each hull. Also termed a semisubmersible catamaran (SSC), this concept has been studied since the early fifties. Thus far, particularly important work has been carried out: 1. by a Netherlands offshore company resulting in the construction of a 1200 ton, 40 m SWATH (DUPLUS) with a service speed of 8 knots; 2. by the U.S. Navy[1-12] resulting in the construction of a 190 ton, 27 m SWATH (SSP KAIMALINO) with a speed of 25 knots; 3. by Mitsui Engineering and Building Co.[13] resulting in the construction of a 370 ton, 35 m SWATH (SSC MESA-80) with a speed of 27 knots after extensive testing of a 12 m sea-going vessel. Published results of theoretical and experimental studies have revealed interest in displacements of up to 30,000 tons, and in speeds of up to 40 knots.

The range of hull form proportions is as follows:

Hull length to hull diameter ratio	12 to 24
Hull length to hull breadth (overall) ratio	1.6 to 4.0
Hull length to hull draught ratio	5 to 15
Hull length x breadth (overall) divided by waterplane area ratio	6 to 15

The benefits of the SWATH concept are derived from their low motions responses in seas which are similar to a conventionl surface ship three times larger due to the significantly reduced waterplane area and the submergence of the main bulk of the displacement volume.[14-33] Figure 3.1.1 shows a typical SWATH configuration taken from Numata.[34]

3.1.2. RESISTANCE INVESTIGATIONS

3.1.2.1 Components of Resistance

As is the case with conventional displacement ships, the main resistance component of SWATH ships at design speed is the frictional resistance. At higher speeds, however, the wave resistance of the hulls and of the struts can be appreciable if careful attention is not directed to the required depth of submergence of the hulls and to the unfavorable interaction of the waves produced by the struts, particularly when each hull has more than one strut.[35,36] The air resistance of SWATH ships is also important. The induced drag of control surfaces becomes significant as soon as appreciable forces are developed to counteract any pitch instability of SWATH ships. At speeds above the primary resistance hump, the spray resistance of struts becomes significant.[37] In a seaway, the added resistance due to waves of SWATH ships is less appreciable than for conventional monohulls.[38] Typical curves of wavemaking resistance due to hulls, struts, and strut and hull interference are given in Figures 3.1.2 and 3.1.3 for a single and a tandem strut configuration (taken from Numata).[34]

3.1.2.2 Resistance Prediction Techniques: Model Test Considerations

3.1.2.2.1 Required Model Size. Models for resistance tests should be sufficiently large so as to avoid unpredictable scale effects. Unpredictable scale effects can occur if the boundary layer flow on hull and stabilizer fins is wholly or partly laminar. The minimum model size is dependent upon the speed range to be tested and the means adopted to stimulate a turbulent boundary layer. The maximum model size is dependent upon the cross-sectional dimensions of the towing tank because blockage and shallow water effects should be avoided and upon the length of the towing tank. If the dimensions of the towing tank are large enough, the minimum model size is often based on a value of the Reynolds number of about 5×10^6 at the minimum test speed when no turbulent stimulation devices are adopted. Recently obtained (unpublished) resistance data with a 1/30-scale model of a tandem strut SWATH configuration using suitable turbulence stimulation devices on hulls and struts, agreed very well with data obtained from an unstimulated 1/12.8-scale model when extrapolated to full scale. The agreement was evident at $R_n \geq 1.8 \times 10^6$ for the 1/30-scale model.

The Reynolds number values of control surfaces is usually too small, even when using very large models. This can result in incorrectly scaled lift and drag coefficient values. To overcome this problem, resistance and propulsions tests are

sometimes carried out with models locked in trim and draft on which no horizontal control surfaces are attached[37,39] and the results corrected using estimated full-scale drag and lift data. This procedure leads to erroneous results if the influence of the control surfaces on heave and trim is not taken into account because the fins are often used to maintain zero trim and design draft throughout the speed range in calm water.[40] One procedure to correctly include the effect of horizontal control surfaces in resistance and powering tests is to stimulate a turbulent boundary layer at the leading edges and to carry out the test at three or four angles of attack of the control surfaces. On using relatively large models, the scale effect on lift and drag of control surfaces can be sufficiently reduced in this way, leading to a satisfactory knowledge of how speed and power are dependent upon their angle-of-attack. This approach also leads to a direct determination of the required angle-of-attack of the foils in order to minimize resistance and/or to maintain zero trim and design draft.

3.1.2.2.2 Possible Scale Effects. Numerous scale effects can occur. Irrespective of the size of the model, a scale effect will always occur in the deduced frictional resistance from the model test results. This is due to the inequality of model and full-scale Reynolds numbers. Use of large models and of turbulent stimulation devices will allow a reasonable estimation of this scale effect. Appreciable scale effects usually occur in the appendage drag. As stated in Section 3.1.2.2.1, the Reynolds number of control surfaces is usually too low to ensure that a turbulent boundary layer exists. The flow along these appendages should also be "tripped" to obtain a turbulent boundary layer. This is also true for rudders and deck-supporting struts. If not only the drag but also the lift of lifting surfaces such as trim-stabilizer fins are not scaled correctly, then scale effects will also occur in the running trim.[37] Because surface tension is not scaled in conventional model testing, the spray caused by the struts at higher speeds is not simulated correctly. Accordingly, a scale effect will occur in the spray resistance.[41] Because models for resistance and propulsion tests usually do not have superstructures, the aerodynamic or wind resistance is not scaled correctly. In certain towing tanks the air velocity under the carriage at the location of the model is considerably affected by the carriage structure. When carrying out tests at high speeds with SWATH models (which can have larger superstructures than conventional ships), attention should be given to the various aspects which could cause an appreciable scale effect in the air resistance. Other scale effects can occur if the model is large relative to the

cross section of the towing tank. In that case, wall effects (blockage) and shallow water effects can occur which are extremely difficult to account for in an adequate way, particularly at certain speeds.

3.1.2.2.3 Turbulence Stimulation. It is nearly always necessary to stimulate a turbulent boundary layer when carrying out tests with SWATH models. As mentioned in Section 3.1.2.2.2 the Reynolds number of struts and control surfaces is such that nearly always laminar flow, or laminar separation, followed by turbulent reattachment, will occur leading to serious scale effects in both drag and lift properties. To stimulate a turbulent boundary layer, trip wires, or studs, a strip of sand or Carborundum particles can be adopted. Each of these have advantages and disadvantages. Preliminary tests are required to find the best location for each of these stimulation devices, and to determine their contribution to the total resistance.

3.1.2.2.4 Influence of Tank Boundaries. Blockage corrections for conventional ships below Froude number values based on a waterline length of 0.35 can be used to estimate the blockage of SWATH models with reasonable accuracy. At higher speeds, no satisfactory procedure exists, other than detailed, three-dimensional wave resistance calculations for the model in the tank using, e.g., newly developed finite element procedures. As already mentioned the draft and beam of SWATH ships is relatively large compared to conventional ships, and it is possible that in some towing tanks the nearness of the tank bottom and sides for SWATH model testing will not be without some effect on resistance (and propulsion). Detailed studies of the effect of shallow water on resistance, squat, and running trim of SWATH ships have not yet been carried out.

3.1.2.2.5 Quantities Measured. The quantities which are commonly measured during calm water resistance tests with SWATH models are model speed, model resistance, sinkage (or rise) of stem, and stern and center of gravity. In addition, photographs are taken of the wave elevation along the side of the struts from which the wetted area of the struts can be deduced. Finally, separate drag and lift force measurements are sometimes carried out in the control surfaces. When tests are carried out with a model locked in heave(draft)and trim, in addition to the resistance force, vertical excitation forces are also measured. This type of test is usually not carried out for the purpose of determining resistance and propulsion properties, but for the design of horizontal control surfaces, or for qualitative comparison of SWATH configurations.[37]

3.1.2.2.6 Extrapolation Procedure. In principle, the results of resistance tests with SWATH models are extrapolated in the conventional way. The frictional resistance of the full-scale hull is accounted for by adopting the International Towing Tank Conference (ITTC) or the American Towing Tank Conference (ATTC) friction coefficient formulation. The frictional resistances of the struts and of the submerged hulls are estimated separately, adopting the length of the strut and hull independently with their respective Reynolds number calculation and wetted surface. The form factor of the cylindrical hulls and of the struts and control surfaces commonly used in SWATH designs have been derived from theoretical and experimental studies.[42] A more accurate estimation of the viscous resistance of SWATH ships is then possible. To the sum of the viscous resistance of struts and hulls should now be added to the viscous resistance of control surfaces, and appendages, as either measured (as is sometimes the case for stabilizer fins) or deduced from semiempirical relations. On subtracting the total viscous resistance, as calculated for the model Reynolds number, from the total measured resistance, the residuary resistance is found which is assumed to be dependent only upon Froude number. This residuary resistance is then extrapolated to full-scale accordingly. When added to the calculated viscous resistance for the full-scale SWATH ship, the total full-scale resistance is found. To this resistance value is to be added the wind resistance which can normally be deduced by calculation or from tests in a wind tunnel.

3.1.2.2.7 Correlation Factors. In extrapolating the results of resistance tests with SWATH models, it is necessary to adopt a model-ship correlation factor to account for the effects of structural hull roughness (plate seams, welds, paint roughness), unknown form drag, and eddy-making. On the basis of a limited number of correlation studies between model tests and full-scale trials,[9] it would seem that an appropriate value for the correlation factor C_A would be between 0 and 0.0005, adopting the extrapolation technique described above (with form factors). The fact that this value has been found to be generally smaller than for conventional ships of comparable length could be due to the fact that the viscous resistance can be assessed with a greater accuracy than for most conventional ships. Also, the wind resistance of SWATH ships, because of its greater importance, is often established explicitly (by tests in a wind tunnel or from detailed calculations) and is not included in the correlation allowance coefficient.

3.1.2.2.8 Systematic Model Test Series. The results of a small series of systematic model tests carried out at the David W. Taylor Naval Ship Research and

Development Center,[43] designated SWATH 1, 2, 3A, 3B, 3C, 3D, 3E, 4, 5A, 5B, 6A, 7 and 8, have been published. Otherwise, very little information of a systematic series is yet available.

3.1.2.2.9 Instrumentation. The instrumentation required for resistance tests with SWATH models is the same as required for resistance tests with models of conventional ships. The only exception is the instrumentation required to measure drag and lift of control surfaces.

3.1.2.2.10 Procedures Unique to SWATH Testing. Procedures to evaluate the effect of horizontal control surfaces on resistance properties of SWATH models, through restraining the trim and (possibly) the rise of the center of gravity, are unique to SWATH testing. Mainly, two techniques are being applied to evaluate the influence of moveable fin-type control surfaces. One of these comprises the technique of adopting a model with all control surfaces and appendages fitted, unrestrained in heave and trim, for which various tests have to be carried out at constant speed to evaluate the influence of angle-of-attack of the moveable, horizontal control surfaces. The other technique comprises the use of a model held locked in heave and trim, for which the vertical force and longitudinal moment on the model have to be measured, without the horizontal control surfaces fitted. In the case of the latter technique it is often required to carry out these tests at various trim and draft values to be able to later ascertain the interaction of the added control surfaces on the resistance through changes in the running trim and rise of the center of gravity.

3.1.2.3 Recommendations to the 16th ITTC for Resistance Studies

3.1.2.3.1 Study and recommend methods for turbulence stimulation in boundary layers of struts and control surfaces of SWATH.

3.1.2.3.2 Study and define procedures for estimating and extrapolating spray resistance. 3.1.2.3.3 Review available methods for determining wall and shallow water effects for SWATH.

3.1.2.3.4 Review available theoretical and experimental formulations for the prediction of the resistance of appendages and control surfaces.

3.1.2.3.5 Review available theoretical and experimental formulations for the prediction of the Reynolds number dependency of the lift of control surfaces for SWATH.

3.1.2.3.6 Document the effects of appendages, control surfaces, and propulsion on the rise of CG and trim of SWATH, particularly as related to the adopted test technique.

3.1.3 SEAKEEPING INVESTIGATIONS

3.1.3.1 Model Considerations

The size of models for seakeeping tests is dependent upon the wavemaking capabilities of the tank, the tank size and water depth, and the sea condition to be simulated. Also, most of the items listed in Section 3.1.2.2.1 are valid here.

Models are usually complete with respect to hull and appendages, freeboard, and superstructure. The weight distribution and logitudinal and transverse moments of inertia are simulated as accurately as possible. The material adopted for model manufacture can be wood, glass-reinforced plastic, or some other strong material.

3.1.3.1 Quantities Measured

The quantities which are important for the seakeeping of SWATH ships are its motions in six degrees-of-freedom; accelerations at the bow and the stern (from which the accelerations elsewhere can be calculated); added resistance (or added thrust); deck wetness; spray and relative motions fore and aft at various stations. To assess hydrodynamic loads and box slamming pressures, bending moments and side forces in struts, deck and other transverse hull connections are measured. Also, the wave characteristics should be accurately known in both regular and irregular sea conditions. Film coverage at high film speeds is extremely useful.

3.1.3.3 Test Wave Environment

Tests in both regular and irregular seas are considered useful. For systematic design studies, often regular seas are adopted (for comparison with calculations). Tests in irregular seas are often carried out in the final design stage. The irregular seas, as simulated in the tank, should be given careful consideration. Heave and pitch motions are more lightly damped than a conventional ship due to the small waterplane area.[44]

It is important to study the behavior in sea environments which contain wave components around the resonance frequency. Because SWATH ships have relatively long periods of motion, conventional irregular wave tests in Pierson-Moskovitz type spectra may not be sufficent.[12,34]

For SWATH ships, the study of the motions in following seas and the structural loading in beam seas is particularly important.[45,46]

3.1.3.4 Test Procedure

Procedurs for SWATH tests in waves are identical to those for displacement ships. The model can be towed at constant speed or with free-to-surge equipment.

Free running tests with self-propelled models, with constant thrust, are also carried out.

When towing the model in waves, careful attention should be given to the simulation of the thrust moment if the towing force is not exerted in the shaft drive of the propulsors. With SWATH ships, this effect is more important than for conventional ships because of their relatively small longitudinal metacentric height GM^L. The report of poor correlations of measured pitch-excited moments with calculations for captive experiments on a SWATH 6A model[43] could be due to this fact.

3.1.3.5 Data Collecting, Processing, and Presentation

Usually both digital and analog signals are recorded for evaluation either during or after the tests by computer. Normally, all test results are presented in tables and graphs for the full-size ship. Measured values are scaled up according to Froude's law. For regular seas, the motions, force, moment, and undisturbed wave signals are analyzed to determine the harmonic components and their nonlinear behavior. For irregular seas, the recorded signals can be divided into four types as follows:

TYPE I

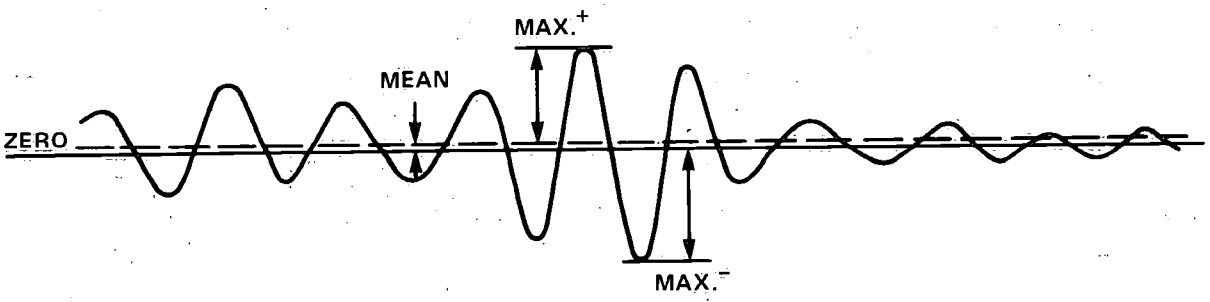

This signal consists of an oscillating motion of which the frequency corresponds with the frequency of the waves.

DEPARTMENT OF THE NAVY
DAVID W. TAYLOR NAVAL SHIP RESEARCH
AND DEVELOPMENT CENTER
HEADQUARTERS
BETHESDA, MARYLAND 20084

ANNAPOLIS LABORATORY
ANNAPOLIS, MD 21402
CARDEROCK LABORATORY
BETHESDA, MD 20084

IN REPLY REFER TO:
1603:RAW
27 July 1981

Dear Delegate to the 16th ITTC:

The David Taylor Naval Ship Research and Development Center published DTNSRDC Report 81/026 entitled, "Status of Hydrodynamic Technology as related to Model Tests of High Speed Marine Vehicles" documenting the complete findings of the 16th ITTC's High Speed Marine Vehicle Panel: the Panel's report submitted to the 16th ITTC is a condensed version of this document. The enclosed copy of the complete report is forwarded for your information. The 16th ITTC High Speed Marine Vehicle Panel considers this report to be a document which hopefully will be continuously reviewed and updated as the technology is further developed.

Very truly yours,

ROBERT A. WILSON
Member, 16th ITTC High Speed
Marine Vehicle Panel

TYPE II

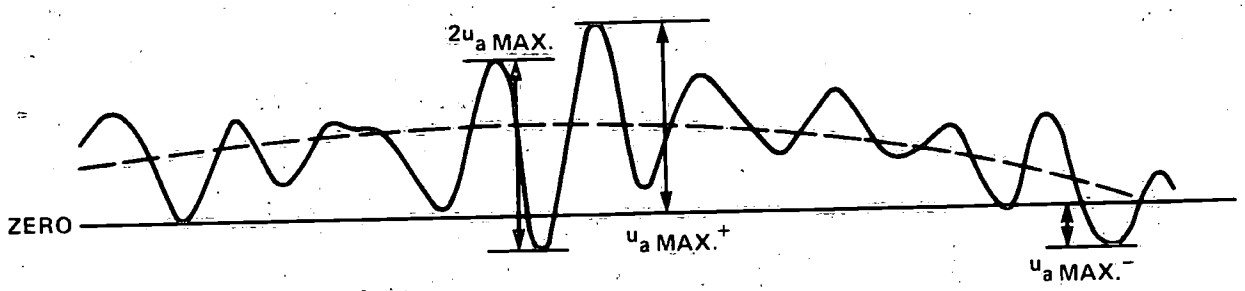

This type of signal consists of a high frequency oscillating motion which is superimposed on slowly varying motion.

TYPE III

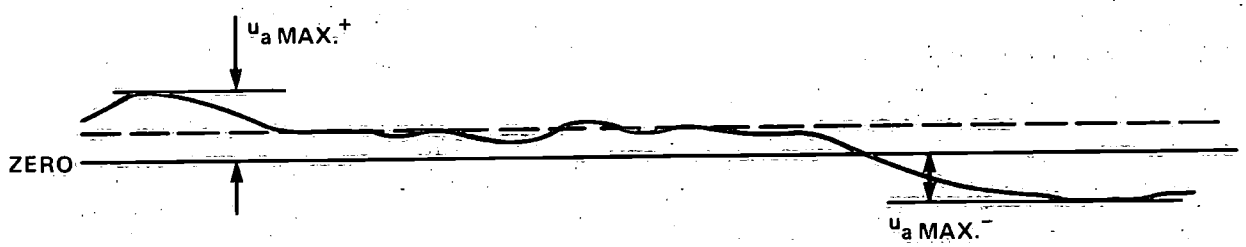

This signal consists also of a high frequency oscillating part, superimposed on a slowly varying part. The amplitude of the high frequency oscillations is small, compared to the slowly oscillating motion.

TYPE IV

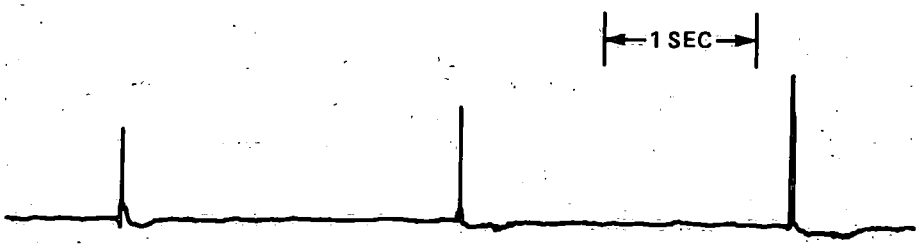

This signal is typical for slamming pressure recordings.

A general classification of the signals obtained or calculated from the various tests is as folows:

TYPE I

Wave heights

Heave motions

Side and shear forces

Bending moments

TYPE II

Surge motions in head and bow quartering seas

Sway motions in bow quartering and beam seas

Roll angles in bow quartering and beam seas

Pitch angles in head and bow quartering seas

Yaw angles in bow quartering seas

Relative motions

TYPE III

Surge motions in beam seas

Sway motions in head seas

Roll angles in head seas

Pitch angles in beam seas

Yaw angles in head and beam seas

TYPE IV

Slamming pressures

From the above recorded signals, usually the following quantities are determined and presented:

3.1.3.5.1 u = Root-mean square value

$$= \frac{1}{N} \sum_{n=1}^{n=N} \left((u_n - \bar{u})^2 \right)^{1/2}$$

3.1.3.5.2 $\bar{u}$ = Mean Value

$$= \frac{1}{N} \sum_{n=1}^{n=N} u_n$$

in which N = number of samples

u_n = value of the n^{th} sample

3.1.3.5.3 $\tilde{u}_{a1/3^+}$ = significant peak value
= which is the mean of the one-third highest crest to zero values (positive, unless states otherwise).

3.1.3.5.4 $\tilde{u}_{a1/3^-}$ = significant trough value
= which is the mean of the one-third highest trough to zero values (positive, unless stated otherwise).

3.1.3.5.5 $2\tilde{u}_{a1/3}$ = significant peak to trough value
= which is the mean of the one-third highest peak to trough values

3.1.3.5.6 $u_{a\ max^+}$ = maximum value
= highest peak value (positive, unless stated otherwise).

3.1.3.5.7 $u_{a\ max^-}$ = maximum value
= highest trough value (positive, unless stated otherwise).

3.1.3.5.8 $2u_{a\ max}$ = maximum value
= highest crest to trough value.

3.1.3.5.9 N_o = number of oscillations.

3.1.3.5.10 Response function:

The response functions of the measured quantities are calculated by dividing their spectral density functions by the wave spectrum and taking the square root of the ratios. Careful attention should be given to the possible nonlinear behavior of SWATH ships in irregular seas, in which case the motion response functions cannot be calculated.[47-55]

3.1.3.6 Correlation of Model Test Results

Very little information is available on the correlation of model test results for SWATH vessels. Recently, the results of full-scale seakeeping measurements on SSP KAIMALINO, a small SWATH vessel of 190 tons displacement, were published by Fein et al.[12] They reported good agreement with the significant motion values found during model tests and obtained from calculations.

3.1.3.7 Systematic Model Test Series

The results of a small series of systematic model tests carried out at DTNSRDC[51] designated SWATH 6A, 6B, 6C, and 6D have been published. Very little other information on a systematic series is available.

3.1.3.8 Outstanding Problems in Rough Water Testing

The small waterplane area of SWATH ships causes the seakeeping properties of these ships to differ markedly from monohulls. While no single outstanding problem in rough water testing can be identified, the seakeeping performance of SWATH ships is a complex subject, and differs sufficiently from monohulls to warrant extensive testing for every new design. As is the case with monohulls, the extent to which motions and accelerations are linear should be further investigated.

3.1.3.9 Recommendations to the 16th ITTC for Seakeeping Studies

3.1.3.9.1 Document the applicability of linearity to the seakeeping performance of SWATH.

3.1.3.9.2 Compare data obtained in free and fixed-in-surge tests in waves and make recommendations as to the extent of the applicability of each experimental procedure.

3.1.3.9.3 Recommend a uniform method for nondimensionalizing transfer functions and encounter frequencies for SWATH.

3.1.3.9.4 Provide a survey of model and full-scale data on seakeeping measurements for SWATH.

3.1.3.9.5 Recommend standard test procedures and data extrapolation methods for SWATH, particularly relative to the choice of sea spectrum in the absence of measured wave data.

3.1.4 MANEUVERABILITY INVESTIGATIONS

Only a few maneuvering investigations of SWATH ships have yet been carried out and reported on. On the basis of available data, it would seem that the large distance between the hulls leads to good low speed maneuvering since the propellers are far apart, while high speed maneuvering is a problem, because of the high directional stability of each of the slender hulls and struts.

3.1.4.1 Influence of Rudder Configuration of SWATH

The first SWATH designs employed rudders that were a movable part of the strut. These rudders produced turning circle diameters which were larger than those of monohulls of the same length.[21] Recent attention to possible alternative rudder configurations have led to designs which have a turning performance comparable to conventional ships.[7,56-59] If the rudder cannot be placed behind the propeller, the required rudder area must be considerably larger to obtain comparable turning performance. The rudder effectiveness for SWATH ships decreases significantly as the level of the flow over the rudders drops.[58,59]

3.1.4.2 Experimental Procedures

The approach adopted to determine the turning characteristics of SWATH ships thus far is to obtain coefficients using the planar motion mechanism (PMM), rotating arm experiments, or radio-controlled models. The coefficients are then fed into a maneuvering simulation adopting the equations of motion. The coefficients include terms for the forces and moments on the ship due to the velocities and acceleration of the ship when in motion. The PMM technique obtains these coefficients by oscillating a model in yaw and sway while moving in a straight line. The model is oscillated at a number of different frequencies for each forward speed tested. This experimental technique will provide the acceleration terms used in the turning simulation. The steady state yaw rate terms are derived by extrapolating the oscillation data to zero frequency, while the steady state sway velocity can be obtained from zero frequency extrapolation or by running straight line drift angle experiments.

The rotating arm technique produces the maneuvering coefficients by running a fully captive model in a circle and recording the forces and moments for different combinations of input parameters such as yaw rate, sway velocity, rudder angle, roll

angle, and forward speed.[17,58] The coefficients are derived by relating the variation of forces and moments to the input parameters at each forward speed. In this way, steady state yaw rate and sway velocity coefficients are obtained. Acceleration terms cannot be obtained in this way. Radio-controlled model experiments in a large basin can also be carried out to determine the most important maneuvering properties.

3.1.4.3 Data Collection, Presentation, and Extrapolation

Preliminary results obtained from maneuvering studies so far indicate that there is no coupling between drift angle and yaw rate at any speed. Also, all the roll angle terms in the equation of motion are nearly zero. Rudder angle-yaw rate and rudder angle-drift angle coupling terms are also nearly zero in all cases. These facts minimize the number of data points necessary to quantify the turning characteristics.[58,59]

The experimental results are usually converted to nondimensional stability and rudder derivatives. On plotting these linear derivatives against the Froude number, the speed dependence of these derivatives is usually found to be significant, particularly near the primary resistance hump.

Normally, the Froude scaling relations are adopted to extrapolate model results to full-scale.

3.1.4.4 Correlation of Model Test Results

Significant comparisons of model and prototype results have not yet been made due to a lack of full-scale information. Full-scale results obtained for SSP KAIMALINO[7,57] agreed very well with results of a maneuvering simulation study based on model tests for speed loss, roll, turn rate, and tactical diameter.

3.1.4.5 Outstanding Problems in Maneuvering Investigations

At speeds higher than presently investigated for SWATH, struts, appendages, and propulsors cavitate severely while maneuvering. The influence of cavitation on lift and drag of struts, appendages, and propulsors are usually not taken into account in the model test results. This fact constitutes an outstanding problem to be addressed for some high-speed SWATH designs presently being studied.

3.1.4.6 Recommendations to the 16th ITTC for Maneuvering Studies

3.1.4.6.1 Recommend procedures for steady and unsteady model tests to provide data for adequately describing the maneuvering characteristics of SWATH.

3.1.4.6.2 Provide a literature survey of the scaling and of the effects of ventilation and cavitation on appendages and propulsors for the maneuvering characteristics of SWATH.

3.1.4.6.3 Examine and report on the utility and applicability of rotating arm tests, planar motion tests, and free-running tests for SWATH ships.

3.1.4.6.4 Establish the applicable equations of motions for SWATH.

3.1.5 PERFORMANCE, PROPULSOR, AND CAVITATION INVESTIGATIONS

SWATH ships have found application in the speed regime of up to about 30 knots. Some studies have included speeds up to 40 knots. Up to 35 knots, the conventional subcavitating propeller is adopted because of its superior efficiency over most other propulsors. Powering, propulsor, and cavitation aspects of SWATH model testing technology is, therefore, identical to those of conventional ships and shall not be addressed here.

3.1.6 PRESENTATION AND INFORMATION

There is a lack of standard symbols associated with SWATH ship geometry and performance. The ITTC should update their list of symbols and definitions to include specific SWATH ship parameters.

3.1.7 REFERENCES

1. Lang, T. and D. Higdon, "Hydrodynamics of the 190-Ton Stable Semisubmerged Platform (SSP)," AIAA/SNAME Meeting, Paper 74-328, San Diego (Feb 1974).

2. Lang, T. et al., "Design and Development of the 190-Ton Stable Semisubmerged Platform (SSP)," presented at the ASME Winter Annual Meeting, Detroit, Mich. (Nov 1973).

3. Lang, T., "Hydrodynamic Design of an S^3 Semisubmerged Ship," presented at the Ninth Symposium on Naval Hydrodynamics, Paris, France (Aug 1972).

4. Lang, T., "S^3 Semisubmerged Ship Concept and Experimental Hydrodynamic Coefficients," Naval Engineers Journal, American Society Naval Engineers, pp. 33-42 (Apr 1972).

5. Lang, T. and D. Higdon, "S^3 Semisubmerged Ship Concept and Dynamic Characteristics," AIAA Paper/72-604 presented at the AIAA/SNAME/USN Advanced Marine Vehicles Meeting, Annapolis, Md. (17-19 Jun 1972).

6. Hightower, J. and R. Seiple, "Operational Experience with the SWATH Ship SSP KAIMALINO," AIAA/SNAME Advanced Marine Vehicles Conference, San Diego, CA, Paper 78-74 (Apr 1978).

7. Fein, J. and R. Waters, "Control Response Trials of the Stable Semisubmerged Platform (SSP KAIMALINO)," DTNSRDC Report SPD 650-02 (Apr 1976).

8. Fein, J. et al., "Seakeeping of the SSP KAIMALINO," AIAA/SNAME Advanced Marine Vehicles Conference, Paper 78-739 (Apr 1978).

9. Stenson, R., "Full-Scale Powering Trials of the Stable Semisubmerged Platform, SSP KAIMALINO," DTNSRDC Report SPD 650-01 (Apr 1976).

10. Fein, J., "Low Speed Seakeeping Trials of the SSP KAIMALINO," DTNSRDC Report SPD 650-04 (Mar 1978).

11. Kallio, J., "Seakeeping Trials of the SSP KAIMALINO," DTNSRDC Report SPE 650-03 (APR 1976).

12. Fein, J. et al., "The Seakeeping Characteristics of a Small Waterplane Area, Twin-Hull (SWATH) Ship," 13th Symposium on Naval Hydrodynamics, Tokyo (1980).

13. Oshima, M. et al., "Experiences with 12-Meter Long Semisubmerged Catamaran (SSC) 'Marine Ace' and Building of SSC Ferry for 446 Passengers," AIAA/SNAME 5th Conference on Advanced Marine Vehicles, Paper 79-2019 (Oct 1979).

14. Lang, T. G., "S^3 New Type of High-Performance Semisubmerged Ship," American Society of Mechanical Engineers, Paper 71-WA/UnT-1, Winter Annual Meeting (28 Nov-2 Dec 1971).

15. Leopold, R., "A New Hull Form for High-Speed Volume-Limited Displacement-Type Ships," Society of Naval Architects and Marine Engineers, Paper 8, Spring Meeting (21-24 May 1969).

16. Boericke, H., Jr., "Unusual Displacement Hull Forms for Higher Speeds," International Shipbuilding Progress, Vol. 6, pp. 249-264 (1959).

17. Mandel, P., "The Potential of Semisubmerged Ships in Rough Water Operations," New England Section, SNAME (Mar 1960).

18. Leopold, R. et al., "The Low Waterplane Area Multi-Hull Ship Principles, Status and Plans," AIAA/SNAME, Advanced Marine Vehicles Conference, Annapolis, Md. (Jul 1972).

19. Childers, K. et al., "SWATH - The VSTOL Aircraft Carrier for the Post 1990's," Naval Engineer Journal (Feb 1977).

20. Pien, P. and C. Lee, "Motion and Resistance of a Low Waterplane Area Catamaran," NSRDC Ninth Symposium on Naval Hydrodynamics, Paris, France (Aug 1972).

21. Hawkins, S. and T. Sarchin, "The Small-Waterplane-Area Twin-Hull (SWATH) Program Status Report," AIAA/SNAME 1974 Advanced Marine Vehicle Conference, San Diego.

22. Lee, C. et al., "Prediction of Motion and Hydrodynamic Loads of Catamarans," Marine Technology, Vol. 10, No. 4, pp. 392-405 (Oct 1973).

23. Kallio, J. and J. Ricci, "Seaworthiness Characteristics of a Small Waterplane Area Twin-Hull (SWATH IV) Part II," DTNSRDC Report SPD 620-02 (1976).

24. Baitis, A. et al., "A Seakeeping Comparison Between Three Monohulls, Two SWATHS, and a Column-Stabilized Catamaran Designed for the Same Mission," DTNSRDC Report SPD-655-01 (1975).

25. Motora, S. and T. Koyama," Wave-Excitationless Ship Forms," 6th Naval Hydrodynamic Symposium, Washington, D.C. Proceedings published by the Office of Naval Research, pp. 383-411 (1966).

26. Curphey R. and C. Lee, "Theoretical Prediction of Dynamic Wave Loads on Small Waterplane Area, Twin HullShip," DTNSRDC Report 77-0027 (1977).

27. Kallio, J., "Seaworthiness Characteristics of 2900-Ton Small Waterplane Area, Twin-Hull (SWATH)," DTNSRDC Report SPD 620-03 (1977).

28. Lee, C., "Theoretical Prediction of Motion of Small-Waterplane Area, Twin-Hull (SWATH) Ships in Waves," DTNSRDC Report 76-0046 (1976).

29. Lee, C. and R.M. Curphey, "Prediction of Motion, Stability, and Wave Load of Small-Waterplane-Area, Twin-Hull Ships," Trans. SNAME, Vol. 85, pp. 94-130 (1977).

30. Lewis E. and J. Berslin, "Semisubmerged Ships for High Speed Operation in Rough Seas," Third Symposium Naval Hydrodynamics, High Performance Ships (ACR-65), pp. 525-560 (Sep 1960).

31. Lang, T., "High Speed Ship with Submerged Hulls," U.S. Patent 3, 623, 444 (Nov 1971).

32. Numata, E., "Model Tests of Lambda SWATH Configurations," SIT Report DL-78-2026 (Jul 1978).

33. Kerr, G. et al., "SWATH Ship Design State-of-the-Art," AIAA/SNAME Advanced Marine Vehicles Conference Paper 78-737 (Apr 1978).

34. Numata, E., "Predicting Hydrodynamic Behavior of Small Waterplane Area, Twin-Hull Ships," presented to the New York Metropolitan Section of SNAME (Apr 1980).

35. Chapman, R., "Hydrodynamic Drag of Semisubmerged Ships," ASME Paper 72-WAOCT-5 (Nov 1972).

36. Chapman, R., "Drag Measurements on Models of SWATH Ships and Basic SWATH Components," Naval Undersea Center Report TN 984 (Apr 1973).

37. Lin, W.-C. and W.G. Day, Jr., "The Still-Water Resistance and Propulsion Characteristics of Small-Waterplane-Area Twin-Hull (SWATH) Ships," AIAA/SNAME Advanced Marine Vehicles Conference Paper 74-325 (Feb 1974).

38. Yeh, H. and E. Neal, "Powering Characteristics of SWATH 6A in Calm Water and Head Seas, Represented by Model 5337-A and Using Propellers 4415-16," DTNSRDC Report SPD 396-20 (Jan 1977).

39. Chapman, R., "Hydrodynamic Drag Measurements on SWATH Ship Components," Naval Undersea Center Report NUC TP-406 (Jul 1974).

40. Chapman, R., "Sinkage and Trim of SWATH Demihulls," AIAA/SNAME 1974 Advanced Marine Vehicles Conference, San Diego.

41. Chapman, R., "Spray Drag of Surface-Piercing Struts," AIAA/SNAME Advanced Marine Vehicles Conference (Jul 1972).

42. Granville, P.S., "Elements of the Drag of Underwater Bodies," DTNSRDC Report SPD 672-01 (Jun 1976).

43. Lamb, G. and J. Fein, "The Developing Technology for SWATH Ships," AIAA/SNAME 5th Conference on Advanced Marine Vehicles, Paper 79-2003 (Oct 1979).

44. Salvesen, N., "A Note on the Seakeeping Characteristics of Small Waterplane Area Twin Hull Ships," AIAA/SNAME Paper 72-606 (Jul 1972).

45. Higdon, D., "Estimation of Critical Hydrodynamic Loads on the SSP," Naval Undersea Systems Command Report TN-533 (1971).

46. Jones, H. and D. Gerzina, "Motion and Hull Induced Bridging Structure Loads for a SWATH Attack Aircraft Carrier in Waves," NSRDC Report 3819 (1973).

47. McCreight, K. and C. Lee, "Manual for Mono-Hull or Twin-Hull Ship Motion Prediction Computer Program," DTNSRDC Report SPD-686-02 (1976).

48. Kim, K., "Determination of Damping Coefficients of SWATH Catamaran Using Thin Ship Theory," Mass. Inst. Tech., Dept. Ocean Eng. Report 75-4 (1975).

49. Lee, C. and M. Martin, "Determination of Size and Stabilizing Fins for Small Waterplane Area, Twin-Hull Ship," DTNSRDC Report 4495 (1974).

50. Dalzell, J., "A Simplified Evaluation Method for Vertical Plane, Zero Speed, Seakeeping Characteristics of SWATH Vessels," Davidson Laboratory, Steven Institute of Technology, SIT Report DL-78-1970 (Jul 1978).

51. Lee, C., "Approximate Evaluation of Added Mass and Damping Coefficients of Two-Dimensional SWATH Sections," DTNSRDC Report 78/084 (Oct 1978).

52. Lee, C. and K. McCreight, "Investigation of Effects of Activated Fins on Vertical Motion of a SWATH Ship in Waves," DTNSRDC Report SPD-763-01 (Feb 1977).

53. Livingston, W., "Generalized Non-Linear Time Domain Predictor for SWATH Craft," DTNSRDC Report SPD-0857-1 (to be published).

54. Day, W. et al., "Results of Exercising a Synthesis Routine for SWATH Ships, and Comparison with Model Experiments," DTNSRDC Report SPD-396-19 (Nov 1975).

55. Kirkman, K. et al., "Model Tests and Engineering Studies of the SWATH 7 Small Waterplane Area Twin-Hull Ship," Hydronautics, Inc. Technical Report 7694-1 (Nov 1976).

56. Lee, C. and L. Murray, "Experimental Investigations of Hydrodynamic Coefficients of a Small Waterplane Area, Twin-Hull Model (SWATH 6a)," DTNSRDC Report SPD 620-03 (1977).

57. Fein, J. and J. Feldman, "Controllability of the Stable Semisubmerged Ship," 3rd Ship Control Symposium, Bath, England (Oct 1972).

58. Fein, J. and R. Waters, "Rotating Arm Experiments on the SWATH 6A Maneuvering Predictions," DTNSRDC Report SPD 698-01 (Jul 1976).

59. Fein, J., "The Application of Rotating Arm Data to the Prediction of Advanced Ship Maneuvering Characteristics," 18th American Towing Tank Conference (Aug 1977).

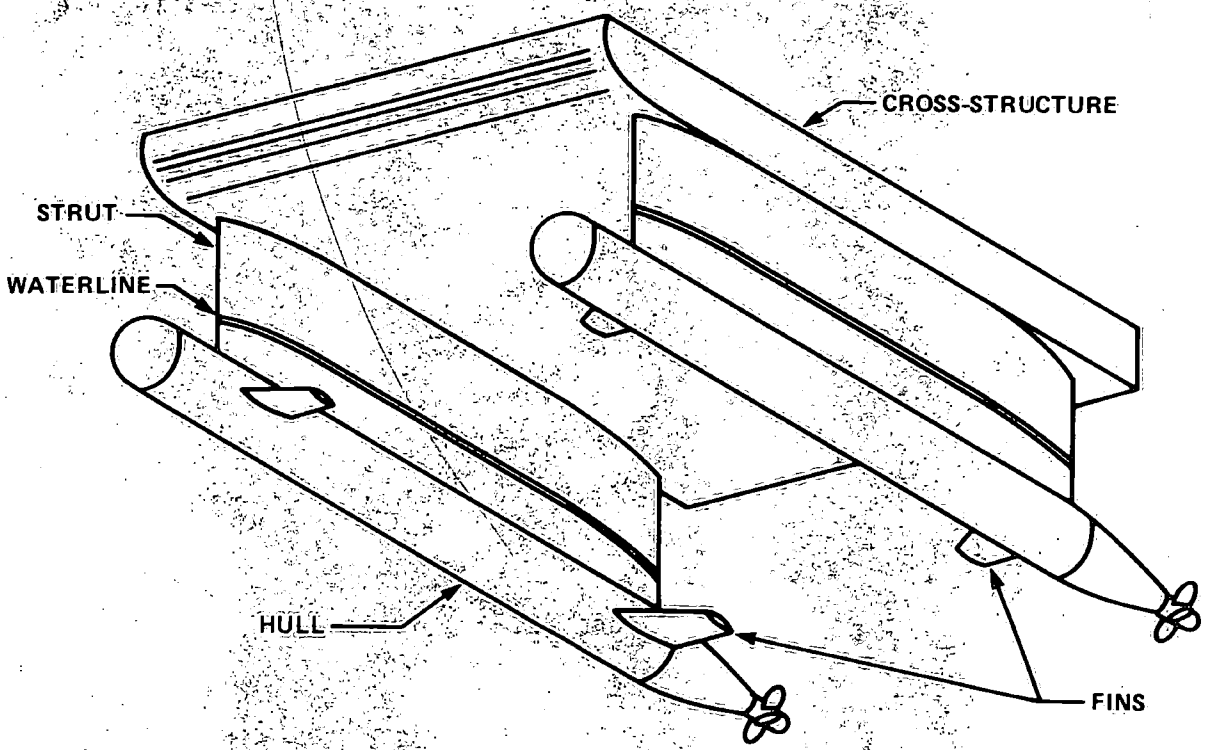

Figure 3.1.1 - SWATH Configuration and Nomenclature

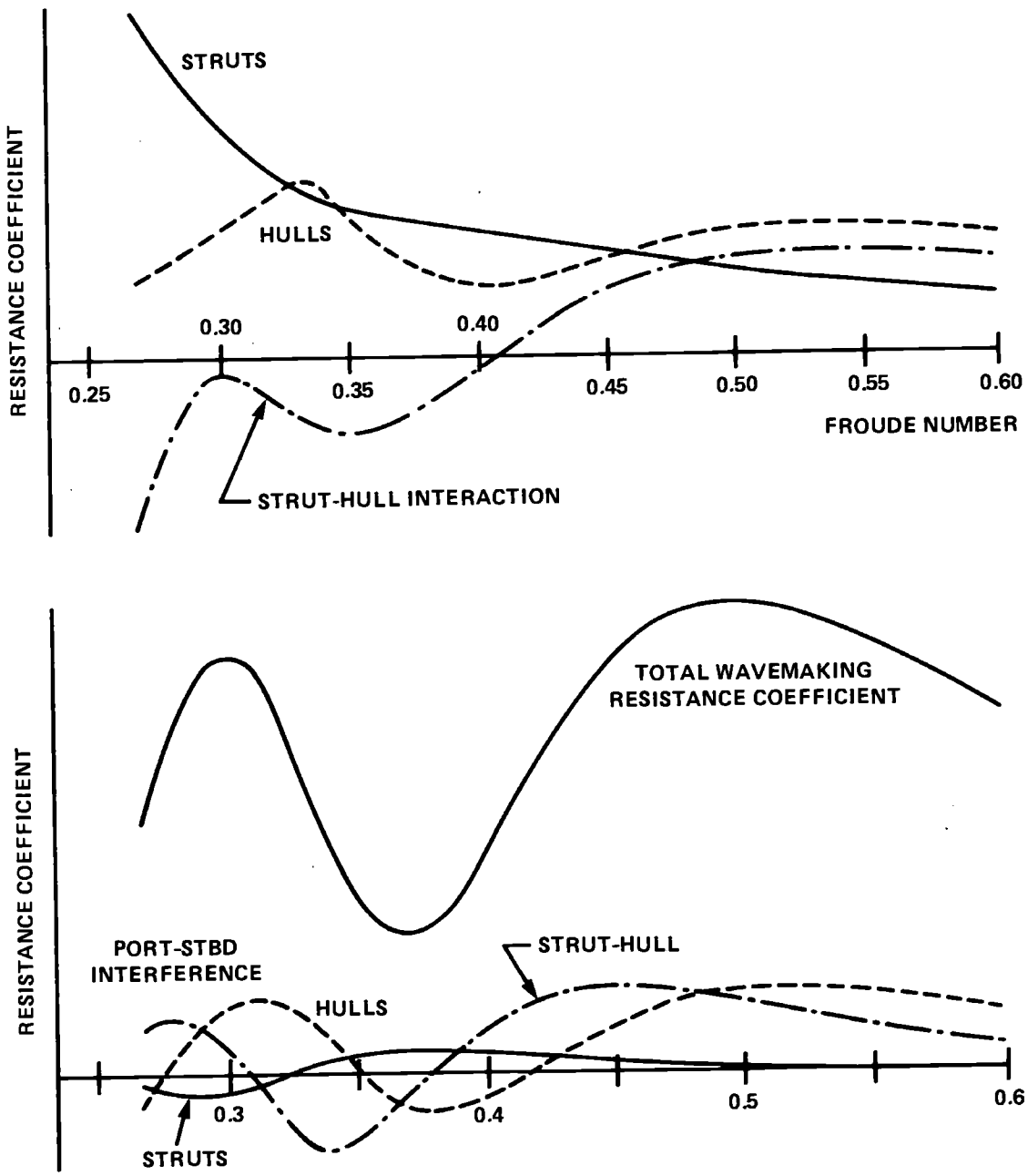

Figure 3.1.2 - Typical Wavemaking Resistance Coefficients versus Froude Number Single-Strut-per-Hull SWATH

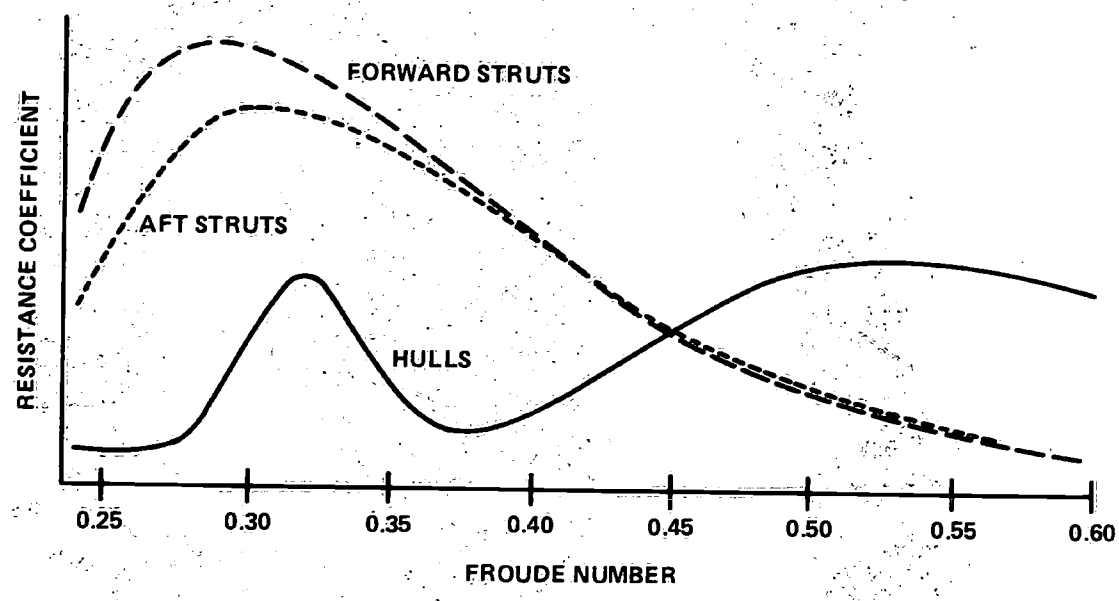

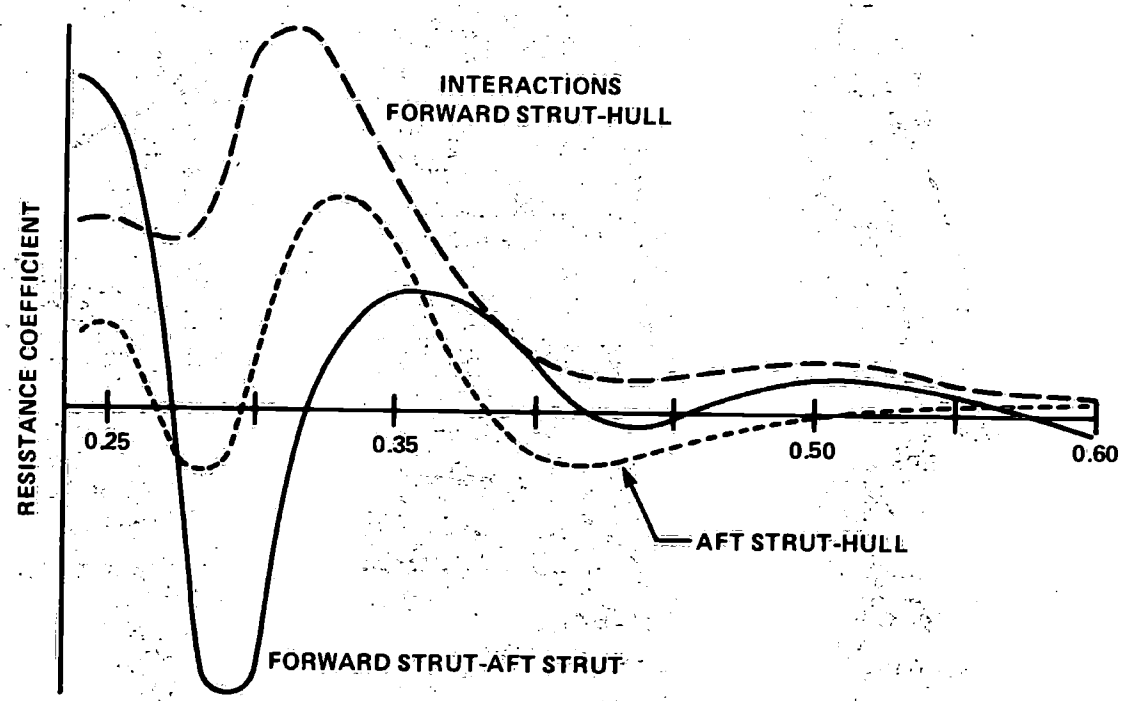

Figure 3.1.3 - Wavemaking Resistance Coefficients versus Froude Number Tandem Strut SWATH (From Reference 15)

3.2 SEMIDISPLACEMENT ROUND BILGE VESSELS

by

Burkhard Müller-Graf

Versuchsanstalt Für Wasserbau Und Schiffbau

3.2.1 CONCEPT DEFINITION

The semidisplacement or semiplaning round bilge vessel operates in a speed range of $0.5, \leq F_n < 1.3$. Its hull form is characterized by:

a. convex section shape
b. high deadrise

} in the forebody,

c. straight and fine entrance waterlines,
d. straight or slightly convex buttock lines in the afterbody rising towards the stern,
e. a center line skeg at the afterbody, and
f. a transom stern.

Rounded sections and convex buttock lines in the afterbody are common for speeds of $F_n < 0.8$; see Figure 3.2.1. For higher speeds straight buttock lines and nearly straight sections with a hard chine before the transom are preferred. To reduce the running trim, the hulls are often equipped with a trailing edge wedge.

The weight of the vessel is mainly supported by hydrostatic lift. Above $F_n = 0.7$ the hull experiences a hydrodynamic lift which increases with speed in the same way as the hydrostatic lift decreases. The rise of longitudinal center of gravity (LCG) above the position at rest indicates the beginning of a positive contribution of hydrodynamic lift. Figure 3.2.2 shows the change of trim and trim angles with speed. Round bilge hulls underway are characterized by the generation of the so-called whisker spray, which increases with speed, in particular above $F_n = 0.7$. Its development and extension are favored by the convexity of the sections and the curvature of the buttock lines in the forebody.

The wetted area varies with speed and with running trim. It can be reduced by means of spray rails or to a small extent by a shift of LCG abaft.

The change of wetted area of a typical round bilge hull without and with spray rails or with a wedge, respectively, is given in Figure 3.2.3.

3.2.1.2 Range of Hull Dimensions, Form Parameters, and Speed

The round bilge form is used for all types of pleasure craft, work boats, fast patrol craft, and small naval ships. Therefore, the main dimensions, the hull form parameters, and the operational speed cover a wide range:

Length (LWL)	6 - 100	m
Length-to-beam ratio	3.2 - 7.5	
Displacement	5 - 2000	tons
Length-Displacement ratio $L/\Delta^{1/3}$	4.4 - 8.3	
Speed	15 - 50	knots

3.2.2 RESISTANCE INVESTIGATIONS (SMOOTH WATER)

3.2.2.1 Resistance Components

The total resistance of a semiplaning round bilge vessel at speeds of $F_n > 0.5$ is the sum of the following components as shown in Figure 3.2.4.

Tank Condition

$$R_T = R_{WP} + R_S + R_P + R_V + R_{AP}$$

Trial Condition

$$R_T = R_{WP} + R_S + R_P + R_V + R_{AP} + R_{AA} + R_{paras} + \Delta R_{AW} + \Delta R_{ST}$$

3.2.2.1.1 The wavemaking resistance R_W, which can be determined on the basis of resistance tests solely, is composed of the first three components of R_T, i.e., of R_{WP}, R_S, and R_P.

3.2.2.1.1.1 The wavepattern resistance R_{WP} is produced by generating gravity waves.

3.2.2.1.1.2 Spray resistance R_S is a component associated with the expenditure of energy in generating the whisker spray. It appears also in the displacement speed range.

The spray resistance R_S consists of a pressure and a viscous drag component

$$R_S = R_{SP} + R_{SV}$$

with the relationships

$$R_S = R_{SP}\ (F_n) + R_{SV}\ (R_n, W_n)$$

where R_n = Reynolds number

W_n = Weber number

A useful method to calculate the pressure drag component is at present not available. This viscous or frictional component cannot be computed likewise, because:

a. The spray wetted area is not accurately definable by visual and photographical observations. This part of the hull is mostly hidden by the spray sheet.

b. The velocity in the spray and the turbulence condition in the boundary layer of the spray area are unknown. A correct specific frictional resistance coefficient cannot determined.

c. At the moment no useful correction method or allowance for the frictional drag is developed taking into account the deviation of the flow direction from the direction of speed.

3.2.2.1.1.3 Induced resistance R_P is given by the horizontal component of the hydrodynamic pressure forces and can be estimated, approximately, only in the case of hulls with straight buttock lines aft by:

$$R_P = \nabla \cdot \rho \cdot g \cdot \operatorname{tg}\tau \ [kN]$$

where ∇ = displacement volume, m^3

ρ = mass density of water, t/m^3

g = acceleration due to gravity, $m\ s^{-2}$

τ = angle of attack of the mean buttock aft, deg

3.2.2.1.2 Viscous resistance R_V, is composed of the frictional resistance R_F and the pressure resistance of viscous origin R_{PV}

$$R_V = R_F + R_{PV}$$

3.2.2.1.2.1 Frictional resistance R_F depends upon R_n and is calculated by

$$R_F = \frac{\rho}{2} S_{WS} \cdot V_S^2 (C_{FS}+C_A) \text{ [KN]}$$

for the full-scale vessel

where V_S = speed of ship, m/s

S_{WS} = wetted surface of the ship, m^2

In most cases, particularly in the design stage, the wetted surface at rest $S_{W(V=0)}$ without the immersed part of the transom is used. The effective wetted surface underway, S_{WE}, including the bottom area, spray area, and the area of side wetting can be determined on the basis of model tests solely by visual and photographical observations of the model.

The 1957-ITTC formulation is generally used for the frictional coefficients of the ship C_{FS}. The values of the Reynolds numbers are calculated on the static waterline length. The change of wetted length with speed, which amounts to 2 to 5 percent of L_{WL}, is considered to be negligible.

The model-ship correlation allowance factor C_A takes into account the resistance increment due to structural shell roughness (welds, waviness, paint roughness, fouling, etc.) and to a certain degree shortcomings of the correlation line.

The formula for C_A, developed and recommended by the ITTC-Performance-Committee[1] leads to impractical high values for small craft. For semidisplacement hulls, an allowance of $C_A = 0.00025$ is generally accepted as an average increment to C_F. For hulls operating in tropical waters, a value of $C_A = 0.0004$ is applied.

3.2.2.1.2.2 Pressure resistance of viscous orgin R_{PV} which includes all the energy losses due to separation and eddy formation, is considered to be negligible for $F_N > 0.7$. Also, a form factor

$$K = \frac{C_V - C_{FO}}{C_V}$$

cannot be applied in calculating the specific total viscous resistance coefficient

$$C_V = (1+K) \cdot C_{FO}$$

as in the case of slow displacement ships, because K depends upon F_n, because S_W varies with speed.

3.2.2.1.3 The appendage drag R_{AP} is the sum of profile drag, frictional drag, and interference drag of struts, strut barrels, propeller shafts, rudders, and stabilizer fins which can amount to 8 to 16 percent of the bare hull resistance. The calculation of these resistance components according to References 2, 3, and 4 results in more realistic full-scale data than the application of a percental allowance of the bare hull resistance.

The common practice to evaluate the appendage drag by means of resistance tests with and without appendages can lead to incorrect full-scale results if laminar flow effects at the model and the influence of cavitation and ventilation on the prototype are not taken into account when necessary.

3.2.2.1.4 Aerodynamic resistance R_{AA} is generated by the super-structures and the above water hull. It is calculated by

$$R_{AA} = \frac{\rho_A}{2} (V_S \pm V_{AA})^2 \cdot A_V \cdot C_{AA} \qquad [kN]$$

where $_A$ = mass density of air, kp/m^2

V_{AA} = velocity of wind relative to ground, m/s

A_V = frontal area of above water superstructure, m^2

C_{AA} = wind resistance coefficient

Special drag coefficients for high speed small craft have not been published. Values of $C_{AA} \approx 0.3$ to 1.0 depending upon the direction of wind relative to the hull are acceptable.

The equation does not take into account the wind and wave induced yawing resistance, the rudder resistance, and the resistance caused by wind induced waves.

3.2.2.1.5 Parasitic drag P_{Paras} is given as well by protruding inlet and outlet openings for cooling water, exhaust, etc. as by zinc anodes and is calculated according to Reference 2.

3.2.2.1.6 The added resistance due to rippling seas, R_{AW} arises from the diffraction of small incident waves at the lowest state of sea 0 to 1.

Because theoretical investigations or model studies concerning the resistance increase of round bilge hulls in small waves are lacking, an allowance of 2 to 3 percent of the naked hull resistance to the total resistance may be acceptable for vessels up to displacements of $\Delta = 500$ tons.

3.2.2.1.7 The added resistance due to coursekeeping, R_{ST} is caused by the induced rudder drag and the resistance due to yawing and swaying motions. These components

components can not be neglected at high speeds. Investigations of R_{ST} concerning fast craft are lacking.

In accordance with the work of Norrbin[5] an allowance of at least 2 percent of the appended hull resistance should be made in case of a twin rudder configuration. An increment of 2.5 percent can be adopted for practical purposes as an average value.

3.2.2.2 Resistance Prediction Techniques

3.2.2.2.1 Resistance Tests. The wavemaking resistance of round bilge hulls is not amenable to direct calculations. Model tests are the unique procedure to determine this resistance component.

3.2.2.2.1.1 Typical models. The model size is selected within the limits given by the tank boundaries and capabilities of the test facility as large as possible to minimize scale effects. To overcome shallow water effects, however, the model length should be smaller than 1.25 times the tank depth h, i.e., $h/L > 0.8$. To reduce tank wall effects, the model length should be smaller than one-half of the tank width.[6] The length of the models varies from 2.0 to 6.0 m; dimensions of 2.3 to 3.8 m are typical.

The models are built of laminated wood or of glass fiber reinforced plastic if the equipment requires a low hull weight. To facilitate the flow separation, the spray rails and hard chines are modeled separately in plastic and fitted to the hull. For determination of wetted area, the hull surface is marked by a net of waterlines and sectionlines. If at low speeds of $R_n < 5 \cdot 10^6$, the models are equipped with boundary layer turbulence stimulators. For round bilge hulls, studs of 2.5 mm diameter have been proven. They are located abaft the stem parallel to its contour terminating at the keel.

3.2.2.2.1.2 Typical smooth water test procedure. The resistance test procedure is very similar to that of displacement ships. The models are free to heave and pitch but fixed in roll, yaw, sway, and surge. The displacement is adjusted by fixed ballast inside of the hull. The LCG of the model is carefully controlled by balancing the fully equipped model in air. The towing force which is applied to the hull in the plane of the propeller shafts at or near LCG is kept in line with the propeller shafts at all running trim conditions. A typical towing set up is given in Figure 3.2.5. The following quantities are measured for a given displacement and LCG:

a. towing speed;

b. total resistance in the direction of towing velocity, i.e., the horizontal component of the towing force;

c. rise and sinkage of the model at fore perpendicular (FP), LCG, and aft perpendicular (AP).

d. trim angles relative to the position of the hull at rest and vertical shift of the LCG; and

e. wetted area of the model by means of above-water photographs from several locations and by visual observations. At $L/B < 5$ underwater photographs are also useful.

To determine the model appendage drag and to take into account the effects of altered trim on hull resistance due to the presence of the appendages, the models are tested without and with appendages. The appendage drag data are required for corrections of the friction deduction in calculating effective power and for corrections of the towing force in the self propulsion test. Tests with the bare hull solely are not usual at round bilge hulls because the influence of the appendage forces on running trim and resistance cannot be estimated theoretically. Therefore, the results of the bare hull tests are of limited value.

3.2.2.2.2 Extrapolation Procedures

3.2.2.2.2.1 General consideration. The results of the resistance tests are scaled up as in the case of displacement ships by the method of Froude. The hydrodynamic resistance of a full-scale bare round bilge hull at $F_n > 0.7$, which is composed of

$$R_{H,S} = R_{WP} + R_P + R_{F,S}$$

is calculated on the basis of the relation

$$R_{H,S} = R_R + R_{FS}$$

where the residuary resistance R_R includes the resistance components R_{WP}, R_S, and R_P. By the equations

$$R_{H,S} = (C_R + C_{FS} + C_A) \cdot \frac{\rho_S}{2} V_S^2 S_{W,S}$$

and

$$R_{H,S} = \left[\frac{R_R}{\Delta_M}\right] \Delta_S + (C_{FS}+C_A) \frac{\rho_S}{2} V_S^2 \cdot S_{W,S}$$

respectively,

where C_R = residuary resistance coefficient, defined by $C_R = C_{T,M} - C_{F,M}$ which is considered to be dependent on Froude number only

M = displacement weight of the model

S = displacement weight of the ship

3.2.2.2.2.2. Practical extrapolation procedures. The effective power P_E is calculated by applying the friction deduction F_{DAP} on the test results, which is given for the model with appendages by

$$F_{DAP} = C_{FM} - (C_{F,S}+C_A) \frac{\rho_M}{2} V_M^2 \cdot S_{W,M} + K \cdot R_{AP}$$

where $S_{W,M}$ = wetted surface of the model without the surface of the appendages

R_{AP} = model appendage drag, obtained as the difference between the model resistance with and without appendages at the same running trim

K = correction factor to compensate the scale effects of appendage drag. On the base of References 7 and 8 the value of K varies with R_n of the appendages from 0.4 to 0.6.

The effective power of the full-scale appended hull is computed by

$$P_E = \frac{\rho_S}{\rho_M} \cdot \lambda^{3.5} (R_{T,M \text{ with App.}} - F_{DAP}) \cdot V_M$$

where λ = scale ratio

3.2.2.2.2.3 Possible scale effects. The full-scale resistance of round bilge hulls, predicted on the basis of model test results is afflicted with scale effects which are involved with:

a. Skin friction resistance

Errors arise by the different R_n of model and full-scale vessel, by the used formulation of the skin friction coefficient and its incomplete consideration of form effects, by the influence of the unknown roughness of the model, by the chosen model

ship correlation factor accounting for the effect of full-scale hull roughness, and by the type of used turbulence stimulator and its resistance.

Further errors can arise by difference in wetted area (side wetting) due to surface tension effects, which can hinder the flow separation.

b. Spray drag

Due to the different Weber numbers W_n of model and full-scale size, the spray formation at the model is not similar to that of the vessel even at the same Froude number. The spray of the model consists of a coherent sheet of water instead of a jet of water droplets as occurring at the vessel. Thus the spray wetted area of the model is greater than that of the prototype. In addition, the reattachment of spray is facilitated.

If the spray wetted area is not taken into account in calculating the frictional resistance of the model, i.e., the wetted surface at rest $S_{W(V=0)}$ is used, the residuary resistance becomes overestimated and by this the total resistance of the prototype likewise.

Because the wetted area of the frictional resistance calculation includes the spray wetted area, the residuary resistance is underestimated. The resistance of the full-scale vessel becomes too small. More reliable predictions can be obtained by using the wetted area underway without the spray region. With the exception of a hull with spray rails, which has a comparatively small spray wetted area, spray drag must be carefully considered in each particular case.

c. Running trim

Due to the relatively larger components of the model frictional resistance and the model appendage drag and due to the different interactions between the appendages and the hull at the model and at the prototype, the running trim of the full-scale vessel can differ from that of the model. By this, errors in the wavemaking resistance R_W and additionally in the frictional resistance due to the change of wetted area, can arise. Moreover the hull resistance of the propelled full-scale vessel can be different from that of the towed model because of the propeller induced pressure field and the propeller shaft forces can alter the running trim.

d. Aerodynamic drag

The drag of the superstructure of the model if not towed behind a wind screen, the blockage effect between model and towing carriage, and the carriage interference effects on the ambient free surface can give rise to changes of attitude and running trim of the model with its consequences on the resistance components.

e. Blockage effects

The tank wall boundaries can cause a change of attitude and running trim of the model.

3.2.2.3 Test Procedures and Instrumentation Unique to Resistance Test of Semidisplacement Hulls

In general the test procedures and the instrumentation are similar to those used for conventional displacement ships. Following techniques are divergent:

a. The application of the towing force in line with the propeller shafts at all trim angles.

b. The use of a wind screen at high model speeds of $V > 6.0$ m/s to eliminate the aerodynamic drag of the model and its superstructure.

c. The determination of the wetted surface by means of underwater photographs in special cases.

3.2.2.4 Outstanding Problems in Prediction of Smooth Water Resistance

The usefulness of the performance prediction must be improved by a correct computation of the spray resistance. The spray phenomenon is not fully explored. Fundamental investigations are necessary relating to:

a. the frictional drag of the spray area,

b. the influence of Weber number on development and extent of spray, and

c. the direction of flow in the spray area.

Additionally, a more practicable method to determine the spray wetted area than by visual and photographical observations is imperative. Another problem is related to the blockage effect at $F_n > 0.4$ and its influence on attitude, trim, and resistance.

3.2.2.5 Recommendations to the 16th ITTC for Resistance Studies

3.2.2.5.1 Study the phenomena of spray.

3.2.2.5.2 Develop methods for calculating and extrapolating the spray drag.

3.2.2.5.3 Investigate the tank wall influence on trim and resistance of round bilge hulls at $F_n > 0.4$.

3.2.2.5.4 Examine the aerodynamic blockage and interference effects between the towing carriage and the ambient free water surface.

3.2.2.5.5 Examine the effect of the appendage forces on running trim and resistance of semidisplacement hulls.

3.2.3 SEAKEEPING INVESTIGATIONS

Because of the absence of adequate theoretical methods to predict the behavior of semidisplacement round bilge hulls in a seaway, seakeeping tests are still required. The model selection, test procedures, quantities measured, instrumentation and data processing and representation are identical to those of planing hulls as reported in the status of hydrodynamic technology of this vessel type (Section 3.3.3). The outstanding problems and the recommendations to the Seakeeping Committee are equal to those of the planing hulls.

3.2.4 MANEUVERABILITY INVESTIGATIONS

Investigations on the maneuverability of round bilge hulls are not usual in commercial test work. This type of vessel is characterized by a high directional stability at speeds of $F_n < 0.8$. Roll induced yaw moments do not occur at moderate speeds. The necessity to perform maneuvering experiments is therefore limited in most cases, to special designs and to low speeds. Experimental data of the maneuvering qualities of round bilge hulls are very rare.

3.2.4.1 Experimental Procedures, Data Collection and Presentation

The test procedures, which can be performed with free running or captive models; the definition of the quantities which identify the maneuvering characteristics of the hull; the data collection; and the presentation are identical to those of displacement ships and shall not be addressed here.

3.2.4.2 Outstanding Problems

At low speeds, the outstanding problems are similar to those of displacement ships. At high speeds, cavitation phenomena can occur at propeller shafts and struts in a turn. Interaction between the cavitating appendages and the hull can possibly influence the running trim of the craft.

Another problem of great interest concerns the course-keeping capabilities of round bilge hulls in quartering and following seas.

A further important problem of this type of vessel is the roll induced directional instability at very high speeds. Due to the decrease of the dynamic pressure in the region of the bilge, at $F_n > 0.8$, the craft indicate a tendency to heel. The unsymmetrical underwater hull in the heeled condition causes yawing moments which can lead to broaching. Fundamental research on the influence of the section curvature on the hull pressure distribution and stability losses is necessary.

3.2.4.3 Recommendation to the 16th ITTC for Maneuverability Studies

3.2.4.3.1 Collect model and full-scale maneuvering data of round bilge hulls.

3.2.4.3.2 Study and recommend suitable test procedures to predict the maneuverability characteristics of round bilge hulls.

3.2.4.3.3 Study the influence of cavitating appendages on running trim in a turn.

3.2.4.3.4 Investigate the pressure distribution in the bilge region at $F_n > 0.8$ and study its influence on the transverse stability underway of round bilge hulls.

3.2.5 PERFORMANCE INVESTIGATIONS

3.2.5.1 Types of Propulsors Used

The following types of propellers with fixed or controllable pitch are used for semiplaning hulls:

a. Subcavitating propellers on inclined shafts,

b. Supercavitating fully submerged propellers on inclined shafts.

c. Subcavitating propellers in tunnel stern, and in special cases,

d. Partially submerged propellers (in tunnel stern).

For all these propulsors, twin or multiple screw installations are common.

3.2.5.2 Forces on Self-Propelled Semidisplacement Round Bilge Hulls

The hull resistance of semidisplacement vessels is very sensitive to the running trim angle. In determining the power performance of this vessel type, all those hydrodynamic forces and moments which can affect the equilibrium condition have to be taken into account accurately.

For the self-propelled vessel, these forces include, besides the hull forces, the appendage and propeller forces. The hull forces are given by the wavemaking and viscous resistance, the buoyant lift, and the hydrodynamic lift. The appendage forces arise by the different drag components of the appendages, and by the lift of the appendage elements inclined to flow, mainly of the propeller shafts. The propeller forces include the shaft forces and the forces induced on the hull. The propeller shaft forces are caused by the shaft inclination and the oblique propeller inflow. They are composed of the horizontal and vertical thrust components T_X and T_Z respectively and of the upward directed propeller transverse force F_Y in the plane of the propeller. Moreover, thrust and torque are higher than in axial inflow at the same advance ratio. The propeller forces induced on the hull are generated by the pressure field of the propeller operating near the bottom. They result, in the case of subcavitating propellers, in a suction force upstream and in a pressure force downstream of the propeller. Depending upon the propeller load, the running trim increases approximately by 0.3 to 0.7 deg. The influence of cavitation on running trim

is not definable at present without tests in a vacuum tank or a large cavitation tunnel. Figure 3.3.7 of the status report of the hydrodynamic technology of the planing hull, which presents the appendage and propeller forces acting on the bottom of a planing hull, is also valid for semidisplacement vessels. Analytical methods to estimate these forces are given in Reference 3.

Because the center of application of the hull forces is not definable, as in the case of prismatic hull forms, the running trim of round bilge hulls is not amenable to theoretical calculations.

3.2.5.3 Self-Propulsion Test

The most reliable performance data of round bilge hulls are obtained on the basis of propulsion tests. These tests take into account all those forces and effects, as described above, which can influence the running trim and by this the power requirements. As well, the propulsive effect of the rudders as the effect of shaft inclination and trim angle on the propeller characteristic is accounted. Solely the development of cavitation which occurs at the prototype and which can have a considerable influence on the performance, cannot be simulated at propulsion tests in open towing basins, where Froude number and cavitation number cannot be realized simultaneously.

3.2.5.3.1 Model Selection. The model size depends mainly on the ratio of the full-scale propeller diameter to the available stock propeller diameter which should guarantee supercritical R_n at 0.7 R of the the blades. The model size is also affected by the weight of the propeller driving gear and the measurement devices. For this reason, the dimensions of models limited by tank boundaries, as described in Section 3.2.2.2.1.1 are mostly larger than required for resistance tests. They are made of glued timber, plywood, or glass reinforced plastic and fitted with appendages. Rudders and fins are often moveable for optimizing the neutral angle of attack at propulsion conditions. Turbulence stimulators at the models are required for $Re < 5. 10^{-6}$.

The diameter of model propellers varies from 0.12 m to 0.2 m, approximately. Due to the high propeller thrust loadings at high speeds, the propulsors are commonly made of brass or gun metal.

3.2.5.3.2 Test Procedure. The self-propulsion tests can be carried out at the ship propulsion point as common for displacement vessels only in the low speed range. For

higher speeds, overload and underload tests, respectively, are more suitable. At these tests the quantity of remaining towing force, which is applied as an external force on the model, is measured together with thrust, torque, rate of rotation, and rise and sinkage at FP and AP. These measurements allow calculation of the delivered power and the propeller revolutions for a range of altered propeller thrust loads. By this, different roughness allowances, altered displacement, and additional drag components for wind, steering, rough water, etc., which cannot be simulated at the model tests, can be taken into account. By means of a modified overload test, the delivered power under trial conditions can be determined directly. The rate of rotation of the model propellers is varied at a fixed speed to that value which yields a remaining towing force corresponding to the frictional deduction reduced by the scaled drag components of the trial condition.

3.2.5.4 Wake Measurements

Measurements of the wake distribution in the propeller plane are limited to special cases, where propeller induced vibrations due to the presence of the strut arms are assumed.

3.2.5.5 Open-Water Tests

The open-water tests are generally performed in the usual manner at axial inflow conditions, thus, at semidisplacement hulls, the propellers are mostly operating in oblique flow. Tests with varied shaft inclinations and cavitation tests are limited to special hull designs. Hence, the effective wake fraction, based on the axial flow open water test is used, in most cases, for designing the full-scale propeller.

3.2.5.6 Full-Scale Performance Estimates

The performance estimation is, in general, quite similar to the procedures used for conventional displacement ships. But unlike this type of vessel, the propulsive performance of semidisplacement hulls to some extent depends upon the effects of oblique propeller inflow and of cavitation phenomena which are intensified by the nonaxial propeller inflow conditions. Both effects must be accounted for carefully. Two methods of full-scale power prediction are common.

3.2.5.6.1 Performance Prediction Based on Propulsion Tests. This method is used mostly for the noncavitating speed range. The delivered power and the propeller revolutions are obtained by direct extrapolation of the measured model values. If the trial conditions are not taken into account at the propulsion tests, trial allowances must be applied on the tank values.

The mean inflow angle relative to the propeller shaft can be assumed to approach:

$$\psi = \delta + \theta \quad \text{(See Figure 3.2.6)}$$

where δ = angle of shaft inclination relative to the mean buttock

θ = trim angle underway

The effective inflow angle is small as reported in Reference 9. Depending upon the hull and shafting geometry, it does not increase proportional to running trim. For moderate nonaxial propeller inflow, the angle is less than six degrees. The propulsive coefficients can be analyzed in the conventional manner. The effective wake fraction W_T, based on thrust identity, is determined with axial flow open-water characteristics as

$$W_T = 1 - \frac{J_O}{\frac{V}{n} \cdot D}$$

The thrust deduction fraction is found with the axial thrust (which is assumed to be horizontal) as

$$t = 1 - \frac{R_T}{T_X}$$

At nonaxial inflow angles of $\psi > 6$ deg, realistic values of the propulsive coefficients can be obtained on the basis of inclined shaft open-water tests or by a correction of the propeller characteristics K_T and K_Q of the axial flow open-water test by a method proposed by Gutsche.[10] The correct values of

$$W_{T_\psi} = 1 - \frac{J_\psi}{\frac{V}{n} \cdot D}$$

which are very low can become negative with increasing inflow angle ψ. The propeller efficiency which is given by

$$\eta_{O_\psi} = \frac{K_{T\psi} \cdot \cos\psi - K_Y \sin\psi}{K_{Q\psi}} \cdot \frac{J_O}{2\pi}$$

where K_Y is the normal force coefficient, is commonly lower than in axial inflow. Correct values of the thrust deduction fraction t_ψ are obtained on the basis of the horizontal or net thrust force T_X as indicated in Figure 3.2.7 as

$$T_X = T_\psi \cos \psi - F \sin \psi$$

where F_Y is the propeller normal force. The calculation with the more convenient axial thrust T , which includes the resistance increment due to the horizontal propeller suction force and the difference between axial and horizontal thrust, leads to higher values of the thrust deduction fraction. The correct hull efficiency η_H is based on the inclined shaft wake fraction W_{T_ψ} and the corrected thrust deduction fraction t_ψ.

3.2.5.6.2 Performance Prediction Based on Resistance Tests. For partially and fully cavitating propellers, propulsion tests are limited to large cavitation tunnels or to vacuun tanks. Therefore, the performance estimates for these full-scale conditions must be derived in most cases from resistance tests and propeller open-water tests at full-scale cavitation numbers. The delivered power is determined by use of the propulsive coefficients:

$$\eta_D = \eta_o \cdot \eta_H \cdot \eta_R$$

where η_o propeller efficiency at full-scale cavitation number

η_H hull efficiency (1-t)/(1-w)

η_R relative rotative efficiency

in the common manner as follows

$$P_D = \frac{P_{EHull} + P_{E\ App} + \Sigma\Delta P_E}{\eta_D}$$

where $\Sigma\Delta P_E$ is the sum of the added effective power due to parasitic drag, aerodynamic drag, rough-water drag, and coursekeeping drag.

The thrust deduction factor t, the wake fraction w, and the relative rotative efficiency are determined from test results of similar hull designs. The reliability of the estimates is improved if the propeller cavitation tests take into account different shaft inclinations. Both components of the hull efficiency should be correct for an inflow angle which is assumed on the basis of test results of a similar vessel. The required propeller speed can be determined by means of K/J^2 and the thrust advance coefficient.

This performance prediction procedure is of limited accuracy. The majority of the moments arising by lift, drag, and propeller forces and which are contributing to the running trim are not taken into account. The different effects of the rudders, which can produce a drag or an additional thrust component, depending upon their position in or outside the propeller slip-stream and depending upon propeller loading and advance ratio as reported by References 11 and 12 are completely neglected.

3.2.5.6.3 Scale Effects. The predicted performance data are influenced by scale effects. Besides those described in Section 3.2.2.2.2.3 for the hull, the propulsor itself and its interactions with the hull are subjected to viscous effects. Differences in the velocity and pressure distribution depending upon R_n but likewise on the development of cavitation on the propeller can result in altered trim conditions with all its effects on hull resistance. The cavitation phenomena are highly afflicted with genuine scale effects and test technique effects. Propeller efficiency, and hull and relative rotative efficiency, which are strongly dependent upon propeller cavitation, are also exposed to scale effects.

3.2.5.6.4 Correlation of Model and Full-Scale Results. For noncavitating conditions, the correlation between predicted power based on propulsion tests and full-scale performance is sufficiently good. Correlation factors for propeller rotational speed as given in References 13 and 14 are useful. For partially and fully cavitating propellers, the thrust and efficiency losses of the prototype are greater than predicted from cavitation tunnel tests. The differences between model and ship propeller performance become smaller if cavitation is fully developed. Correlation factors for delivered power and propeller speed, taking into account the cavitation condition, are not available for round bilge hulls. Some information about the influence of cavitation on the propulsive characteristics of planing hulls, as given in Reference 15 are also useful for semidisplacement hulls.

3.2.5.7 Outstanding Problems in Performance Investigations

3.2.5.7.1 Effects of propeller induced forces on running trim for partially and fully cavitated flow

3.2.5.7.2 Scale effects of propeller forces and propeller induced forces in axial and nonaxial flow

3.2.5.7.3 Useful analytical power prediction method for the cavitation range based on resistance or propulsion test results

3.2.5.7.4 Effect of highly loaded propellers on rudder drag and rudder thrust of high speed vessels

3.2.5.8 Recommendations to the 16th ITTC for Propulsion Studies

3.2.5.8.1 Collect all available full-scale performance data of semidisplacement hulls at speed $F_n > 0.5$

3.2.5.8.2 Investigate the effects of cavitation and shaft inclination on the propeller hull interactions and the propulsive coefficients

3.2.5.8.3 Develop a method for estimating the net rudder force of high speed round bilge hulls

3.2.5.8.4 Develop a useful power prediction method based on the resistance or propulsion test data for cavitating propellers

3.2.6 PROPULSOR INVESTIGATIONS

3.2.6.1 Propulsor Problems Unique to High Speed Semidisplacement Hulls

Typical propulsor problems are discussed in Section 3.2.5.1. Propulsor problems which are unique to semidisplacement hulls do not exist at present. The main problems of interest arising also at other vessel types are:

3.2.6.1.1 Propeller characteristics for oblique inflow at $\psi > 6$ deg and for noncavitating and cavitating conditions

3.2.6.1.2 Propeller induced forces on hull, shafting, and struts at fully or partially cavitating conditions

3.2.6.1.3 Propeller characteristics of partially emerged propulsors in a tunnel stern

3.2.6.2 Recommendations to 16th ITTC for Propulsor Studies

No special recommendations to the propulsor committee are necessary at present. The problems of interest in Section 3.2.6.1 are a matter of permanent research work.

3.2.7 CAVITATION INVESTIGATIONS

The cavitation problems at the propellers of high speed semiplaning hulls are not very different from those arising at the other vessel types. A special problem of interest is the effect of oblique propeller inflow on cavitation and its inception at inflow angles $\psi > 6$ deg. No special recommendations to the cavitation committee, which is concerned with the problems of high speed propulsors, are necessary.

3.2.8 PRESENTATION AND INFORMATION

The list of the ITTC Standard Symbols does not include special terms and symbols which are used for the ship geometry, resistance components, and performance of semi-displacement hulls. The ITTC Standard Symbols and the ITTC Dictionary of Ship Hydrodynamics should be supplemented by these symbols and terms in accordance with those which are applied to the field of planing hulls.

3.2.9 REFERENCES

1. "Report of Performance Committee," 15th International Towing Tank Conference Proceedings, Part I, Wageningen, The Netherlands (1978).

2. Hoerner, S.F., "Fluid Dynamic Drag," published by the author, USA (1965).

3. Hadler, J.B., "The Prediction of Power Performance on Planing Craft," Trans. Soc. Naval Arch. and Marine Eng., Vol. 74 (1966).

4. Kirkman, K.L. and J.W. Kloetzli, "Scaling Problems of Model Appendages," 19th American Towing Tank Conference, University of Michigan, Ann Arbor, Michigan (Jul 1980).

5. Norrbin, N.H., "On the Added Resistance due to Steering on a Straight Course," Appendix 8, Performance Committee Report to the 13th International Towing Tank Conference, Berlin - Hamburg (Sep 1972).

6. Schuster, S., "Untersuchungen über Strömungs- und Widerstandsverhältnisse bei Fahrt von Schiffen in beschranktem Wasser," Jahrbuch der Schiffbautechnischen Gesellschaft, Bd 46 (1952).

7. Clement, E.P., "Scale Effect on the Drag of a Typical Set of Planing Boat Appendages," David Taylor Model Basin Report 1165 (Aug 1957).

8. Müller-Graf, B., "Bestimmung des Widerstandes von Motorbootsanhängen," Versuchsanstalt fur Wasserbau und Schiffbau, VWS-Bericht 205/61, Berlin (1961)

9. Rutgersson, O., "Cavitation on High Speed Propellers in Oblique Flow. Influence of Propeller Design and Interaction with Ship Hull," 13th Symposium on Naval Hydrodynamics, Tokyo (1980).

10. Gutsche, F., "Untersuchung von Schiffsschrauben in schräger Anströmung," Schiffbauforschung 3 (3/4 Mar 1964).

11. Suhrbier, R., "An Experimental Investigation on the Propulsive Effect of a Rudder in a Slipstream," International Shipbuilding Progress, Vol. 21, No. 234, pp. 31-39 (Feb 1974).

12. Rutgersson, O., "On the Importance of Rudder and Hull Influences at Cavitation Tests of High Speed Propellers," Conference Papers of High Speed Surface Craft Exhibition and Conference, Kalerghi Publication (1980).

13. Bailey, D., "The NPL High Speed Round Bilge Displacement Hull Series," The Royal Institution of Naval Arch., Maritime Technology Monograph (1976).

14. Rader, P., "Die Bedeutung des Nachstroms für die Wechselwirkung zwischen Schiffsrumpf und Propeller," Institut fur Schiffbau der Universität Hamburg, II. Fortbildungskurs (Oct 1976).

15. Blount, D.L. and D.W. Hankley, "Full-Scale Trial and Analysis of High Performance Planing Craft Data," SNAME, Vol. 84 (1976).

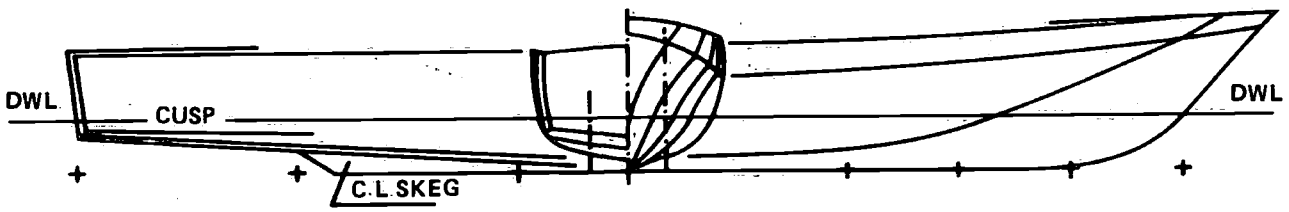

Figure 3.2.1 - Typical Body Plan of a Round-Bilge Hull

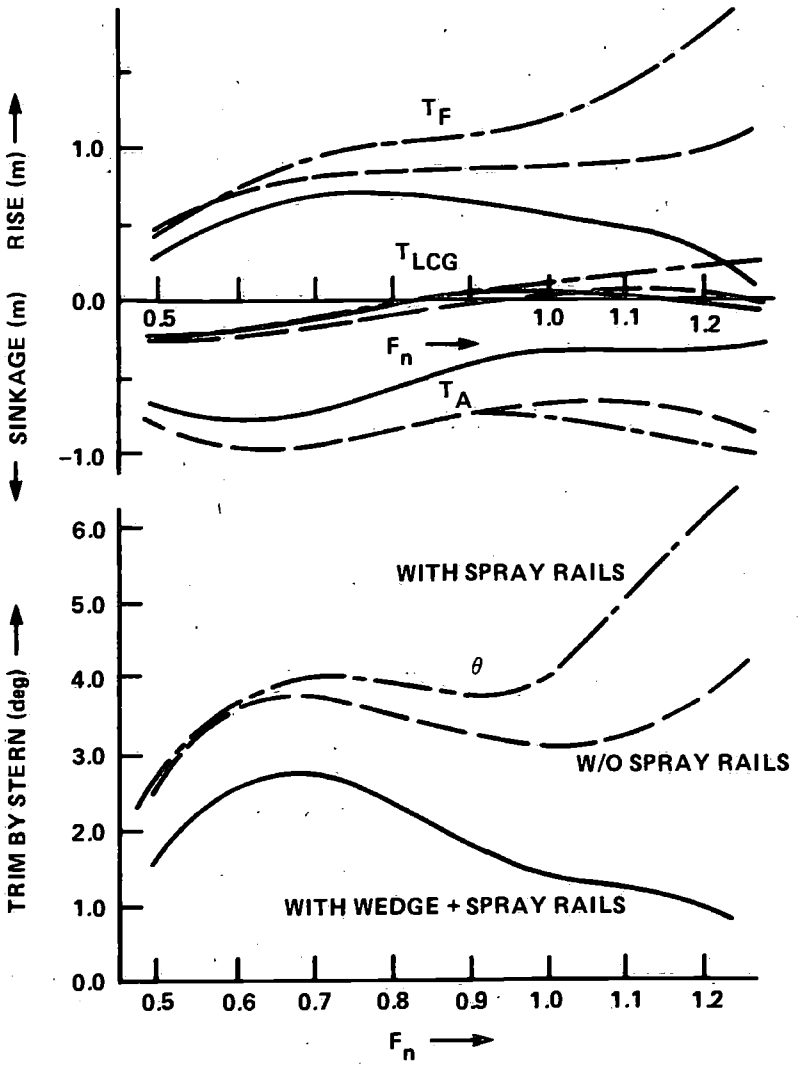

Figure 3.2.2 - Trim Variations

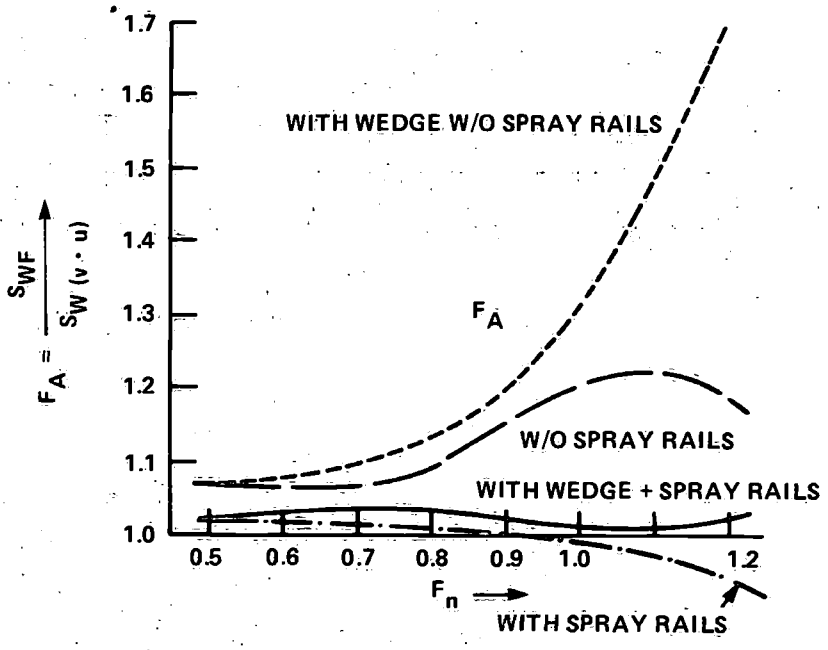

Figure 3.2.3 - Change of Wetted Area

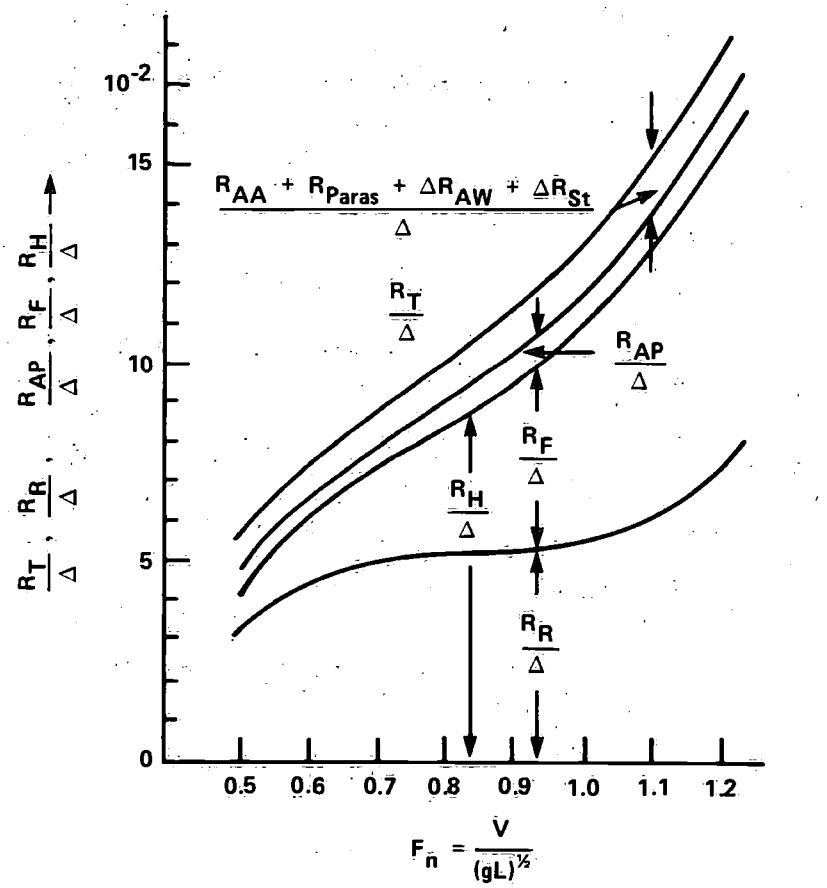

Figure 3.2.4 - Drag-Weight Ratios of Full-Scale Round-Bilge Hull

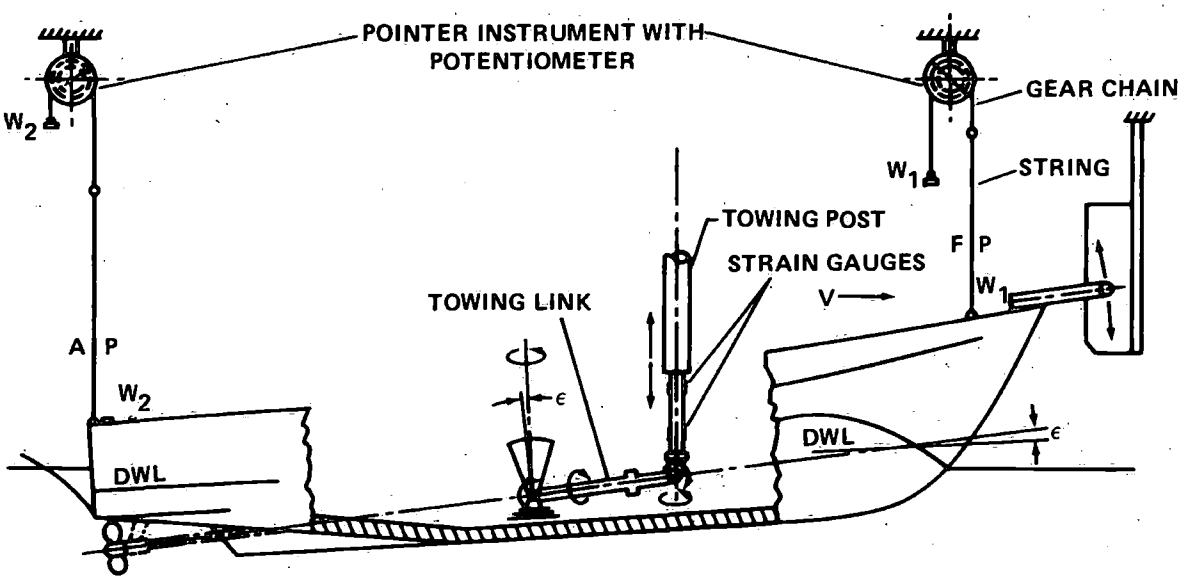

Figure 3.2.5 - Towing Setup for Resistance Tests

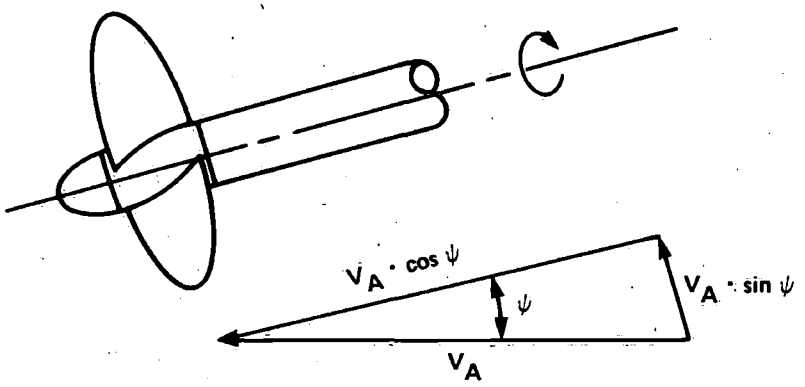

$$\psi = \delta + \theta$$

Figure 3.2.6 - Velocities at Propeller in Oblique Flow

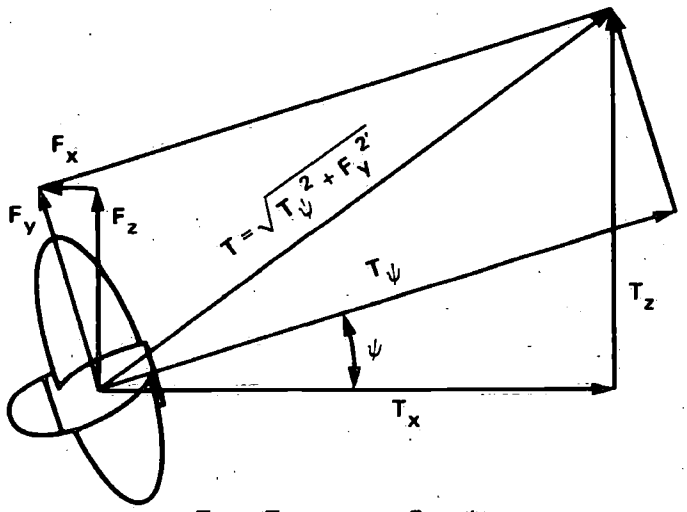

$$T_x = T_\psi \cdot \cos\psi - F_y \cdot \sin\psi$$

$$T_z = T_\psi \cdot \sin\psi + F_y \cdot \cos\psi$$

Figure 3.2.7 - Forces at Propeller in Oblique Flow

3.3 PLANING HULLS

by
Daniel Savitsky

Stevens Institute of Technology
Davidson Laboratory

3.3.1 CONCEPT DEFINITION

3.3.1.1. Configuration

The planing hull is designed for operation in the speed range $F_n > 1.0$. The hull form is characterized by:

a. Sharp chines and transom stern to induce flow separation at the stern and along the sides;

b. Straight buttock lines, especially the avoidance of convex sections aft of the bow area, to prevent development of negative dynamic bottom pressures;

c. Bottom deadrise, increasing rapidly in the bow area, to reduce impact loads in waves and to provide lateral area for maneuvering; and

d. Fine entrance waterlines to reduce low speed resistance.

Typical high-speed planing hull geometry is shown in Figure 3.3.1.

When the planing hull is driven beyond the displacement ship speed range ($F_n>1.0$), it develops positive hydrodynamic bottom pressures. As the hydrodynamic lift increases with increasing speed, the amount of hydrostatic lift decreases accordingly. Figure 3.3.2 shows the relation between hydrostatic and hydrodynamic lift components versus F_n for a typical planing hull, and indicates the approximate speed coefficient at which the center-of-gravity initially rises. In the planing condition, the flow separates from the transom and chines, and the drag-to-lift ratio is essentially constant for a given trim angle.

Figure 3.3.3 illustrates typical flow patterns over the wetted bottom area when planing. The stagnation line separates the pressure area from the forward, so-called "whisker-spray" area. The geometry and extent of these wetted regions vary with speed, deadrise, and trim angle. Underwater photographs of planing surfaces clearly identify the pressure area which is used to normalize the frictional drag component. The spray area does not appear in underwater photographs, but can be estimated from overwater visual observations.[1]

Figure 3.3.4 contains plots of typical variations of resistance-to-weight ratio and trim as a function of Froude number for various hull length-to-beam ratios. It is apparent that, especially for low length-to-beam ratios, the trim angle variations are substantial. Although not shown, the wetted bottom area also varies with speed. In the planing speed range, there is no side wetting for moderate to low length-to-beam ratio hulls. There is some aft side wetting due to flow reattachment for moderate to high length-to-beam ratio hulls. The extent of this side wetting is a function of trim angle, speed, and length-to-beam ratio.[2]

3.3.1.2 Range of Geometric And Operational Variables

The planing hull form is extensively used for military patrol craft, crew boats, recreational craft, high-speed ferries, and racing craft. The following range of geometric and operational parameters are typical for existing and projected planing hull designs:

Length (LOA)	4 - 60 m
Length-to-Beam Ratio	3 - 7
Displacement	5 - 600 long tons
Speed	20 - 60 knots

3.3.2 RESISTANCE INVESTIGATIONS (SMOOTH WATER)

3.3.2.1 Resistance Components

The total resistance of a hard chine planing hull is the sum of the following components:

$$R_T = R_{WF} + R_{WB} + R_P + R_S + R_V + R_{AP} + R_{AA}$$

where R_{WF} = wavemaking resistance

R_{WB} = wavebreaking resistance

R_P = pressure or induced drag

R_S = spray resistance in whisker spray area; essentially a viscous drag component which is presently taken to be dependent upon Reynolds number. (Not developed in the displacement speed range.[1])

R_V = viscous resistance in pressure area. Dependent upon Reynolds number.[1]

R_{AP} = appendage resistance, including struts, shafts, rudders, water scoops, interference drag, etc.[3]

R_{AA} = aerodynamic drag. Dependent upon frontal area of superstructure and fineness of bow. In model tests, the superstructure is usually omitted.[4]

In the preplaning speed range, the spray resistance is negligible and the remaining components of resistance are identical to those for displacement ships with their usual dependence upon Froude number and Reynolds number.

For a planing prismatic hull with straight buttock lines aft, the following simple relationship exists when planing:

$$R_{WF} + R_{WB} + R_P = \Delta \tan \tau$$

where Δ = displacement

τ = trim angle

so that the hydrodynamic resistance R_H of an unappended prismatic hull operating in the planing condition is:

$$R_H = \underbrace{\Delta \tan \tau}_{\text{pressure drag}} + \underbrace{R_V + R_S}_{\text{viscous drag}}$$

Figure 3.3.5 identifies the distribution between viscous drag and pressure drag for various trim angles as a function of deadrise angle. For each deadrise surface, there is a specific trim angle at which the drag is a minimum. In the usual planing hull tests, the sum of viscous and spray drag is called total viscous drag.

3.3.2.2. Resistance Prediction Techniques

3.3.2.2.1 Typical Model. Unappended models which vary in length from 1 m to 5 m are used for effective horsepower (EHP) tests. The scale is selected such that (a) the hump speed is less than the critical speed of the tank and (b) because the same model will most likely also be used in seakeeping tests, the model scale should allow for simulation of the full-scale sea state within the wavemaking capabilities of the test facility.

Models are usually constructed of wood or glass reinforced plastic (GRP) with a strip of thin mylar plastic attached to the vertical edges of the chine and extending approximately 1/32-in. below the chine in order to promote separation. Also, the transom is slightly recessed to promote flow separation at the stern. Lucite models can be used providing the chines and transom are sharpened to promote flow separation. Every effort would be made to avoid extraneous convex surfaces in the model because at high test speeds, they will develop significant negative pressures.

For deep water testing, it is believed that there are minimal wall effects if the tank width is at least seven times the model beam. It is strongly recommended that appropriate studies be undertaken to identify the effect of tank boundaries over the entire speed range of planing hulls.

3.3.2.2.2 Typical Smooth Water Test Procedure. The EHP tests are typically conducted with the unappended model free-to-trim and heave, but fixed in roll, yaw, sway, and surge. The model is ballasted with various combinations of fixed ballast weights inside the hull to enable easy simulation of the various loading conditions (normally three displacements and three longitudinal centers of gravity (LCG)) required by the designer. A pivot box, from which the model is towed, is installed in the model so that the tow point corresponds with the shaft line, usually in the midship vicinity. Provision is made to unload the model for the vertical component of thrust in order to assure that the resultant "simulated" tow force acts along the shaft line. Unloading tables are usually generated in advance so as to expedite the test program. For combinations of large trim angles and shaft angles, the unloading correction can be significant.

Because the drag of planing hulls is sensitive to running trim angle, consideration should be given to the pitching moments created by the lift and drag of the appendages and by the induced propeller forces and moments. Analytical estimates of these effects can be made using the procedures of Reference 3. If these induced forces and moments appear to have an important influence on trim angle, then their effect on hull drag can be accounted for by interpolating within the bare hull drag data obtained for the range of loadings and LCG positions originally specified. For routine commercial tests of planing hulls, the usual procedure is to only represent the propeller thrust along the shaft line.

It is recommended that further research be directed to quantifying the effects of propeller and appendages on planing hull performance. Reference 5 presents a

further discussion of this subject and suggests a model test procedure for representing these effects.

Boundary layer turbulence simulation is required in the planing regime when the Reynolds number (based on mean wetted length) is less than 5×10^6. Because of variable wetted areas, some test facilities tow turbulence-inducing struts ahead of and along the model centerline. The effectiveness of 0.040-in. diameter strut is demonstrated in Reference 6 and Figure 3.3.6 which is taken from that reference. Other facilities use turbulence stimulators, such as studs, mounted at various longitudinal locations along the bottom. The usual Reynolds number for model appendages is so small that turbulence stimulation is not likely; hence, appendages are not included on the model and their full-scale drag is best calculated.[4]

The chine and keel lines are striped to indicate distance from transom. From underwater photographs, the wetted length of the keel (L_K) and chine (L_C) are determined and used to define:

$$\text{Wetted Pressure Area} = \left(\frac{L_K + L_C}{2}\right) b$$

$$\text{Mean Wetted Length} = \left(\frac{L_K + L_C}{2}\right)$$

$$\text{Reynolds Number} = \left(\frac{L_K + L_C}{2}\right) \frac{V}{\nu}$$

where V = model speed

ν = kinematic viscosity

b = beam

all in appropriately consistent units.

In a typical model test, the sum of the viscous drag in the spray and pressure areas is normalized on the basis of the wetted pressure area.

For a given displacement and LCG, the quantities measured during an EHP test include:

a. Total resistance in direction of towing velocity,

b. Trim angle of hull relative to base line,

c. Vertical position of center-of-gravity relative to static location for the entire speed range.

d. Towing speed.

e. Wetted pressure area from underwater photography,

f. Whisker spray area from visual observations (optional), and

g. Photograph of model underway.

3.3.2.2.3 Extrapolation Procedures. The bare hull resistance data are extrapolated for full-scale values in accordance with the Froude hypothesis. Estimates of the appendage forces and aerodynamic forces are then added to the hull drag.

$$C_{TS} = (C_{TM} - C_{FM}) + C_{FS}$$

where C_{TS} = total resistance coefficient of unappended full-scale hull

C_{TM} = total resistance coefficient of unappended model hull

C_{FM} = viscous friction coefficient of model using ATTC Schoenherr or ITT friction line

C_{FS} = viscous friction coefficient of full-scale hull

All coefficients are normalized on the basis of wetted area exclusive of spray area. A suitable correlation allowance C_A is selected in collaboration with the client. It is usual, however, to take C_A=0 because the bottom surface of planing hulls are generally quite smooth.

The use of the flat plate friction lines is somewhat questionable because, as shown in Figure 3.3.3, there is a large accelerated flow in the pressure area just aft of the stagnation line. Research studies should investigate this matter. Equally important is the development of a basic understanding of the frictional drag in the "whisker-spray" area.

Several limited geoseim tests of planing hulls have been inconclusive as related to uncertain "scale-effects" on running trim angle and viscous drag. A basic, thorough geoseim test program is recommended.

3.3.2.3 Procedures, Instrumentation, Tests, etc., Unique to Resistance Tests of Planing Hulls

Except for the special considerations mentioned in Section 3.3.2.2., the procedures, instrumentation, and test procedures are similar to those used for conventional displacement ships.

3.3.2.4 Outstanding Problems in Prediction of Smooth Water Resistance

The application of the flat plate skin friction line to planing surfaces should be examined in view of the large accelerating flows aft of the stagnation line. The frictional drag in the whisker spray region should be examined and properly formulated in terms of Reynolds number, Weber number, and extent and direction of spray velocity. Reexamination of methods for stimulating turbulence in the boundary layer is required for model Reynolds numbers less than 5×10^6. The effect of tank boundary conditions on planing hull resistance should be defined.

3.3.2.5 Recommendations for Resistance Studies to the 16th ITTC

3.3.2.5.1 Examine and recommend methods for turbulence stimulation in boundary layers subjected to large accelerated flows.

3.3.2.5.2 Examine the applicability of flat plate frictional coefficients to the large accelerated flows on planing surfaces.

3.3.2.5.3 Examine and recommend methods for estimating spray drag and extrapolating to full-scale values.

3.3.2.5.4 Examine and recommend methods for separate expansion of appendage drag. Especially consider the advisability of including appendages in EHP model tests.

3.3.2.5.5 Document carriage interference effects on ambient free surface conditions.

3.3.2.5.6 Review and investigate all available information on wall and shallow water effects for $F_n > 0.3$.

3.3.2.5.7 Examine effects of appendages and propeller-induced effects on running trim and performance of planing hulls.

3.3.3 SEAKEEPING INVESTIGATIONS

At the present time, there is no completely developed theoretical method for computing accelerations and motions of hard-chine planing hulls in irregular seas--especially in the planing speed region. References 7 and 8 describe the most recent theoretical efforts in this regard and indicate fairly good agreement with measured motions. The predicted accelerations, however, indicate that further theoretical developments are necessary. Hence, model tests are essential. Because planing hull responses are nonlinear, the superposition procedures are not applicable so that meaningful tests can only be made in irregular seas.

3.3.3.1 Model Selection

The model scale used for seakeeping tests is usually identical to that used in the previously described EHP tests. Of special concern is that the model size be suitable to allow for proper simulation of the desired sea state within the wave-making capabilities of the test tank. Further, the model should not be so small as to prevent simultaneous scaling of the mass and moments of inertia when the necessary test apparatus and instrumentation are installed.

The test model is fully appended with proper location of the deck house, breakwaters, etc., to evaluate the probability of superstructure impact and spray wetting resulting from waves breaking over the bow.

The model is attached to the towing carriage by suitable pivots located at the center of gravity. Provision is made within the model to relocate the pivot box as necessary in order to represent various CG locations. The model deck area is made watertight to avoid shipping water. The moments of inertia are obtained from free-oscillation of the model when suspended from a knife edge and considering the system to be a compound pendulum. Standard formulations are used to translate these results into values of radius of gyration.

3.3.3.2 Typical Model Tests

Planing hull tests in head or following seas are usually accomplished by constraining an unpowered model in surge, yaw, roll, and sway and running at constant speed. Reference 9 demonstrates that constant speed tests in head seas produce essentially the same motions, oscillations, and added resistance as the more complex, free-to-surge tests where the model is towed with constant thrust. Constant speed tests in waves increase the tank productivity and expedite data analysis when performance analysis is to be made at selected speeds. It is recommended that all towing tank facilities relate their experience in comparing fixed and free-to-surge test results.

Planing hull seakeeping test objectives and procedures are basically similar to the displacement ship except for the following differences:

a. Because of high model test speeds, there are fewer numbers of wave encounters in a given tank length so that repeat runs are necessary in different sections of the irregular wave system to obtain at least 100 wave encounters. The data from the separate runs are "pieced" together and statistically analyzed as one continuous run.

b. High-speed tests in oblique seas are usually not attainable because of the low speed and dimensional limitations of existing maneuvering tank facilities. Low-speed tests, however, can be carried out to a limited extent using small model lengths.

c. In the planing speed range, hull slamming is very common and special consideration must be given to assure proper frequency response of installed accelerometers.

d. Simulation of surf zone operation is necessary for occasional tests of planing hull landing craft.

Although most tests are conducted in irregular seas, regular waves are occasionally used for basic studies such as examining the extent of linearity, etc.

3.3.3.3 Quantities Measured During Tests

The quantities measured during seakeeping tests depend upon the clients' needs, but usually include:

a. Speed of model,

b. Total resistance,

c. Accelerations at the CG, bow and stern,

d. Trim angle,

e. Heave motion, usually of CG,

f. Relative bow motion,

g. Wave height, at stationary point in tank,

h. Closed-circuit television and/or movie coverage of model behavior,

i. Roll motions; and

j. Natural periods and damping ratios in heave, pitch, and roll at zero speed.

3.3.3.4 Instrumentation Used in Wave Tests

The wave profile in the test section is usually measured by a stationary wave probe of resistance, capacitance, or ultrasonic type. Moving wave probes have been somewhat inconsistent--perhaps due to spray generation or other uncertain effects, mainly at high towing speeds.

The accelerometers must measure (a) wave-induced hull motion accelerations where the maximum frequency can be estimated from the energy content of the spectrum in the frequency of encounter domain and (b) hull-wave impact accelerations which are of substantially higher frequency. In either case, the accelerometers that are selected should have a damping constant equal to 70 percent critical (to obtain a linear output to as large a frequency as possible) and a natural frequency at least 2.5 times

greater than the expected frequency of a hull-wave impact. Some guidance in this regard is the following empirical solution for the maximum frequency component (in hertz) of the hull wave impact acceleration for typical planing hulls:

$$f_{impact} = \frac{9\left(\eta_{1/10}\right)^{1/2}}{\Delta^{1/6}}, \text{ Hz}$$

where Δ = craft displacement, metric tons

$\eta_{1/10}$ = 1/10 highest CG acceleration, g (see Reference 2)

This formula is still to be verified and, thus, it is recommended that all towing tanks compare their methods for selecting accelerometers and perhaps agree on one procedure.

The intent in model testing is to measure the rigid body accelerations; hence, the model construction should be as stiff as possible. Even so, it will be found that all models do have an elastic response of their own and steps must be taken to prevent the model's structural response from contaminating the acceleration record. This contamination, apart from affecting the magnitude of the acceleration (magnification factor) will affect the statistical measures by causing extraneous vibrations. A system of low-pass filtering is used to compensate for and isolate the structural vibration of the model (first mode). It is recommended that the cut-off frequency of this filter be, at most, one-half the model frequency and also be larger than the expected impact acceleration frequency. Because this filtering affects the phase of the response, identical filters must be applied to all relevant data channels, i.e., wave elevation, and heave and pitch motions, wherever relative phase informations is required. It is recommended that existing towing tanks compare methods for isolating the structural vibrations. This is of particular importance if the frequency content of the impact acceleration contains the first mode structural vibration frequency of the model.

Selection of the drag balance capacity requires the calculation of the maximum anticipated drag load in calm water, using either series data or the standard prediction equations. A balance should then be chosen having a capacity equal to twice the maximum calm water drag. This will allow an adequate margin for the balance to expand linearly to wave-induced loads and for noise-induced in the balance by the towing system. This assumes that the measurement required is the average drag in

waves. Time histories of the drag force require that the dynamic response of the balance be given consideration somewhat in the manner of an accelerometer.

The problem in measuring heave and pitch motions is one of gearing down the large motion displacements to a displacement transducer. Although similar considerations apply to displacement ship model tests, the motions are relatively larger for planing hull models. Care must be taken that the gearing and transducer do not impede the motion of the model and yet follow the motion under dynamic conditions, e.g., must be free of backlash. This is not a simple problem because the reduction ratio can be on the order of 500 to 1.

3.3.3.5 Test Wave Environment

Most planing hull model tests are conducted in irregular head and/or following seas over a wide speed range. The sea spectra used vary with the tank facility and clients' desires, but are usually the deep water spectra defined by the ITTC, the ISSC, or the Pierson-Moskowitz formulation which are reproduced as unidirectional waves. Because most planing craft operate in coastal waters, a finite depth spectrum would be more suitable if a representative formulation can be agreed upon. It is recommended that consideration be given to the Jonswap and Darbyshire spectra.

To provide some guidance as to the sea states of interest, a 100-ft long high-speed planing hull should have operational capability in a state of sea having a significant wave height of at least 5 ft and a survival capability, at low speed, in a significant wave height of at least 10 to 12 ft. Because these sea states are considerably smaller than used in displacement ship tests, wavemakers in existing tanks may experience difficulty in producing good quality wave forms as required by the usual small size planing model.

3.3.3.6 Data Collection and Processing

Data collection and processing are highly computerized in most existing tank facilities. Usually both analog and digital signals are simultaneously recorded. The analog signal is used for diagnostic purposes (if digital outputs appear to be suspicious) and the digital data, which are usually obtained at a scanning rate of 250 Hz, is used to develop the statistics of the model behavior.

It is important that the data-scanning system ignore extraneous noise or carriage vibration signals, or else the statistical representation of results will be seriously distorted. To avoid this problem buffers are installed which will ignore these small voltage inputs. The buffer size is selected by running the model at the same speed in calm water and finding the average 1/3-highest peak and trough for each

acceleration and motion channel. The algebraic difference of these values is selected as the size of the buffer.

For most development tests, data are processed on-line so that results are available tankside immediately after the run. The following data are typically presented:

Weight of model

Speed

Average drag

Significant wave height

Number of wave encounters for pitch, heave, and accelerations:

Mean values

rms

Number of oscillations

Average 1/3, 1/10; extremes of maxima and minima

Television coverage on tape cassette

Properly time-scaled movies

Continued emphasis is currently being placed on interpretation of the seakeeping results--expecially relative to habitability. For this purpose, the vertical acceleration data are also presented as a plot of RMS in 1/3-octave bands and, for intermediate frequencies $\geq$ 1 Hz, are compared with the International Standards Organization standard for fatigue-decreased proficiency. The criteria for lower frequencies is that of von Gierke for motion sickness incidence.

The 1/10-highest vertical accelerations are usually the basis for structural design.

3.3.3.7 Data Presentation

The tankside computer outputs described in Section 3.3.3.6 may constitute the data section of the final test report. These results are plotted as required to complement the discussion, analysis, and recommendation sections of the final report.

Motion and acceleration transfer functions are not calculated from the energy spectra of the motions and encountered waves because of the nonlinear behavior of planing craft in irregular seas.

3.3.3.8 Extrapolation of Model Results to Prototype

The extrapolation of model test results to prototype values is based on Froude's scaling laws and is basically similar to that in displacement ship technology.

3.3.3.9 Correlation of Model Test Results

At the present time, there are only limited model, full-scale comparisons of planing hull seakeeping characteristics. Reference 10 shows that, if proper adjustments are made to account for differences in model-prototype state of sea, mean trim angle, displacement, etc., then the model accelerations are just slightly larger than full-scale values. Differences between model and full-scale elasticity, method of mounting the accelerations, and methods of data processing do influence the comparisons and should be further investigated.

It is essential that more seakeeping data be collected for correlation purposes. All tank superintendants are urged to contribute comparative results whenever possible.

3.3.3.10 Outstanding Problems in Rough Water Model Tests

Operation in oblique seas is an important operational mode and yet only a very limited number of test facilities are available to represent this condition and these are restricted to medium speeds using small models. Self-propelled, rudder-controlled, model tests have been employed in oblique sea tests.

Present methods for recording wave profile using a wave probe moving at high speed are unsatisfactory.

The effect of model elasticity in influencing the accelerations in the model is yet to be properly established.

Acceptable wave spectra for water of finite depth are lacking.

The degree of motion, resistance, and acceleration linearity in a seaway should be identified in a parametric fashion.

3.3.3.11 Recommendations for Seakeeping Studies to 16th ITTC

3.3.3.11.1 Investigate the extent of linearity as applied to hard-chine, high-speed planing hulls in irregular seas.

3.3.3.11.2 Recommend sea spectra for finite water depth.

3.3.3.11.3 Collect and correlate model, analytical, and full-scale seakeeping data.

3.3.3.11.4 Provide guidance for the selection of appropriate accelerometer characteristics and the location in the model to properly account for model elasticity and acceleration frequency in order to obtain "rigid-body" impact accelerations.

3.3.3.11.5 Establish the model test procedure for performance evaluations in following seas.

3.3.3.11.6 Establish a distribution function for the relation between the statistics of impact accelerations.

3.3.3.11.7 Establish the relation between natural damping characteristics, Froude number, and Reynolds number.

3.3.4 MANEUVERABILITY INVESTIGATIONS

Maneuverability investigations of high-speed planing hulls are not routinely undertaken in towing tanks. Occasionally there are requests for such evaluations, but these are limited to simple tests which will identify the turning diameter and/or the dynamic directional stability index for a specific design. At the moment, there is no complete set of six-degree-of-freedom equations of motions and accompanying definitions of the various coupled and uncoupled hydrodynamic coefficients required to simulate the maneuvering characteristics of hard-chine planing hulls. The amount of experimental data available relative to maneuvering and control of planing craft is very limited and fragmentary. Results of elemental dynamic tests are almost nonexistent.

3.3.4.1 Quantities Which Have a Major Influence on Maneuvering Characteristics

3.3.4.1.1 Basic Hull Form. It is important to understand that the hydrodynamic forces and moments on the hull are highly nonlinear, and are strongly dependent upon wetted hull geometry, trim angle, roll angle, yaw angle, wetted length, and Froude number--all of which vary significantly during a maneuver. Further, there is evidence of strong yaw-roll coupling which is dependent upon trim angle and speed. While there may be some success in analytical or semiempirical representations of the static stability derivatives, there has been no demonstrated success in the prediction of the dynamic (damping and added mass) derivatives.

Model details, especially chine and keel sharpness, may have a significant effect upon all hydrodynamic coefficients when planing asymmetrically. For instance, a hard-chine boat will experience a slight increase in roll moment with roll angle at high speed, whereas a round-bilge hull, which does not provide for flow separation at the chine, may actually demonstrate a decrease in roll moment with roll angle.

3.3.4.1.2 Appendages. These are typified by large propeller shaft angles, shaft support struts, and either bottom-mounted or stern-mounted surface-piercing rudders. At high planing speeds, these appendages will likely experience some degree of cavitation and ventilation in a turn and seriously upset any predictions based on the

assumption of fully wetted flows. Hull interaction with these cavitated appendages can also influence the equilibrium of the craft.

3.3.4.1.3 Propulsion System. The large horsepowers presently being installed in small planing craft can impose large propeller-induced torques which provide a roll bias to the craft. Transom-mounted trim-flaps can correct for this when deflected asymmetrically and should be included in any analytical or model simulation.

Because of the possibility of combined large hull trim angles and shaft angles, the propeller will develop a laterally displaced (relative to the shaft line) thrust which, particularly in small craft, can introduce large steering torques on the craft. The magnitude of this effect is dependent upon whether the propeller is fully wetted or cavitated and should be considered in any simulation of maneuvering. Further, the hydrodynamic moments on the strut of outdrive units are strongly influenced by the Munk moment developed by the conical fairing ahead of the propeller and should be accounted for.

The majority of the hydrodynamic effects described above have not been quantified, especially for ventilated and cavitated flows.

3.3.4.2 Experimental Procedures

Three basic test methods can be used in exploratory studies of planing craft maneuvering. They are:

a. Captive model tests on rotating arm and straight course
b. Captive model tests on planar-motion mechanisms
c. Radio-controlled free-running models

The rotating arm tests provide data useful for predicting directional stability and turning circles, but do not provide trim, roll and heave damping, and added mass terms. A planar-motion mechanism can provide these quantities, but contains a frequency dependence which must still be identified. The radio-controlled model does not provide basic hydrodynamic data. All three methods are deficient in not representing the cavitation effects on propellers, rudders, skegs, support struts, etc.

It must be concluded that the development of model test procedures or analytical methods for simulation of maneuvering of planing craft has been severely neglected.

3.3.4.3 Data Collection and Presentation

Reference 11 presents an example of a limited test program using straight-course tests and rotating-arm tests to define the coursekeeping stability and turning performance of a hard-chine planing hull. It is not known whether similar studies have been made using a planar motion mechanism.

The procedure is to mount, on the rotating arm or straight-course apparatus, an appended model which is free-to-heave and pitch, but restrained at fixed values of yaw and roll and locked in surge and sway. The drag, side force, yaw moment, and roll moment are measured at various speeds, turning radii, and rudder deflection.

For dynamic course stability (neglecting yaw-roll coupling), the data for zero roll are plotted as a function of yaw angle and radius for each test speed and, from these, values of N_v, N_r, Y_v, and Y_r are obtained. The course stability is found from linear differential equations of motion using these hydrodynamic derivatives and introducing appendage and propulsor effects which have not been included in the test model.

The equilibrium turning diameter, roll angle, and rudder deflection at each test speed is found by solving the simultaneous equations of yaw, roll, and side force equilibrium, including the estimated propeller and appendage effects which have not been included in the test model.

The uncertainty in both procedures stems from the omission of unknown cavitation, ventilation, and interference effects.

3.3.4.4 Extrapolation of Model Results to Prototype

The usual Froude scaling relations are used.

3.3.4.5 Correlation of Model Test Results with Full-Scale

Comparisons of model and prototype results are extemely limited because of the scarcity of model predictions. Those few comparisons that have been made indicate the directional stability predictions have been confirmed, but that the prototype turning radius is slightly larger than predicted, probably due to partial cavitation of the full-scale appendages and rudders.

3.3.4.6 Outstanding Problems

The major problems concerning the predictability of the maneuvering characteristics of the hard-chine, high-speed planing hull are:

a. Lack of developed six-degree-of-freedom equations of motion for self-propelled, controlled, high-speed, hard-chine hull forms;

b. Scarcity of basic hydrodynamic data on hull forms, appendages, propulsors, and their interactions in ventilated and cavitated conditions;

c. Lack of development of suitable experimental and/or combined analytical and experimental methods for predicting maneuvering characteristics; and

d. Dearth of full-scale data and even fewer attempts at model-to-full-scale correlations.

3.3.4.7 Recommendations for Maneuverability Studies to 16th ITTC

In view of its present undeveloped state of technology, it is recommended that a basic study of all aspects of planing hull maneuverability be undertaken and recommendations be made for suitable model test procedures to predict these characteristics.

3.3.5 PERFORMANCE (SHP) INVESTIGATIONS

3.3.5.1 Types of Propulsors Used

Nearly every form of propulsor has been used to propel planing hulls. These include:

a. Subcavitating propellers on inclined shafts;
b. Subcavitating propellers in tunnel sterns;
c. Subcavitating propellers on outdrive and outboard units;
d. Fully cavitated propellers installed as in (a),(b), and (c) above;
e. Surface-piercing propellers;
f. Supercavitating propellers;
g. Waterjets; and
h. Single- and multiscrew installations.

3.3.5.2 Equilibrium Condition of Self-Propelled Planing Hull

As described in section 3.3.2.2, the forces that contribute to the equilibruim running trim and total drag of a self-propelled planing hull include the hydrodynamic lift and drag of the hull, the hydrodynamic lift and drag of the appendages, and the propeller forces--both direct and induced. These effects have a substantially larger influence on the performance of planing hulls than in the case of displacement ships.

Figure 3.3.7 shows the forces present on a planing hull with submerged propellers on waterline shafts. This figure, taken from Reference 3, shows separately the forces on the hull, the appendage forces, and the propeller forces.

3.3.5.2.1 Hull Forces. The lift and drag forces on the hull, together with the location of their lines of action and dependence upon hull geometry, speed, and loading are given in Reference 1.

3.3.5.2.2 Appendage Forces. For the case of planing hulls, appendage lift, as well as drag, must be considered. Reference 3 presents numerical methods for predicting these forces for typical elements of planing craft appendages, including inclined propeller shafts, struts, strut bossing, strut palms, interference drag, rudders (ventilated and fully wetted), etc. Many of these appendage shapes are unique to

planing craft and are not considered in the case of typical displacement ships. On a model scale, the Reynolds numbers of these appendages are usually so small that turbulence stimulation in their boundary layers is unlikely.

3.3.5.2.3 Propeller Shaft Forces. Propellers on planing hulls are typically mounted on inclined shafts, resulting in a sinusoidal variation in tangential velocity which is a function of angular position of each propeller blade. The effect of this inclination is to result in (a) higher total thrust and torque than for the same advance ratio in axial flow, and (b) an upward vertical force in the plane of the propeller. Reference 3 presents analytical methods for estimating these forces.

3.3.5.2.4 Propeller Forces Induced on Hull. The effect of the propeller operating near the bottom of a planing hull is to induce small pressures acting over large areas of the bottom. These induced propeller forces result in a net suction force forward of the propeller and a positive pressure force aft of the propeller. The total effect is to tend to increase the hull trim angle. Again, Reference 3 provides analytical methods for estimating these forces.

3.3.5.2.5 Propeller-Induced Drag on Rudder. When located in the propeller slipstream the rudder experiences (a) an axial flow greater than the free-stream velocity, and (b) a normal component of velocity due to the rotational component of flow in the propeller wash. As a result, the rudder profile drag is increased by the increased flow velocity and an induced drag results from the "effective angle of attack" of the rudder relative to the resultant incident velocity. Reference 3 provides a method for estimating the propeller-induced drag.

The lines of action of all the above forces is pictorially shown in Figure 3.3.7. It is seen that each appendage has a direct drag contribution and, through their effect on the pitching moment, influence the equilibrium trim and, hence, the hull drag which is a major component of the total resistance. The EHP tests with unappended models only account for the unloading effect of the propeller thrust along the shaft line (Section 3.3.2.2). Full-scale predictions for the propelled planing craft must account for the appendage and propulsion effects described previously.

3.3.5.3 Self-Propulsion Tests

Model tests to determine shaft horsepower (SHP) are made with fully appended, self-propelled models--even though it is recognized that turbulence stimulation of the appendages may not be adequate and the model propellers may not represent the cavitation expected to be experienced by the full-scale craft. This procedure is

accepted because of the inherent limitations of atmospheric pressure towing tanks and economic considerations for limiting the size of the test model.

Resistance tests are first performed on a fully appended model without the propulsor in order to provide baseline data useful to develop the propulsive coefficients. The self-propelled tests are then conducted to obtain the effective wake fraction, relative rotative efficiency and the thrust deduction coefficients. These results are used to design the full-scale propeller and predict delivered horsepower requirements. Although the procedure appears to be acceptable for noncavitated flows, there are uncertainties, yet to be resolved, when appendages and/or prototype propellers are cavitated because conventional towing tanks cannot simulate simultaneously Froude number and cavitation number.

The self-propelled tests are usually carried out for overload and underload conditions where a group of test runs are carried out at fixed speed and various rates of propeller rotation. During these tests, a tow force is applied which corresponds to a difference between model and ship specific resistances (assuming incomplete turbulence stimulation over the appendages). This type of test provides information which may be applied for any desired assumptions concerning roughness allowance, scale ratio, air drag, rough-water drag increment, etc.

It is unusual for wake surveys to be taken with planing hulls so that the full-scale propeller design is adapted to the mean wake as determined from the wake fraction.

Open-water tests of the model propellers are usually made at zero incidence to the flow and at fully wetted conditions. Thus, the propulsive coefficients include the effect of flow incidence due to shaft inclination and propeller-induced effects on the model trim angle.

Although other propulsor types (waterjets, tunnel propellers, partially submerged propellers, etc.) have been used on planing craft, self-propelled model tests using these devices are so limited that it is premature to discuss the results and procedures.

3.3.5.4 Measurements of Full-Scale Performance

As stated in Reference 10, speed-power prediction for planing craft has little documented correlation evidence to indicate the magnitude or type, or even if a correlation allowance is required.

There is some doubt in assuming that the measured model propulsive coefficients apply directly to full-scale, as all factors are liable to scale effect and, with the

invariable existence of full-scale propeller cavitation at high spped, there is an undefined complex interaction between propulsion system, appendages, and hull.

Relatively few planing craft designs have been supported by model propulsion tests in the design stage due to economics and a lack of understanding of how the results must be interpreted to be applicable. These limitations have resulted in most speed-power predictions being made using bare hull resistance tests (EHP) and making appropriate engineering allowances for appendages, propulsors, and interference effects. A suggested computerized procedure for using bare hull resistance data to estimate SHP while fully accounting for the appendage and propeller effects is given in Reference 5. It is recommended that this and similar methods be evaluated.

Because of the relatively low cost of planing hull propellers, it is not unusual, in the case of a cavitated propeller, to provide a second propeller design based on the full-scale experience of the initial design, particularly if full-scale torque and RPM are measured.

3.3.5.5 Correlation of Model and Prototype Results

For noncavitating propellers, correlation between predicted (using bare hull EHP results and estimates of appendage drag and propulsive coefficients offered by Reference 4) and full-scale performance has been good. For cavitated flows, the correlations have not been good. However, recent procedures developed in Reference 10 do provide correlation factors for operation at low cavitation numbers. These are based on limited data and should be expanded as more full-scale results become available.

3.3.5.6 Outstanding Problems

It is important to identify the scale effects on hull form, appendage and propulsor forces and moments because the equilibrium condition of a planing hull depends upon a balance of all forces and moments. Should there be scale effects on any or all of these forces and their centers of application, then full-scale and model trim and rise will be at variance.

Further, it is important that direct and indirect ventilation and cavitation effects be identified. In this regard, there is a need for characterizing cavitated and partially cavitated propellers in inclined flows in proximity of a free water surface and a rigid surface representative of hull bottoms.

Finally, a reliable experimental and analytical method needs to be established for speed-power predictions.

3.3.5.7 Recommendations for Propulsion Studies to 16th ITTC

3.3.5.7.1 Identify scale effects in noncavitated self-propulsion tests.

3.3.5.7.2 Identify the effect of cavitation on the propeller-hull interaction.

3.3.5.7.3 Identify characteristics of the cavitated propeller in inclined flows.

3.3.5.7.4 Investigate methods for obtaining powering predictions of water-jet propelled craft.

3.3.5.7.5 Examine the following predictive techniques and recommend an acceptable test method:

a. Self-propelled model;

b. Towed, bare-hull model combined with analytical estimates of appendage and propulsor forces; and

c. Analytical model.

3.3.6 PROPULSOR INVESTIGATIONS

3.3.6.1 Typical Propulsors

Section 3.3.5.1 provides information regarding typical propulsors.

3.3.6.2 Propulsor Problems Unique to Planing Craft

There is a general lack of performance characteristics of the following:

a. Cavitated and noncavitated propellers in inclined flow near a free surface or near a rigid plate typical of hull bottoms;

b. Tunnel-stern propeller systems;

c. Effect of aeration over the hull bottom on the performance of various propulsors;

d. Propeller-induced vibratory forces on the hull bottom, especially with cavitated propellers; and

e. Effect of air ingestion on performance of water jets.

3.3.6.3 Recommendations on Propulsor Studies to 16th ITTC

Essentially to recommend a study of problems described in section 3.3.6.2.

3.3.7 CAVITATION INVESTIGATION

The current studies of the Cavitation Committee include areas of major interest to the designer of planing hulls and this work should be continued in cooperation with the activities of a High-Speed Marine Vehicles Committee.

3.3.8 PRESENTATION AND INFORMATION

It is recommended that inquiries be made of the various technical societies, towing tanks, etc., as to their use of particular symbols, coefficients, etc., which have been accepted and used by each of these groups in their evaluations of planing hulls and then to incorporate these symbols, etc., into the Standard Symbols and ITTC Dictionary of Ship Hydrodynamics.

3.3.9 REFERENCES

1. Savitsky, D., "Hydrodynamic Design of Planing Hulls," Marine Technology, Vol. 1, No. 1 (Oct 1964).

2. Savitsky, D. and P.W. Brown, "Procedures for Hydrodynamic Evaluation of Planing Hulls in Smooth and Rough Water," Marine Technology, Vol. 13, No. 4 (Oct 1976).

3. Hadler, J.B., "The Prediction of Power Performance on Planing Craft," Transactions Society of Naval Architects and Marine Engineers, Vol. 74 (1966).

4. Blount, D. and D.L. Fox, "Small Craft Power Prediction," SNAME, Marine Technology, Vol. 14 (Jan 1976).

5. Kirkman, K.L. and J.W. Kloetzli, "Scaling Problems of Model Appendages," 19th ATTC, University of Michigan, Ann Arbor, Michigan (Jul 1980).

6. Savitsky, D. and E. Ross, "Turbulence Stimulation in the Boundary Layer of Planing Surfaces," Davidson Laboratory, Stevens Institute of Technology, Report 444 (Aug 1952).

7. Zarnick, E.E., "A Non-Linear Mathematical Model of Motions of a Planing Boat in Regular Waves," David W. Taylor Naval Ship Research and Development Center Report 78/032 (Mar 1978).

8. Zarnick, E.E., "A Non-Linear Mathematical Model of Motions of a Planing Boat in Irregular Waves," David W. Taylor Naval Ship Research and Development Center Report SPD-0867-01 (Sep 1979).

9. Fridsma, G., "A Systematic Study of the Rough-Water Performance of Planing Hulls, Irregular Waves, Part II," Davidson Laboratory, Stevens Institute of Technology Report 1495 (Mar 1971).

10. Blount, D.L. and D.W. Hankley, "Full-Scale Trials and Analysis of High Performance Planing Craft Data," SNAME Transactions, Vol. 84 (1976).

11. Savitsky, D. et al., "Hydrodynamic Development of a High-Speed Planing Hull for Rough Water," Ninth ONR Symposium on Naval Hydrodynamics (Aug 1972).

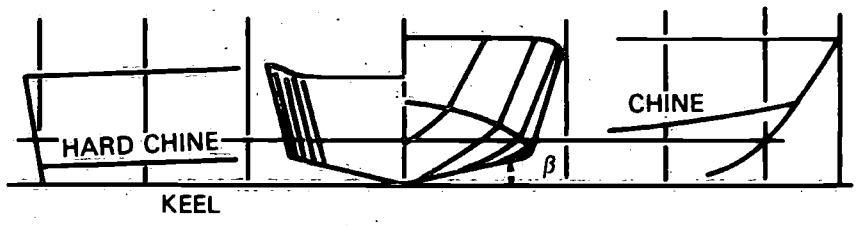

Figure 3.3.1 - Typical High Speed Planing Hull Geometry (Series 62)

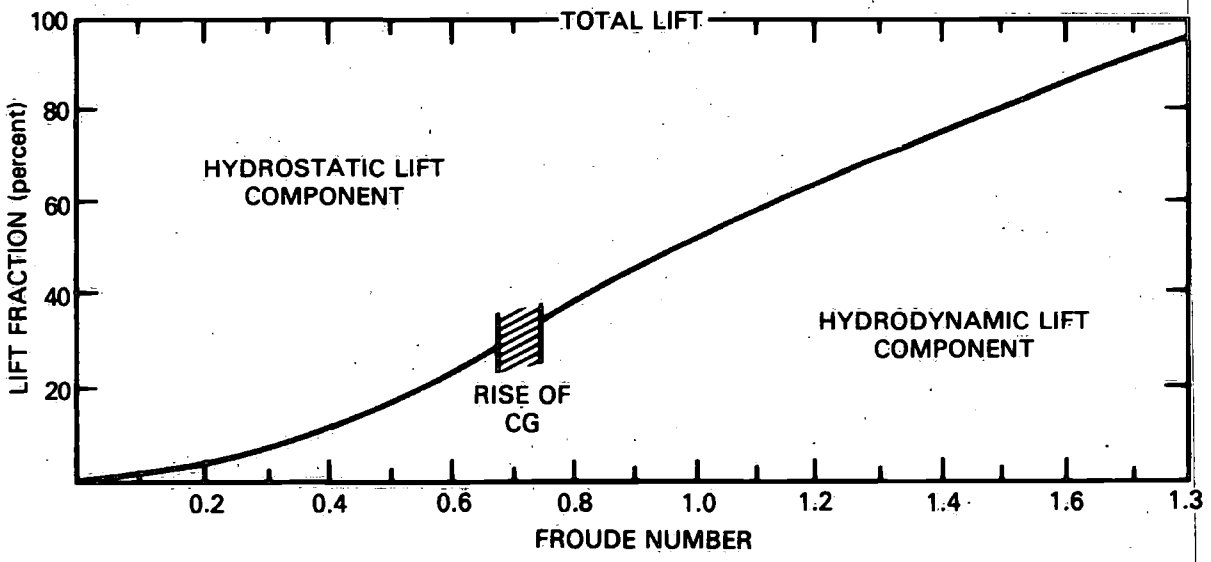

Figure 3.3.2 - Distribution of Hydrostatic and Hydrodynamic Lift

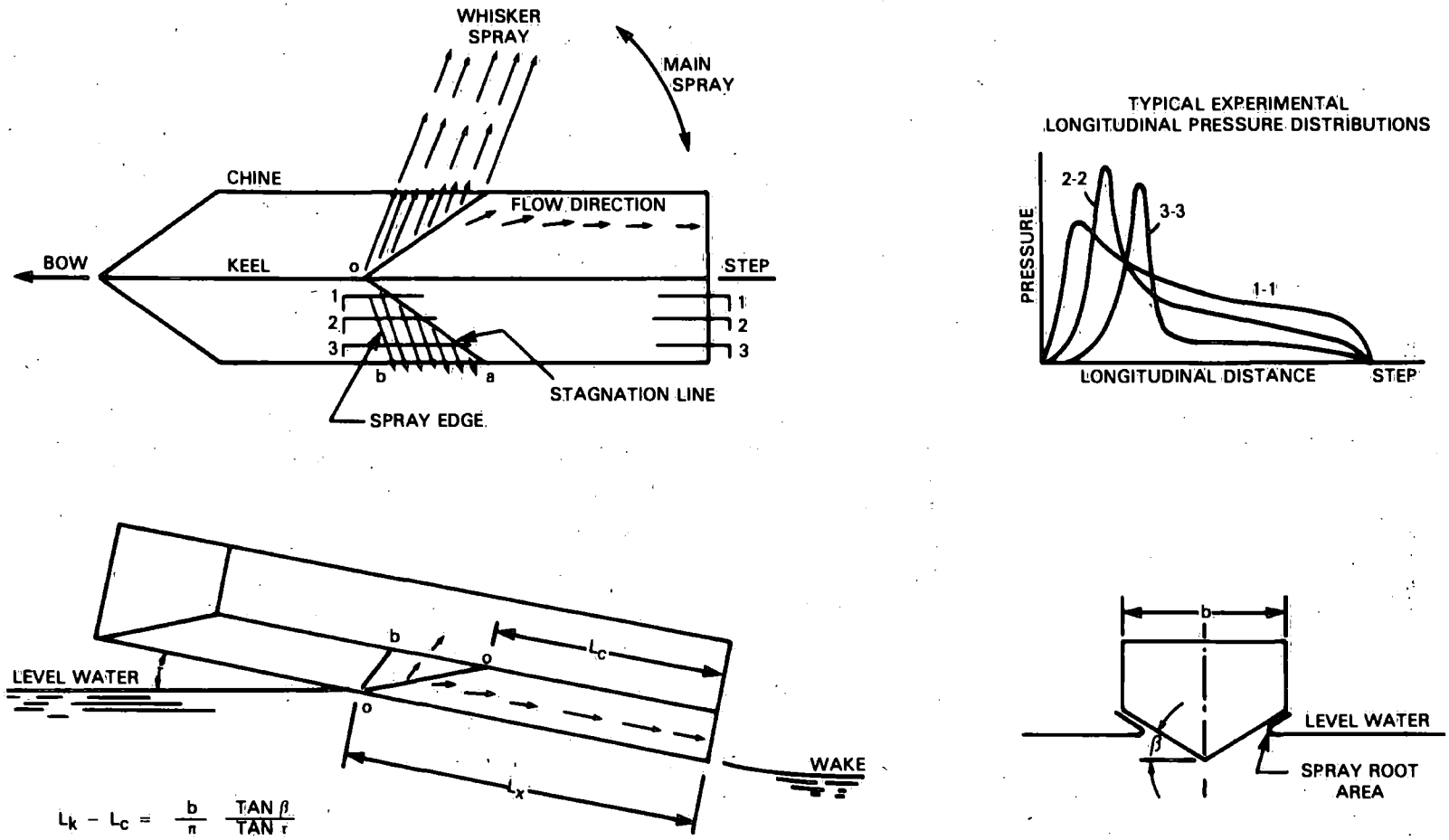

Figure 3.3.3 - Flow Phenomena Associated With Planing Surfaces

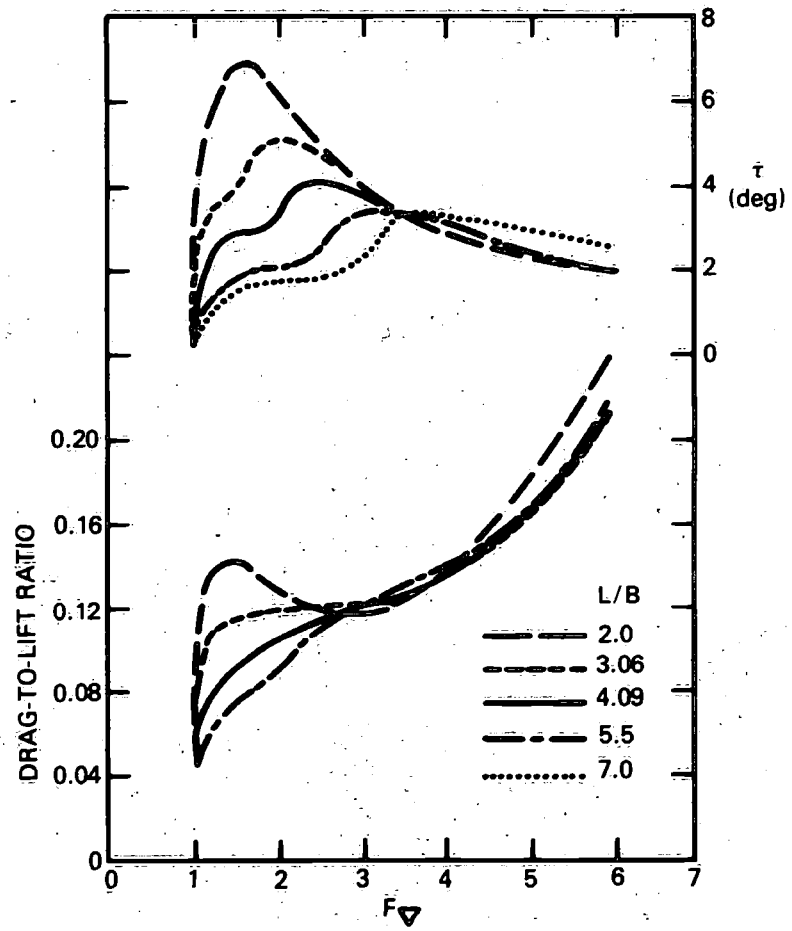

Figure 3.3.4 - Drag-to-Lift Ratio and Angle of Attack Versus Froude Number for Series 62

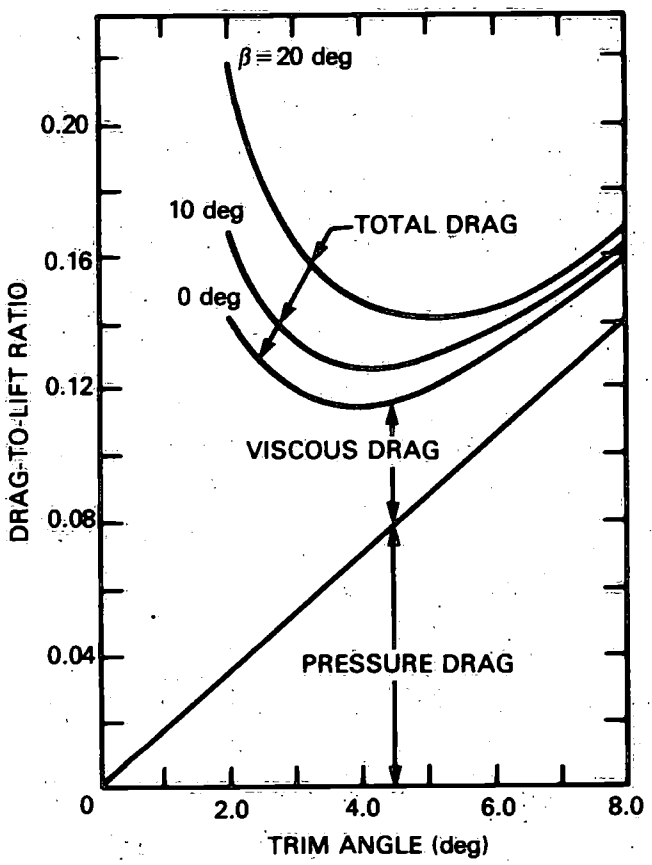

Figure 3.3.5 - Variation of Drag-to-Lift Ratio for Prismatic Planing Surfaces

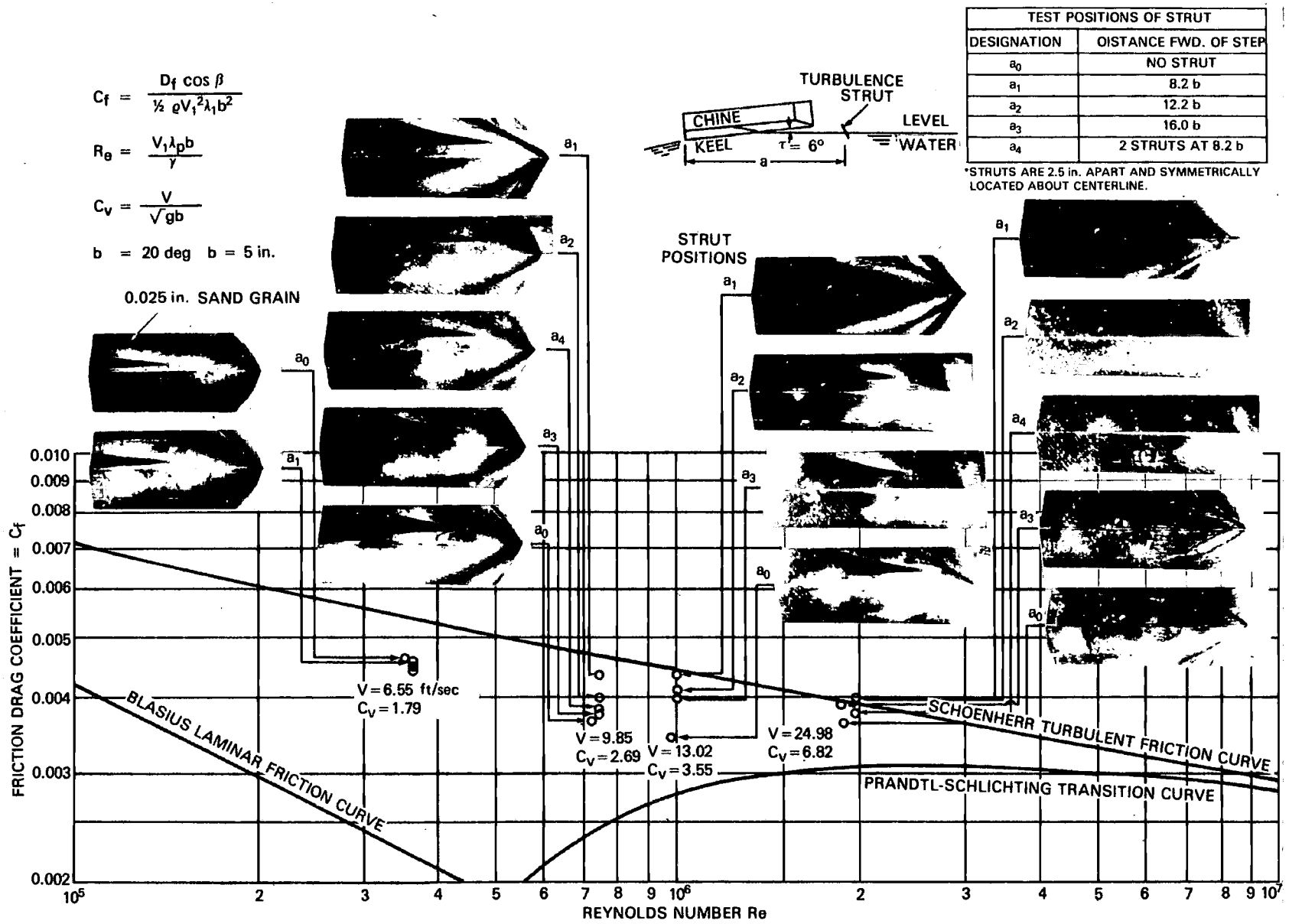

TEST POSITIONS OF STRUT	
DESIGNATION	DISTANCE FWD. OF STEP
a_0	NO STRUT
a_1	8.2 b
a_2	12.2 b
a_3	16.0 b
a_4	2 STRUTS AT 8.2 b

*STRUTS ARE 2.5 in. APART AND SYMMETRICALLY LOCATED ABOUT CENTERLINE.

Figure 3.3.6 - Effect on Friction Coefficient and State of Boundary Layer of Various Longitudinal Positions of a 0.040 Inch Diameter Turbulence Strut

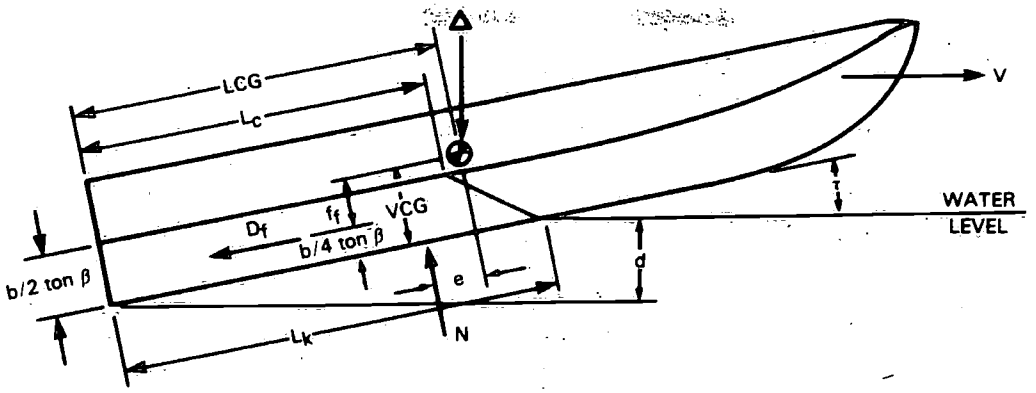

Figure 3.3.7a- Forces and Moments on a Planing Surface

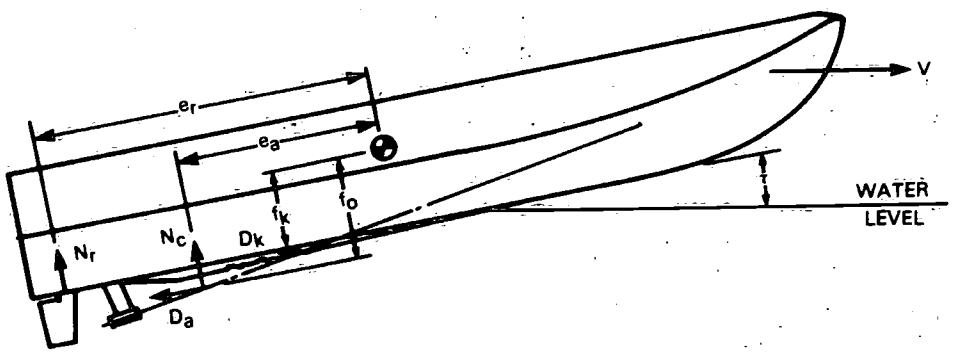

Figure 3.3.7b - Appendage Forces and Moments on a Planing Hull

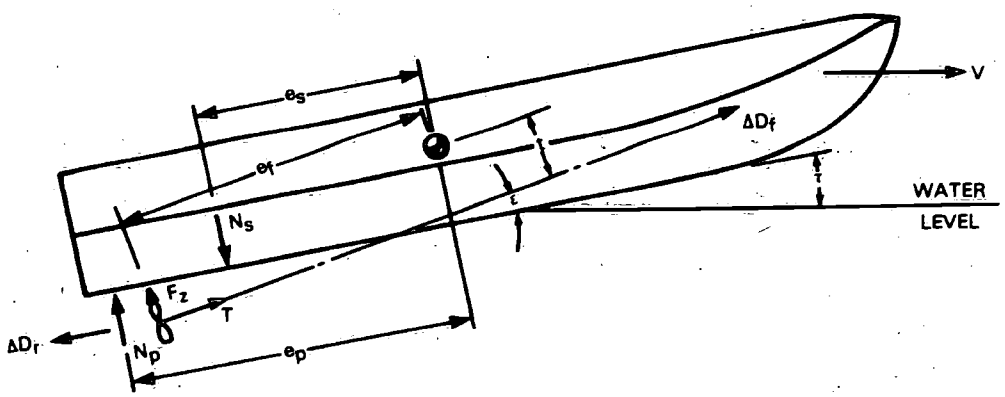

Figure 3.3.7c - Propeller Forces and Moments on a Planing Hull

Figure 3.3.7 - Forces and Moments on Self-Propelled Planing Hull

3.4 SEMISUBMERGED HYDROFOIL CRAFT

by

Burkhard Müller-Graf

Versuchsanstalt Fur Wasserbau Und Schiffbau

3.4.1 CONCEPT DEFINITION

3.4.1.1 Configuration

Hydrofoil craft with semisubmerged foil systems are designed to operate in a speed range of 28 to 45 knots, and in exceptional cases up to V = 60 knots. In the hullborne mode, at speeds $V < 0.4\ V_{max}$ ($F_{n\Delta} \leq 4$) the weight of the vessel is supported by buoyant lift. During the take-off period ($F_{n\Delta} \approx 4$ to 5) the buoyant lift and the dynamic lift of the hull decrease in the same way as the hydrodynamic lift of the foils increases. In the foilborne mode, $V > 0.6\ V_{max}$ or $F_{n\Delta} > 8$, the weight is totally supported by the lift of the foils. The resistance of the foilborne vessel, comprising foil, appendage, and aerodynamic drag, is less than 50 percent of a comparable displacement supported vessel. Further merits of surface piercing hydrofoil crafts (SPH) are their good seakeeping qualities and the small speed loss in waves.

3.4.1.1.1 Foil System. The surface piercing foil systems are characterized by:

3.4.1.1.1.1 Dihedral or anhedral foils, hoops, or ladder foils. In the foilborne mode the foil area is partially submerged. The reserve area is clear above the water surface (Figure 3.4.1).

3.4.1.1.1.2 Inherent static and dynamic stability in pitch, roll, yaw, and heave. The foilborne craft is automatically stabilized by area stabilization. A deviation from the equilibrium condition causes a change of the lift producing wetted foil area which creates restoring forces and moments. The requisite reserve lifting area is mostly provided by trapezoidal foil tips (Figure 3.4.1) or in some cases by ladder shaped foil systems (Figure 3.4.2).

3.4.1.1.1.3 Wave disturbances. Marked effects of wave disturbances on dynamic longitudinal and lateral hull response, resulting from area stabilization.

3.4.1.1.1.4 Low take-off speed. Take-off begins at, $V_T \approx 0.5\ V_{max}$. The lift is generated predominantly by two foil units, a bow foil and a rear foil. The foil arrangement is categorized as:

a. Conventional or airplane type. The main foil, arranged nearly midships but before the longitudinal center of gravity (LCG), carries 90 percent of the total weight; the auxiliary stern foil carries the remainder.

b. Tandem type. The front foil near the bow supports 55 to 65 percent of the total weight. The rear foil is fitted at the transom.

c. Canard type. The rear foil near the transom carries 90 percent of the total weight.

The area of each foil unit is mostly unsplit, but for foil retraction the area can be split laterally in two. Sweep-back of the foils is unusual.

During the take-off period the lift of the foils can be controlled by changes of the angle of incidence of the foil unit, by flaps or by air feeding.

The cross-section of the foils are mostly of the subcavitating type. At speeds above V = 50 knots supercavitating and superventilated profiles have to be used. The cross-sections of the struts and the supporting legs are streamlined or base ventilated. Fences are used to control ventilation on foils and struts.

3.4.1.1.2 Hull Form. The hull shape mainly depends upon the type of longitudinal foil arrangement and the required interplay between foil and hull lift during the take-off period. For vehicles with aeroplane foil configuration, unconventional bluff bowed monohull forms are used.[1] Tandem foils require hard chine planing hull types with moderate or high deadrise.[2,3] To facilitate the hull emersion, transversal or oblique wedges or steps are provided at the bottom (Figure 3.4.3). For canard foil configuration, hulls with fine forward lines and a high deadrise are preferred.

3.4.1.2 Range of Hull Dimensions and Operational Limits

Hydrofoil vessels with surface piercing foil systems are used for high speed passenger transport in coastal waters and in some cases for military purposes. The following dimensions are typical for crew beats and ferries:

Length (LOA)	9 - 40 m
Length-to-Beam Ratio L/B (Hull)	3.5 - 6.0
B_{max} (overfoils)	2.5 - 16.0 m
Displacement	4 - 200 tons
Speed (foilborne)	30 - 45 knots

The seakeeping capability of the craft increases with its size, especially with the hull clearance. Hulls of 30 m length with 60 to 80 tons displacement can operate foilborne in a State 4 sea with 2.0 m significant wave height. Vessels of 150 to 180

tons displacement can perform safely in a State 5 sea with significant wave heights of 2.5 m. In the following seas the marginal wave heights are smaller; broaching of foils is a fairly frequent phenomenon but seldom violent and never a threat to safety. Quick take-off in waves proposes no problems. The comfort of ride in beam swell is excellent.

3.4.1.3 Foil Specification

Commercial and paramilitary vessels are equipped with the Supramar or Schertel-Sachsenberg tandem foil system with front foils carrying approximately 60 to 65 percent of the total weight. At displacement $\Delta < 100$ tons the front and rear foils are the surface piercing unsplit V-type. Depending upon the size of the craft, the lift can be controlled either by adjustable foil units or by flaps. Craft with displacements $\Delta > 100$ tons are equipped with the Supramar hybrid foil system, consisting of a surface piercing w-shaped front foil and a fully submerged rear foil; see Figure 3.4.4. The lift is controlled by flaps and airfeeding. The stability of the vessel is maintained by the autostability of the front foil combined with an artifical air-stabilization.

3.4.1.4 Steering and Power Transmission

The rudder assembly which includes one or two rudder stems with flaps, is attached to the rear foil. The propellers, driven by inclined shafts are located ahead or astern of the rear foil (mostly below it); z-drive systems are seldom used.

3.4.2 RESISTANCE INVESTIGATIONS (SMOOTH WATER)

3.4.2.1 Total Resistance

3.4.2.1.1 Hullborne. Below the take-off speed, $V < 0.5\ V_{max}$, the craft behaves like a planing boat. The total resistance includes the hull resistance with all its components and the drag of the foil-strut systems:

$$R_{T,S} = R_{H,S} + D_{F,S}$$

The hull resistance at speeds $F_n > 0.4$ is composed of

$$R_{H,S} = R_{WP} + R_P + R_S + R_V + R_{AP} + R_{AA} + R_{Paras} + \Delta R_{AW} + \Delta R_{ST}$$

with

$$R_V = R_F + R_{VP}$$

At the hump speed, F_n = 0.45 to 0.5 close below the take-off speed, the resistance of the bare hull amounts to, approximately, 60 to 65 percent of the total resistance; see Figure 3.4.5.

The drag of the foil units is the sum of the following components:

$$D_{F,S} = \Sigma D_P + \Sigma D_I + \Sigma D_W + \Sigma D_{Interf.} + \Sigma D_S + \Sigma D_{Vent}$$

3.4.2.1.2 Foilborne. Above the take-off speed, when the hull is clear out of the water (Figure 3.4.6), the total resistance is given by:

$$R_{T,S} = \Sigma D_{F,L} + \Sigma D_{Strut} + R_{AP} + R_{AA} + \Delta D_{AW}$$

The foil drag $D_{F,L}$ is the greatest resistance component with, approximately, 60 percent of the total resistance.

3.4.2.2 Resistance Components

The contribution of the different resistance components versus speed is shown in Figure 3.4.5.

3.4.2.2.1 Hull Resistance. The resistance components of the appended hull at F_n> 0.4 are:

R_{WP} = Wave Pattern resistance
R_P = Pressure or induced resistance
R_S = Spray resistance
R_V = Viscous resistance
R_F = Frictional resistance
R_{VP} = Pressure resistance of viscous origin
R_{AP} = Appendage drag
R_{AA} = Aerodynamic drag
ΔR_{AW} = Added resistance due to small waves
ΔR_{ST} = Added resistance due to course keeping

and the methods of their determination are described in detail in Section 3.4.2.1.1.

The lower aerodynamic drag coefficient of the hydrofoil vessel, C_{AA} = 0.6 to 0.8, and the effects of ventilation and spray generation on the drag of the inclined surface piercing shafts, must be taken into account. Due to the high directional

stability of the foil-strut systems the added resistance caused by coursekeeping can be neglected.

3.4.2.2.2 Foil-Strut Drag. The drag of the lift generating foil elements, $D_{F,L}$, and those of the nonlift generating struts, D_{Struts}, are composed of the following components:

D_P = Profile or section drag. The streamline drag depends upon R_n, thickness ratio t/c, camber ratio m/c, surface roughness, and angle of attack.[4]

D_I = Induced drag. The drag due to lift depends upon the dihedral angle, aspect ratio, induced angle of attack, submergence of the foil, taper ratio, and thickness ratio. This drag component which amounts to approximately 30 percent of the total foilborne resistance is obvious by the trough behind the foil unit and by the lateral waves originating at the foils at the region of surface penetration (Figure 3.4.7). The volume weight of the trough is of the same size as the foil's lift. The induced drag of the front foil can be recovered partially if the rear foil is positioned just under half the wavelength behind the former.

D_W = Wave drag. The wave drag of surface piercing nonlift generating foils and struts arises by generating gravity waves. It decreases rapidly at $F_{nc} > 1$. Due to the high values of the Froude number F_{nc}, based on chord length, this type of wave drag is very small and can be neglected at speeds above the take-off condition.[4]

D_{Interf} = Interference drag. It arises from the mutual interaction of the boundary layers at the junctions of foils and struts or air fences.

D_S = Spray drag. This resistance is associated with generating spray at the surface piercing struts, rudders, and foils. It increases with thickness ratio t/c and depends upon Froude number relating to chord length.

D_{Vent} = Drag due to ventilation. It is caused by the reduced pressure at the rear side of surface piercing struts or at the upper side of air-fed submerged foils.

ΔD_{AW} = Added resistance due to rippling seas. This component amounts to, approximately, 2 to 3 percent of the foilborne drag.[5]

3.4.2.3 Resistance Prediction Technique

3.4.2.3.1 General Consideration. The wave resistance and the spray drag of the hull, both components strongly affected by the presence of the foil-strut units, cannot be calculated directly. In the foilborne mode the analytical determination of the foil

drag is not accurate enough to define realistic power requirements. The computation does not take into account the interdependency of both foil units on lift and drag, nor the effects of the bow foil trough on the inflow direction at the shafts, rudders, and stern struts. Hence, model tests are the unique procedure to determine the wavemaking resistance of the hull and the total foil drag with sufficient accuracy.

In addition, tests with the isolated foil system are often required to obtain the foil characteristics at atmospheric and cavitation conditions.

3.4.2.3.2 Typical Models. The model scale of foils and hulls is scaled according to Froude's law of similarity. The chosen chord length has to guarantee super-critical R_n numbers (based on section length) at least at speeds where the takeoff starts. To overcome blockage effects on hull resistance, the hull length should be smaller than 1.25 times the tank depth and smaller than one half of the tank width.

The length of the model hulls varies for 1.8 to 3.4 m, the displacement from 0.04 to 0.15 m^3, approximately. The models, made of plywood or glass reinforced plastic (GRP) are fitted with adjustable bow and rear foil units, with rudders and propeller shafts (Figure 3.4.8). The foil sections of the model may be different from those of the full-scale vessel to guarantee the same lift curve slope $dC_L/d\alpha$. The foils consist of corrosion resistant material to minimize surface roughness effects. They are manufactured very carefully to ensure uniformity of the foil sections. Chord lengths of 0.1 to 0.18 m are typical. Alterations of the angle of attack due to deformations of the foil system by hydrodynamic loads should be limited to $\Delta\alpha \leq 0.1$ deg. The accuracy of the foil adjustment must be of the same value.

Hull, struts, and foils are marked with a net of waterlines. At $R_n < 5 \times 10^5$ in the hullborne mode, turbulence stimulators (studs of 2.5 mm diameter located abaft the stem) are provided.

For basic investigations of the mutual interference of bow and rear foil, the foil units are attached to a lattice or plate girder (Figure 3.4.9).

3.4.2.3.3 Typical Hull-Foil Test Procedure. The resistance test procedure for the complete hull-foil system is very similar to that of planing hulls or semidisplacement hulls. The model is free to heave and pitch, restrained in roll and yaw, and fixed in sway and surge.

The towing force, which is applied to the hull in the plane of the propeller shafts at or near LCG is kept in line with the shaft axis at all running conditions. The towing setup is the same as shown in Figure 3.2.5 of Section 3.2.2.2 Resistance,

which is the horizontal component of the towing force, attitude, trim angle, and towing speed are measured.

At each displacement tests are made with different combinations of the angle of incidence of bow and rear foil to determine the minimum drag-to-lift ratio at each speed of interest (Figure 3.4.10). Tests of the bare hull are normally not carried out.

3.4.2.3.4 Typical Foil Tests. Tests with isolated foil systems in the subcavitating range are performed in towing basins, circulating water tanks, and whirling tanks. The foil systems are mounted on three or six component foil balances. Lift, drag, and sideforce, and rolling, and pitching moments are measured for various angles of attack, roll, and sideslip at supercritical R_n numbers.[6-9] In addition, the dimensions of the trough and the flow direction behind the foil system are measured; see Figures 3.4.11 and 3.4.12.[10]

Effects of cavitation and aeration on the foil lift-to-drag characteristics are investigated by full-scale high speed tests or by model tests in cavitation tunnels with large cross sections.

3.4.2.3.5 Extrapolation Procedures. The model test results cannot be applied directly to the full-scale vessel by Froude's method. Due to the unknown boundary layer condition at the foil and strut elements caused by the low local R_n numbers, correct specific frictional resistance coefficients $C_{F,M}$ are difficult to define. The residual resistance coeffcient of the hullborne vessel is

$$C_R = C_T - C_{F,M}$$

which are usually assumed to be the same for the model and the ship; experience has shown this to be an unrealistic value. Similarly, the extrapolation of the foilborne resistance suffers from the same uncertainty. Hence, the test results are scaled by Froude's law and by using empirical correction factors

$$R_{T,S} = \epsilon_M \cdot \Delta_S \cdot (1+k)$$

where $R_{T,S}$ = Total resistance of prototype

ϵ_M = Drag-to-lift ratio of the model

Δ_S = Displacement weight of the full-scale vessel

k = Correction factor, based on full-scale trial results

In the case of Schertel-Sachsenberg foil systems, correction factors

$k = 0.1$ for the hump speed, and

$k = 0.2$ for V_{max}

have been proven.[5] The effective power is calculated conventionally by

$$P_E = R_T \cdot V_S \qquad \text{[units of kW or hp]}$$

3.4.2.3.6 Possible scale Effects. The predicted resistance of the prototype is affected by different scale effects, which are caused by:

3.4.2.3.6.1 Viscous effects. The lift and drag of model foils and struts which are operating in the transition region between $10^5 < R_n < 10^6$ can vary appreciably. The foil and appendage drag suffer laminar effects, because turbulence stimulation is not practicable. The roughness of the model foils as well as that of the full-scale foils has an important influence on lift and drag and as a result, also influences flight position and angle of attack of the foils. Foil roughness can change rapidly by separation of foil paint, by long port times, and by service in tropical waters. The applied roughness allowance is a matter of experience.

3.4.2.3.6.2 Surface tension effects. The spray drag is influenced by the dissimilarity of the Weber numbers.

3.4.2.3.6.3 Cavitation and aeration. Both phenomena which can affect the lift, and by this flight position and drag of the full-scale vessel, do not occur at the model foil system. Froude number and cavitation number cannot be realized simultaneously at model tests in open towing tanks.

3.4.2.3.6.4 Foil geometry. To obtain the lift coefficient slope of the full-scale vessel also at the low R_n numbers of the model, circular arc sections with smaller profile drag are used instead of modified airfoil sections of the prototype. In addition, the requirements of strength are leading to larger thickness ratios which also increase the profile drag. Due to the absence of air fences and flaps, and the gap between foils and control surfaces, further differences in foil drag are established. Inaccuracies in section shape and differences in the angle of attack can cause small angles of heel which increase the drag of the model or prototype noticeably.

3.4.2.3.6.5 Aerodynamic effects. These effects are the same as described in Section 3.2.2.1.4.

3.4.2.3.6.6 Blockage effects. In the hullborne mode, the tank wall boundaries can cause a change in attitude and running trim of the model.

3.4.2.3.6.7 Effects of foil deformation. Differences in the deformation of model and full-scale foil units can lead to different lift-to-drag ratios.

3.4.2.4 Test Procedures and Instrumentation unique to Resistance Tests of Hydrofoil Vessels

The test procedures and the instrumentation used in determining hull-foil resistance are very similar to those used on conventional displacement ships with the exception of the following cases.

3.4.2.4.1 The towing force is applied to the model in line with the propeller shaft axis at all running trim angles and hull attitudes.

3.4.2.4.2 The use of a wind screen at model speeds $V > 6.0$ m/s.

3.4.2.4.3 Resistance tests with isolated model foil systems or complete hull foil models under full-scale cavitation conditions in large cavitation tanks.

3.4.2.5 Outstanding Problems in Predicting smooth Water Resistance

Methods to achieve boundary turbulence stimulation at the model foil and strut elements should be examined. Basic research is necessary in the field of aeration and cavitation inception but also in spray phenomena.

3.4.2.6 Recommendations for Resistance Studies to the 16th ITTC

3.4.2.6.1 Examine and recommend methods for turbulence stimulation in the boundary layer of the foil and strut elements.

3.4.2.6.2 Investigate the influence of aeration on the foil and strut characteristics in axial and nonaxial flow.

3.4.2.6.3 Examine the spray phenomena of struts in axial and nonaxial flow and recommend methods in extrapolation of full-scale spray drag.

3.4.2.6.4 Investigate the tank wall influence on the resistance of hullborne hydrofoil craft with a surface piercing foil system.

3.4.3 SEAKEEPING INVESTIGATIONS

Several analytical methods based on linear and nonlinear theories have been developed to predict the longitudinal response of surface piercing hydrofoil systems

in waves.[11-14] The agreement between predicted motions and accelerations, and full-scale results is due to nonlinear effects and is not always satisfying. Model tests in regular or irregular waves are still necessary to improve the theories and to investigate or predict on the basis of experimental transfer functions the seakeeping characteristics of a special design.

3.4.3.1 Model Selection

The model scale for seakeeping tests is selected in accordance with the requirements of the smooth water tests. It depends upon the capability of the wavemaker, which should ensure tests under the operational sea conditions. In addition, the scaled mass of inertia should be achieved including the weight of the instrumentation.

For basic research, the foils are mounted on a lattice girder (Figure 3.4.9). For commercial tests, fully appended model hulls with water tight decks are used.

The models are correctly ballasted for scaled weight, center of gravity, and mass of inertia about the three axes of freedom. The proper radii of gyration are set by oscillating techniques. The longitudinal moment of inertia of the model is mostly increased due to the relatively increased weight of the foil systems.

3.4.3.2 Typical Test Procedures

3.4.3.2.1 Isolated Foils. For basic research isolated foils attached to a three or a six component balance are tested in waves by measuring oscillatory forces and moments at varied angles of attack and sideslip in head and following seas.[15]

3.4.3.2.2 Complete Foil Configuration. Tests are performed in head and following seas at constant speed with an unpowered model. The model is free to pitch and heave but restrained in surge, roll, and yaw. It is towed at the LCG and connected with the resistance balance by a shock absorber. Provisions are made to restrict the downward motion of the model in following seas.

The models are tested at different speeds with varied combinations of bow and rear foil incidence. The flight position of the model is attained before meeting the waves.

Tests in oblique waves are not attainable even in special seakeeping basins. These tests are practicable with manned and self-propelled models in open water environments.

3.4.3.3 Test Wave Environment

Seakeeping tests are performed in irregular and regular waves. The behavior of different designs is compared better in regular waves. The test results imply an additional margin of safety, because the conditions are much more severe due to resonance effects than those of irregular waves with the same average wave height. Tests in irregular waves need more repeat runs to obtain enough wave encounters for statistical analysis. Wavelengths in irregular seas should be selected in such a manner that platforming and contouring can be tested.

Tests in following seas are of the greatest importance to estimate the seakeeping qualities of a hydrofoil vessel.[16]

3.4.3.4 Quantities Measured during Tests, Instrumentation Used in Waves, Data Collection and Processing, Data Presentation

All these items are identical, with some exceptions to those as reported in Section 3.3.3.

3.4.3.5 Extrapolation of Model Results to Prototype

The extrapolation of the model test results follows Froude's scaling and is basically similar to the procedure for conventional ships.

3.4.3.6 Correlation of Model Test Results

The limited model and full-scale seakeeping data do not always correlate. The discrepancy is caused by resonance effects, by damping effects of full-scale aeration and cavitation, by differences in the elasticity of model and full-scale hull, by differences in the radius of gyration, by the multidirectional characteristics of the full-scale sea state, and by the lack of accuracy in full-scale wave measurements.

3.4.3.7 Outstanding Problems

Outstanding problems concern the foil characteristics and the interference effects between the front and rear foils in following seas and the damping effects of aeration and cavitation on vertical motions and accelerations. The scale effects of the aeration and cavitation phenomena are also of great interest. Further research on the effect of nonlinearities on heave and pitch is required.

3.4.3.8 Recommendations for Seakeeping Studies of the 16th ITTC

3.4.3.8.1 Investigate the effects of nonlinearities on the foil motions.

3.4.3.8.2 Investigate the interference effects between the front and rear foils in the following seas.

3.4.3.8.3 Examine the effects of aeration and cavitation on motions and accelerations.

3.4.3.8.4 Collect and correlate model test results with analytical and full-scale seakeeping data.

3.4.4 MANEUVERABILITY INVESTIGATIONS

Maneuverability tests are not usually conducted for commercial hydrofoil designs in the foilborne mode. This is true for the following reasons:

a. Tests with free running models are not attainable in towing basins.

b. At model tests, aeration and ventilation, which mainly affect the sideforces, do not occur in a correct scale.

c. The required vertical area distribution and the required sideforce curve slope of rudders and foils for good directional stability, which is a characteristic feature of surface piercing hydrofoil crafts, can be determined analytically in most cases.

d. Forces and moments, roll angle, and sideslip angle in a turn can be calculated.[17]

Basic research is performed with captive models attached to a planar motion mechanism or running on a straight course. The most reliable results are obtained with experimental craft, i.e., with free running manned models.

3.4.4.1 Experimental Procedures, Data Collection, and Presentation

Experimental procedures, data collection, and presentation are identical to those of conventional ships.

3.4.4.2 Outstanding Problems

The most important problems concern ventilation and aeration in a turn and their effects on sideforces and lift.

3.4.4.3 Recommendations for Maneuverability Studies to the 16th ITTC

3.4.4.3.1 Collect model and full-scale maneuvering data of surface piercing hydrofoil crafts.

3.4.4.3.2 Study the effects of ventilation and aeration on strut sideforces and foil lift at small sideslip angles.

3.4.5 PERFORMANCE INVESTIGATIONS

For hydrofoil craft, subcavitating and supercavitating propellers, mostly with fixed pitch, are used. Inclined shafts or z-drives with single or twin screw installations are common.

3.4.5.1 Self Propulsion Tests

Propulsion tests with hydrofoil craft are not usually conducted in towing basins. Model sizes which guarantee supercritical R_n numbers at 0.7 R of the propeller blade become too great and too fast for most of the test capabilities. Self-propulsion tests are performed in some cases with experimental boats of 5 to 10 m length having a displacement weight of 0.5 to 2.5 tons. The manned craft are built of plywood, GRP, or alloy with a model scale between one third and one sixth. They are propelled by gas engines of the outboard type or, in the case of scaled inclined shaft systems, of the inboard type. Speed of craft, thrust, torque, rate of rotation, and engine output are measured.

3.4.5.2 Wake Measurements

Measurements of wake distributions in the propeller plane are limited to such cases where the propeller is fitted to the propulsion nacelle of a z-drive system.

3.4.5.3 Open Water Tests

Propeller tests under cavitation conditions and in oblique inflow can be of greater interest than the conventional axial inflow tests.

3.4.5.4 Full-Scale Performance Estimates

On the basis of experimental craft tests the full-scale delivered power and propeller revolutions are obtained by direct extrapolation of the measured values using Froude's law of similarity. Empirical corrections are applied for viscous effects. Generally, the full-scale performance prediction is based on resistance test results. Quite similar to conventional ship procedure, the delivered power is determined by

$$P_D = \frac{R_{T,S} \cdot V_S}{\eta_D}$$

with η_D the quasi-propulsive coefficient

$$\eta_D = \eta_o \cdot \eta_H \cdot \eta_R$$

where η_o = propeller efficiency at full-scale cavitation number

η_H = hull efficiency $(1-t)/(1-w)$

η_R = relative rotative efficiency

The thrust deduction fraction t takes into account the effects of the inclined thrust axis by using the net thrust force

$$T_x = T_\psi \cdot \cos \psi + F_y \cdot \sin \psi$$

where T_ψ = axial thrust

ψ = propeller inflow angle, $\psi = \delta + \theta$

δ = shaft inclination

θ = running trim

F_y = propeller normal force

Force F_y can be determined by empirical expressions or, more correctly, by the method of Gutsche.[18] The wake fraction w has solely to account for the change in propeller inflow velocity due to the oblique flow condition:

$$V_\psi = V_S \cdot \cos \psi$$

The value of η_R becomes unity in most cases of inclined shaft systems. Because the propeller is placed abaft the rear foil, the effects of oblique propeller inflow are noticeably reduced because the rear foil acts like a guide van.

The required propeller speed is determined by means of K_T/J^2 and the thrust advance coefficient J_T. On the propeller calculated for rate of rotation, no allowance is applied. A propulsion prediction factor (1+k), with k = 0.04, is used to compensate for the drop of propeller efficiency due to propeller roughness.

3.4.5.5 Recommendations for Propulsion Studies to the 16th ITTC

No special recommendations are necessary at present.

3.4.6 PROPULSOR INVESTIGATIONS

3.4.6.1 Propulsor Problems Unique to Hydrofoil Craft

Propulsor problems which are unique to surface piercing hydrofoil craft do not presently exist. The problems of interest, propeller characteristics for oblique inflow for subcavitating and supercavitating condition, are also valid for other vehicle types.

3.4.6.2 Recommendations on Propulsor Studies to 16th ITTC

No special recommendations to the propulsor committee are necessary at present.

3.4.7 CAVITATION INVESTIGATIONS

3.4.7.1 Cavitation Problems Unique to Hydrofoil Craft

The cavitation problems at the propellers of hydrofoil vessels are similar to those arising on other types of vessels. However, the phenomena of cavitation and aeration on oscillating hydrofoil systems running near the water surface are of great interest.

3.4.7.2 Recommendation on Cavitation Studies to the 16th ITTC

Collect data concerning the influence of cavitation and aeration on lift and drag characteristics of hydrofoils running near the water surface.

3.4.8 PRESENTATION AND INFORMATION

The list of the ITTC Standard Symbols does not include special terms and symbols which are used for foil geometry and resistance components of hydrofoil craft. The ITTC-Standard Symbols and the ITTC Dictionary of Ship Hydrodynamics should be supplemented by these symbols in accordance with those which are applied in the field of fully submerged hydrofoils.

3.4.9 REFERENCES

1. Pieroth, C.G., "Hydrofoil Hullform Selection," Hovering Craft and Hydrofoil, Vol. 16, No. 3 (Dec 1976).

2. Müller-Graf, B., "Widerstandsversuche für ein 41-t-Tragflügelboot," (Resistance Tests for a 41 ts Supramar Hydrofoil Boat), 262/63, Versuchsanstalt für Wasserbau und Schiffbau Report 247/63, Berlin (1963).

3. Müller-Graf, B., "Widerstandsversuche für ein 40-t-Tragflügelboot," (Resistance Tests for a 40 ts Supramar Hydrofoil Boat), Versuchsanstalt für Wasserbau und Schiffbau Report 340/66, Berlin (1966).

4. Hoerner, S.F., "Fluid Dynamic Drag," published by the author, USA (1975).

5. Graff, W. et al., "Theorie der Tragflügelboote," Schertel - Sachsenberg AG and Supramar AG (1949 and 1955).

6. Müller-Graf, B., "Widerstandversuche für ein 150-ts-Tragflügelboot," (Resistance Tests for Hull and Foil Units of a 150 ts Supramar Hydrofoil Boat), Versuchsanstalt fur Wasserbau und Schiffbau Report 529/70, Berlin (1970).

7. Müller-Graf, B., "Kennlinien-Bestimmung von Wassertragflügeln," (Characteristics of Surface Piercing Hydrofoils), Versuchsanstalt für Wasserbau und Schiffbau Report 295/65, (1965).

8. Schwanecke, H., "Einfluss der freien Wasseroberfläche auf den Strömungszustand an Wassertragflügeln," (Effect of Water Surface on Flow Conditions of Hydrofoils), Versuchsanstalt für Wasserbau und Schiffbau Report 100/58, Berlin (1958).

9. Schuster, S. and H. Schwanecke, "On Hydrofoils Running Near a Free Surface," Third Symposium on Naval Hydrodynamics, ONR ACR-65 (1960).

10. Müller-Graf, B., "Bestimmung der Anströmwinkel am Heckflügel und am Ruder," (Determination of Inflow Angles at Rear Foil and Rudder), Versuchsanstalt fur Wasserbau und Schiffbau Reports 326/66 and 518/69, Berlin (1966 and 1969).

11. Weinblum, G.P., "Approximate Theory of Heaving and Pitching of Hydrofoils in Regular Shallow Waves," David Taylor Model Basin Report C-479 (Oct 1954).

12. Ogilvie, T.F., "The Theoretical Predictions of the Longitudinal Motions of a Hydrofoil Craft," David Taylor Model Basin Report 1138 (Nov 1958).

13. de Witt, H., "Lineare Theorie der symmetrischen Schwingungen von Tragflügeltandems in flachen sinusförmigen Wellen," Doctoral thesis, T.H. Braunschweig (1966).

14. de Witt, H., "Numerical Results of Forced Antimetric Oscillations of a Hydrofoil Boat in a Seaway," Hovering Craft and Hydrofoil, Vol. 8, No. 1 (Oct 1968).

15. Schuster, S. and H. Schwanecke, "On Oscillating Hydrofoils," Part I, Part II, ONR N. 62558-2236 (1960) and 2552 (1962), VWS-Reports (1960 and 1962).

16. Müller-Graf, B., "Seakeeping Tests with a Model of a 150 ts Supramar Hydrofoil Craft," Versuchsanstalt für Wasserbau und Schiffbau Report 343/66, Berlin (1966).

17. Schuster, S., "Über Seitenbewegungen und Seitenstabilität von Tragflügelbooten," Versuchsabteilung der Gebr. Sachsenberg AG, Bericht Nr. 39-42 (1945).

18. Gutsche, F., "Untersuchung von Schiffschrauben in Schräger Anströmung," Schiffbauforschung 3 (3/4 Mar 1964).

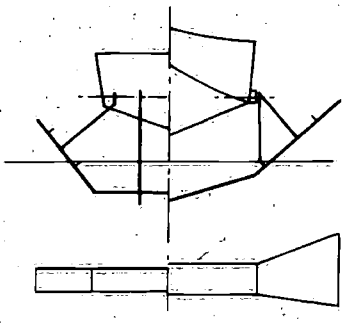

Figure 3.4.1 - Schertel-Sachsenberg Foil-System

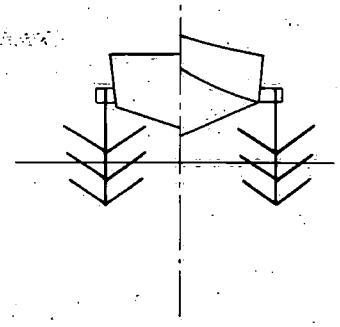

Figure 3.4.2 - Ladder Foil System

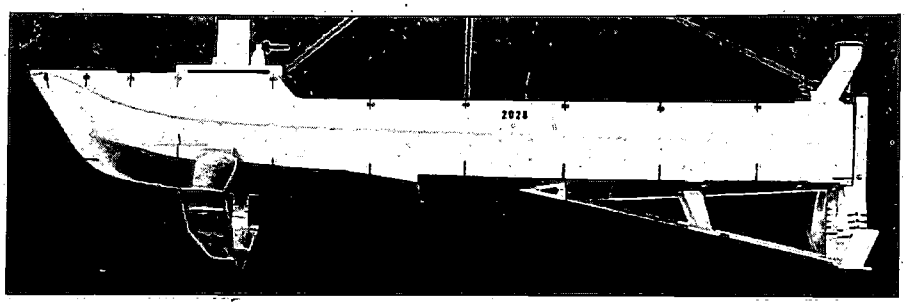

Figure 3.4.3 - Hull With Midships Wedge

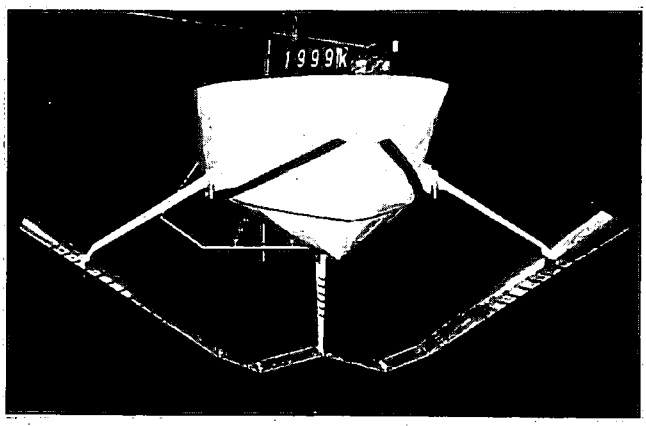

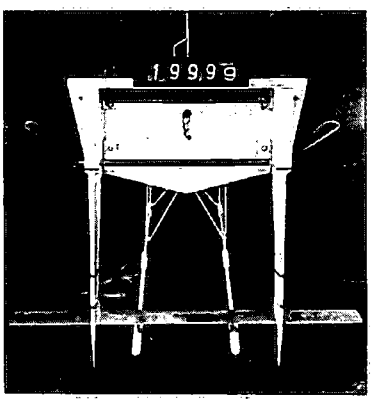

Figure 3.4.4 - Typical Tandem Hybrid Foil Arrangements

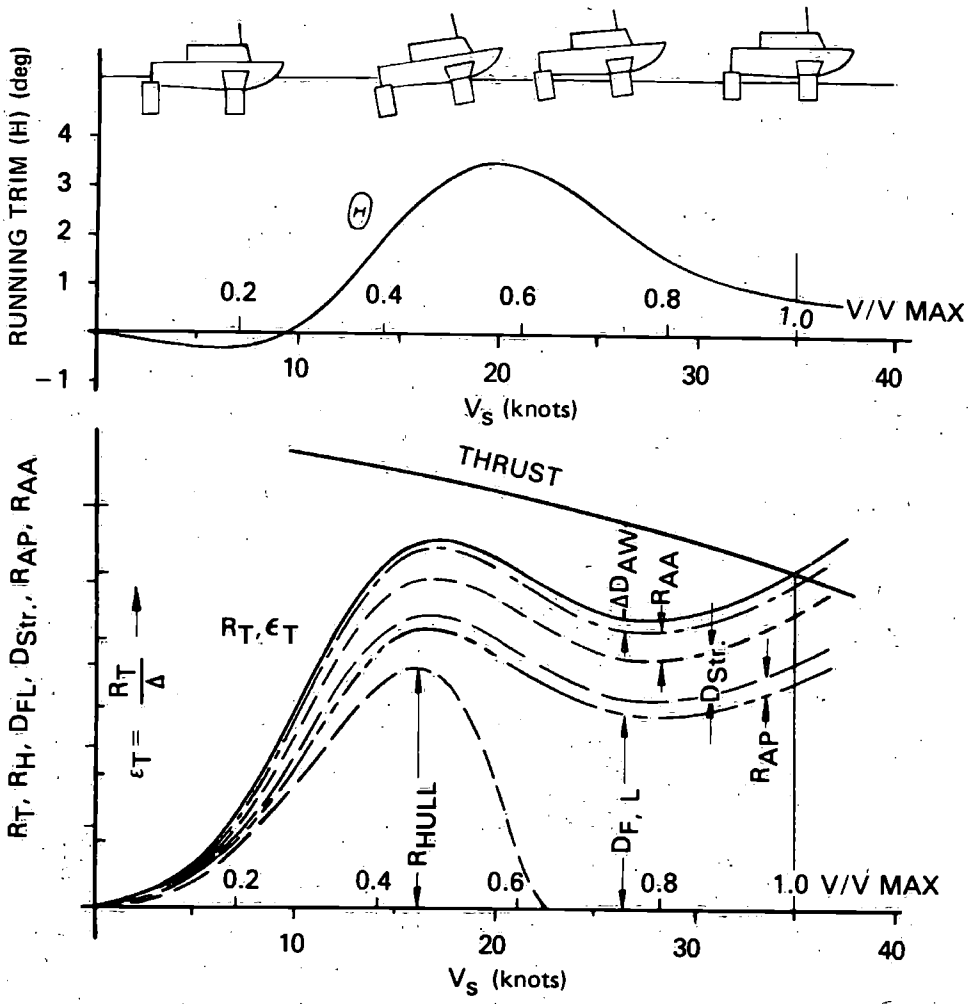

Figure 3.4.5 - Distribution of Resistance Components, Running Trim, Attitude

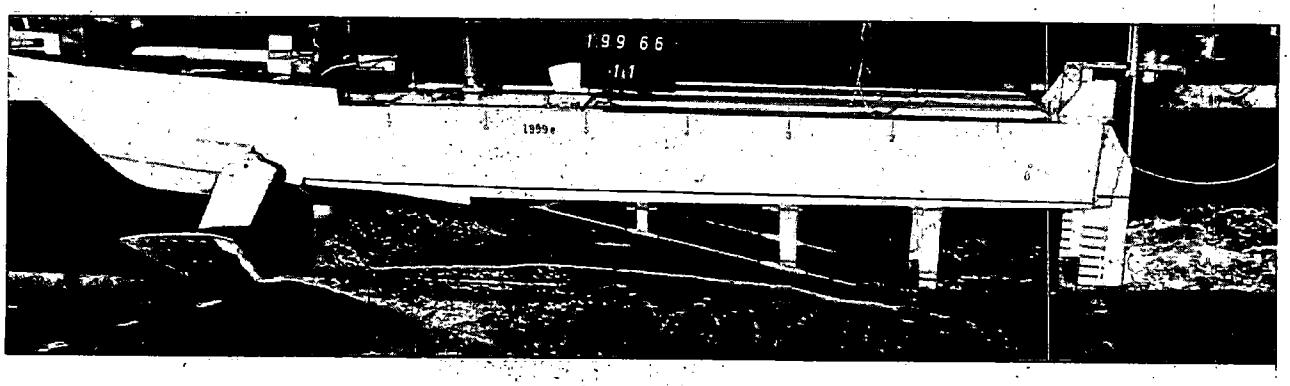

Figure 3.4.6 - Foilborne Mode

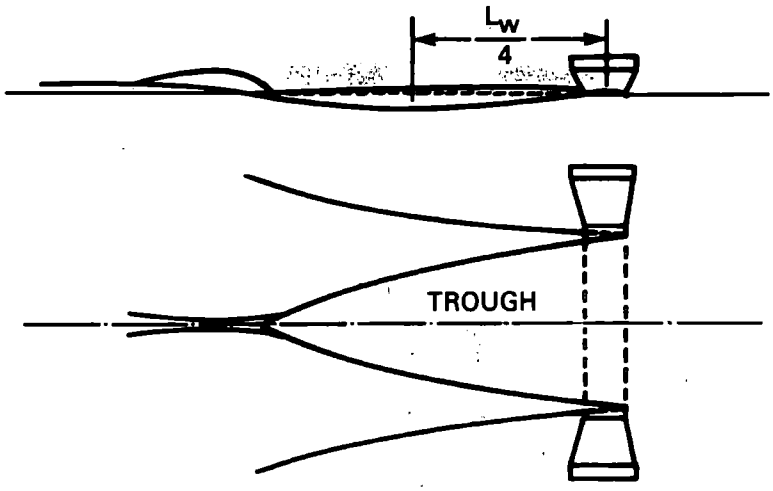

Figure 3.4.7 - Bow Foil Trough

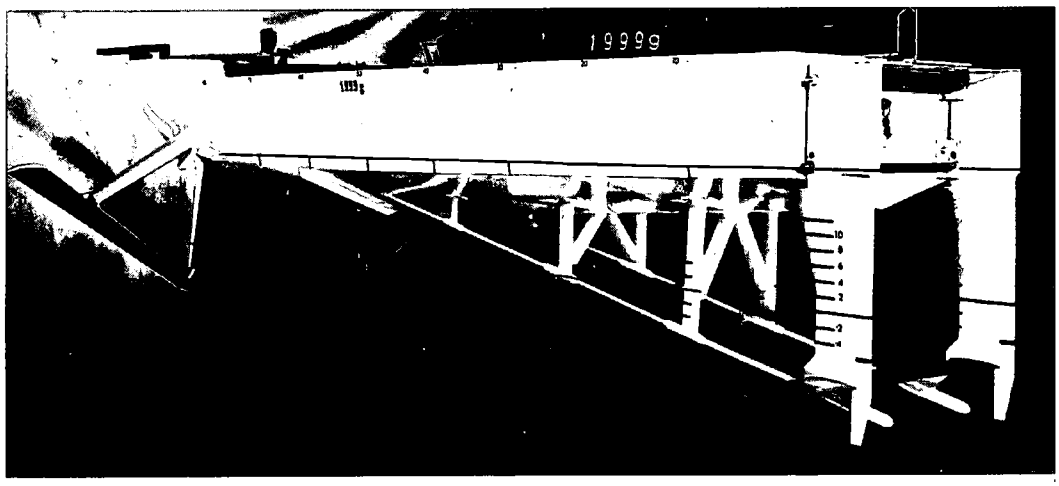

Figure 3.4.8 - Complete Hydrofoil Model

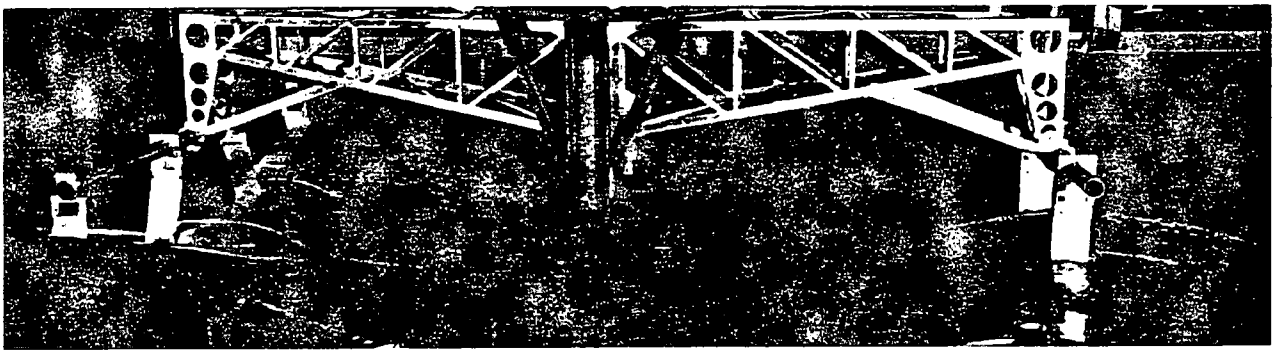

Figure 3.4.9 - Hydrofoil Tandem

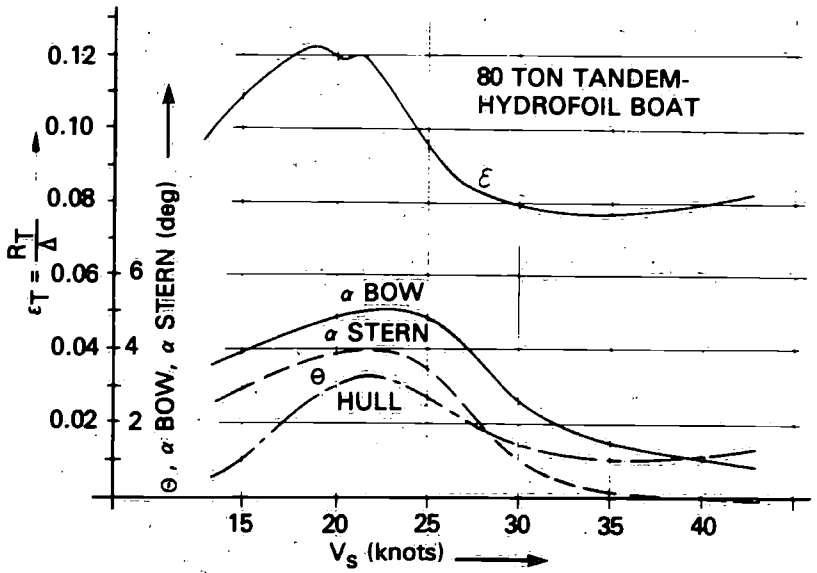

Figure 3.4.10 - Angles of Foil Incidence for Optimal Drag-to-Lift Ratio

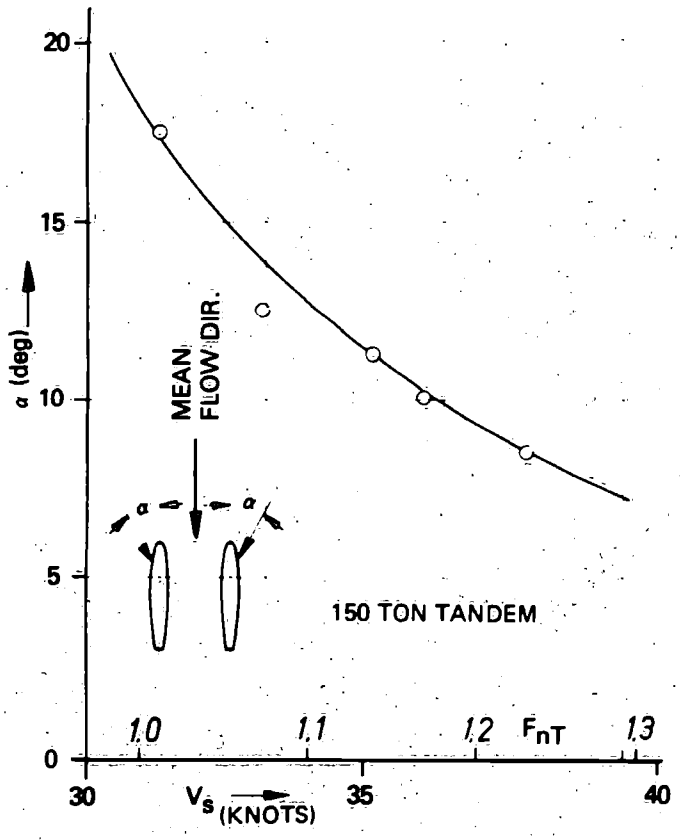

Figure 3.4.11 - Angle of Attack of Rudder Stems

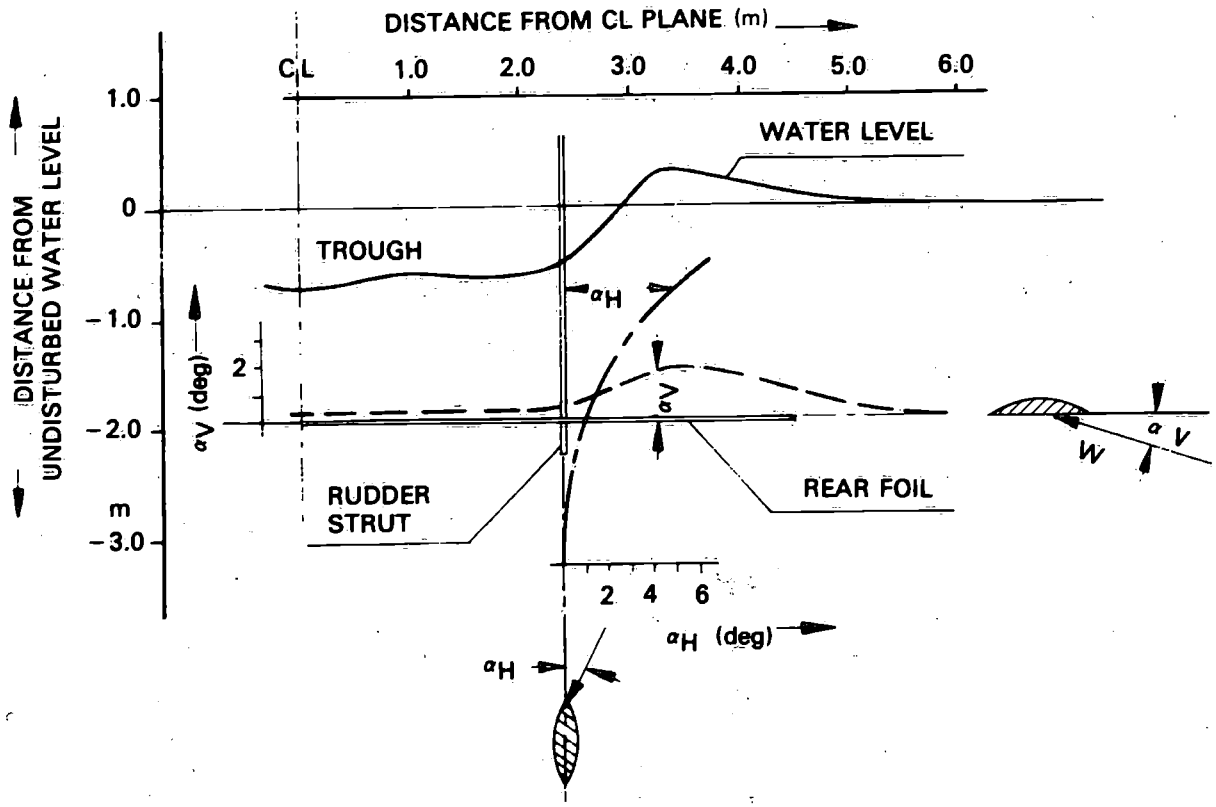

Figure 3.4.12 - Cross-Section of Bow Foil Trough, Inflow Angles at Rear Foil and Rudder Strut at V = 38.0 Knots

3.5 SURFACE EFFECT SHIPS

by

Robert A. Wilson
David W. Taylor Naval Ship Research and Development Center

and

Toshikazu Murakami
Technical Research and Development Institute
Japan Defense Agency

3.5.1 CONCEPT DEFINITION

3.5.1.1 Configuration

The surface effect ship (SES) is an air-cushion-supported vehicle where the cushion air is enclosed on the sides by rigid sidewalls and on the bow and stern by compliant seals of the bag and finger or planing type. The air for the cushion and seals is supplied by fans. Directional stability and turning moments are provided by rudders or ventral fins located on the keels of each sidewall near the transom. Thrust is provided by propellers or waterjets located on each sidewall at the transom. Figure 3.5.1 is a schematic of an SES as viewed from beneath.

Surface effect ship models do not generally incorporate a propulsion system during resistance, motions, and stability investigations (because these effects can be added to the data at a later time and because there is little interaction between the propulsor and the hull) but in other respects are good scale replicas of the prototype vehicle. Figure 3.5.2 presents several views of a typical SES model. They are generally constructed with lightweight aluminum centerbodies. The sidewalls are constructed of thin plywood structural members, lightweight foam filler, and a fiberglass covering. The centerbody and sidewalls of structurally scaled models are sometimes constructed of polyvinyl chloride. The seals are constructed of neoprene impregnated nylon or dacron cloth and thin layers of fiberglass. The model seals are designed to scale the weight and dynamic response characteristics of the full-scale seals. The lift fans do not have to be geometrical models of the full-scale fans, but the airflow rate as well as the shape of the pressure versus airflow rate characteristics of the fans must be correctly scaled to the full-scale craft. Weights and moments of inertia should be similarly scaled. If moments of inertia are not known, a nominal radius of gyration should be selected and maintained for the range of weights for the vehicle.

3.5.1.2 Range of Geometric and Operational Variables

Parametric designs of surface effect ships discussed in Reference 1 indicate the cushion length-to-beam (L/B) ratio of an SES may vary from approximately 2 to 8 with displacements ranging up to 12,000 long tons. The cushion height from the keel to the wet deck may vary from 25 to 35 percent of the cushion beam. The overall beam is nominally 1.25 times the cushion beam. The speeds of interest for an SES of a L/B of 2 to 3.5 is nominally of Froude numbers (based on cushion length) up to 2.0. Usually SES's of L/B of 5 and greater have design Froude numbers of nominally 0.6 to 0.8.

An upper limit to model size is somewhat determined by the water depth dimension of the facility in which it will be tested as well as the maximum speed of the towing carriage. It is desirable to ensure that the water depth is greater than 75 percent of the cushion length in order to eliminate or minimize wave resistance scaling corrections. Cushion beam dimensions have ranged from 2 to 3 ft (0.6 to 0.9 m) with cushion lengths varying from 5 to 16 ft (1.5 to 4.7 m). Speed variations are determined by Froude scaling as previously described. Models are presently tested at weights up to 800 lb (360 kg) but this is not a limit; practical considerations prevent model weights less than 100 lb (45 kg). Construction costs and data accuracy are also very important in determining the size of a model.

3.5.1.3 Dynamic Similitude

The forces acting on a SES are complex functions of aerodynamic, aerostatic, hydrodynamic, and hydrostatic forces. Therefore, to scale the forces, the proper scaling relationships must be understood. In general, Froude scaling prevails. The displacement, speed, vehicle attitude, and immersion scale with Froude number based on cushion length (F_ℓ). For ease of understanding the design trends for various L/B designs, Froude number based on the square root of the cushion area is sometimes used (F_s). The specific loading or cushion density of the vehicles are examined in terms of pressure-to-length ratio (P/ℓ) or weight-to-cushion area ratio raised to the 1.5 power. While scaling resistance, Reynolds number is used using the appropriate characteristic length (e.g., sidewall length at the on-cushion water line for sidewall resistance and the mean chord of a rudder for rudder resistance). Cushion pressures and airflow rates also are Froude scaled. The stability forces and moments from the cushion and sidewalls Froude scale but the data from rudders and ventral fins must correctly account for the proper cavitation number. Aerodynamic forces and moments should be evaluated at the proper Reynolds number. Seal material

properties are examined in terms of Young's modulus as well as unit weight and elastic properties (e.g., material strength in terms of force per unit length). Spray is examined in terms of Weber number. Wave heights are usually dimensionally scaled based on the characteristic length of the cushion.

3.5.2 RESISTANCE INVESTIGATIONS

3.5.2.1 Resistance Components

The primary components of resistance of an SES are the wavemaking resistance of the cushion and the sidewalls, the frictional drag of the sidewalls, the frictional and induced drag of the seals, the resistance of the appendages, and the aerodynamic resistance. The wavemaking component is calculated from theory, the frictional resistance determined by studying the wetted areas (usually from photographs), and the aerodynamic resistance of the model is determine from special tare runs. The remaining resistance (which is primarily the seal component) is found by subtraction and is called the residual drag. Typical component distributions for low and high L/B designs are presented in Figure 3.5.3.

Model resistance experiments are normally conducted with the model free in heave and pitch. The weight of the model is corrected for salt water density so as to ensure that the trim of the craft, which is determined from the wave slope of the cushion, is correct. A good design will have the same longitudinal center-of-gravity (LCG) location for minimum drag at all speeds. Because a low drag design will have little lift carried by the seals, the optimum trim of the craft as a function of Froude number can be determined from the slope of the wave which is $\theta = \tan^{-1} D_w/W$. This is verified experimentally. Experience has shown that the best LCG of an SES should be located 51 percent of the cushion length forward of the trailing edge of the stern seal.

3.5.2.2 Test Procedures

Resistance experiments should be conducted in both calm water and in seas. The primary measurements in calm water are: drag, pitch angle, immersion of the keels at the pitch pivot relative to the undisturbed water surface, pressures in the seals and in the cushion, and speed. In waves, the additional measurement of wave profile must be taken. Photographs are taken of the model from abovewater and underwater to assist in analyzing the wetted areas. Figure 3.5.4 shows typical wetted areas during a calm water experiment of a L/B = 8 model.

The model test procedure in calm water is to set the LCG at 51 percent and then vary the seal-to-cushion pressure ratios so as to minimize drag. (These pressure ratios may vary from 1.05 to 1.4 depending upon the type of seal used.) Pitch angle (or LCG) is then varied in small increments to select the best value as shown in Figure 3.5.5; note that the best pitch attitude is speed dependent. Airflow rate is then varied to evaluate its effect (which is small at low speeds and large at high speeds as shown in Figure 3.5.6). The best value of airflow rate for each speed is when the total equivalent drag (summation of the drag plus the equivalent drag of the lift system (D + (PQ/V)) is a minimum is shown in Figure 3.5.7. (This calculation is valid when the efficiency of the lift and propulsion systems are the same, which is in general, true.) Because the wavemaking drag and the immersion vary with weight, weight variations should also be made as shown in Figure 3.5.8.

Experience has shown that the best seal-to-cushion pressure ratio, LCG, and airflow rate in calm water are usually also the best values for the design in seas; the ability of a specific seal design to adjust to wave conditions, however, can affect the results. Experiments in seas are usually conducted with the model fixed in surge because comparative experiments with the model both fixed and free in surge have shown that the same time average drag value is produced in both cases. (It should be noted, however, that trim instabilities can be aggravated when testing fixed in surge by forcing the model forward at constant speed when it would normally slow down due to increased drag.) Testing fixed in surge requires, therefore, that the model be operated at a number of fixed speeds for each scaled state of sea considered. Operating at fixed speeds both simplifies data analysis and minimizes testing time. The results are plotted as drag versus significant wave height, as shown in Figure 3.5.9. Then, curves of drag versus speed for a constant sea state can be plotted (by interpolation); a typical family of curves for a low L/B SES is shown in Figure 3.5.10.

3.5.2.3 Resistance Scaling

The resistance of an SES is scaled using the technique presented by Wilson et al. in Reference 2. This technique uses the theoretically calculated wavemaking drag component as determined using Doctors' method[3] and shown in Figure 3.5.11. The frictional drag component is calculated using the wetted areas as determined from photographs. (If underwater photographs are not available, an assumed value of an inside wetting equalling 10 percent of the outside wetting can be assumed.) The residual drag, which is primarily seal drag and includes both frictional and induced

drag components, is scaled using Figure 3.5.12. The aerodynamic drag, which for the model was determined as a tare value and subtracted from the model results, is added based on wind tunnel results. If wind tunnel results are not available, an assumed value of a drag coefficient of 0.5 times the dynamic pressure times the entire frontal area of the vehicle will produce acceptable values. Figure 3.5.13 from Reference 2 shows that this technique has produced acceptable levels of correlation.

3.5.2.4 Outstanding Problems in Resistance Investigations

The technique described in Referene 2 for scaling resistance is one, documented approach used for scaling model resistance. This approach can be improved upon, especially in the areas of sidewall wetted areas over the broad range of length-to-beam ratios and displacements and for scaling the residual drag which is primarily seal drag. A better understanding of these components as a function of speed, sea condition, and loading is needed. Photography is used extensively to determine sidewall wetting; if the wetted area could be measured, it would improve accuracy and save time. Engineers predicting the drag of sidewalls often use aircraft procedures used for establishing surface roughness as determined by Schlicting.[4] Acceptance of this technique should be examined. The SES sidewalls are subject to spray sheets which vary with Reynolds number and Weber number and which contain three-dimensional flow fields, an area that needs to be studied. The materials used in the seals of SES's and ACV's must be properly scaled for weight, strength, and dynamic characteristics. Because incorrectly scaled seals can affect the results of the experiments, guidelines for this component design and fabrication should be established.

3.5.2.5 Recommendations for Resistance Studies to the 16th ITTC

3.5.2.5.1 Broadly examine methods used to determine the drag components of surface effect ships and the scaling of these components.

3.5.2.5.2 Examine methods of determining the inside and outside wetting of SES sidewalls over a broad range of Froude numbers and craft displacements (or cushion loadings).

3.5.2.5.3 Examine techniques for determining the skin friction coefficient for high-speed vessels including the three-dimensional flow.

3.5.2.5.4 Examine the skin friction coefficient which would be used for planing surfaces in contact with an air-water mixture such as that in contact with the stern seal of an SES.

3.5.2.5.5 Examine the scaling of the spray sheet drag associated with the flow on the sidewalls of high-speed surface effect ships.

3.5.2.5.6 Examine techniques for scaling the materials used to fabricate the seals on SES's and ACV's to scale weight and dynamic characteristics.

3.5.3 SEAKEEPING INVESTIGATIONS

3.5.3.1 Model Characteristics

The models used in seakeeping experiments are usually the same models used in resistance experiments. Added care is taken, however, to position ballast weights on the model such that the vertical center-of-gravity is at the estimated location for a prototype.

3.5.3.2 Wave Environment

Surface effect ship model experiments are conducted primarily in irregular seas; regular wave experiments have been conducted during limited-technlogy related experimental programs. Seakeeping experiments are principally done in head seas, but following and oblique sea experiments also have been performed. (Oblique sea experiments have been conducted only at low speeds due to facility limitations.) A Pierson-Moskowitz spectrum is used for SES model experiments because, to date, designs have not been made for proposed operation in a specific ocean region.

3.5.3.3 Test Procedures

The seakeeping experiments on an SES model are conducted in both irregular as well as regular seas. The proper moment of inertia (I_{yy}) is set on the model and confirmed using the spring-oscillation or compound pendulum technique. If the moment of inertia of the prototype vehicle is not known, an appropriate radius of gyration is selected and maintained for all displacements evaluated. (Subsequent full-scale predictions using model data must include corrections for the radius of gyration.)

The measurements made during seakeeping experiments are the same as those during resistance experiments with the addition of accelerometers at the bow, LCG, and stern. A minimum of three accelerometers are required because the center-of-rotation for an SES is nominally near the aft quarter point and the accelerations vary (often by a factor of two) from the bow to the more aft locations. Impact pressures and strains are measured on structurally scaled models where structural loads are needed.

3.5.3.4 Data Presentation

When the characteristics of a specific design are being determined, seakeeping experiments are usually conducted only in irregular seas; regular wave experiments are used in more parametrically-related studies. Pitch, heave, and acceleration data are analyzed to determine rms, and average, significant, one-tenth highest values as

well as maximum values experienced for the peaks and troughs of the motions. Typical plots of rms g's, and significant double amplitude pitch and heave motions (in irregular seas) are shown versus significant wave height for constant speed in Figures 3.5.14, 3.5.15, and 3.5.16. Histograms of model responses are prepared in some laboratories to reveal how frequently values in different class intervals occur and to provide input for developing empirical probability distributions to be used for future predictions.

Model experiments in regular waves have been conducted at various wave heights for fixed wavelengths and speeds to examine the linearity of the SES. Reference 5 has shown a length-to-beam ratio 6.5 SES to be linear with respect to wave height. References 6, 7, and 8 have shown that the response amplitude operators obtained by experiments in regular, irregular, and transient waves for the same SES design also show relatively good agreement. Pitch and heave data obtained in regular waves for an L/B 2.5 SES design at various Froude numbers, wavelengths, and wave heights are presented in Figures 3.5.17 and 3.5.18. The results also show a reasonable degree of linearity.

3.5.3.5 Correlation of Model Test Results

Data from model and full-scale trials on the SES-100B have been analyzed to permit comparisons of transfer functions versus a nondimensional encounter frequency for pitch and heave. Figure 3.5.19 shows good agreement between model and full-scale pitch responses for frequencies above 3.5 at a Froude number of 1.31. In the resonance frequency range below 3.5, however, the shape of the model and full-scale pitch response curves are different, indicating that the pitch damping of the full-scale craft is less than that of the model. Model and full-scale heave transfer functions are presented in Figure 3.5.20. This figure shows good agreement between model and full-scale response over the entire frequency range.

Even though the results presented in Figures 3.5.19 and 3.5.20 indicate that the motions of a full-scale craft can be predicted from model motions, References 9 and 10 note that due to air compressibility, the motions of large ships (especially those with relatively small cushion airflow rates such as the SES) do not scale. The ability to characterize the dynamic responses of the lift system (fans, ducts, and internal seal aerodynamics) as discussed in Reference 11 also bring model to full-scale motion predictions under question. Using these arguments, full-scale predictions can only be made using predictive techniques which have been correlated with model results and that adequately address compressibility and the various subsystems on

the vehicle. Special experimental investigations need to be conducted which address these matters.

3.5.3.6 Outstanding Problems in Seakeeping Investigations

Present analyses of models and small testcraft show that the motions of surface effect ships appear to be linear but theoretical predictions of motions simulating the cushion as a piston with a compressible fluid indicate that model results cannot be used for predicting full-scale motions. Reduced atmospheric experiments as well as other, specialized experiments and measurements directed at high frequency responses of models and testcraft must be conducted and analyzed to provide the answer. While surveying the motions of numerous ships, one finds that different authors and facilities use different nondimensionalizing techniques for transfer functions and frequencies; therefore, a standard is needed. The use of cross-spectral analysis techniques eliminates noise in the data and allows for coherency determination. This technique needs to studied further and possibly established as a standard. This will help in providing a common base for comparing the motions of different craft. High-speed vessels need a great deal of accurate seakeeping data in all headings to the sea. Means of providing these data must be determined.

3.5.3.7 Recommendations for Seakeeping Studies to the 16th ITTC

3.5.3.7.1 Examine the area of atmospheric pressure scaling (compressibility effects) with special emphasis on recommended experimental programs, techniques, and measurements.

3.5.3.7.2 Continue to examine the area of linearity with emphasis on the linearity of the model, the dynamics of the lift and seal systems, and compressibility.

3.5.3.7.3 Continue the examination of model and full-scale motion correlations.

3.5.3.7.4 Establish a uniform method for nondimensionalizing transfer functions and frequencies.

3.5.3.7.5 Examine the use of cross-spectral analysis techniques which eliminates noise in data as a recommended standard for motion data analysis.

3.5.3.7.6 Extensive data are needed for high-speed vessels in various headings to the sea, but present facility limitations do not permit obtaining these data. Examine this problem and make any recommendations.

3.5.4 MANEUVERABILITY INVESTIGATIONS

3.5.4.1 Typical Evaluations

The determination of the maneuvering characteristics of a surface effect ship requires a good understanding of the various forces involved. The sidewalls, seals,

and appendages all interact and the forces on these components vary significantly with speed, vehicle attitude (yaw, roll, and pitch); therefore, extensive model experiments must be conducted to provide data for maneuvering simulations. Various levels of sophistication require different types and amounts of data.

The conservative design approach, which requires that the craft demonstrate static or inherent stability over its operating range (including all attitudes anticipated during any failure conditions), require only that static stability data be determined, but this may result in the need for large ventral fins or rudders. If a more complete simulation is required, then dynamic stability data must be included. This nessitates the use of a planar motion mechanism to supplement the static stability information. The more complete simulations use the approach shown in Figure 3.5.21; this schematic also points out the need to include propulsion forces as well as appendage ventilation and control effects.

The static and dynamic stability characteristics of an SES vary with configuration, attitude, and speed and are only linear over a very small attitude range. Thus, to date, extensive model experiments used in conjunction with maneuvering simulations of varying complexity have been the only successful ways of predicting the maneuvering and safety characteristics of an SES.

3.5.4.2 Test Procedures

SES model stability experiments are conducted with the model in heave equilibrium (free in heave) but usually restrained in all other axes. The gage zero reading taken prior to each run are done with the model hanging in air so that the running reading will measure all forces acting on the model (e.g., aerostatic, hydrostatic, aerodynamic, and hydrodynamic). A set of aerodynamic tare runs are made at the beginning of the experiment with the model in close proximity to the water to measure the aerodynamic forces (which can be large in drag and pitch moment); these values are often replaced with wind tunnel data during further analysis.

A normal test matrix will involve examining pitch angles ± 2 deg about the normal trim condition for each speed. Roll angle variations include ± 3 deg in increments adequate to define the curve. Yaw angles examined include speed variations such that 0 to 8 deg are examined at low speeds and 0 to 5 deg at high speeds. This matrix is evaluated over the speed range with more emphasis of the high speeds where significant force changes often occur due to appendage and cushion pressure ventilation.

Roll damping information can also be determined from the log decrement of the roll oscillation obtained from a static stability experiment. Figure 3.5.22 shows

the craft to be well damped in roll. Experiments of this type also show that roll damping increases with displacement. A similar evaluation can be done in pitch.

3.5.4.3 Data Processing

The measurements taken are longitudinal and side forces, and pitch, yaw, and roll moments. Figure 3.5.23 shows how the forces and moments on a characteristic SES model vary with speed for a fixed rudder (fin) angle, roll angle, and pitch angle. Figure 3.5.24 shows the effect of rudder size and pitch angle on yaw moment. Figures 3.5.25 and 3.5.26 (for a different SES design) show the nonlinear characteristics of yaw moment and side force respectively, which can appear at angles that may be quite small. It is these nonlinearities which can often necessitate large test matrices.

Planar motion experiments provide velocity and acceleration dependent terms. Figure 3.5.27 shows a SES model attached to the planar motion mechanism (PMM) at DTNSRDC. The key data from these experiments are the N_r, K_p, and $N_{r_{vv}}$ terms. The cross coupling terms become very important when simulating failure conditions.

Sample velocity and acceleration derivatives for a SES model are presented in tables 3.5.1 and 3.5.2. The acceleration dependent coefficients $Y'_{\dot{r}}$, $N'_{\dot{r}}$, and $K'_{\dot{r}}$ are small compared to the velocity dependent coefficients Y'_r, N'_r, and K'_r and can be considered negligible compared to the model's mass inertia. An overall comparison of the results in Tables 3.5.1 and 3.5.2 shows that the rudder markedly contributes to the N'_r and $N'_{\dot{r}}$ coefficients. Also, the coefficients do not remain constant with a change in model velocity for the same model attitude. Model roll variation does not have any substantial effect on the coefficients. This effect is clearly shown in the bare hull configuration of Tables 3.5.1 and 3.5.2.

3.5.4.4 Outstanding Problems in Manueuverability Investigations

Surface Effect Ship maneuverability can be approached in a conservative manner which may produce a poor performing vehicle or, in a much more elaborate manner with extensive simulations, using extensive PMM (unsteady) data. The degree to which each investigation is conducted should be recommended to the customer based on need and cost. A stability criterion of SES's is also needed. Because appendage forces at high speed are affected by ventilation and cavitation, a series of appendage experiments in various facilities should be conducted to provide uniform guidelines for data to be used in maneuvering simulations.

3.5.4.5 Recommendations for Maneuverability and Cavitation Studies to the 16th ITTC

3.5.4.5.1 Establish guidelines or outlines for steady and unsteady stability experiments to be used to adequately describe the maneuvering of high-speed vessels.

3.5.4.5.2 Survey the literature on scaling of ventilation and cavitation on end-plated appendages in high-speed flow to provide consistent data needed for use in maneuvering predictions.

3.5.5 PERFORMANCE INVESTIGATIONS

3.5.5.1 Types of Propulsors Used

The propulsors used on the SES are either subcavitating propellers on inclined shafts, semisubmerged supercavitating propellers located at the keel of the transom, or waterjets. Air propellers can be used also. Propulsors used on surface effect ships are discussed in References 12, 13, 14, and 15.

3.5.5.2 Model Completeness

Models used to determine the performance of an SES have a properly scaled lift system which is studied parametrically during resistance investigations. The models generally do not contain propulsion systems; the thrust and vertical force components are analytically applied to the scaled resistance characteristics.

3.5.5.3 Data Presentation

The resistance of a surface effect ship is scaled using the techniques described in Section 3.5.2.3. The airflow rate for the resistance values used is scaled using the relationship that $Q_{F_S} = Q_M 2.5$. This relationship assumes Froude scaling of the pressures, exit velocity of the cushion air, and the area through which the air passes. The lift power is then the product of the Froude-scaled pressure and airflow rate. The efficiency used with the Froude-scaled lift power comes from experimental investigations of the lift fans using standards established for fans. (These lift fan experiments are conducted in wind tunnels or facilities with calibrated orifices and standard duct lengths.)

The propulsors used on the SES are either subcavitating propellers on inclined shafts, semisubmerged supercavitating propellers located at the transom at the keel, or waterjets. With the thrust versus speed characteristics of the selected propulsion system known, the maximum speed capability of the ship can be determined. The interaction of the propulsor and the vehicle are reviewed in Reference 16.

Range calculations are made using the resistance values at various displacements, and the lift and propulsion power relationships. Ranges are calculated at constant speed and constant power. Because the cushion pressure varies with displacement, lift power will also vary with displacement and must be adequately accounted for. The immersion of the keels also varies with displacement and if immersion

affects the performance of the propulsion system, it is also taken into account. This is especially important when working with waterjet inlets to ingest air from the cushion or along the sidewalls.

3.5.5.4 Outstanding Problem in Performance Investigations

The surface effect ship rides very close to the surface of the water to minimize frictional resistance. This causes broaching or air ingestion problems for the propulsors. Likewise, the pressure fields on the hull in the area of the propulsor can become great which must be understood in order to evaluate the optimum longitudinal center-of-gravity for the ship -- which in turn, affects the manner in which the ship is loaded.

3.5.5.5 Recommendations for Performance Studies to the 16th ITTC

Examine the source and scaling of the air which gets into waterjet inlets on SES's and study its trajectory to assist a designer in designing a proper "fence" to minimize air ingestion.

3.5.6 PROPULSOR INVESTIGATIONS

3.5.6.1 Propulsor Experiments

Propellers are experimentally examined in the manner conventional to displacement hulls except that they are often tested behind a foreshortened sidewall. Waterjet experiments are conducted on complete models to study broaching effects. They are also conducted in cavitation scaled facilities to study subsystem components such as inlet and lip designs as well as the complete performance of the system.

3.5.6.2 Outstanding Problem in Propulsor Investigations

Semisubmerged, super-cavitating propellers will probably be the future propulsor for SES's due to their increased efficiency. They will probably be mounted at the transom of the sidewalls but may require special sidewall lines to get proper flow to them in various operating speed conditions. Also, when operating in a seaway, the forces felt by the propellers will see oscillating loads which will affect their performance. This propeller-sidewall interface area needs to be investigated.

3.5.6.3 Recommendations for Propulsors Studies to the 16th ITTC

Examine the effects of oscillating flows on thrust, torque, efficiency and structural and vibratory loads on the semisubmerged propellers on surface effect ships.

3.5.7 INSTRUMENTATION

3.5.7.1 Outstanding Problems in Instrumentation

The wetted areas of sidewalls and seals of surface effect ships are determined by studying numerous photographs of test conditions. A more accurate, less time consuming method is needed. Crude measurement systems have been designed and used to measure air-water quality in the ducts of waterjet systems. These systems include photocells and electric wire grids. Improved, more accurate system are needed.

3.5.7.2 Recommendations for Instrumentation Studies to the 16th ITTC

3.5.7.2.1 Examine and recommend ways of measuring the wetted areas on sidewalls of surface effect ship models.

3.5.7.2.2 Examine methods for developing a good system to determine the air-water mixture in ducts and pumps used with the waterjet propulsion system on surface effect ships.

3.5.8 REFERENCES

1. Ford, A.C. et al., "High Length-to Beam Ratio Surface Effect Ship," American Institute of Aeronautics and Astronautics and the Society of Naval Architects and Marine Engineers Report 78-745 (1978).

2. Wilson, R.A. et al., "Powering Prediction for Surface Effect Ships Based on Model Results," David W. Taylor Naval Ship Research and Development Center Report 78/602 (Jul 1978).

3. Doctors, L.J., "The Wave Resistance of An Air Cushion Vehicle," University of Michigan (Dec 1970).

4. Schlichting, H., "Boundary-Layer Theory," McGraw-Hill, Sixth Edition, 1968.

5. Magnuson, A.H. and K.K. Wolff, "Seakeeping Characteristics of the XR-5, A High Length-to-Beam Ratio Manned Surface Effect Testcraft : I. XR-5 Model Response in Regular Head Waves," NSRDC SPD 616-01 (1975).

6. Magnuson, A.H. and K.K. Wolff, "Seakeeping Characteristics of the XR-5, A High Length-to-Beam Ratio Manned Surface Effect Testcraft : II. Results of Linearity Investigation, Effects of Changes from Reference Operating Condition and Trim and Draft in Regular Waves," NSRDC SPD 616-02 (1975).

7. Ricci, J.J. and A.H. Magnuson, "Seakeeping Characteristics of the XR-5, A High Length-to-Beam Ratio Manned Surface Effect Testcraft : III. Results of Random Wave Experiments, Investigation of Linear Superposition for Ship Motions and Trim and Draft in Random Waves," DTNSRDC SPD 616-03 (May 1976).

8. Moran, D.D. et al., "The Seakeeping Characteristics of a High Length-to-Beam Ratio Surface Effect Ship," AIAA/SNAME Advanced Marine Vehicles Conference (1976).

9. Kaplan, P. and S. Davis, "A Simplified Representation of the Vertical Plane Dynamics of SES Craft," AIAA (1974).

10. Doctors, L., "The Effect of Air Compressibility on the Nonlinear Motion of an Air-Cushion Vehicle over Waves," Eleventh Symposium on Naval Hydrodynamics, Sessions III-IV, London (1970).

11. Durkin, J.M. and L.W. Luehr, "Dynamic Response of Lift Fans Subject to Varying Backpressure," AIAA/SNAME Advance Marine Vehicles Conference (1978).

12. Chaplin, J.B., "SES Technology Developments," AIAA/SNAME Advanced Marine Vehicles Conference (1978).

13. Barr, R.A. and R.J. Etter, "Selection of Propulsion Systems for High Speed Advanced Marine Vehicles," AIAA/SNAME Advanced Vehicles Conference (1974).

14. Arcand, L. and C.R. Comolli, "Waterjet Propulsion for High-Speed Ship," AIAA/SNAME Advanced Marine Vehicles Meeting (1967).

15. Contractor, D.N. and V.E. Johnson, Jr., "Waterjet Propulsion," AIAA/SNAME Advanced Marine Vehicles Meeting (1967).

16. Wilson, M.B., "A Survey of Propulsion-Vehicle Interactions on High Performance Marine Craft," 18th American Towing Tank Conference (1978).

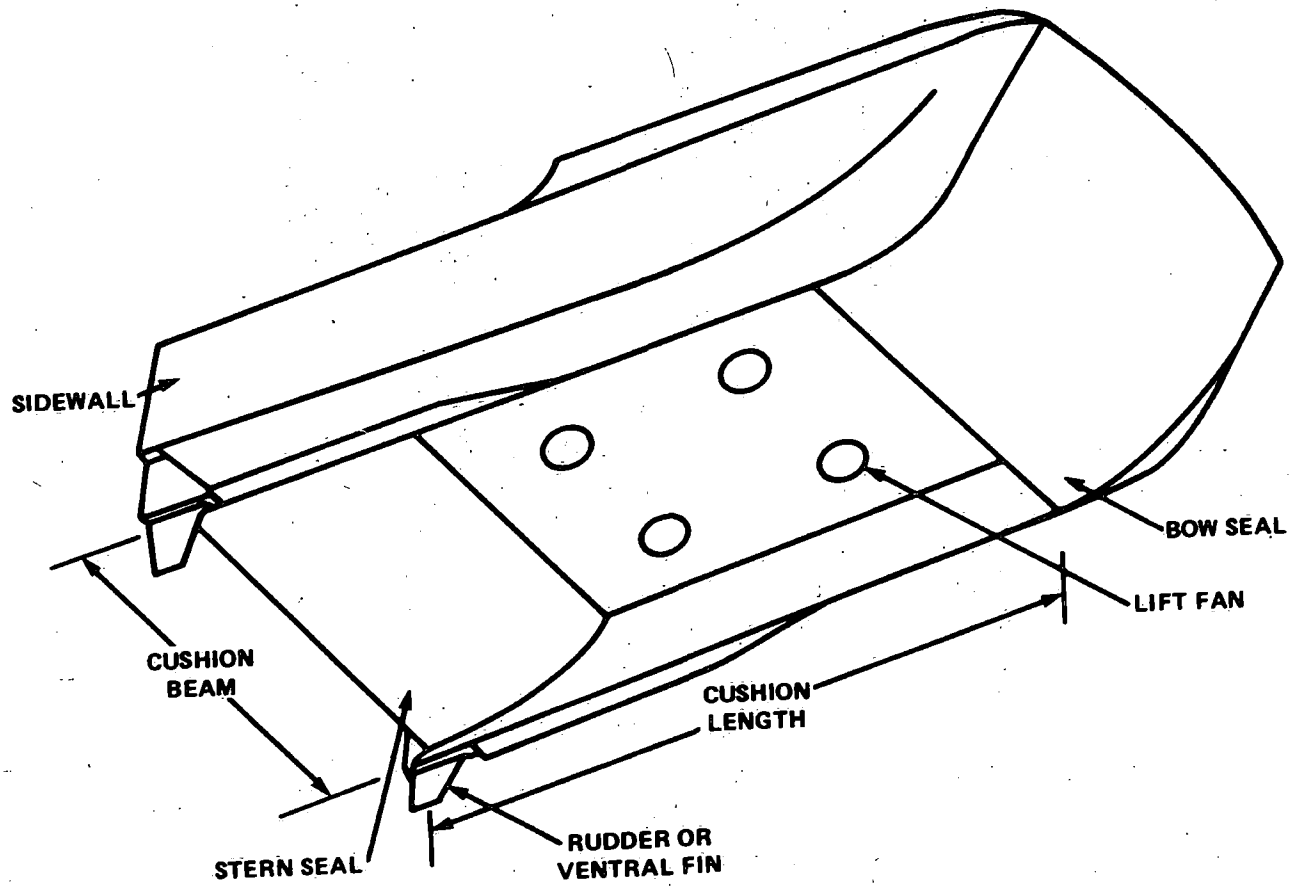

Figure 3.5.1 - Surface Effect Ship

Figure 3.5.2 - Surface Effect Ship Model and Components

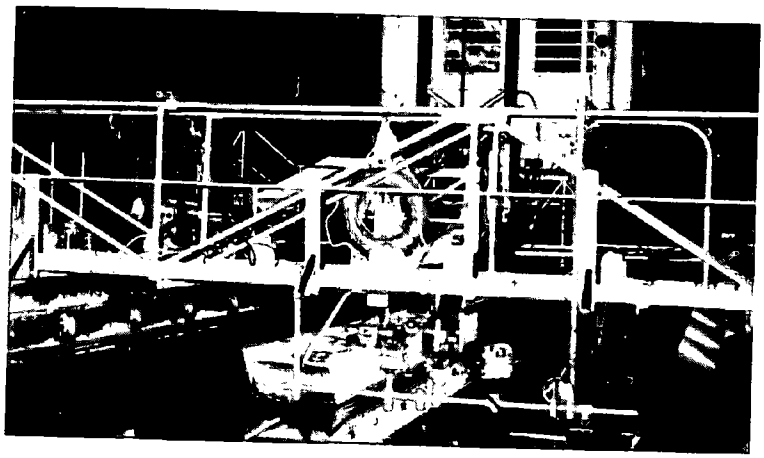

Figure 3.5.2a - Model on Carriage

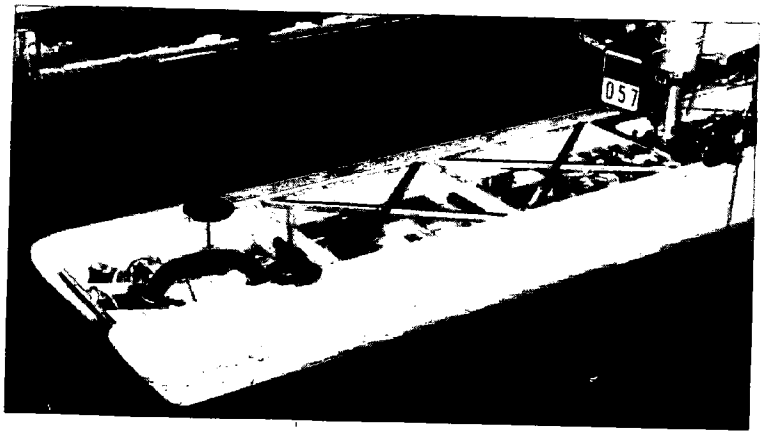

Figure 3.5.2b - Model Centerbody Construction and Tow Post

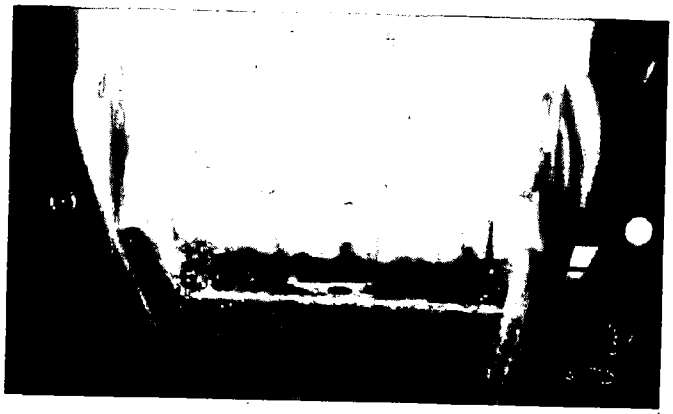

Figure 3.5.2c - Model Viewed From Below With Bag and Finger Bow Seal

Figure 3.5.2 - (Continued)

Figure 3.5.2d - Flexible Planing Bow Seal

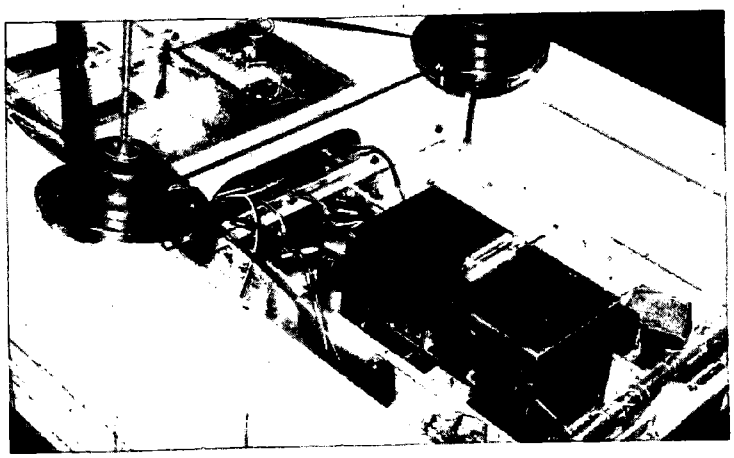

Figure 3.5.2e - Model Fans, Cross Flow Duct, Ballast Weights, and Accelerometer

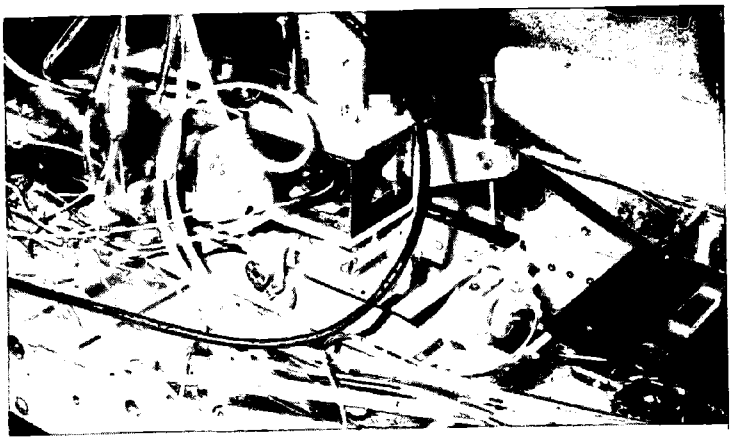

Figure 3.5.2f - Model Tow Post, Force Gage, Gimbal, and Pitch and Roll Potentiometers

Figure 3.5.3 - Drag Components of a SES

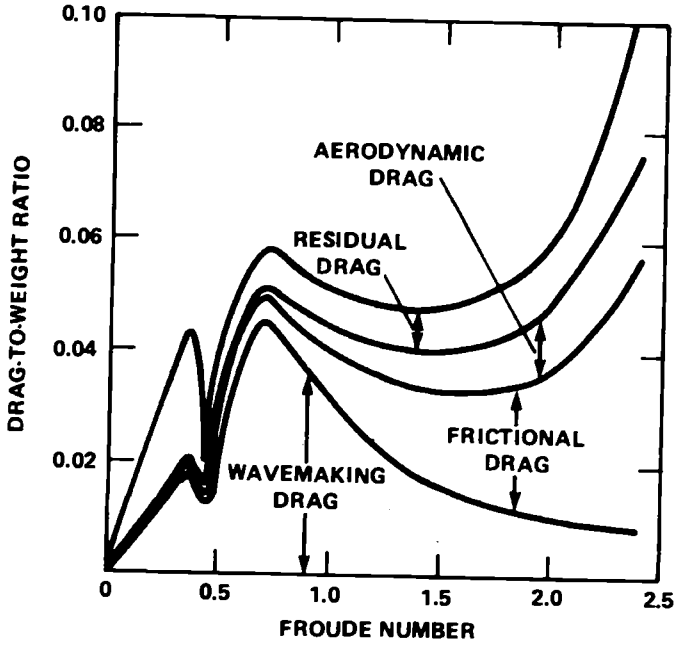

Figure 3.5.3a - Cushion L/B = 2.0

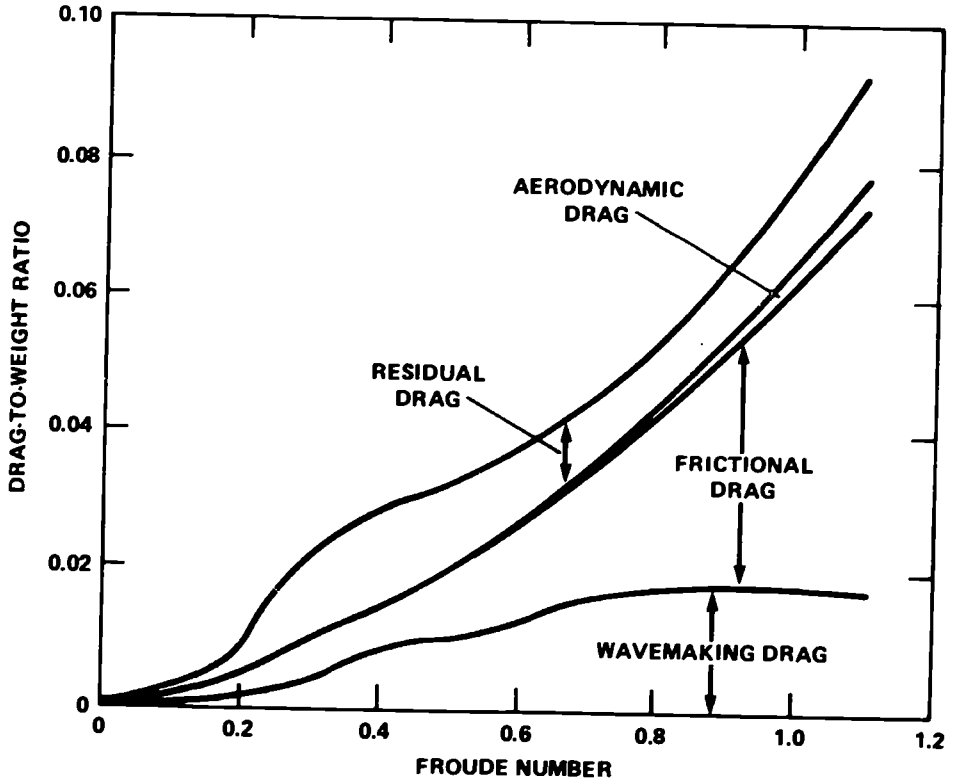

Figure 3.5.3b - Cushion L/B = 6.0

Figure 3.5.4 - Typical Abovewater and Underwater Photographs for an L/B 8 SES Model

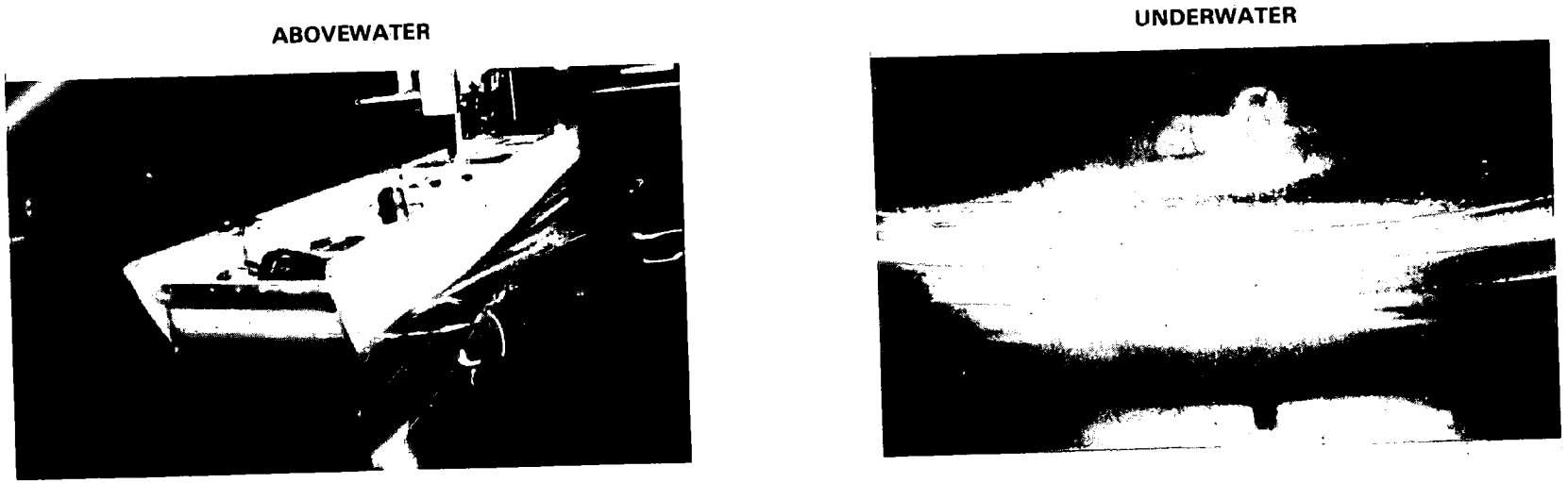

Figure 3.5.4a - Froude Number = 0.25

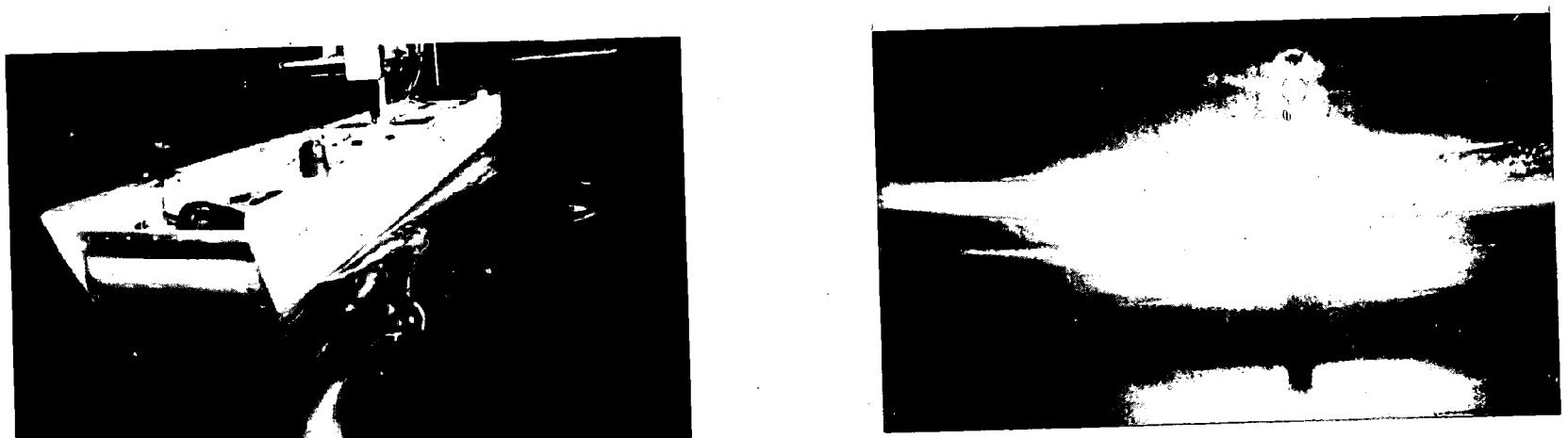

Figure 3.5.4b - Froude Number = 0.37

Figure 3.5.4 - (Continued)

ABOVEWATER

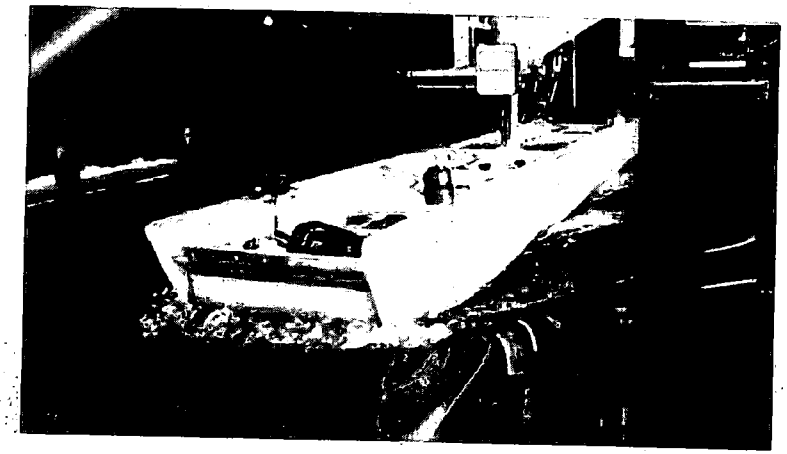

UNDERWATER

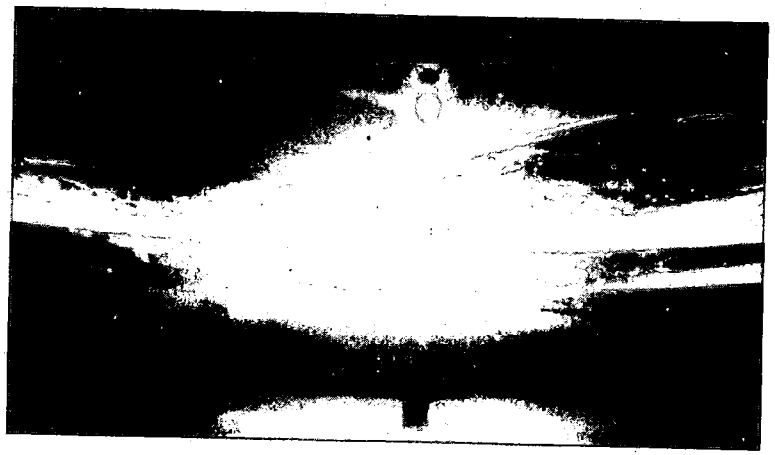

Figure 3.5.4c - Froude Number = 0.42

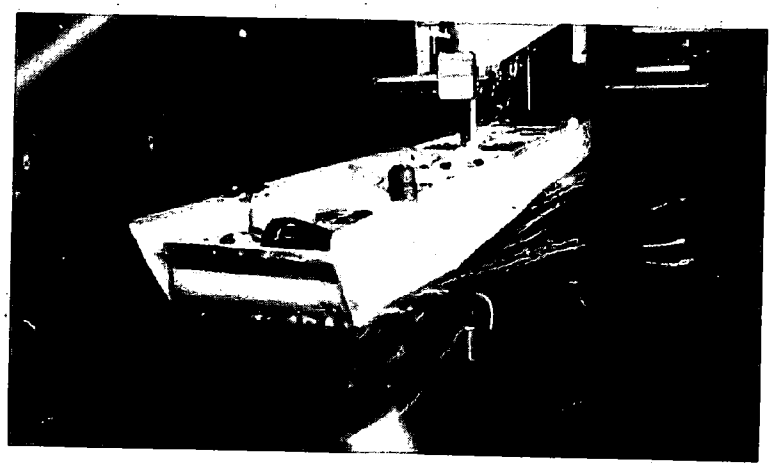

Figure 3.5.4d - Froude Number = 0.76

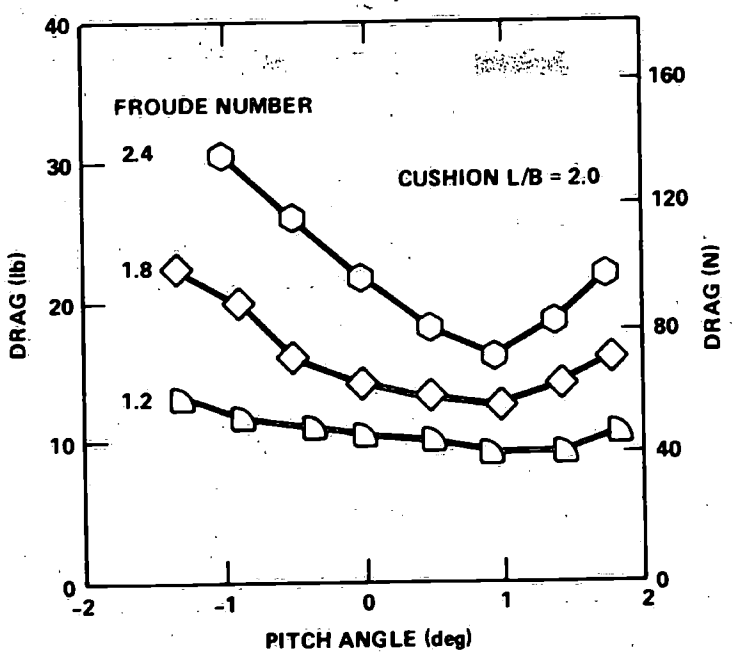

Figure 3.5.5 - Drag Variations with Pitch Angle and Froude Number

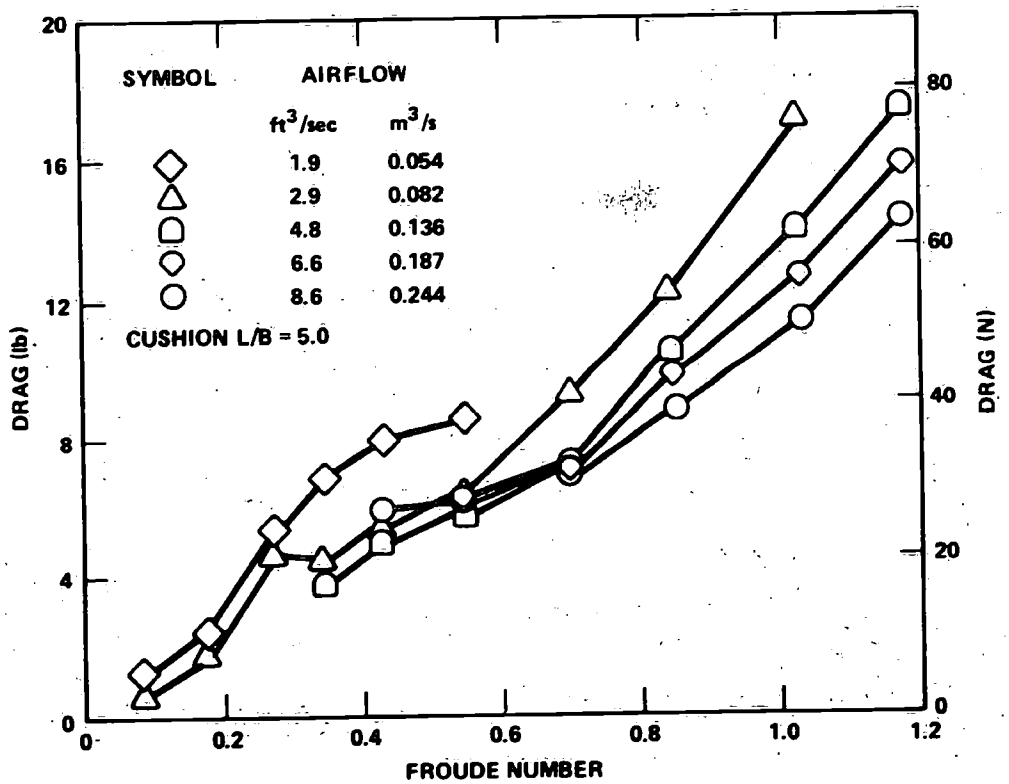

Figure 3.5.6 - Drag Variations Due to Total Airflow Rate

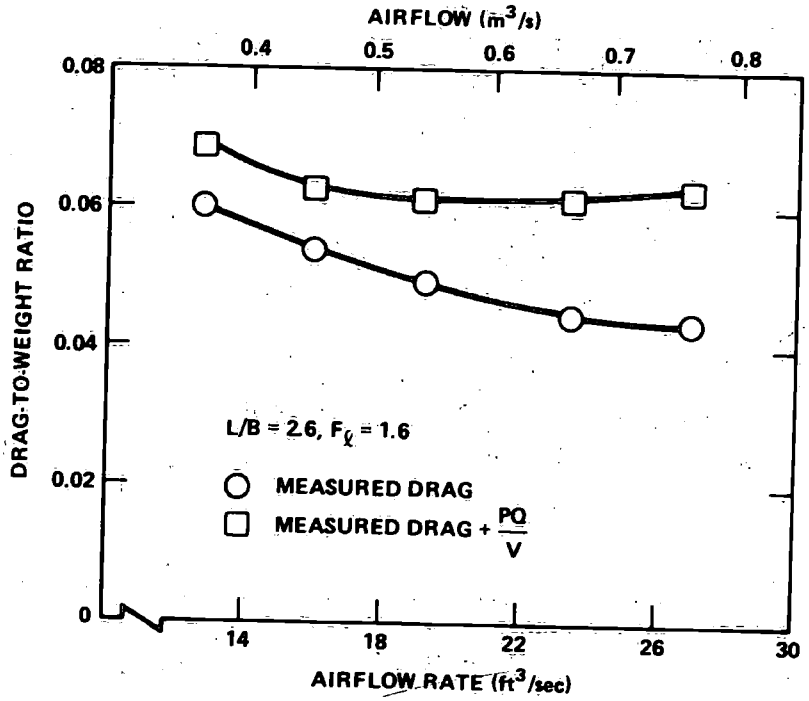

Figure 3.5.7 - Effect of Airflow Rate on Drag

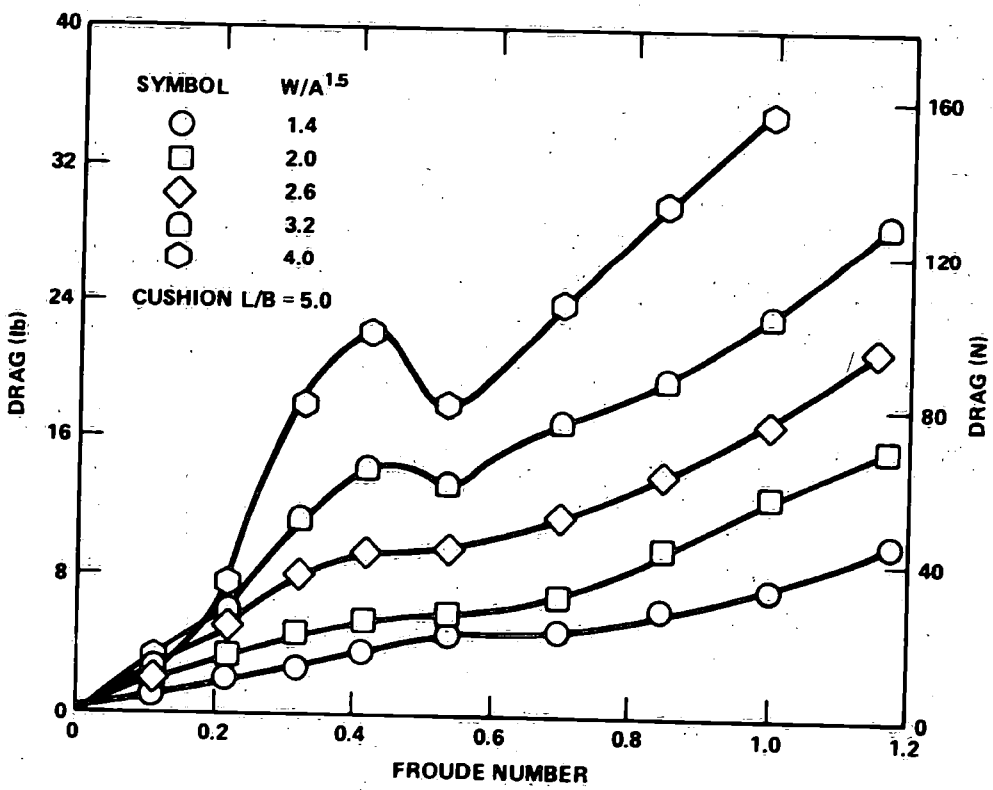

Figure 3.5.8 - Effect of Weight on Drag

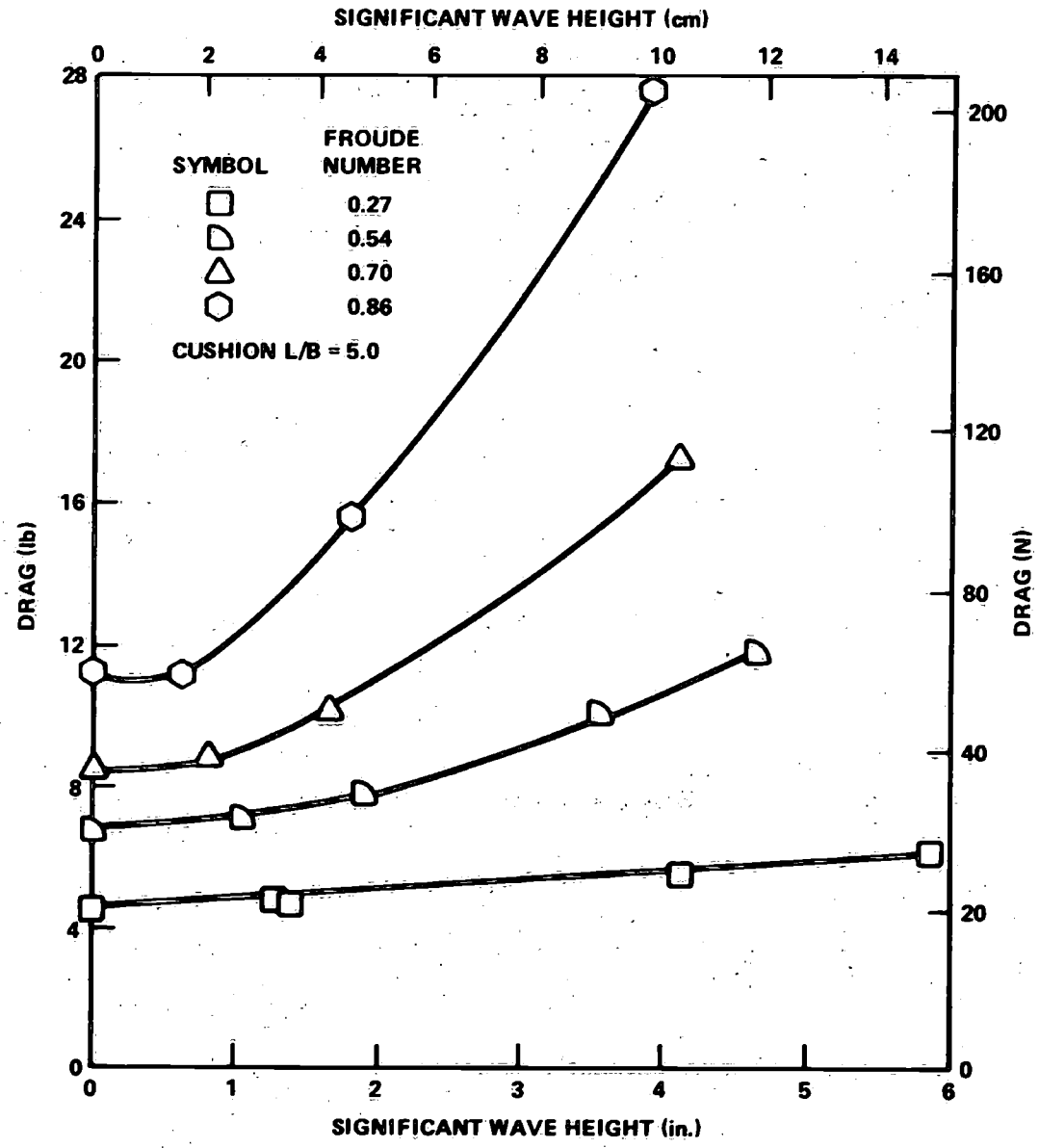

Figure 3.5.9 - Drag Variation with Significant Wave Height for Constant Froude Numbers

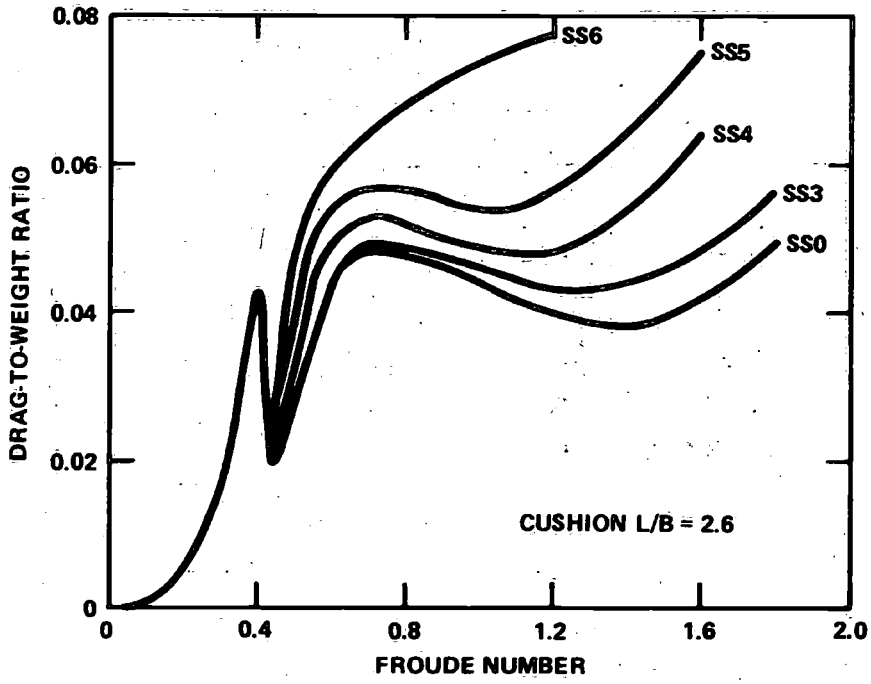

Figure 3.5.10 - State of Sea Effect on Drag

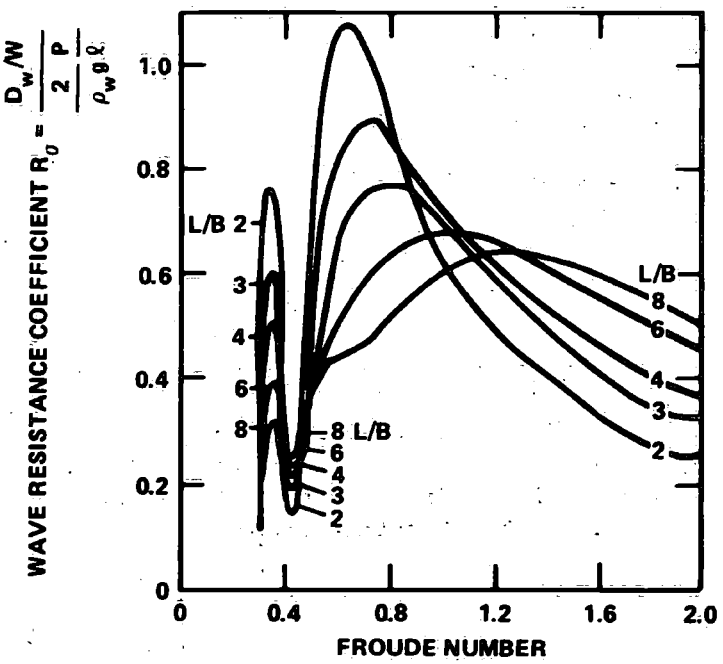

Figure 3.5.11 - Doctors' Wave Resistance Coefficient

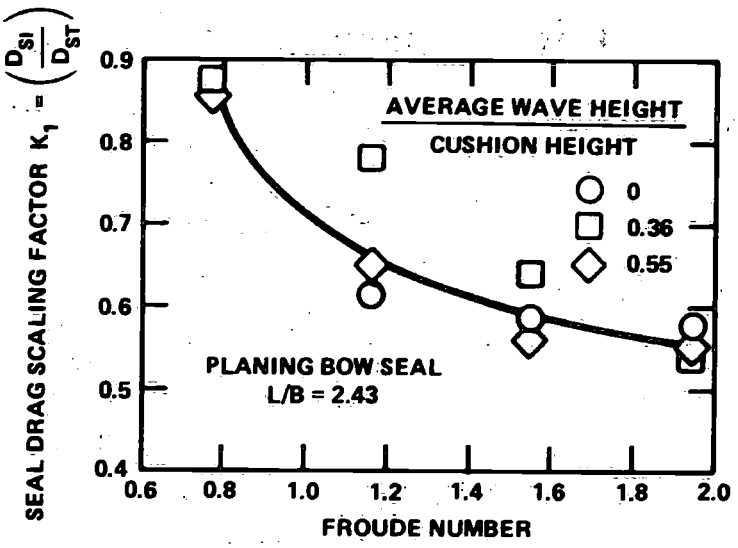

$$\left(\frac{D_R}{W}\right)_P = \left[K_1 + (1-K_1)\left(\frac{C_{f_P}}{C_{f_M}}\right)\right]\left(\frac{D_R}{W}\right)_M$$

Figure 3.5.12 - Residual (Seal) Drag Scaling Factor and Equation

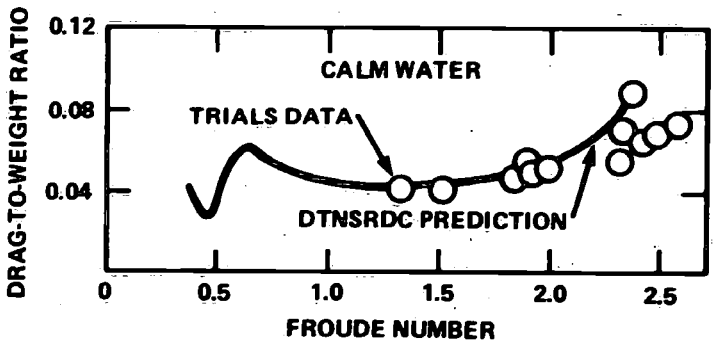

Figure 3.5.13 - Comparison of Scaled and Measured SES-100B Drag (From Reference 2)

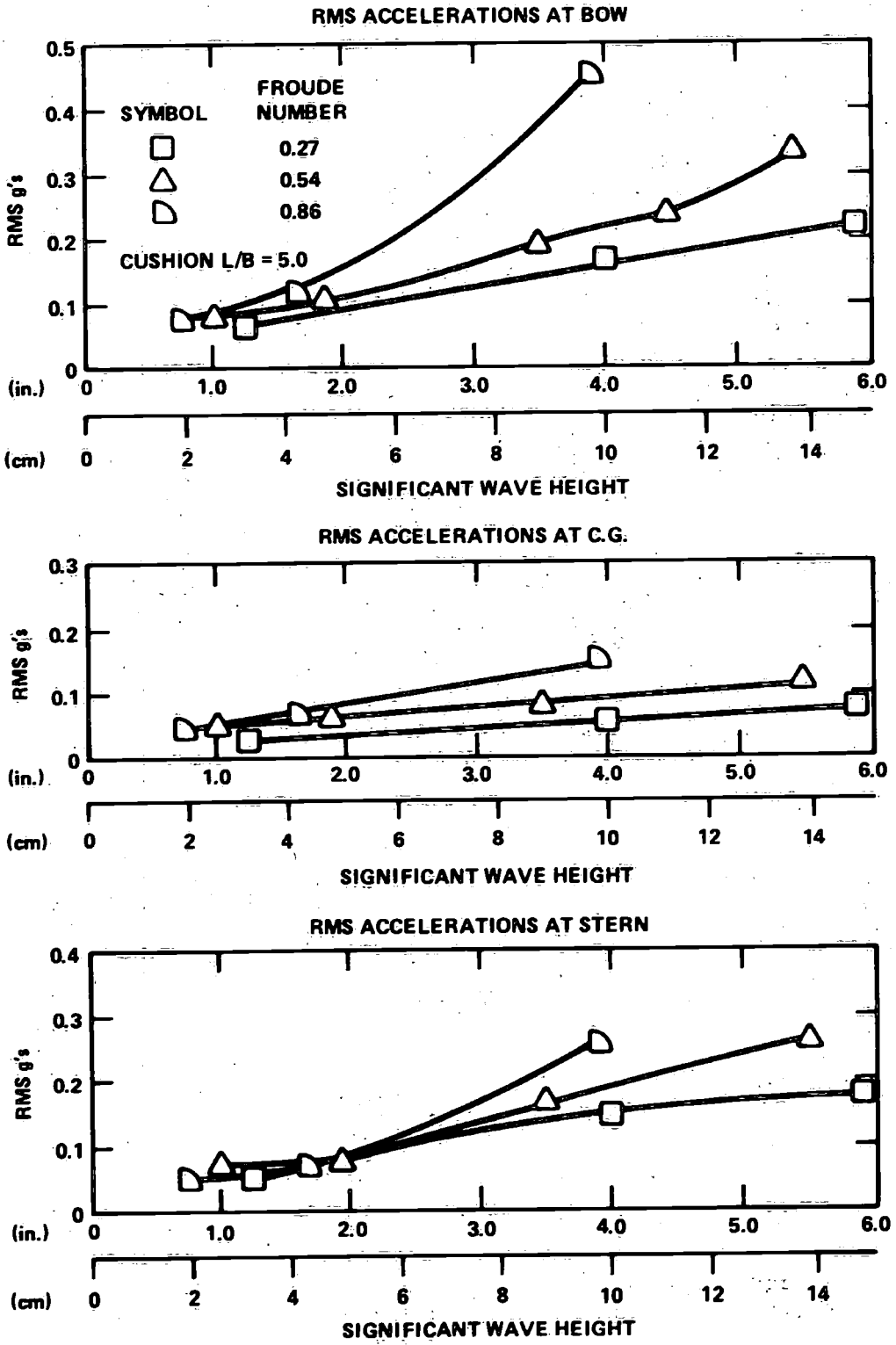

Figure 3.5.14 - Root Mean Square Accelerations for Various Significant Wave Heights and Froude Numbers

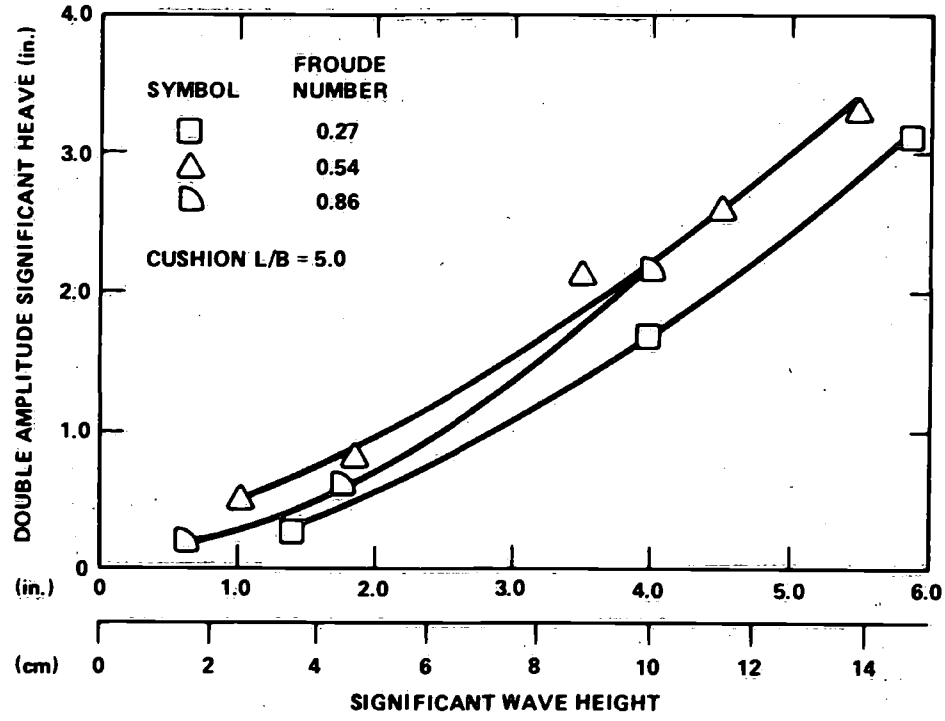

Figure 3.5.15 - Double Amplitude Significant Heave Oscillations

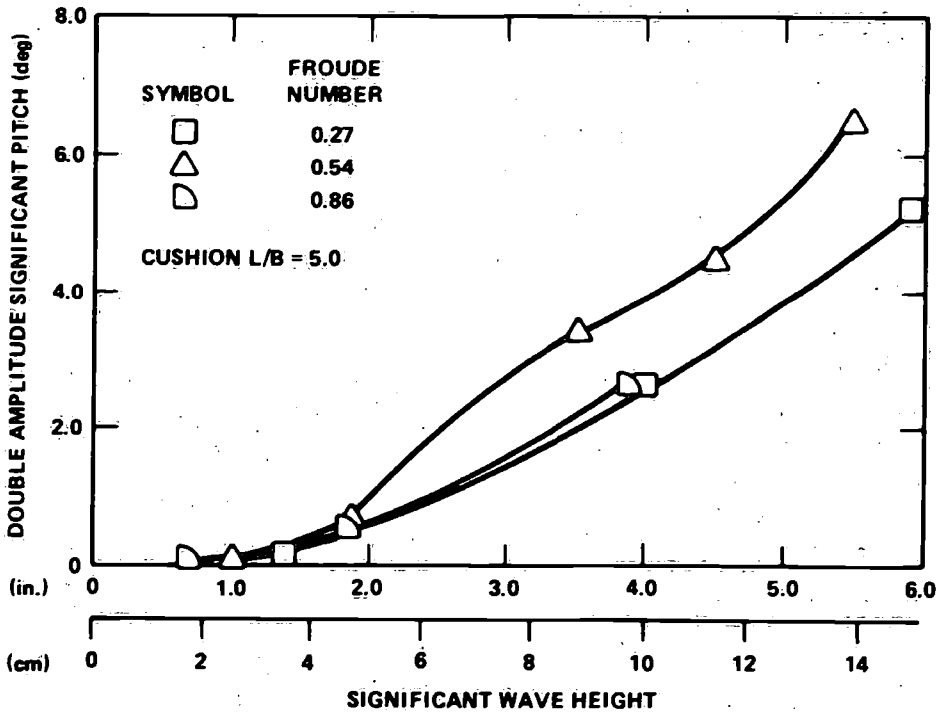

Figure 3.5.16 - Double Amplitude Significant Pitch Oscillations

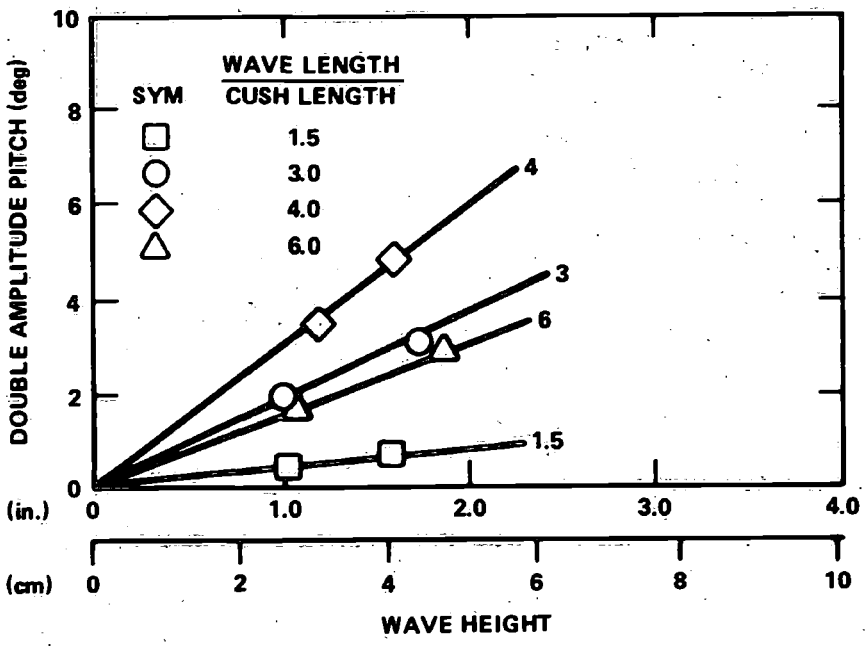

Figure 3.5.17a - Froude Number = 1.72

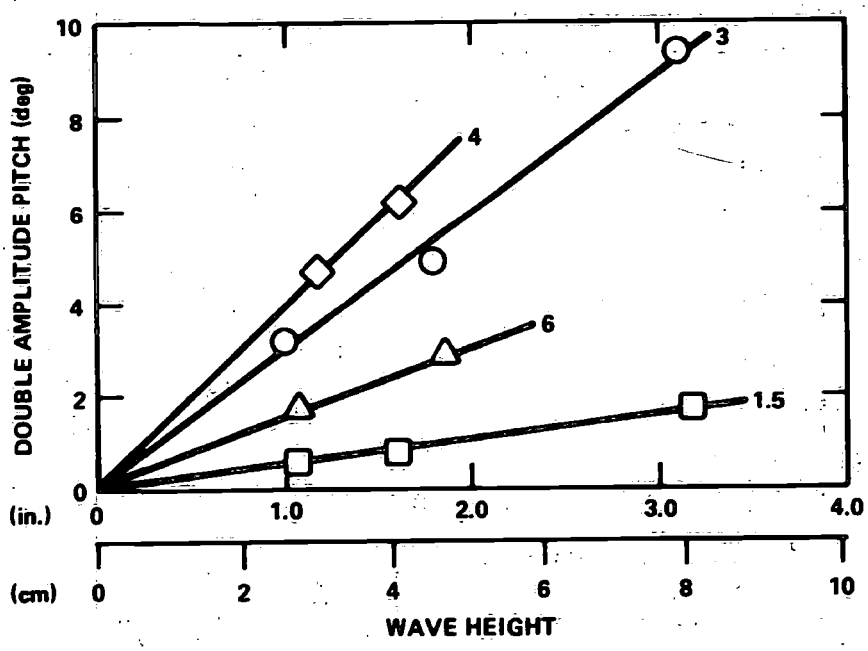

Figure 3.5.17b - Froude Number = 1.28

Figure 3.5.17 - Pitch Linearity in Regular Head Seas for an L/B 2.5 SES Model

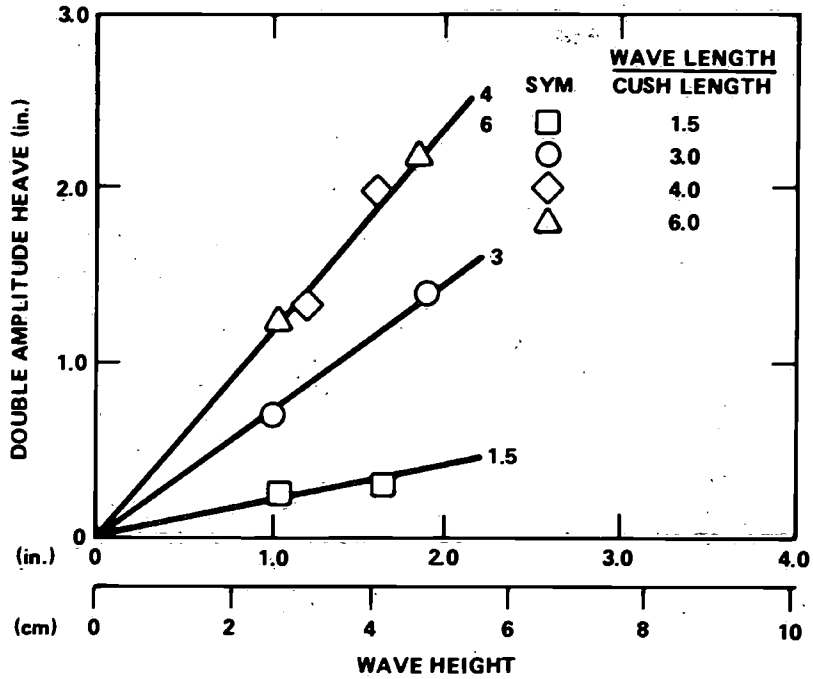

Figure 3.5.18a - Froude Number = 1.72

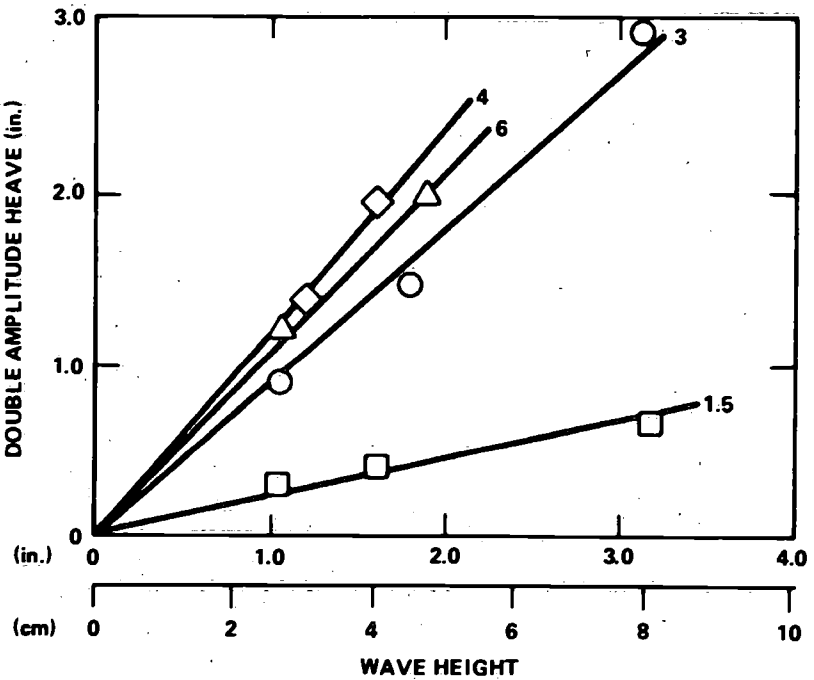

Figure 3.5.18b - Froude Number = 1.28

Figure 3.5.18 - Heave Linearity in Regular Head Seas for an L/B 2.5 SES Model

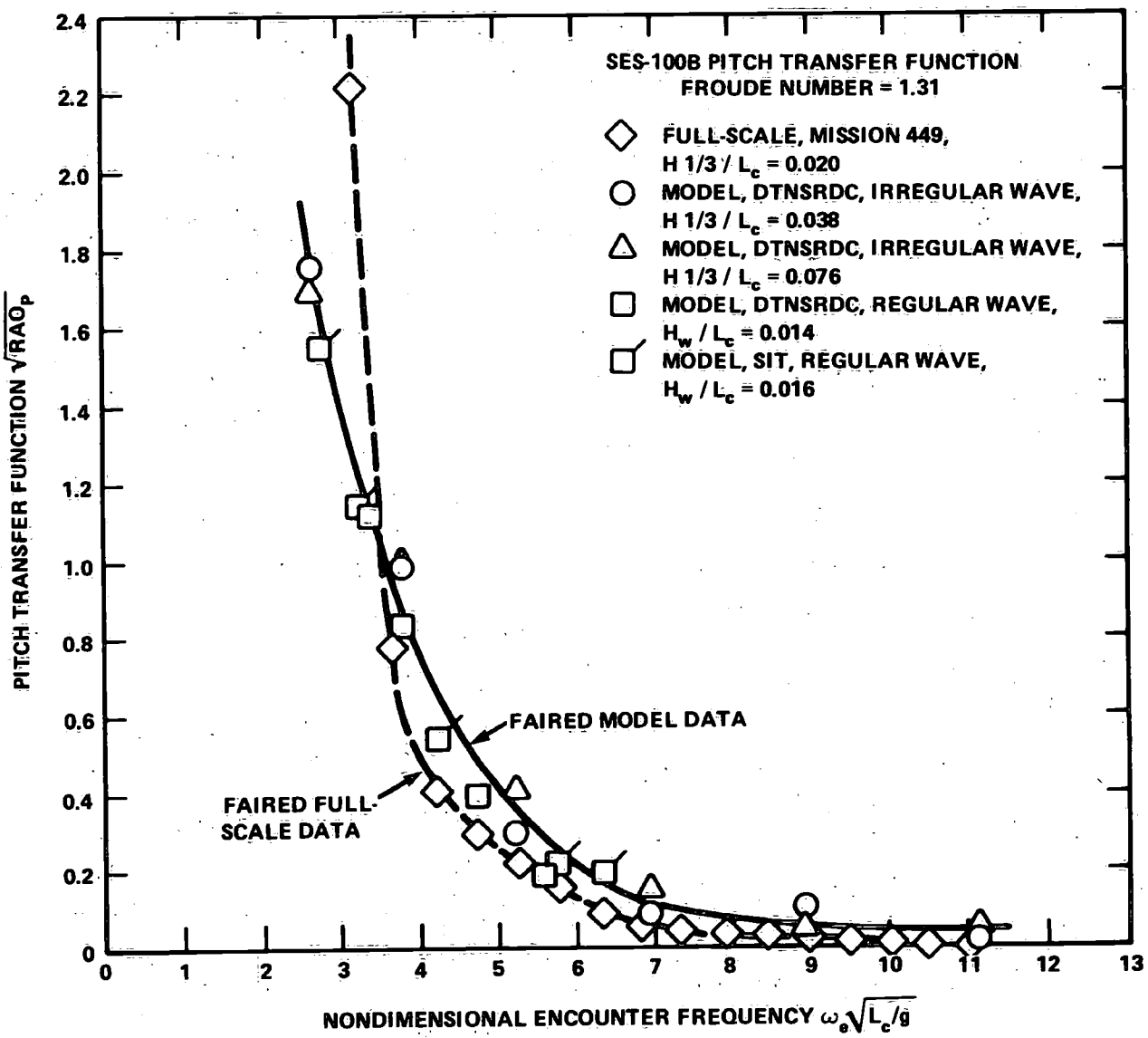

Figure 3.5.19 - SES-100B Model and Full-Scale Pitch Response Comparison at a Froude Number of 1.31

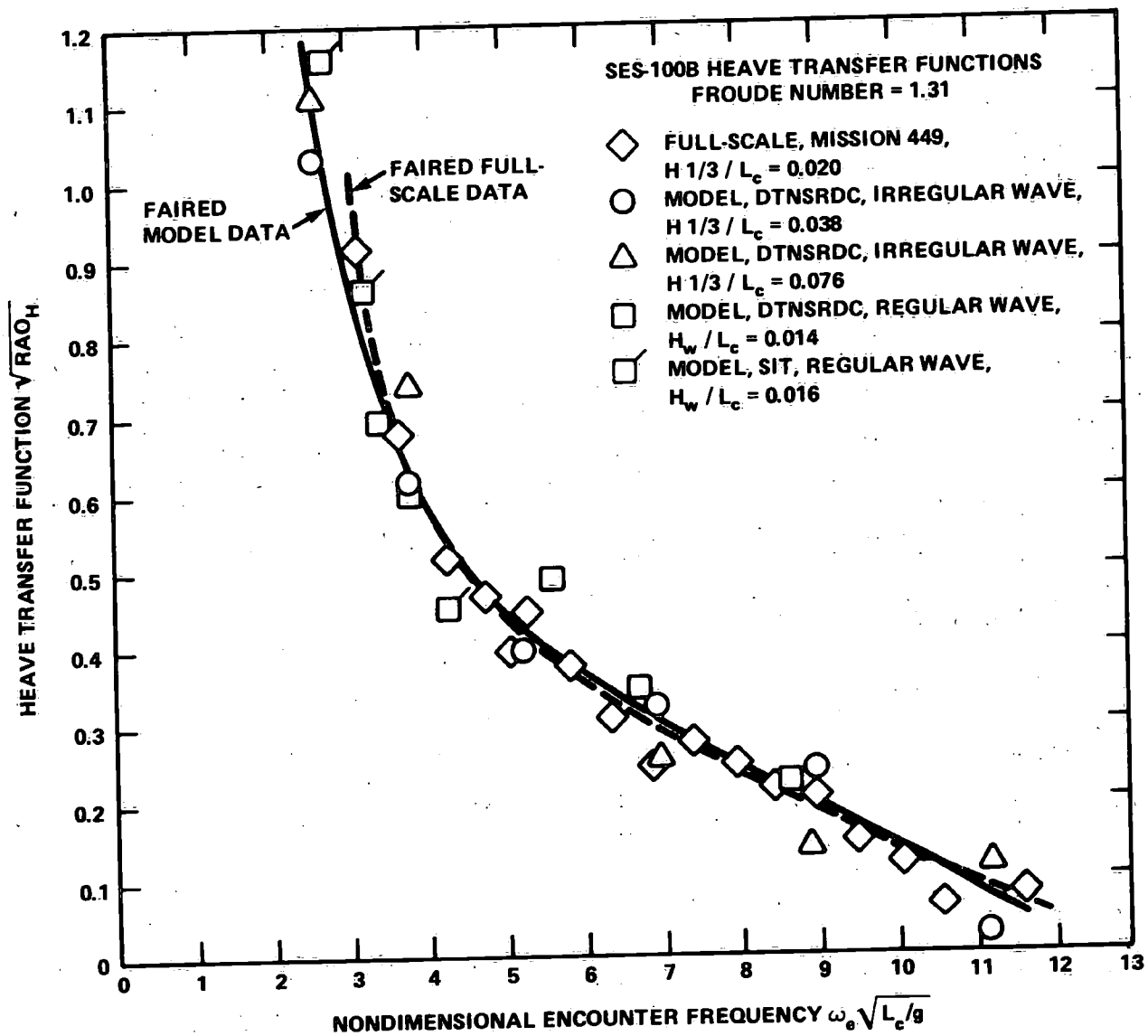

Figure 3.5.20 - SES-100B Model and Full-Scale Heave Response Comparison at a Froude Number of 1.31

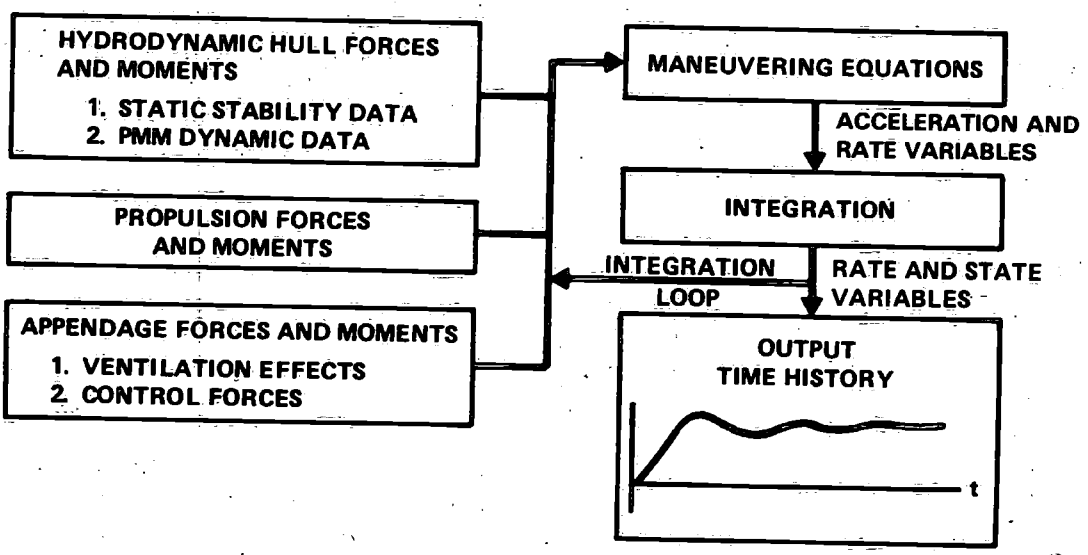

Figure 3.5.21 - Data-Based Maneuvering Simulation Schematic of a SES

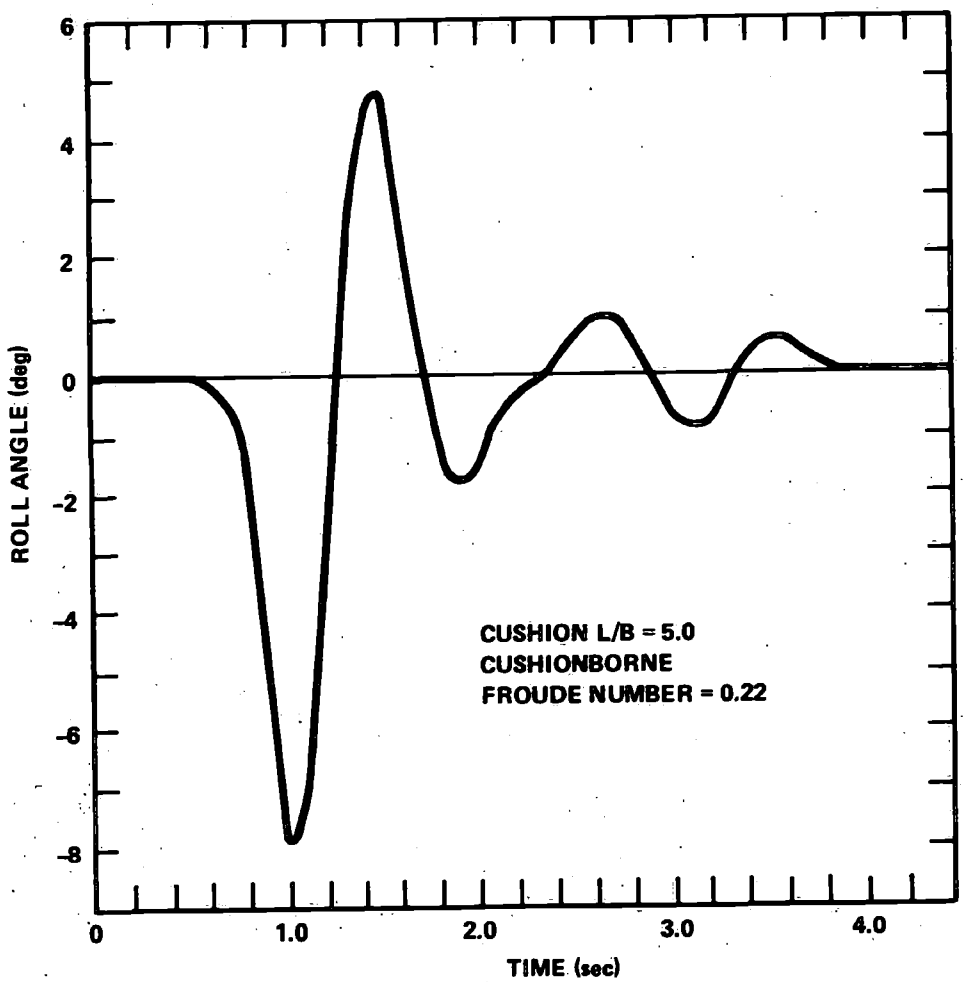

Figure 3.5.22 - Roll Damping Determination Using a Single Forced Roll

Figure 3.5.23 - Static Stability Data

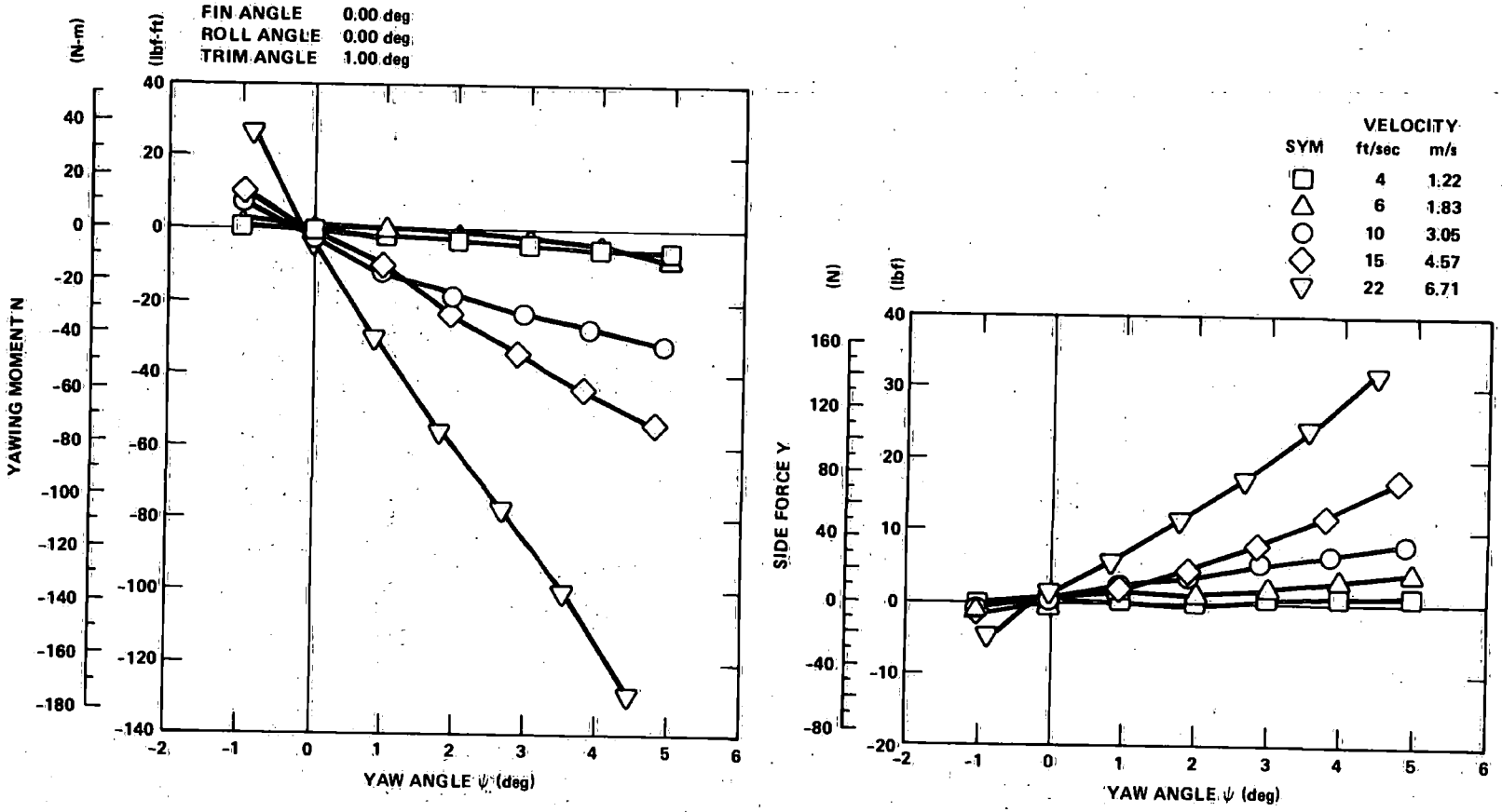

Figure 3.5.23a - Yawing Moment and Side Force Data

Figure 3.5.23 - (Continued)

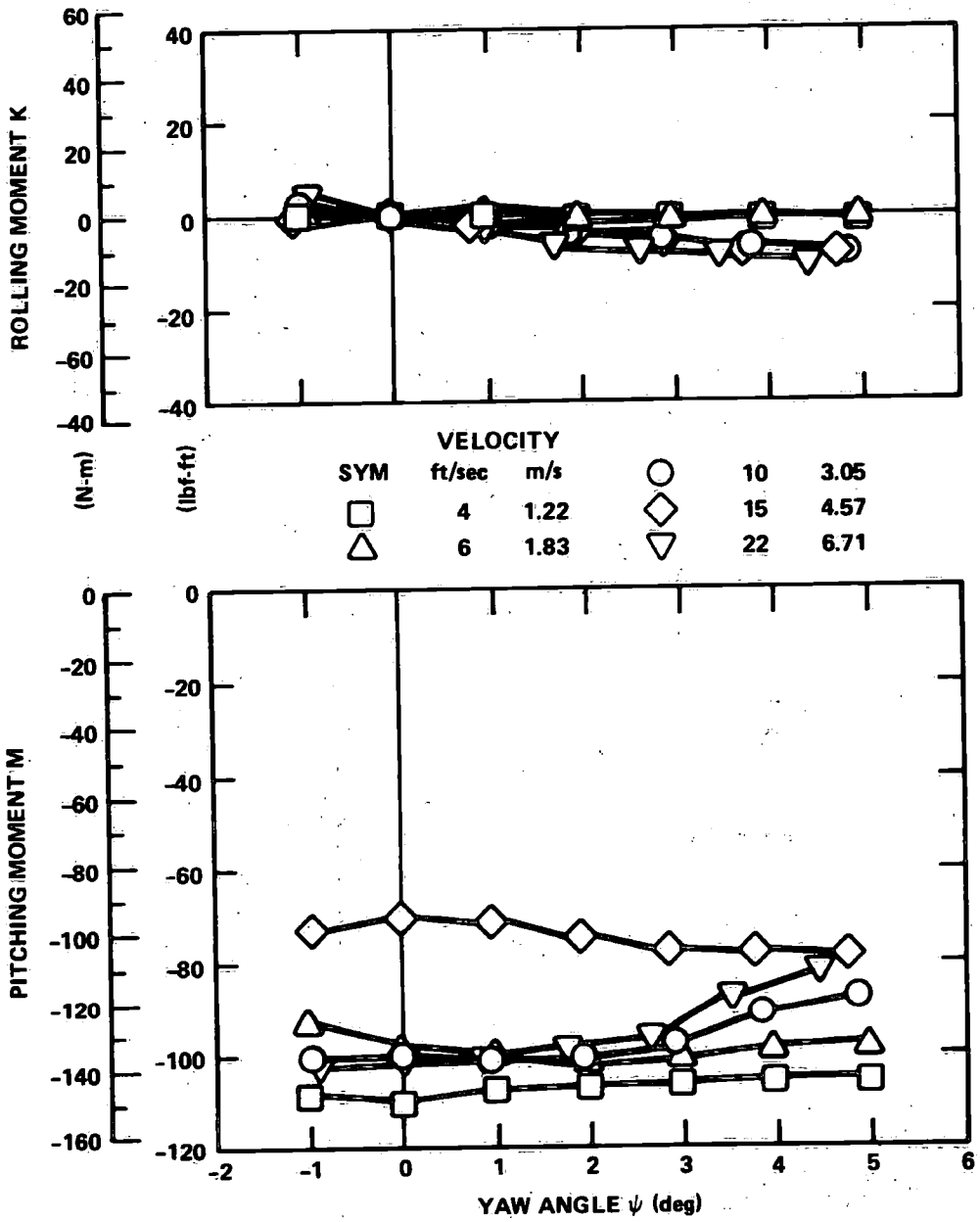

Figure 3.5.23b - Rolling Moment and Pitching Moment Data

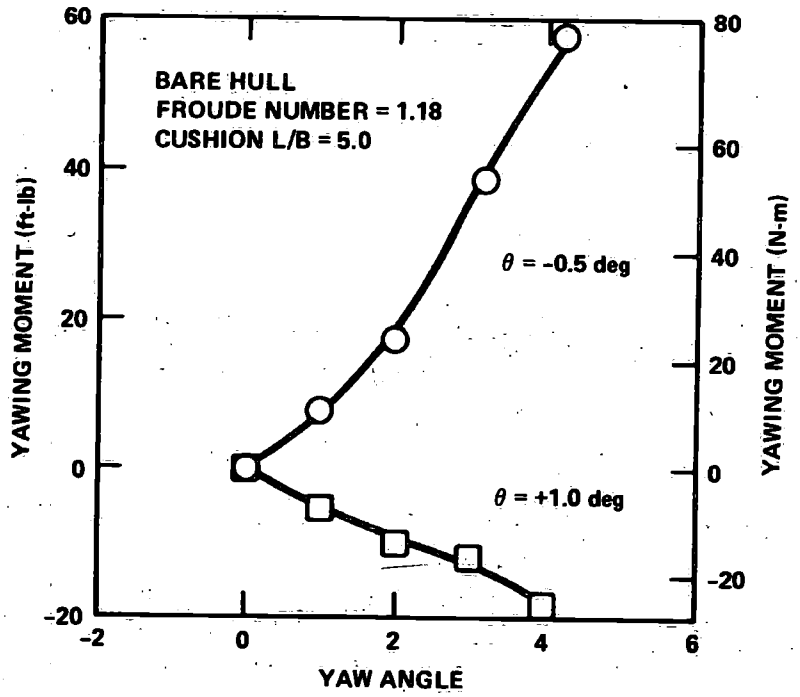

Figure 3.5.24a - Pitch Attitude Effect on Yaw Moment

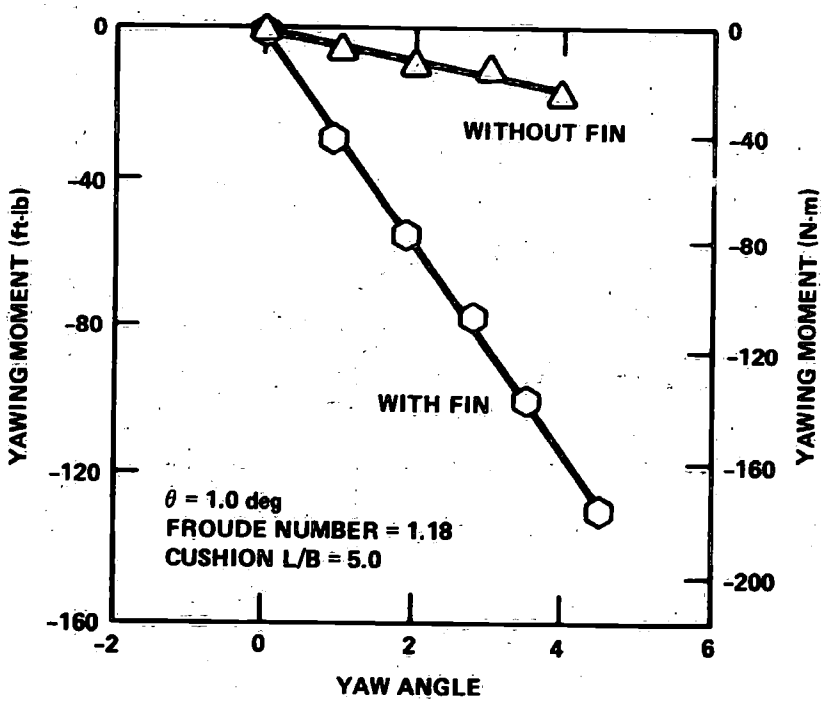

Figure 3.5.24b - Ventral Fin Effect on Yaw Moment

Figure 3.5.24 - Yaw Stability Trends

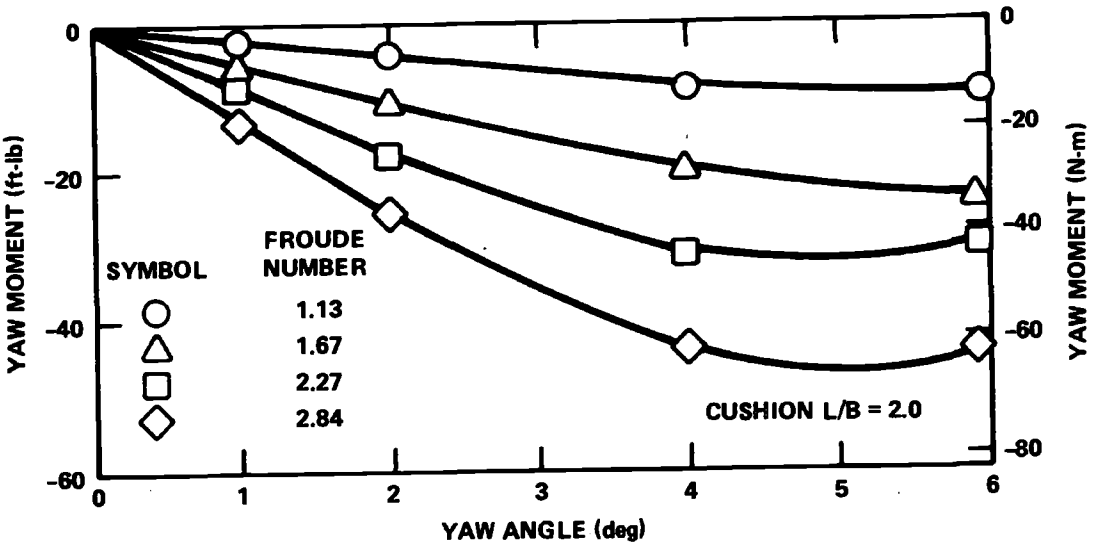

Figure 3.5.25 - Yaw Moment Nonlinearities

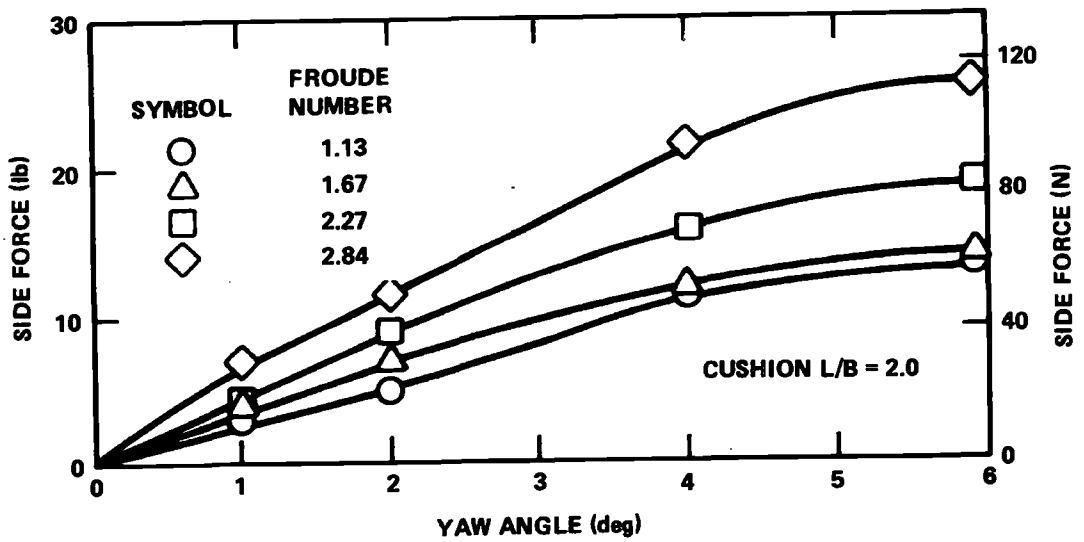

Figure 3.5.26 - Side Force Nonlinearities

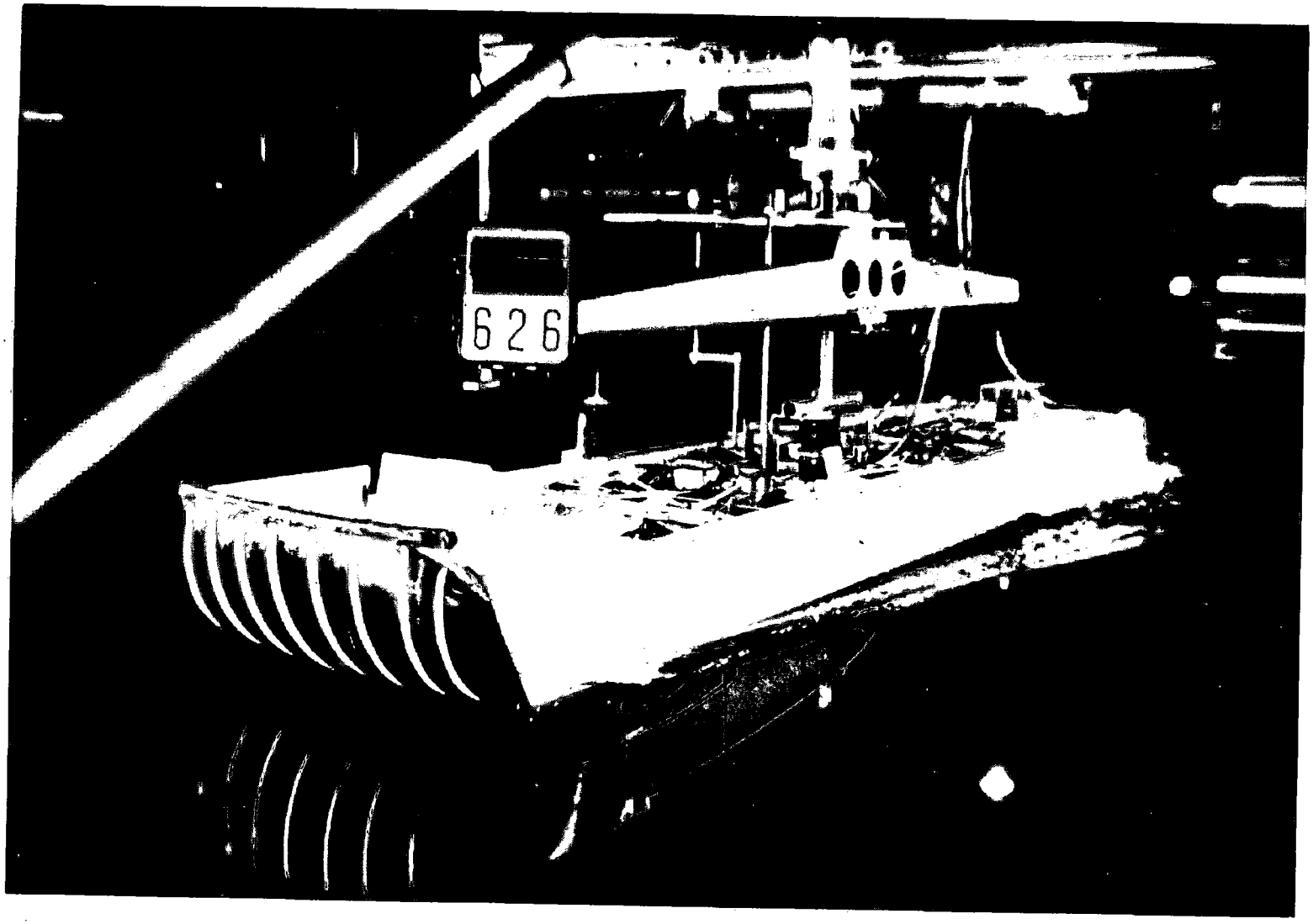

Figure 3.5.27 - Planar Motion Mechanism on Which an L/B 5.0 SES Model is Installed

TABLE 3.5.1 - A SUMMARY OF HYDRODYNAMIC YAW VELOCITY DERIVATIVES FOR A LENGTH-TO-BEAM RATIO 5 MODEL

Bare Hull Configuration								
Model Test Condition					Planar Motion Derivatives			
U (ft/sec)	θ (deg)	d (in.)	ϕ (deg)	β (deg)	δ (deg)	$Y'_r \times 10^5$	$K'_r \times 10^5$	$N'_r \times 10^5$
10.0	0.25	2.05	0	0	NA	-166.52	-8.29	-136.40
10.0	1.25	1.80	0	0		-62.60	-12.61	-104.10
10.0	0.25	2.05	1.0	0		-134.72	-7.41	-126.99
10.0	1.25	1.80	1.0	0		-38.48	-10.75	-110.88
22.0	0.25	1.05	0	0		-24.25	-0.96	-50.61
22.0	1.25	1.40	0	0		-76.04	-0.31	-36.73
22.0	0.25	1.05	1.0	0		-27.95	-0.72	-52.22
22.0	1.25	1.40	1.0	0		56.24	-1.97	-39.35

With Rudder Configuration								
Model Test Condition					Planar Motion Derivatives			
U (ft/sec)	θ (deg)	d (in.)	ϕ (deg)	β (deg)	δ (deg)	$Y'_r \times 10^5$	$K'_r \times 10^5$	$N'_r \times 10^5$
10	0.25	2.05	0	0	0	33.2	-29.15	-300.5
22	0.25	1.05	0	0	0	57.9	-3.54	-94.7
10	1.25	1.80	0	0	0	204.9	-30.99	-254.1
					-2	202.3	-32.51	-269.2
					-6	212.1	-32.25	-274.8
22	1.25	1.40	0	0	0	235.6	-13.97	-144.0
					-2	192.5	-17.06	-163.6
					-6	181.2	-3.87	-123.6

TABLE 3.5.2 - A SUMMARY OF HYDRODYNAMIC YAW ACCELERATION DERIVATIVES FOR A LENGTH-TO-BEAM RATIO 5 MODEL

Bare Hull Configuration								
Model Test Condition					Planar Motion Derivatives			
U (ft/sec)	θ (deg)	d (in.)	ϕ (deg)	β (deg)	δ (deg)	$Y'_{\dot{r}} \times 10^5$	$K'_{\dot{r}} \times 10^5$	$N'_{\dot{r}} \times 10^5$
10	0.25	2.05	0	NA	NA	-19.98	8.95	1.62
			1			7.24	3.59	2.06
	1.25	1.80	0	NA	NA			
			1			5.31	3.60	6.03
22	0.25	1.05	0			3.09	1.58	3.26
			1			33.85	1.32	2.76
	1.25	1.40	0			20.71	-0.96	1.30
			1			19.53	0.92	4.09

With Rudder Configuration								
Model Test Condition					Planar Motion Derivatives			
U (ft/sec)	θ (deg)	d (in.)	ϕ (deg)	β (deg)	δ (deg)	$Y'_{\dot{r}} \times 10^5$	$K'_{\dot{r}} \times 10^5$	$N'_{\dot{r}} \times 10^5$
10	0.25	2.05	0	NA	0	-29.95	9.137	33.89
	1.25	1.80	0	NA	0	-21.17	5.85	22.01
			0		-2	-19.49	6.66	24.86
					-6	-15.78	6.69	26.86
22	0.25	1.05			0	20.63	5.86	8.53
	1.25	1.40			0	-24.90	2.08	29.33
					-2	-21.14	4.43	34.93
					-6	-1.06	3.75	22.58

3.6 AIR CUSHION VEHICLES

by

Martin J. Stevens

Experimental and Electronic Laboratory

British Hovercraft Corporation

and

Sergei D. Prokhorov

Krylov Ship Research Institute

3.6.1 CONCEPT DEFINITION

For the present purposes, the term air cushion vehicle (ACV) has been used as a name for a class of vehicle which causes air pressure, higher than atmospheric, to be exerted on the surface of the water directly below it, such that the integral of this additional air pressure over the vehicle's planform projected on the water surface produces a force equal in magnitude to the vehicle weight. The space between the water surface and the vehicle is called the air cushion.

3.6.1.1 Craft Configuration

Typically, the air cushion is contained by a flexible skirt, consisting of a flexible structure separating the air cushion area from the atmospheric air around the whole perimeter of the craft. There may also be flexible elements subdividing the cushion area in plan view. (See Figure 3.6.1). The detailed configuration of the flexible skirts varies considerably but a typical scheme, consisting of a bag component with "finger" type segments attached, is shown in Figure 3.6.2.

The ACVs usually employ air propulsion, normally either ducted propulsors or airscrews and sometimes ducted plenum air, making them amphibious. Control is largely aerodynamic in form, comprising aerodynamic lifting surfaces (e.g., fins, rudders, and elevators) often sited in the propeller slipstream. Thrust vectoring is achieved by swivelling pylon-mounted propellers and also cushion or plenum bleed systems (primarily for low speed control). Also pitch and roll control may be achieved by either a fuel or water ballast system and/or a controlled movement of the center of pressure relative to the craft center of gravity (C.G.) by means of either skirt lifting or shifting systems.

Craft are typically of rectangular planform with a semicircular bow. Current operational craft vary in size up to a maximum displacement of about 300 tons and 50 meters in length, having maximum Froude number, based on cushion length, in the region of 2.0. Typical service speeds are usually in the range of F_n (based on cushion length) between 0.8 and 1.5. Cushion length-to-beam ratios are generally on the order of 1.5 to 2.7 and the cushion pressures on modern marine vehicles tend to vary up to 5000 N/m^2.

It is often convenient to express various parameters in coefficient form (e.g., cushion aspect ratio, cushion loading coefficient, flow rate coefficient), and examples of these are defined in Reference 2, which provides the terminology and notation currently in use with ACV's in the United Kingdom. No internationally agreed list of symbols and terminology for ACV's exists at the present time and it is recommended that these should be reviewed with regard to extension of the present list of Standard ITTC symbols to include ACV's.

3.6.1.2 Model Configuration

The models used in the development of ACV's range from relatively simple, two-dimensional representations, through small scale solid or partial models for wind tunnel use, to special test rigs, and finally, to dynamic models for use in a towing tank and also, possibly, in free running form on natural test sites.

If the complete model is intended for multipurpose use, it is likely that it will be both visually and dynamically representative of the full-scale craft, and be ballasted to the correct scale weight, center of gravity, and inertias about the axes of freedom.

The scale chosen for the dynamic model will vary depending upon the test facilities available and also the use to which it may be put. If it is intended to use the model in free-flight, radio-controlled form, as well as on a towing tank, it is likely that this will dictate the minimum size of model which can accommodate the radio control gear and instrumentation package. Also from the practicable considerations of scaling the structure, lift fans, skirts, etc., a larger model is likely to be preferable.

The maximum size of the model is governed by the size of the towing tank, bearing in mind the sea conditions in which the full-scale craft is to operate in relation to the wavemaking capability of the tank, and also the scale speed which may be required. Provided the tank width is four to six times the model beam, wall effects are generally negligible but corrections to the results will be necessary in smaller

tanks. The tank water depth is a further parameter to consider, and unless tests are specifically required in shallow water, the model length should be limited to about twice the water depth in order to keep wave resistance corrections within reasonable limits (Figure 3.6.3). Particular care should be taken to ensure that, for the model scale selected, the hump speed does not coincide with the critical speed for the tank ($gh/V^2 = 1$, where h is the water depth). This speed is associated with a discontinuity in the wavemaking drag (see Figure 3.6.4), but provided the hump speed is situated well below the critical tank speed, the wavemaking resistance (and hence the change in resistance) at the critical speed will be small.

In some facilities the lift system is reproduced in considerable detail to ensure that the damping and stiffness of the vehicle are modeled as accurately as possible. Geometrically scaled fans are used and, to ensure the correct scale volume flow, the fans may, where appropriate, be run at a slightly higher than scale speed on the model. The necessary speed correction can be estimated by the use of formulas such as those of Moody (Reference 3), from which can be derived the following relationship between model and full-scale impeller efficiency.

$$\frac{1 - \eta_m}{1 - \eta_f} = \lambda^{0.2}$$

where m and f refer to model and full-scale, respectively, and λ is the scale ratio. Such formulas generally apply only at the maximum total efficiency point, but available evidence suggests that they should also be reasonably accurate over flow excursions on the order of ± 25 percent of the design value. Because the efficiency difference is essentially due to a difference in pressure loss, it is possible to suggest a change in impeller speed which would approximately compensate for this pressure difference. Depending upon the scale of the model this can imply that the model fans have to be run up to approximately 5 percent faster than the scaled rpm to provide the correct volume flow. Alternatively, it may be accepted that the model will provide a slightly pessimistic answer when the scaled rpm is used.

The problems become more difficult for large craft as the model scale, and hence fan size, is reduced. In particular, it may become difficult to accurately represent the fan to intake junction, which can have a substantial effect on the lift system performance. For this reason, some establishments do not employ geometrical models

of the full-scale fans, and instead develop representations which provide the scaled airflow rate and have the correct pressure versus airflow characteristics.

Typically, models are constructed to scales between 1:6 and 1:12, providing models in the range 2 m to 4 m in length. For a multipurpose model the minimum weight is likely to be approximately 70 kg (equipped with radio control gear and some instrumentation) while the maximum weight for a towing tank model is approximately 250 kg. The structural stiffness is not usually scaled. Models are constructed in lightweight materials such as wood, glass reinforced plastic (GRP), carbon fiber, light alloy, and polyvinyl chloride (PVC), foams etc. The latter material can have advantages since it simplifies structural modifications which may be required during a development program. Further examples of constructional techniques are given in Reference 4.

Skirts are manufactured from commercially available proofed fabrics or specially produced synthetic rubber coated fabrics. Material properties considered in the choice of material are bending stiffness (Youngs modulus), elastic properties, and weight. With commercially available materials it is unlikely that both stiffness and weight will scale correctly, but for certain applications this can be overcome by adding mass at discrete points in the skirt. One method of scaling bending stiffness is outlined in Section 3.6.8.

3.6.1.3 Scaling Approach

In accordance with accepted tank testing practice, Froude scaling laws are generally applied to ensure that gravitational as well as fluid dynamic pressure effects are correctly scaled. There are, however, several effects which are not accounted for by this method of scaling.

Aerodynamic forces and moments should be evaluated at the proper Reynolds number. When scaling hydrodynamic wetting drag, account should be taken of the difference in Reynolds number between the model and full-scale regimes. However, because of the indeterminate wetted area of the skirts, it may be impracticable to apply this correction in the case of an amphibious hovercraft. Furthermore, the influences of viscosity and surface tension on water wetting and spray drag must also be considered, in particular the fine spray generated by the escape of cushion air is not amendable to Froude scaling.

When operating in waves, the effects of absolute ambient pressure on the behavior of the cushion system must also be considered. In these unsteady conditions, air compressibility effects might be expected to arise, and a suggested criterion,

for scale effects of this nature, which is a modification of the criterion from Reference 5, has the following form

$$\frac{\Delta PV}{P_0\ QT} \ll 1$$

and the process is considered to be isothermal.

where ΔP = steady state cushion pressure (gage)
Q = airflow rate
V = cushion volume
P_0 = absolute atmospheric pressure
T = period of oscillation

Meeting the said condition indicates that there is no significant scale effect. From the form of this expression it follows that with an increase in the flow rate Q the scale effect is smaller, all other conditions being equal.

Experience to date on conventional fully skirted craft suggests that compressibility effects are small as regards the air cushion as a whole, and further model/full-scale correlation experience is required to substantiate the above expression which is based on theoretical considerations alone.

Special arrangements need to be made with regard to any portion of the skirt which acts like a sealed bag (where flow rate is very small or zero) to ensure that the pressure-volume relationship is, at least approximately, correctly scaled. This can be achieved by connecting each bag section to a spring loaded sealed pressure compensator designed so that the pressure-volume relationship of the bag and compensator combination is approximately correct (Figure 3.6.5).

3.6.2 TESTS (GENERAL)

Prior to towing tank tests on an ACV development work is likely to be implemented on individual craft components and bench tests conducted with the complete model. These are discussed in Section 3.6.3. Self-propulsion tests are not normally conducted on ACV's and performance is derived from calm water resistance tests, seakeeping tests, and separate propulsor investigations (see Sections 3.6.4, 3.6.5, and 3.6.7, respectively).

The ability of an ACV to operate over very shallow water and to negotiate various types of terrain and size of obstacle may also need to be investigated. This type of work often requires special facilities and the test methods employed are not described in this document.

3.6.3 PRELIMINARY TESTS

3.6.3.1 Flexible Skirts

During the development of new flexible skirt schemes, it is convenient to use stationary test rigs for testing two-dimensional flexible skirt components. In this way it is possible to evaluate the agreement of flexible skirt form parameters to their design values, the degree of stability, and flexible skirt component stiffness, as well as to the frequency response of the skirt design.[1] When necessary, similar model tests can be carried out over the water surface.

3.6.3.2 Fans

The characteristics of lift fans are often studied in special test rigs, both in an "idealized" environment and when installed in a typical craft plenum system. The characteristics may also be studied under fluctuating output flow conditions.[6]

3.6.3.3 Complete Craft at Zero Speed

Bench model tests for estimating supporting forces and stability characteristics are a necessary phase preceeding model tests in a towing tank. Test facilities are used which enable tests to be carried out over a solid ground board as well as over water.

The model is free to perform vertical oscillations, heel, and trim. When the model is loaded or during the action of heeling and trim moments, kinematic parameters, and also side and longitudinal forces may be recorded using a two component dynamometer at the model attachment point. Heel and trim are measured by potentiometers. To measure static pressures use is made of liquid manometers or elecrical gages.

Tests over a solid ground board and over water are carried out to find the relationships between model hovering height, loading, and air flow rate as well as stability characteristics.

3.6.4 RESISTANCE (SMOOTH WATER)

3.6.4.1 Components of Resistance

Depending upon the purpose of investigations, various authors use various approaches when subdividing resistance into components. The following classification

of drag components can serve as an example with fairly wide application. As with many others, this classification does not take into account the interdependence of components and probably does not exhaust all possibilities. The following hovercraft calm water resistance components are considered.

Aerodynamic profile drag

Intake momentum drag

Wavemaking drag

Residual drag (including wetting drag of the skirts, jet component due to the air outflow form the cushion, etc.)

3.6.4.1.1 Aerodynamic Drag

3.6.4.1.1.1 Profile drag. This comprises the sum of the aerodynamic skin friction and form drag of the craft. It is customary to express the profile drag in terms of a nondimensional drag coefficient, C_{dp} such that:

$$D_p = \frac{1}{2} \rho_a V_a^2 A_f C_{dp} \tag{3.6.1}$$

where

ρ_a = air density

V_a = air speed

A_f = craft frontal area

C_{dp} = profile drag coefficient

Profile drag coefficients typically vary from 0.3 to approximately 0.8 depending upon the craft.

3.6.4.1.1.2 Intake momentum drag. This is caused by having to accelerate the air entering the lift fans from rest up to the velocity of the craft. To evaluate the momentum drag it is usually most convenient to assume that all the air taken in by the lift fans finally leaves the craft in a symmetrical pattern. The drag can then be expressed as:

$$D_m = \rho_a \cdot Q_{sum} \cdot V_a \tag{3.6.2}$$

where Q_{sum} is the total volume flow entering the lift fans per unit time.

Any significant departures from the symmetrical situation, due for example, to air leaking through relatively large gaps in the rear skirts or exhausting through the main engines, are then taken into account by evaluating the associated thrust terms.

3.6.4.1.2 Over Water Drag

3.6.4.1.2.1 Wavemaking drag. When a pressure distribution, such as that under a hovercraft cushion, moves over the surface of the water, a wave system is set up, the shape of which depends upon the speed of the craft and the characteristics of the pressure distribution. This disturbance to the surface gives rise to a drag term known as wavemaking drag. As speed increases, the drag rises and falls through a series of humps and hollows until the primary hump if reached. Thereafter, the wavemaking drag decreases, becoming almost negligble at very high speeds. In practice, as the craft accelerates, the theoretical lower speed wave humps may not fully develop or may be steepness limited. An example of the wavemaking drag at low speed is shown in Figure 3.6.4.

The theory developed by Newman and Poole[8] for sharp edged rectangular pressure distributions is most commonly used to predict the magnitude of this component of drag. However, some researchers feel that more recent work published by Doctors,[9] which assumes a smooth pressure drop-off at the edges of the cushion, gives more realistic results particularly at speeds below the main hump.

3.6.4.1.2.2 Calm water wetting drag (or residual drag). This is another, largely hydrodynamic, drag term which is experienced in the calm water case. It is generally interpreted as being the difference between the total calm water drag and the sum of the components discussed above, i.e., the profile, momentum and wavemaking drags, and at present can only be derived from model tests or estimated empirically.

It is called 'wetting drag' because it is primarily due to water contact, either from direct immersion or spray impact. However, it also includes a number of other force components the most significant of which is a trim term associated with the pitch attitude of the craft. In calm water, optimum performance is often achieved at bow down trim conditions in which a sizable forward thrust is produced by additional air leakage at the rear. If the calm water wetting drag is separated from this "trim thrust" it can be expressed as follows:

$$D_{wet} = D_{tot} - D_p - D_m - D_{wm} - D_{trim}$$

where D_{wm} = wavemaking drag

D_{trim} = trim drag (or thrust)

D_{tot} = total calm water drag

3.6.4.2 Tests

As implied by Equation (3.6.3), the experimental determination of ACV resistance can involve the use of both towing tanks and wind tunnels. The test techniques employed vary depending upon the facilities available and the type of craft being considered. In a towing tank it may not be possible to obtain correct scale values of aerodynamic profile drag (D_p) and momentum drag (D_m) and the wavemaking drag may be subject to boundary effects if the tank size is limited. Thus, the test techniques employed are devised to enable these components to be isolated as far as possible and scaled separately when extrapolating to the full-scale regime.

3.6.4.2.1 Wind Tunnel Tests. The use of wind tunnel experimental facilities for investigations of hovering craft resistance is desirable for two main reasons: (1) developing hull forms with minimum aerodynamic resistance and (2) obtaining aerodynamic characteristics necessary for the calculation of total full-scale resistance.

With a new craft design it is likely that the aerodynamic characteristics will be established using simple solid models. The techniques involved generally follow conventional wind tunnel practice.[10,11]

The aerodynamic control system may be developed with the aid of either partial models or possibly the complete dynamic test model. Similarly, either specialized models or the dynamic model may be used to develop the lift system air intakes and to study the effects of interaction between the lift and propulsion systems.

3.6.4.2.2 Towing Tank Tests with Screened Models. The usual towing scheme uses a vertical post to tow the model at constant speed with freedom in heave and pitch. The total resistance to model movement is recorded by a one-component dynamometer. The center-of-gravity rise and angle of trim are recorded by potentiometer gages.

The distortion of the velocity field in the airstream (see Section 3.6.4.2.3) as well as the comparatively small Reynolds numbers which often apply, sometimes make it attractive to exclude air resistance when measuring total ACV model resistance in the model tank. This is achieved by the installation of a screen ahead of the model which insulates the model from oncoming air flow.

The disadvantage of this method is that it does not guarantee complete insulation of the model. That is why, to some extent, profile and momentum drag, a well as

components due to the interaction between the air outflow from the air cushion with the oncoming flow, are excluded form the measurement. These factors are difficult to account for.

The unrepresentative aerodynamic action upon the model during its towing in the model basin, in particular the longitudinal moment, has an effect upon model trim and, consequently, distorts its hydrodynamic characteristics in comparison with the full-scale vessel for the same longitudinal C.G. location. Thus, the model has to be towed with a longitudinal C.G. location such that its trim corresponds to that of a full-scale craft with the moment from the propulsors also taken into account. The moment characteristics necessary to correct the trim of the model are obtained by calculations and by the results of wind tunnel tests.

3.6.4.2.3 Towing Tank Tests with Unscreened Models. The determination of the calm water resistance is only a small part of the total performance envelope. Therefore, because a screen can only be used in the calm water case, many establishments prefer to conduct tests with unscreened models.

Due to the comparatively large above water area and high speeds of an ACV it is important to ensure that the model is not subject to aerodynamic interference effects from the towing carriage. The air flow beneath a conventional tank carriage can be severely disturbed. To minimize these effects, either a small permeable carriage, connected with the main one and running ahead of it, or a self-contained unmanned carriage is employed.

The detailed treatment of the aerodynamic profile drag component depends upon the superstructure configuration and the extent to which it can be accurately modeled. In many cases, with a suitably representative superstructure, experience has indicated that at least approximate similarity of the external flow around the model is obtained. It is sometimes assumed that the aerodynamic drag coefficient is the same on the model as on the prototype vehicle.

In some instances this may not be sufficiently accurate and corrections are then applied using data from wind tunnel tests. The model may also be towed in the tank in the hovering position without the air cushion to obtain an aerodynamic drag coefficient for the model, however, this is not always practical with fully skirted craft.

Measurements made comprise total resistance, C.G. rise, trim, and often skirt and cushion pressures and lift power.

3.6.4.2.4 Tests to Determine the Resistance of Particular Craft Components. For investigation purposes, alongside total resistance measurements, the resistance of flexible skirt components is determined by mounting these components on separate dynamometers. Generally speaking, in the case of flexible skirts, the longitudinal force along the hinge line on the solid hull structure is measured rather than the flexible skirt resistance. An example of such test results is shown in Figure 3.6.7. The technique of these experiments is complicated by the specific features of the hovering craft supporting system. The estimation of the resistance of flexible skirt components, for example, is possible only by simultaneous measurement of the forces, air cushion pressure, flexible skirt form, and area of its wetted surface.

3.6.4.3 Extrapolation of Model Results in Smooth Water to Prototype

The principle hydrodynamic scale effects as regard calm water resistance are due to the influences of viscosity and surface tension on water wetting and spray.

Water wetting can be corrected for in the usual way provided that the wetted areas can be determined and that the boundary layer is turbulent. This is the normal procedure for surface-piercing rigid structure such as skegs, etc., but is generally impractical on flexible skirts. However, it can be postulated that the expected reduction in full-scale skin friction drag coefficient due to Reynolds number effects is offset by an increase in spray drag or some other nonscale phenomenon. This premise is supported by correlation experience obtained to date which indicates that full-scale calm water resistance can be satisfactorily predicted by direct Froude scaling of the model residual drag component given by Equation (3.6.3) (see Reference 12).

When tests are conducted with a screened model (see Section 3.6.4.2.2), the full-scale aerodynamic drag terms (D_p and D_m) must be calculated using wind tunnel data (see Section 3.6.4.3.1) and added to the Froude-scaled model hydrodynamic resistance. As noted previously, however, some errors are likely to be introduced because some aerodynamic effects are not accounted for fully. The effect of the oncoming flow upon the amount of air jet response can be taken into account using the results of wind tunnel tests on a model with flexible skirts and working fans, but such a procedure is not usual during routine testing.

For tests with an unscreened model, the total measured resistance may sometimes be scaled directly to full-scale using Froude scaling. However, it is more usual to separate the aerodynamic drag components to enable corrections to be applied (see Section 3.6.4.2.3).

Where tank size is limited, the wavemaking drag of the model in the restricted water of the test tank may then be calculated using the Newman and Poole method[8] so that the wetting (or residual) drag of the model can be obtained (see Equation 3.6.3). This is scaled up to full-scale using direct Froude scaling. The full-scale estimates of the aerodynamic and wavemaking drag components for unrestricted water are then added to the full-scale residual drag to give the total full-scale calm water drag.

3.6.4.4 Outstanding Problems in the Prediction of Smooth Water Resistance

Calm water resistance prediction techniques, as already described, give satisfactory correlation with full-scale trials for many existing craft. Nevertheless the spray drag scale effects due to surface tension are not fully understood and this may become important on future craft designs when the apparent balance, which exists at present between water wetting and spray scale effects, may no longer apply.

3.6.4.5 Recommendations to the 16-ITTC in the Area of Smooth Water Resistance

3.6.4.5.1 Assess the hydrodynamic skin friction scale effects on flexible structures and the theoretical calculations of wetting drag.

3.6.4.5.2 Determine the effects of spray drag and the scale effects associated with spray generation.

3.6.4.5.3 Develop techniques suitable for the investigation of separate drag components.

3.6.4.5.4 Develop techniques for scaling skirt material characteristics and the effect of material properties on the resistance.

3.6.5 SEAKEEPING (PERFORMANCE AND MOTIONS)

3.6.5.1 General

Seakeeping qualities of hovering craft are characterized by the craft resistance and various accelerations, the value of the largest impact loads in a sea-way and the amplitudes of pressure fluctuations in the air cushion.

3.6.5.2 Test Wave Environment

The value of regular wave tests is limited since ACVs are often specifically designed to have nonlinear response characteristics, and, except for detailed investigation of this aspect, most tests are conducted in irregular waves.

The energy spectra employed should be representative of the area and conditions under which the craft is expected to operate. Either British Towing Tank Panel (BTTP) Inshore (Darbyshire 100 nm fetch) or Jonswap formulations are frequently

employed for all but the largest vehicles where Pierson-Moskowitz and Bretschneider formulations may be more appropriate. For comparative tests between, for example, different craft configurations, it is important to test each in the same wave train at each speed.

3.6.5.3. Test Procedures

Tests are either conducted in the towing tank or occasionally with free running models at sea in wind generated waves.

For tests in the towing tank the model is restrained in roll, sway, and yaw but is free to pitch and heave. In general, freedom in surge is also felt to be highly desirable for ACVs because it is reasonable to assume that scale motion characteristics will only be reproduced if the model is free to recover correctly from the decelerating effects of large waves.

Depending upon the wavelength and height relative to the cushion length and height the amount of surge movement may be small, and in some facilities overwave tests are conducted without surge freedom.

Tests are normally conducted with the model locked at zero roll and yaw. However, with an amphibious hovercraft it is likely that, in a seaway, the craft will be operated at some angle of yaw relative to its track. For certain applications, therefore, roll and limited yaw freedom may be provided during the model tests.

The model is towed at constant thrust (or constant speed) from the center of gravity and a pitching moment correction applied to account for the difference in height between the thrust line and the vertical C.G., by moving ballast within the model.

The quantities measured generally comprise mean resistance, trim, C.G. rise, vertical accelerations, skirt and cushion pressures, and, where appropriate, surge motion. Wave height is recorded by means of a probe attached to the tank carriage. In limiting sea conditions impact pressures may also be recorded. It is usual to obtain video motion picture film coverage for qualitative evaluation.

3.6.5.4 Data Collection and Processing

The methods of data collection and processing employed vary depending upon the facilities available.

Either digital or analog methods may be employed for recording the data depending upon the preference of the establishment. The high encounter frequencies experienced require that the digitizing sample rates should be high (on the order of 100

samples per second on each channel may be necessary to ensure sampling rates on the order of five times the frequency of the data). In many cases, these recording methods are supported by analog paper trace records, which are used for direct visual appraisal and as an aid for correct interpretation of the results of subsequent analysis.

Time domain analysis is emphasized in many cases because of the nonlinear nature of ACV motions, accelerations, etc. Statistics such as: the largest response, the second largest, etc. the significant; the average of the largest one-tenth; and the average are calculated from actual peaks and troughs in the time history. For ACV motion analysis these peaks and troughs in the time histories are usually treated separately because experience has shown that this minimizes the effects of large amplitude very low frequency motions which are of little significance from the point of view of ride comfort.

Motions, accelerations, and waves are normally presented either as energy spectra on a frequency base or as significant values.

Significant values of motion and acceleration are also sometimes divided by significant wave height to provide significant responses for comparative purposes.

Histograms are sometimes provided, especially where impact pressures are measured. Accelerations may be compared against a habitability standard to evaluate habitability of the design in question.

3.6.5.5 Extrapolation of Model Results in Rough Water to Prototype

3.6.5.5.1 Correlation of Model and Full-Scale Motion Data. Direct correlation of model motion data obtained on the towing tank with full-scale behavior is difficult to establish because the full-scale behavior is influenced to a large extent by driver technique, craft heading, and multidirectional characteristics of the full-scale sea state. There are also difficulties in obtaining a good measure of the full-scale waves.

Qualitative evidence that has been obtained by "flying" the full-scale craft with fixed control settings in reasonably long crested waves, however, suggests that direct correlation of craft motions is obtained using Froude scaling providing the conditions prevailing in the tank and in the full-scale regime are the same.

3.6.5.5.2 Prediction of Rough Water Performance. The rough water performance is calculated using the drag measurements obtained form the model tests which, when the calm water resistance is subtracted, give values of the overwave increment drag (D_{inc}).

At the present time there is no adequate theoretical treatment available for this term and like the calm water wetting, it can only be established from model tests or estimated using empirical techniques.

It arises mainly from the additional water contact which occurs as the craft passes through the natural waves, but in rough conditions additional terms can arise from local impacts with the craft structure or cushion compartmentation devices. In addition, work by J.R. Richardson[13] suggests that a rough water drag may occur as a result of the craft motion even if no water contact occurs. This arises because the craft damping in pitch and heave alters the phase between the craft motion and the wave in such a way that the resultant of the pressure fluctuations has a net rearwards component.

Experience has shown that in rough water, full-scale performance may be better than that indicated by direct Froude scaling of model test data. This discrepancy between model and full-scale performance in waves has been attributed to the fact that models are normally tested in linear towing tanks where the simulated waves are two-dimensional as opposed to natural sea waves which have a finite width. It is also possible that a portion of the discrepancy is due to other effects such as skin friction or nonscale skirt dynamic characteristics. Because skirt wetting is higher in waves than in calm water, the apparent balance which exists between the scale effects in calm water may not apply in waves.

To allow for the fact that model overwave drags tend to be pessimistic, a wave-height correlation factor (W.H.C.F.) to relate the tank wave to its full-scale equivalent, is often applied. This factor may vary with the type of craft and at present can only be established as a result of previous model-to-full-scale correlation experience.

However, model-to-full-scale trials with a number of craft of widely different sizes, but similar planform shape and skirt configurations, have suggested that this factor is essentially constant for a particular class of vehicle (typically with a value in the region of 1.5).

3.6.5.6 Analysis Methods

Figure 3.6.7 shows typical curves of craft drag variation with speed in calm water and at three wave conditions, all at optimum longitudinal C.G. positions. If necessary, tank boundary corrections are applied to the calm water drags and the total rough water drag curves established by adding the measured D_{inc} to the

corrected calm water resistance. As shown on the figure, the aerodynamic (i.e., momentum and profile) and wavemaking drag components are estimated (see Equations (3.6.1) and (3.6.2)) so that the variation of calm water wetting drag with speed may be deduced (see Equation (3.6.3)). Hence, the total hydrodynamic drag (D_H) may be defined for each sea condition (i.e., total craft drag less total aerodynamic drag, with allowances for cushion thrust if appropriate). That is,

$$D_H = D_{tot} + D_{inc} - D_m - D_p \qquad (3.6.4)$$

To predict the full-scale speed performance using the drag figures derived from the tests, the total thrust (e.g., propeller and exhaust) is determined for the appropriate propeller rpm and thrust power condition, and the aerodynamic drags appropriate to a range of airspeeds are subtracted. It is then possible to construct curves of total thrust less aerodynamic drag ($T-D_m-D_p$) against water speed for various headwind conditions (see Figure 3.6.8). Curves of total hydrodynamic drag for calm water at each test wave height factored by the appropriate WHCF, when superimposed on Figure 3.6.8, enable a performance prediction to be made for an assumed wind speed wave height relationship. This is illustrated in Figure 3.6.9 in terms of the variation of predicted into wind water speed with significant wave height.

In assessing the overall performance of a vehicle it should be appreciated that seakeeping behavior with respect to ride comfort is often of considerable importance and may dictate a limiting speed independent of the available power.

3.6.5.7 Outstanding Problems in Model Tests in Rough Water

The major problem area is associated with the comparatively nonrepresentative environment of the towing tank where the model is conventionally tested at constant control settings at zero yaw in unidirectional head seas. As previously discussed, the full-scale vehicle is effectively "flown" by the pilot sometimes at a significant yaw angle in multidirectional seas. In developmental work, model towing tank data are normally employed on a comparative basis, using a design for which the full-scale behavior is known as the reference.

At present the satisfactory prediction of rough water performance often depends upon empirical correlation factors appropriate to a particular class of vehicle and are determined as a result of previously obtained correlation data. More correlation experience is required on a wide range of vehicle types with a view to determining the parameters which govern the choice of correlation factors. Such correlation data might also assist in the determination of following sea performance and the influence of craft yaw angle on performance prediction.

3.6.5.8 Recommendations to the 16th ITTC in the Area of Rough Water Performance

3.6.5.8.1 Establish more clearly the effect of surge restraint on performance, motions, and plow-in for different types of ACV since many test facilities use a locked-in surge towing technique.

3.6.5.8.2 Establish the extent of linearity of the response of practical ACV configurations.

3.6.5.8.3 Establish the effects of driver techniques on craft response and its significance with respect to towing tank data.

3.6.5.8.4 Investigate the applicability and application of the various methods of calculating significant values.

3.6.5.8.5 Examine analytical methods for the prediction of calm water residual resistance and overwave drag increment.

3.6.5.8.6 Examine methods of predicting craft performance in beam and following seas, and the effect of craft yaw on performance predictions.

3.6.5.8.7 Investigate the significance of the waveheight correlation factors currently employed for model-to-full-scale performance correlation in rough water.

3.6.6 MANEUVERING AND STABILITY CHARACTERISTICS

3.6.6.1 General Description

The maneuvering and stability characteristics of an amphibious hovercraft are often interlinked and a change in one may have serious repercussions on the other. In this context it is worth noting a comment made in Reference 14 "...when handling a hovercraft the line between controlling the hovercraft and the hovercraft controlling the situation may be very thin, and it is very easy to slip to the wrong side of this line."

For this reason, considerable emphasis is placed on model investigations of these aspects to define critical situations and to assist with the preparation of the operators manual.

Adequate control must be available to enable the craft to maintain, and turn off, any chosen heading within the specified range of wind and sea conditions. The parameters normally used to describe the maneuvering characteristics of the vehicle are the tactical turning circle diameter, advance, and maximum safe rate of turn which can be achieved without excessive outward roll. The response of the vehicle to control and motive power failure, and to sudden changes of environmental conditions must also be examined.

3.6.6.2 Tests

3.6.6.2.1 Free Running Tests in the Open Sea. This technique compliments, rather than supersedes, experiments in the controlled environment of a towing tank and, because of the complex interaction between the aerodynamic and hydrodynamic forces, can highlight phenomena having an importance that would not otherwise be appreciated.

Other features include the realism of the environment, in that the waves are wind-generated and multidirectional; the model has all six degrees of freedom, and can be run at any heading to the wind and waves.

The tests can be carried out with manned or, more usually, radio-controlled models of varying degrees of sophistication depending upon the requirements of the work. For an initial investigation, a relatively simple model with no instrumentation can provide much useful information. For more detailed studies, a model having all the full-scale control functions represented and carrying comprehensive instrumentation, using either an onboard recorder or radio telemetry, depending upon the size of the model, is likely to be used.

The models are usually powered by air-cooled two-stroke gasoline engines. Instrumentation may include: accelerometers (longitudinal, vertical, and lateral); a gyro for pitch and roll angles; and for yaw angle, air speed, and control settings. Model track is determined using techniques similar to those employed for conventional low speed ships. High speed film records are normally obtained for visual appraisal.

Tests are carried out in a wide range of sea states, to cover the worst intended environmental conditions proposed for the full-scale vehicle. A variety of maneuveres are carried out over a range of headings to establish the turning performance, the maximum yaw angles for safe operations, the longitudinal C.G. range available before the onset of plow-in, and the behavior following a control system or engine failure.

3.6.6.2.2. Towing Tank Tests. Stability investigations on the towing tank use two basically different test techniques. In the first, the model is provided with surge freedom and the dynamic situation is represented as closely as possible within the limitations imposed by the towing tank. With the second technique the model is locked in surge, and sometimes in all other five degrees of freedom, and measurements of forces are obtained, usually for application in a computer simulation.

In the first method longitudinal stability is investigated with the model free to surge, heave, and trim and usually restrained in roll, yaw, and sway. It is

normally towed at constant thrust from the C.G. position with appropriate thrust moment corrections applied to account for the correct position of the thrust line. Stability boundaries are investigated by variations of the longitudinal L.C.G. position in calm water and when entering disturbed water, such as a ship's wake (simulated in the tank by operating the wavemaker for only a very short period of time). Emergency situations and engine failure cases may also be studied. Clearly this method requires a free-to-surge facility with considerable travel; experience suggests a travel on the order of four times the model length is desirable.

For investigation of transverse stability, and the limits of safe operation at yaw angles up to 90 degrees, similar techniques are employed and tests are also carried out in steep following seas and the effects of wind, C.G. shifts and control, and skirt failures may be investigated. In these cases the model is restrained in yaw and sway (i.e., perpendicular to the wave direction) only.

In this context it should be noted that, while the initiating maneuver may commence at a high speed, the final large attitude change and possible overturn is most likely to occur at a relatively low speed, with the craft traveling essentially beam-on and rolling about the immersing leading side structure.[15]

This critical overturn speed has been defined in model beam-on towing tests in calm water as the speed at which the applied roll moment produces the maximum roll angle, as illustrated by the example in Figure 3.6.10. The parameters influencing craft safety are discussed in detail in Reference 14.

The second type of technique follows more closely conventional displacement ship practice in that the model is locked in surge. Longitudinal stability is the simplest for evaluation and using measurements of trim angle for various C.G. locations relative to model length, it is possible to evaluate the stiffness as a function of the Froude number, load coefficient, etc. The critical modes preceeding the loss of stability due to plow-in may also be approximately evaluated.

To estimate the longitudinal and transverse stability in conditions of three-dimensional model motions, a tracking installation may be used.[16] In this case, the model has five degrees of freedom, i.e., vertical emergence, side displacement, heeling, yawing, and trimming. In the case of side displacement, the model is relieved of inertial and frictional forces in the moving components of the installation by means of a special servosystem. The significant element of the installation is a servosystem bringing the towing force direction at each given moment of time into coincidence with the model centerline plane irrespective of the course angle.

On apparatus such as that described, one can determine model amplitude, phase, and frequency characteristics or directly estimate model behavior in a given conditions such as the case of flexible skirt rupture or failure of fans, etc.

Naturally, because the model is restrained in surge and the towing speed is always constant, it is not possible to obtain a complete simulation of vehicle behavior. However, this is not necessarily a barrier to solving a wide variety of practical problems because errors are often on the side of safety.

The determination of directional stability derivatives can be carried out in a circulating basin with a rotating arm. Superstructures may be simulated while the effects of propellers are not. For the tests in the circulating basin, the model is attached to a dynamometer on the rotating arm with defined drift and heel angles and with freedom in vertical motion and trimming. Such factors as side force, resistance, moments of heel and yaw, as well as the angle of trim and center of gravity rise are measured. During the tests the linear model towing speed, radius of circular trajectory, angle of heel, and drift are varied. The form of the test result presentation depends upon the use of the material and the pattern of curves obtained. Stability derivatives may also be obtained using a horizontal planar motion mechanism. The model generally has freedom in heave and pitch and as a rule the superstructure and aerodynamic control surfaces are not represented. In both of the above cases, the techniques are similar to conventional low speed ship practice with the exception that wind tunnel tests may also be required to determine the aerodynamic characteristics. Such tests employ conventional wind tunnel techniques.[16]

3.6.6.3 Extrapolation to Prototype

Model to full-scale correlation of directly simulated processes (such as free-running tests) are carried out by direct Froude scaling without any additional scale-effect corrections. Reynolds number effects are considered to be insignificant in most practical cases. This has been found adequate for the prediction of full-scale behavior.

The stability derivatives and coefficients obtained from captive model tests are generally employed in a computer simulation to predict the maneuvering characteristics of the full-scale vehicle.

3.6.6.4 Outstanding Problem Areas in Maneuverability and Recommendations

The interaction and cross coupling between the various aerodynamic and hydrodynamic characteristics governing the maneuvering capability of ACV's present serious

problems when attempting to assess the maneuvering performance by means of mathematical models. Nevertheless, a better understanding of the problems is desirable for the long term development of ACV's in general.

It is recommended that investigations be made into the aerodynamic and hydrodynamic characteristics governing the maneuvering capabilities of ACV's, and the most suitable methods for obtaining these characteristics experimentally.

3.6.7 PROPULSOR INVESTIGATIONS

3.6.7.1 Typical Propulsors

Typical propulsors are discussed in Section 3.6.1.1

3.6.7.2 Testing

The testing of air propellers normally lies outside the realm of towing tanks, although, as mentioned in Section 3.6.4.2.1, wind tunnel tests are often conducted to investigate lift and propulsion system interactions, control effectiveness, etc. The data obtained from separate wind tunnel tests on airscrews are employed in the prediction of performance as described in Section 3.6.5.6.

3.6.7.3 Outstanding Problems and Recommendations

As already mentioned airscrews are the most common form of propulsor used for ACV's and the problems that arise are normally outside the realm of towing tanks.

When water screws are employed the problems are similar to those for other screw propelled high speed vehicles.

3.6.8 - SCALING OF SKIRT MATERIAL CHARACTERISTICS

The correct bending stiffness is generally determined by comparing the deformation to load characteristics of similar model and full-scale specimens when deformed in the same way. For example, a rectangular sample of material can be clamped at one end as a cantilever and its deformation under its own weight measured. Hence, if we consider the full-scale material sample of length l_f, weight per square meter W_f, thickness t_f, and Youngs modulus E_f we have:

$$\delta_f = \frac{12 W_f l_f}{8 E_f t_f^3} \qquad (3.6.5)$$

where δ_f is the deflection of the full-scale sample at the free end.

At model scale

$$\delta_m = \frac{12 W_m l_m^4}{8 E_m t_m^3} \qquad (3.6.6)$$

and from, Equation (3.6.5)

$$E_f = \frac{12 W_f l_f^4}{8 \delta_f t_f^3} = \lambda E_m \qquad (3.6.7)$$

where λ = scale ratio

Hence, substituting for E_m in Equation (3.6.7) we have:

$$\frac{\delta_m}{\delta_f} = \frac{Wm}{W_f} \cdot \frac{l_m^4}{l_f^4} \cdot \frac{t_f^3}{t_m^3} \lambda \qquad (3.6.8)$$

Alternative methods are in use but they follow similar principles.

3.6.9 REFERENCES

1. Plackett, M.J. and R.B. Wade, "Design Aspects of Seal Systems for Air Cushion Vehicles," Advanced Marine Vehicles Conference, AIAA Paper 78-755 (1978).

2. "Report of the A.R.B. Special Committee on Hovercraft Stability and Control," Civil Aviation Authority Paper 75077 (1975).

3. Shepherd, D.C., "Principles of Turbo Machinery," MacMillan (1956).

4. Clarke, B.G., "Some Techniques used in the Testing of Hovercraft Models," Royal Aeronautical Society (Southampton Branch) and U.K. Hovercraft Society (1979).

5. Prokhorov, S.D. and B.M. Zelensby, "On Towing Tank Simulation of Unsteady Outflow from the Hovercraft Air Cushion," 16th ITTC Newsletter, No. 2 (Jun 1980).

6. Wheeler, R.L., "Recent United Kingdom Hovercraft Development," Advanced Marine Vehicles Conference, AIAA Paper 76-863 (1976).

7. Doctors, L.J. and S.D. Sharma, "The Acceleration of an Air Cushion Vehicle Under the Action of a Propulsor," Journal of Ship Research, Vol. 17, No. 2 (Jun 1973).

8. Newman, J.N. and F.A.P. Poole, "The Wave Resistance of a Moving Pressure Distribution in a Canal," DTMB Report 1619 (Mar 1962).

9. Doctors, L.J., "The Wave Resistance of an Air Cushion Vehicle," University of Michigan (1970).

10. Andrews, E.J., "The Aerodynamic Characteristic of a Family of Related Hovercraft Shapes," College of Aeronautics Memorandum 133 (1967).

11. Treshchevsky, V.N. et al., "Aerodinamichesky Experiment v Sudostroenii," Leningrad (1972).

12. Clarke, B.G., "The Use of Scale Models for the Prediction of Performance," Advanced Marine Vehicle Course, Computational Mechanics Centre, Southampton, England (Oct 1980).

13. Richardson, J.R., "A Mechanism of Rough Water Drag," National Physical Laboratory, Hovercraft Unit Report (Jan 1971).

14. "Stability and Control of Hovercraft, (Notes for Commanders)," Ship and Marine Technology Requirements Board, Department of Industry (1980).

15. Crago, W.A., "Problems Associated with the Use of Skirts on Hovercraft," Institute of Mechanical Engineers (Dec 1967).

16. Prokhorov, S.D. et al., "On the Determination of Aerohydrodynamic Performance of Air Cushion Vehicles," 9th Symposium on Naval Hydrodynamics, Paris (1972).

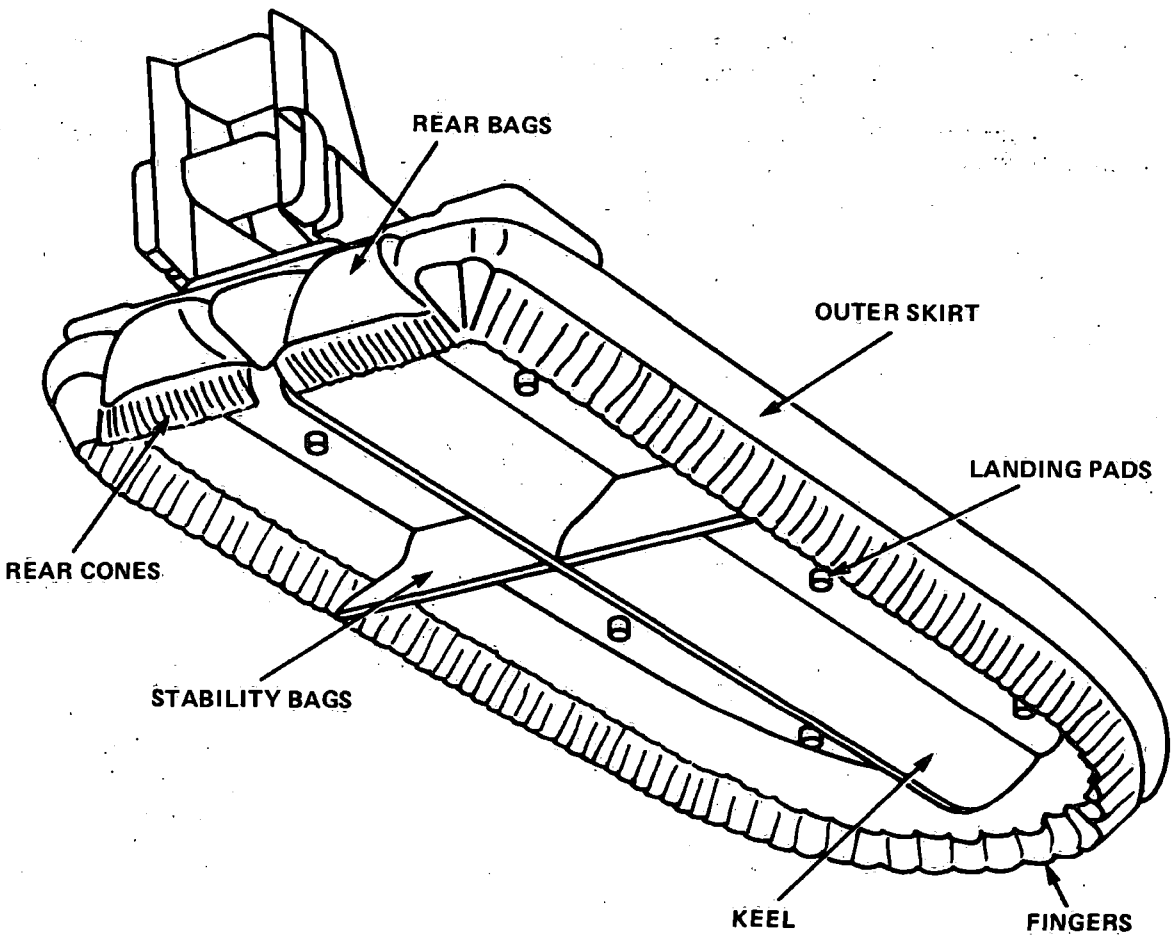

Figure 3.6.1 - Typical Small ACV Fitted with BHC Type Peripheral Skirt

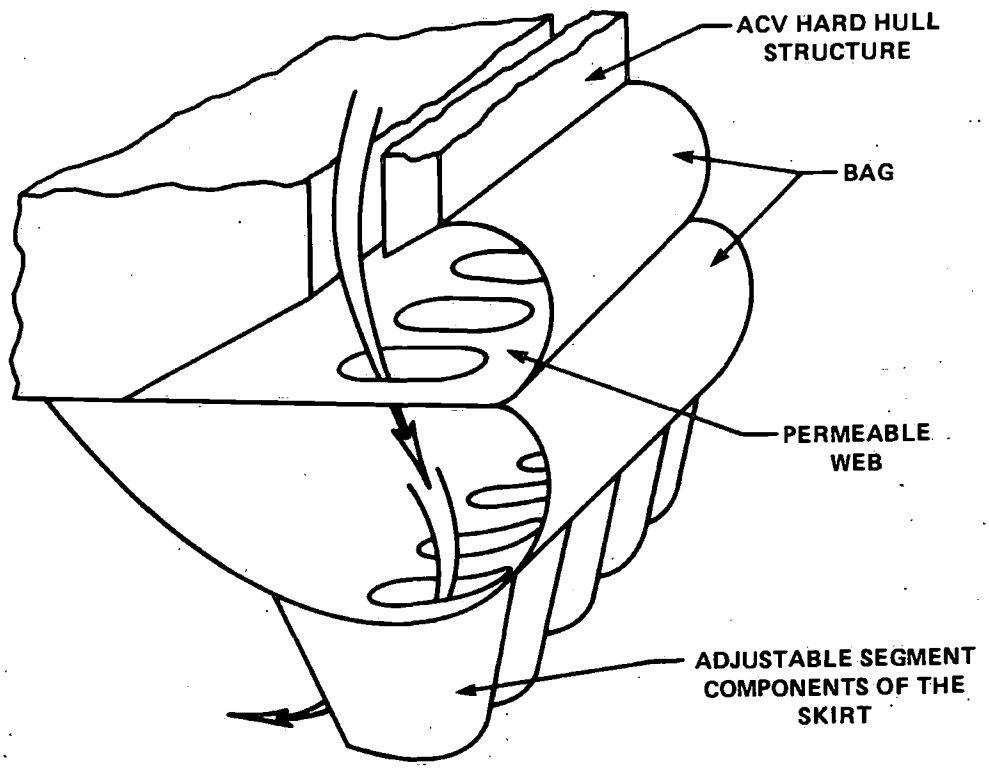

Figure 3.6.2 - Scheme of the Side Part of the ACV Peripheral Flexible Skirt

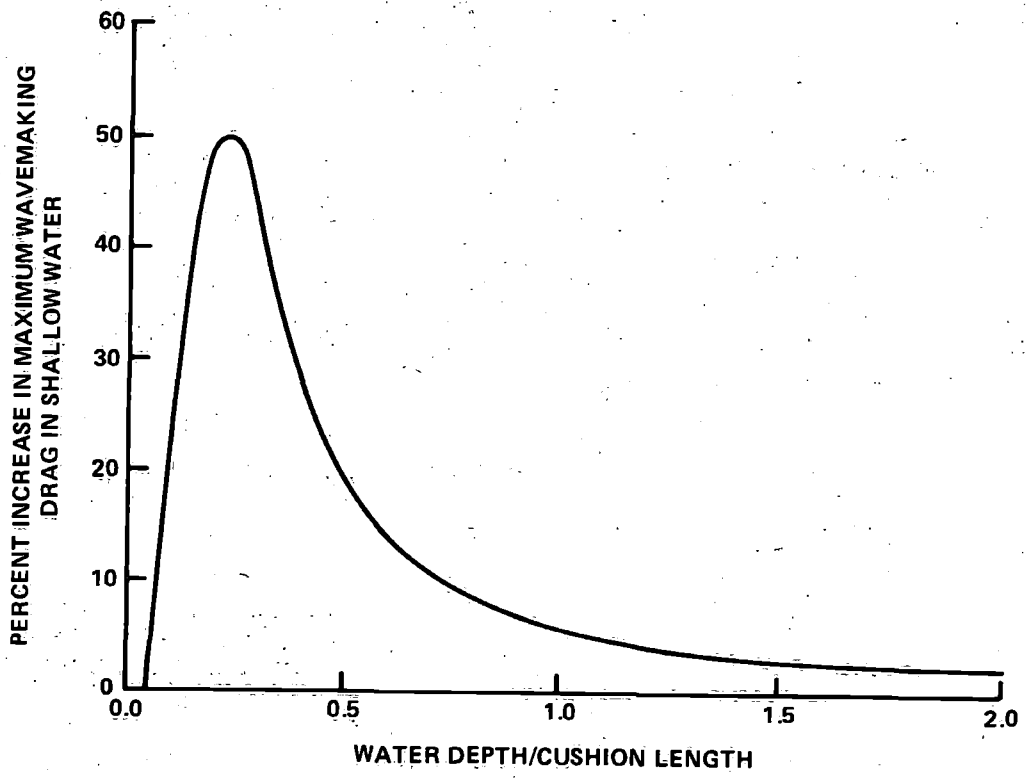

Figure 3.6.3 - Typical Increase of Wavemaking Drag in Shallow Water

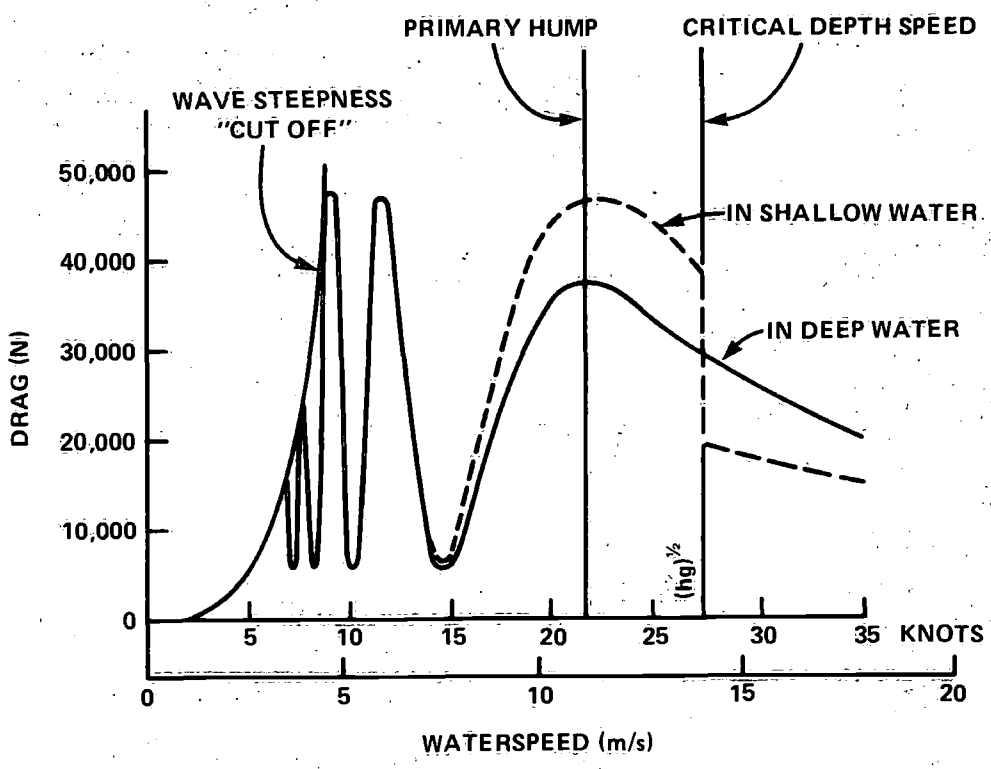

Figure 3.6.4 - Typical Wavemaking Drag Characteristics

Figure 3.6.5 - Scaling of Enclosed Bags

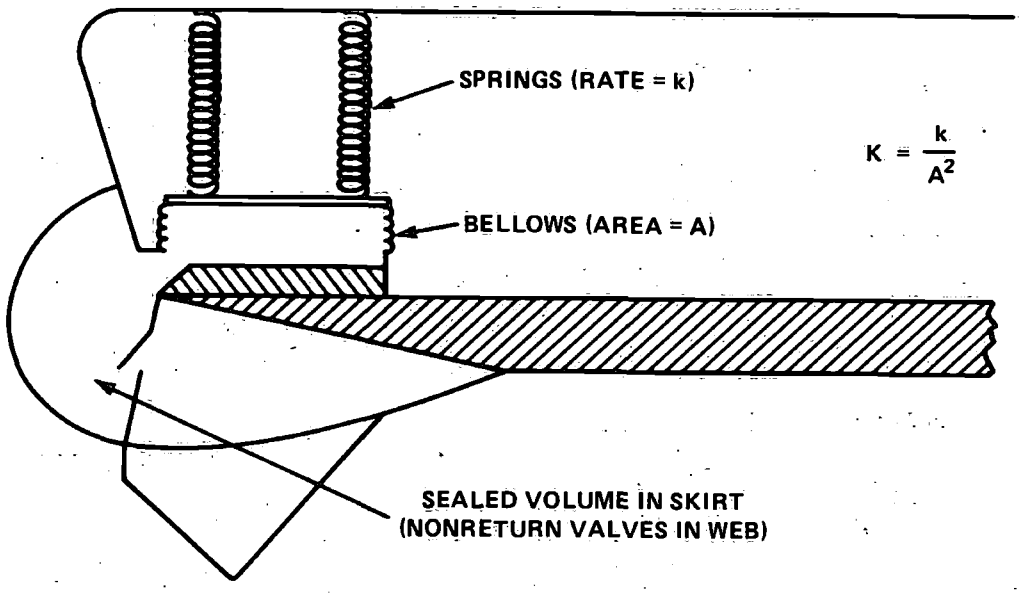

Figure 3.6.5a - Typical Installation of Pressure Compensator in a Model

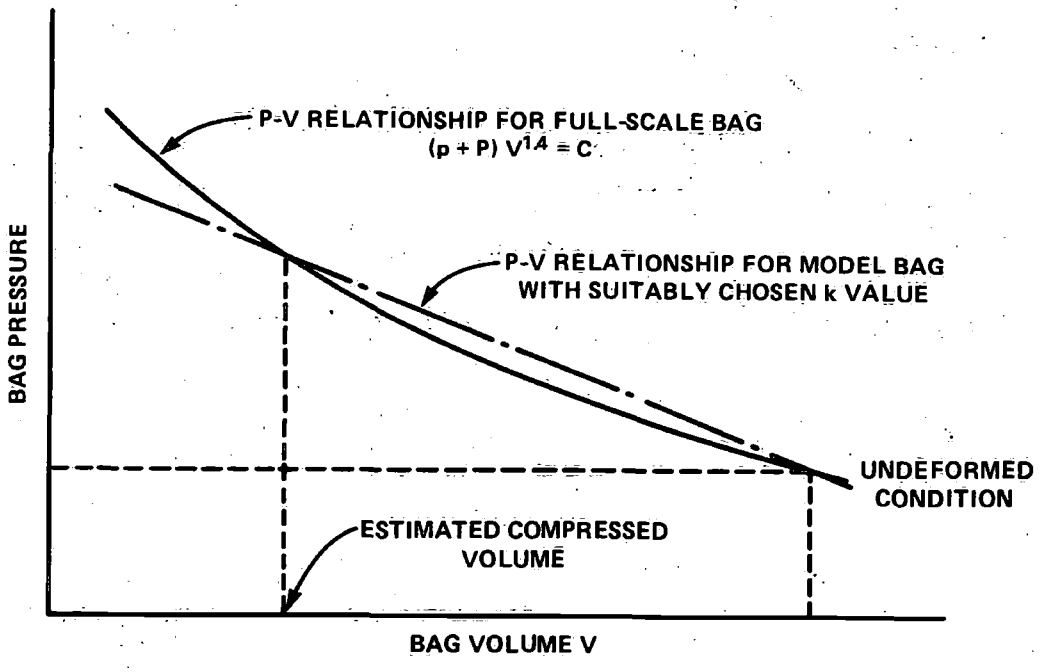

Figure 3.6.5b - Example of Pressure Volume Relationship

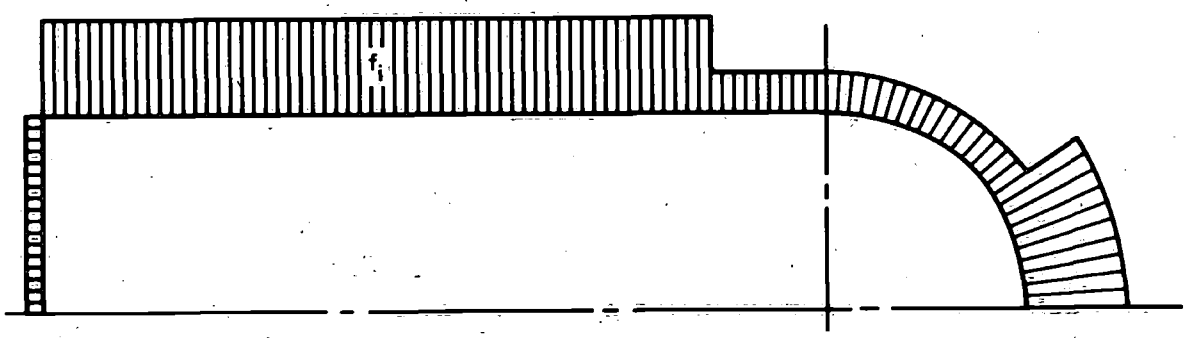

$$f_i = \frac{F_i \ell}{\ell_i G}$$

F_i – LONGITUDINAL FORCE MEASURED AT THE FLEXIBLE SKIRT HINGE LINE.
ℓ_i – FLEXIBLE SKIRT LENGTH.
ℓ – FLEXIBLE SKIRT PERIMETER LENGTH.
G – MODEL WEIGHT.

Figure 3.6.6 - A Schematic of the Relative Specific Load Distribution for the Flexible Skirt of an ACV Model

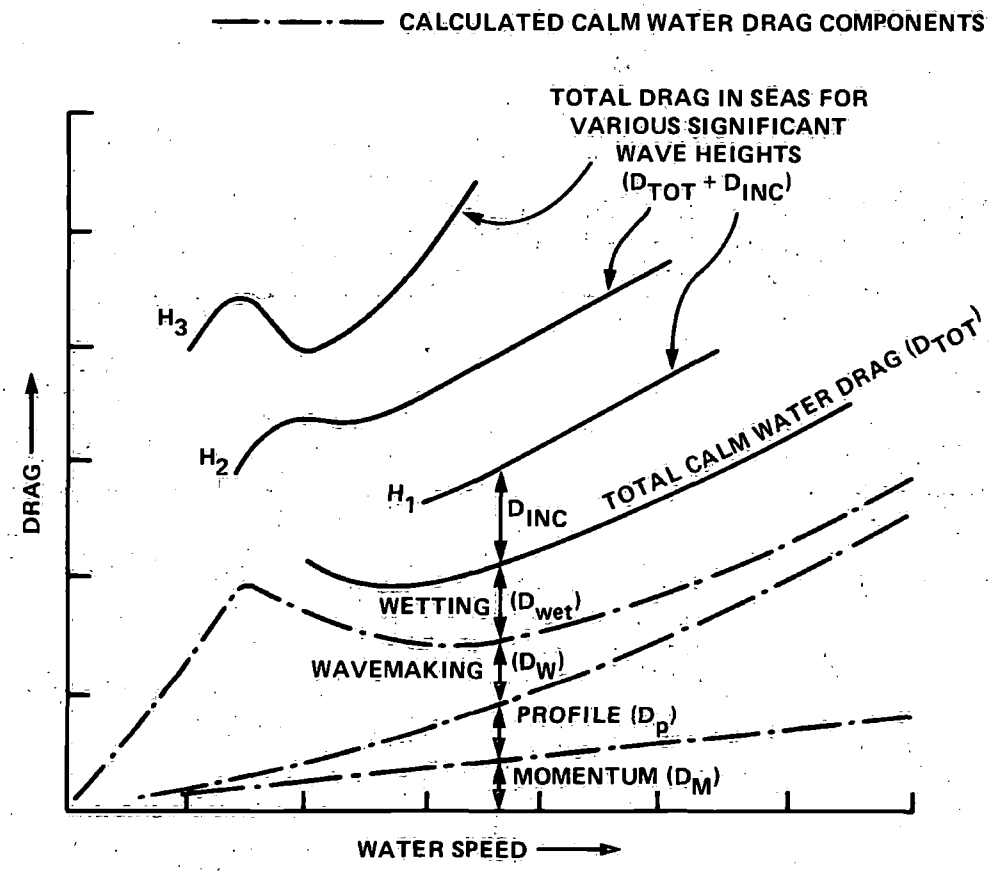

Figure 3.6.7 - Towing Tank Drag Measurement at Optimum Longitudinal Center of Gravity

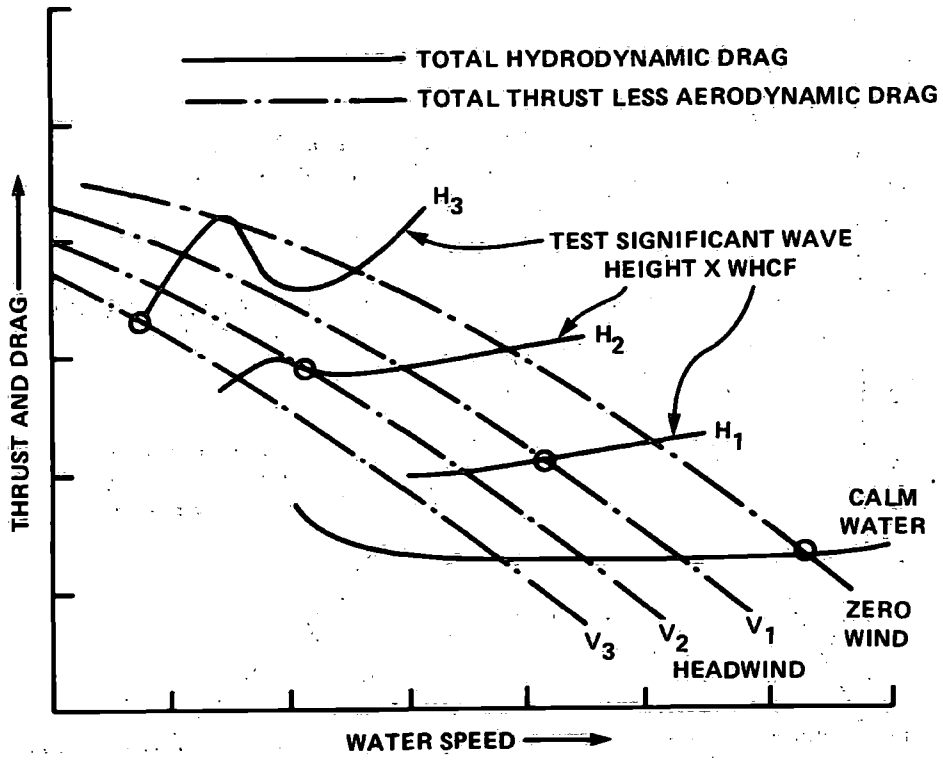

Figure 3.6.8 - Thrust and Drag

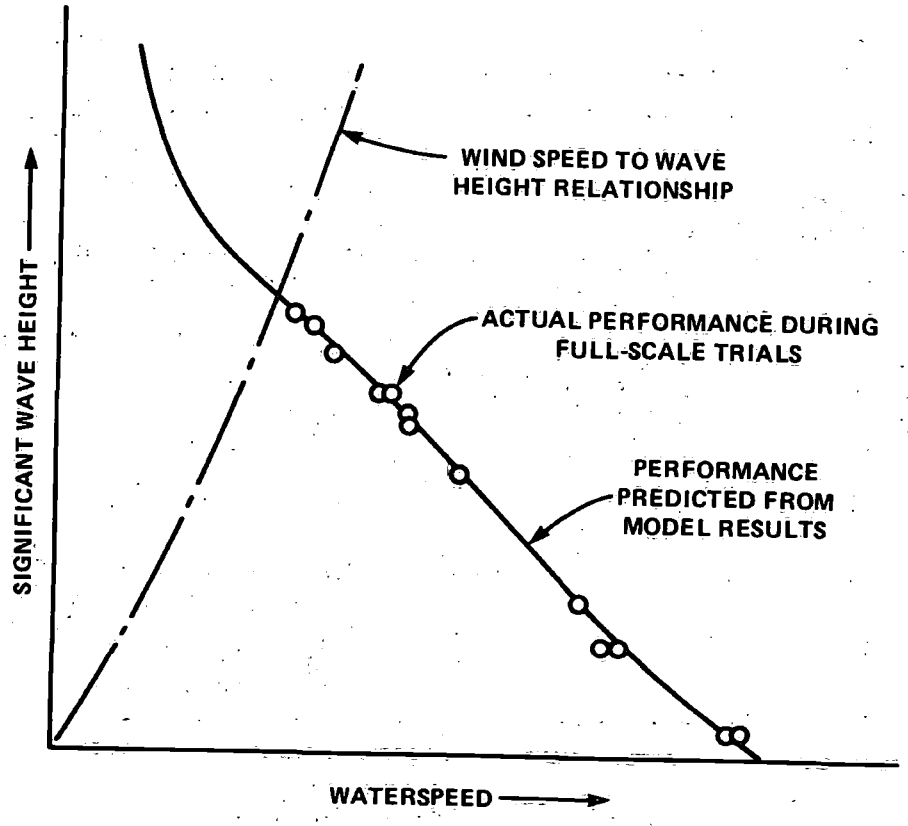

Figure 3.6.9 - Actual and Predicted into Wind Waterspeed Performance

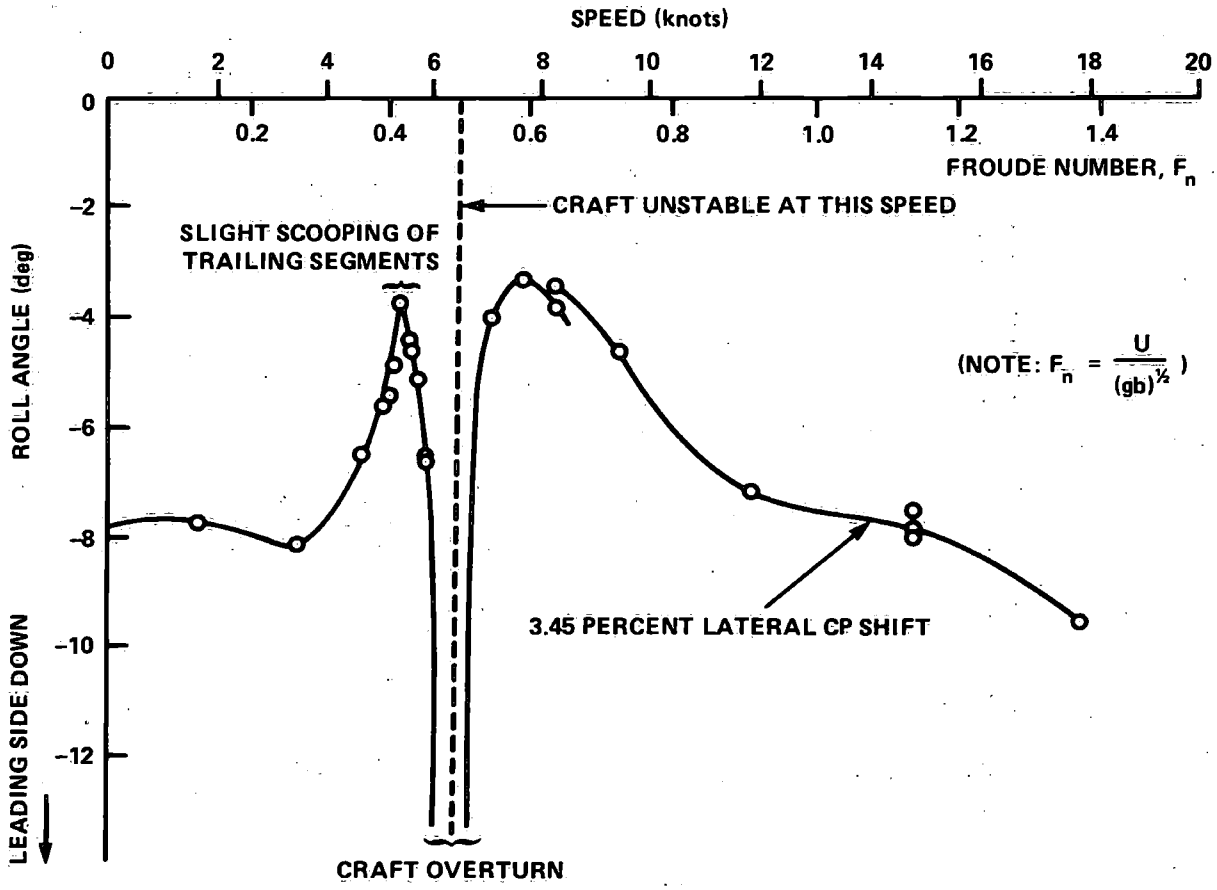

Figure 3.6.10 - Example of Critical Speed Definition from Model Tests

INITIAL DISTRIBUTION

Copies	
4	U.S. Army, Cold Regions R&E Lab 2 Library 1 G. Frenkenstein 1 Prof. G.P. Vance
4	USNA 2 Library 1 Prof. R. Bhattacharyya 1 Prof. B. Johnson
8	Naval Sea Systems Command 1 SEA 003/N. Kobitz 1 SEA 3213/R. Keane 5 PMS 304/S. Davis 1 PMS 377/R. Kenefick
12	DTIC
1	U.S. Department of Commerce Office of Marine Technology 1 R. Falls
1	CIT/Prof. T. Wu
2	University of California 1 Prof. W. Webster 1 Prof. J. Wehausen
1	University of Hawaii 1 Prof. M. St. Denis
1	MIT/Prof. M.A. Abkowitz
4	University of Michigan 2 Library 1 Dr. A. Troesch 1 Prof. R.B. Couch
1	Penn State Univ/Dr. B. Parkin
1	Arctec, Inc./R.A. Major
1	Fluid Dynamic Branch Office 1 Dr. R. Whitehead
5	Hydronautics, Inc. 2 Library 1 Dr. R. Barr 1 P. Eisenberg 1 A. Goodman
2	Institute of Hydraulic Research 1 Prof. V. Patel 1 Prof. L. Landweber
1	Lockheed Ocean Lab/W. Barkley
2	Offshore Tech Corp/Library
5	SIT 2 Library 1 Prof. Dr. J. Breslin 1 Dr. H. Eda 1 Dr. D. Savitsky

CENTER DISTRIBUTION

Copies	Code	Name
1	01	Dr. A. Powell
1	1100	W.M. Ellsworth
1	1113	G.R. Lamb
1	1170	M. Brown
1	1500	Dr. W.B. Morgan
1	1500	W.C. Cummins
1	1500	Dr. K. Schonherr
1	1508	Dr. F. Peterson
1	1524	Dr. W. Lin
1	1532	G. Dobay
1	1552	Dr. J. McCarthy
1	1568	G. Cox
1	1600	Dr. H.R. Chaplin
10	1603	R.A. Wilson
5	1630	A.G. Ford

CENTER DISTRIBUTION (Continued)

Copies	Code	Name
10	5211.1	Reports Distribution
2	522.1	Unclassified Lib
2	522.3	Aero Lib